

**Synthesis and Characterization of Novel Ion-Conducting Highly Sulfonated
Poly(phenylene sulfone)s for Electrochemical Application**

Nodar Dumbadze

*Dissertation has been submitted to the Joint Science Dissertation Board of Free University of
Tbilisi and Agricultural University of Georgia to obtain the academic degree of PhD in
Chemistry*

Scientific Supervisor: Prof. Giorgi Titvinidze, PhD in Chemistry

Agricultural University of Georgia

Tbilisi, 2025

სამეცნიერო მიმართულების კომისიის რეკომენდაცია

დისერტანტი: ნოდარ დუმბაძე

დისერტაციის სათაური: „ახალი იონგამტარი მაღალი სულფირების ხარისხის მქონე პოლი(ფენილენ სულფონების) სინთეზი და კვლევა ელექტროქიმიური გამოყენებისთვის“. „Synthesis and Characterization of Novel Ion-Conducting Highly Sulfonated Poly(phenylene sulfone)s for Electrochemical Application“.

დისერტაციის დაცვის თარიღი: 28.02.2025

დისერტაციის დაცვის კომისია:

რეცენზენტი 1: /ელიზბარ ელიზბარაშვილი/

რეცენზენტი 2: /მაია მერლანი/

თავმჯდომარე/რევაზ კორაშვილი/: _____(ხელმოწერა)

წევრი/სამეცნიერო ხელმძღვანელი/გიორგი ტიტვინიძე/: _____(ხელმოწერა)

წევრი/გია ხატისაშვილი/: _____(ხელმოწერა)

წევრი/რამაზ ქაცარავა/: _____(ხელმოწერა)

რეკომენდებულია დაცვისათვის ქიმიის სამეცნიერო მიმართულების კომისიის მიერ.

თავმჯდომარე/გიორგი ტიტვინიძე/: _____(ხელმოწერა)

წევრი/ელიზბარ ელიზბარაშვილი/: _____(ხელმოწერა)

წევრი/რევაზ კორაშვილი/: _____(ხელმოწერა)

წევრი/რამაზ ქაცარავა/: _____(ხელმოწერა)

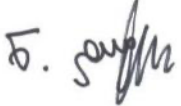
წევრი/ნატო კობახიძე/: _____(ხელმოწერა)

სადოქტორო სკოლის კოორდინატორი: _____/ნატო კობახიძე/

თარიღი: 28.02.2025

Declaration of Authorship

“As the author of the submitted doctoral dissertation, I declare that my dissertation is an original work and that the materials published or defended by other authors in it are used in accordance with the proper citation rules.”

Nodar Dumbadze  (signature)

Date: 28.02.2025

Abstract

Modern electrochemical energy conversion devices require proton-exchange membranes with more advanced properties than the state-of-the-art perfluorosulfonic acid (PFSA) ionomers. Hydrocarbon-based membranes are an attractive alternative to PFSA in proton exchange membrane fuel cells (PEMFC) due to their low gas permeability, high mechanical properties and good thermal stability. Coming from above mentioned there is an increased interest in new aromatic proton conductive polyelectrolytes.

Novel sulfonated poly(phenylene sulfone)s (sPPS) with a backbone consisting of merely phenyl rings connected with electron-accepting sulfone units ($-\text{SO}_2-$) were synthesized and studied. These types of ionomers deserve special interest due to the several advantages over frequently reported sulfonated poly(arylene)s containing electron-donating units in the main chain:

- a. higher oxidative and hydrolytic stability caused by the presence of electron-withdrawing groups ($-\text{SO}_2-$) in the ortho-position to the sulfonic acid groups;
- b. higher acidity of sulfonic acid groups caused by electron-deficiency of the aromatic ring;
- c. rigidity of backbone allowing preparation of water-insoluble ionomers with high ion-exchange capacity.

Within the current PhD thesis we have synthesized sPPS copolymers having long unsulfonated segments, which allowed to prepare water insoluble sPPSs with higher IECs and in addition, such type of polymers showed lower water uptake. To prepare mentioned copolymers corresponding long-chain difluoro monomers were prepared for the first time. For all prepared monomers and polymers molecular characterizations were carried out.

From the developed novel ionomers acid-base blend membranes with different polybenzimidazoles were prepared. The increase of IEC of sPPS copolymers correspondingly allows to increase as IEC of the blend membranes, as well as the content of polybenzimidazoles in them, which leads as to the increased proton conductivity, as well as to the increased

mechanical properties. Water uptake, IEC and leaching out measurements were carried out for the prepared membranes.

In the frames of the PhD thesis structure-property relation were studied (e.g. water uptake — chemical structure, chemical stability — chemical structure, proton conductivity — chemical structure, monomer structure — molecular weight, etc.).

Key Words: ion-exchange membranes, step-growth polymerization, fuel cells, poly(phenylene sulfone)s, water electrolyzers

Supervisor, Giorgi Titvinidze



(signature)

რეზიუმე

თანამედროვე ელექტროქიმიური ენერჯის გარდამქმნელი ხელსაწყოებისათვის აუცილებელია ისეთი პროტონმიმოცვლითი მემბრანები, რომელთაც გააჩნიათ დღესდღეობით გამოყენებულ პერფორირებულ სულფომჟავა ჯგუფის შემცველ იონომერებზე უფრო მოწინავე თვისებები. ნახშირწყალბადზე დაფუძნებული მემბრანები წარმოადგენენ ხსენებული იონომერების მიმზიდველ ალტერნატივას პროტონმიმოცვლით მემბრანიან საწვავ ელემენტებში გამოსაყენებლად, რაც ეფუძნება მათ აირის დაბალ შეღწევადობას, მაღალ მექანიკურ სიმტკიცესა და კარგ თერმულ თვისებებს. აქედან გამომდინარე, გაზრდილია ინტერესი ახალი ტიპის არომატული პროტონგამტარი პოლიელექტროლიტებისადმი.

დასინთეზდა და შესწავლილ იქნა ახალი ტიპის სულფირებული პოლი(ფენილენ სულფონები), რომელთა მთავარი ჯაჭვი შედგება მხოლოდ ფენილის ბირთვებისგან, რომლებიც, თავის მხრივ, ერთმანეთთან ელექტრონაქცეპტორული სულფონის ჯგუფებით (-SO₂-) არიან დაკავშირებული. ამ ტიპის იონომერები, ხშირად მოხსენებულ ელექტრონდონორული ერთეულების შემცველ პოლი(არილენებთან) შედარებით, განსაკუთრებულ ინტერესს იმსახურებენ რამდენიმე უპირატესობის გამო:

ა. მაღალი ჟანგვითი და ჰიდროლიზური სტაბილურობა, რაც გამოწვეულია სულფომჟავა ჯგუფებთან ორთო-პოზიციაში მყოფი ელექტრონაქცეპტორული ჯგუფების (-SO₂-) არსებობით;

ბ. სულფომჟავა ჯგუფების მაღალი მჟავურობა, რაც გამოწვეულია არომატული ბირთვის ელექტრონდეფიციტურობით;

გ. მთავარი ჯაჭვის სიხისტე, რაც წყალში უხსნადი და მაღალი იონმიმოცვლითი ტევადობების მქონე იონომერების სინთეზის საშუალებას იძლევა.

დისერტაციის ფარგლებში განხორციელდა გრძელი არასულფირებული სეგმენტების შემცველი სულფირებული პოლი(ფენილენ სულფონების) თანაპოლიმერების

სინთეზი, რამაც მაღალი იონშემცველობის მქონე, წყალში უხსნადი სულფირებული პოლი(ფენილენ სულფონების) სინთეზის საშუალება მოგვცა და, გარდა ამისა, ამ ტიპის პოლიმერებს აღმოაჩნდათ დაბალი წყლის აღება. აღნიშნული თანაპოლიმერების მომზადების მიზნით, საწყის ეტაპზე განხორციელდა შესაბამისი გრძელჯაჭვიანი დიფთორ-მონომერების სინთეზი. ყველა დასინთეზებული მონომერისა და პოლიმერისათვის ჩატარდა მოლეკულური დახასიათება.

სინთეზირებული ახალი ტიპის იონომერებისა და სხვადასხვა პოლიბენზ-იმიდაზოლების მკვა-ფუძე პოლიმერული ნარევების საფუძველზე მომზადდა მემბრანები. სულფირებული პოლი(ფენილენ სულფონების) თანაპოლიმერების იონშემცველობის ზრდა იძლევა საშუალებას, რომ გაიზარდოს როგორც პოლიმერული ნარევებისგან დამზადებული მემბრანების იონშემცველობა, ასევე მათში პოლიბენზ-იმიდაზოლების შემცველობა, რასაც პროტონგამტარობისა და მექანიკური თვისებების გაზრდამდე მივყავართ. მომზადებული მემბრანებისათვის განხორციელდა წყლის აღების, იონშემცველობისა და გამორეცხვის გაზომვები.

დისერტაციის ფარგლებში განხორციელდა სტრუქტურასა და თვისებებს შორის კავშირის შესწავლა (მაგ.: წყლის აღება — ქიმიური სტრუქტურა, ქიმიური სტაბილურობა — ქიმიური სტრუქტურა, პროტონგამტარობა — ქიმიური სტრუქტურა, მონომერის სტრუქტურა — მოლეკულური მასა და ა.შ.).

საკვანძო სიტყვები: იონმიმოცვლითი მემბრანები, საფეხურებრივი ზრდის პოლიმერიზაცია, საწვავი ელემენტები, პოლი(ფენილენ სულფონები), წყლის ელექტროლიზერები

სამეცნიერო ხელმძღვანელი, გიორგი ტიტვინიძე  (ხელმოწერა)

Acknowledgements

I want to take this moment to express my profound gratitude to my scientific supervisor – Prof. Dr. Giorgi Titvinidze, for his unwavering support, guidance, motivation and engaging discussions in the realm of polymer science. Additionally, I appreciate him for generously sharing his wealth of experience and knowledge with me throughout our research journey. His understanding and advices proved to be invaluable and studying under the mentorship of Prof. Dr. Giorgi Titvinidze was a tremendous honor.

In addition, I would like to thank the Free University of Tbilisi, Agricultural University of Georgia and its rector – Prof. Vakhtang Lejava for outstanding kindness and unwavering support, including the opportunity to join the university's staff during my Ph.D. studies.

I would like to express my gratitude to a former member of our group, Zviad Katcharava, who taught me the synthesis of poly(phenylene sulfone)s and various other techniques during my undergraduate studies. The knowledge and skills I gained under his guidance played a significant role in the development of my doctoral dissertation.

I would also like to acknowledge the valuable assistance of our collaborators in Germany: Dr. Klaus-Dieter Kreuer from Max Plank Institute for Solid State Research and the junior research group “Electrochemical Energy Systems” from Hahn-Schickard Institute for the outstanding friendly attitude and the characterization of polymer membranes by various electrochemical methods.

I am especially grateful to the head of the synthesis laboratory Dr. Marco Viviani, who kindly hosted me during my 3-month visit to Freiburg and provided assistance in learning various new synthetic methods and further refining my synthesis skills.

In addition, I thank Andreas Münchinger, Annette Fuchs and Klaus-Dieter Kreuer for providing the proton conductivity measurements.

This research [PHDF-22-299] has been supported by Shota Rustaveli National Science Foundation of Georgia (SRNSFG) and German Federal Ministry of Education and Research, project “Fluorfreie-MEA” (Grant No. O3HY106A) and “Beyond-PFSA” (Grant No. O3SF0643C).

Table of Contents

სამეცნიერო მიმართულების კომისიის რეკომენდაცია	ii
Declaration of Authorship	iii
Abstract.....	iv
რეზიუმე.....	vi
Acknowledgements.....	viii
Table of Contents	ix
List of Tables	xiii
List of Figures.....	xv
List of Schemes	xix
List of Pictures	xxiv
List of Abbreviations	xxv
Introduction	1
1. Literature Review	11
1.1. Main candidates for proton-exchange membranes.....	11
1.1.1. Nafion and other perfluorinated copolymers.....	11
1.1.2. Poly(arylene ether sulfone)-based proton-exchange membranes.....	13
1.1.3. Polyimide-based proton-exchange membranes.....	25
1.1.4. Block copolymer-based proton-exchange membranes	29
1.1.5. Polybenzimidazoles.....	36
1.1.6. Poly(2,6-dimethyl-1,4-phenylene oxide) — PPO	38
1.1.7. Poly(arylene ether ketone)s.....	39
1.1.8. Poly(phenylene)s	46
2. Materials and Methods	58
2.1. Materials.....	58
2.2. Characterization of monomers and polymers	59
2.3. Synthesis of monomers with high sulfonation degree	61

2.3.1. Synthesis of SDFDPS	61
2.3.2. Synthesis of SBFPP0	62
2.3.3. Synthesis of DS-1,3-DFB.....	62
2.3.4. Synthesis of DS-1,4-DFB.....	62
2.3.5. Synthesis of DS-1,3-DCB.....	63
2.3.6. Synthesis of DS-1,4-DCB.....	63
2.4. Synthesis of poly(phenylene sulfone) based statistical copolymers with different linking groups via TBBT route	63
2.4.1. Synthesis of sPPS-435	63
2.4.2. Synthesis of sPPS-435-CO.....	64
2.4.3. Synthesis of sPPS-435-0	65
2.5. Synthesis of poly(phenylene sulfone) based statistical copolymers with different equivalent weights via Li ₂ S route	66
2.5.1. Synthesis of sPPS-240	66
2.5.2. Synthesis of sPPS-253.5.....	67
2.5.3. Synthesis of sPPS-260	68
2.5.4. Synthesis of sPPS-275	69
2.5.5. Synthesis of sPPS-280	70
2.5.6. Synthesis of sPPS-300	71
2.5.7. Synthesis of statistical sPPS-360	72
2.6. Experimental study of polymer leaching from polymer blends	73
2.6.1. Preparation of the blends of sPPS-240 and sPPS-260 with PBI-OO.....	73
2.6.2. Leaching experiments on sPPS-240 and sPPS-260 blends with PBI-OO	73
2.7. Synthesis of microblock copolymers containing an alkyl and perfluoroalkyl main chains	74

2.7.1. Synthesis of microblock monomers containing an alkyl and perfluoroalkyl main chains.....	74
2.7.2. Synthesis of poly(phenylene sulfone)s containing alkyl and perfluoroalkyl main chains.....	77
2.8. Synthesis of microblock copolymers containing phenylene moieties	82
2.8.1. Synthesis of microblock monomers containing phenylene moieties	82
2.8.2. Synthesis of poly(phenylene sulfone)s containing phenylene moieties	83
2.9. Synthesis of microblock copolymers containing merely sulfone units.....	89
2.9.1. Synthesis of microblock monomers containing sulfur and sulfone units.....	89
2.9.2. Synthesis of poly(phenylene sulfone)s with microblock segments containing merely sulfone units.....	90
2.10. Synthesis of microblock copolymers with different branching degree	92
2.10.1. Synthesis of the branching agent.....	92
2.10.2. Synthesis of branched poly(phenylene sulfone)s with microblock segments....	93
3. Results and Discussion.....	98
3.1. Synthesis of monomers with high sulfonation degree	98
3.1.1. Optimized synthesis of SDFDPS	98
3.1.2. Optimized synthesis of SBFPPO	103
3.1.3. Synthesis of DS-1,3-DFB and DS-1,4-DFB.....	106
3.1.4. Synthesis of DS-1,3-DCB and DS-1,4-DCB.....	112
3.1.5. An outlook of the practical application of highly sulfonated monomers	117
3.2. Evaluating the radical stability of sulfonated poly(phenylene sulfone)s with different heteroatoms in the main chain	118
3.3. Synthesis of poly(phenylene sulfone) based statistical copolymers with different equivalent weights via Li ₂ S route	121
3.3.1. Influence of Li ₂ S particle size on sPPSs molecular weights	125
3.3.2. Preparation of the blends of sPPSs with PBI-00	126

3.3.3. Water uptakes of sPPSs and their blends	128
3.3.4. Study of the kinetics on the sample of the unoxidized precursor of sPPS-260 ...	132
3.3.5. NMR spectra of sPPSs	134
3.3.6. Solubilities of statistical sPPSs with different equivalent weights	137
3.4. General introduction to the synthesis strategy of polymers with different non-sulfonated microblock segments	138
3.4.1. Synthesis of microblock copolymers containing an alkyl and perfluoroalkyl main chains	143
3.4.1.1. Synthesis of microblock monomers containing an alkyl and perfluoroalkyl main chains	143
3.4.1.2. Synthesis of poly(phenylene sulfone)s containing an alkyl and perfluorinated chains	149
3.4.2. Synthesis of microblock copolymers containing phenylene moieties.....	158
3.4.2.1. Synthesis of microblock monomers containing phenylene moieties	159
3.5.2.2. Synthesis of poly(phenylene sulfone)s containing phenylene moieties	162
3.4.3. Synthesis of microblock copolymers containing merely sulfone units.....	169
3.4.3.1. Synthesis of microblock monomers containing merely sulfur and sulfone units	169
3.4.3.2. Synthesis of poly(phenylene sulfone)s with microblock segments containing merely sulfone units.....	172
3.4.4. Synthesis of microblock copolymers with different branching degree	180
3.4.4.1. Synthesis of the branching agent.....	180
3.4.4.2. Synthesis of branched poly(phenylene sulfone)s with microblock segments.	183
4. Conclusions	187
References.....	190

List of Tables

Table 1. Glass transition temperatures of poly(arylene ether sulfone)s produced using DCDPS and diverse biphenols	15
Table 2. Thermal properties of some representatives of the PAEK family [106,]	40
Table 3. Solubilities of statistical sPPSs with different EW's in various common solvents	137
Table 4. Intrinsic viscosities of microblock copolymers containing alkyl and perfluorinated fragments	152
Table 5. Film forming abilities of microblock copolymers containing alkyl and perfluorinated fragments	153
Table 6. Solubilities of microblock copolymers containing alkyl and perfluorinated fragments in different solvents.....	153
Table 7. λ values of microblock copolymers containing alkyl and perfluorinated segments at 80 °C	155
Table 8. Intrinsic viscosities of microblock copolymers containing phenylene fragments	167
Table 9. Film forming abilities of microblock copolymers containing phenylene fragments	167
Table 10. Solubilities of microblock copolymers containing phenylene fragments in different solvents	167
Table 11. λ values of microblock copolymers containing phenylene fragments at 80 °C....	168
Table 12. Intrinsic viscosities of microblock copolymers containing merely sulfone units	176
Table 13. Film forming abilities of microblock copolymers containing merely sulfone units	176
Table 14. Solubilities of microblock copolymers containing merely sulfone units in different solvents	177
Table 15. λ values of microblock copolymers containing merely sulfone units at 80 °C	177

Table 16. Intrinsic viscosities of branched microblock copolymers containing merely sulfone units.....	185
Table 17. Film forming abilities of branched microblock copolymers containing merely sulfone units	185
Table 18. Solubilities of branched microblock copolymers containing merely sulfone units in different solvents.....	185
Table 19. λ values of microblock copolymers containing merely sulfone units at 80 °C.....	186

List of Figures

Figure 1. Proton-Exchange Membrane Fuel Cell (PEMFC) []	1
Figure 2. Proton-Exchange Membrane Electrolyzer (PEMWE) []	2
Figure 3. TGA analysis of sPPSs [14].....	5
Figure 4. Proton conductivities of sPPS-360, sPPS-220 and Nafion.....	7
Figure 5. Figure of the ion-network model of hydrated Nafion	30
Figure 6. Different types of block copolymers	31
Figure 7. ^1H NMR spectrum of SDFDPS in D_2O showing DMSO contamination	100
Figure 8. ^1H NMR spectrum of pure SDFDPS in D_2O	101
Figure 9. ^{19}F NMR spectrum of pure SDFDPS in D_2O	101
Figure 10. ^{13}C NMR spectrum of pure SDFDPS in D_2O	102
Figure 11. IR spectrum of SDFDPS.....	102
Figure 12. ^1H NMR spectrum of pure SBFPPO in D_2O	105
Figure 13. ^{19}F NMR spectrum of SBFPPO in D_2O showing the presence of traces impurities (ca. 2 % mol).....	105
Figure 14. ^{13}C NMR spectrum of SBFPPO in D_2O	105
Figure 15. IR spectrum of SBFPPO.....	106
Figure 16. ^1H NMR spectrum of crude mixture of 2,5-difluorobenzene-1,3-disulfonate and 2,5-difluorobenzene-1,4-disulfonate obtained after sulfonation in D_2O	108
Figure 17. ^1H NMR spectrum of DS-1,3-DFB in D_2O	108
Figure 18. ^{19}F NMR spectrum of DS-1,3-DFB in D_2O	109
Figure 19. ^{13}C NMR spectrum of DS-1,3-DFB in D_2O	109
Figure 20. ^1H NMR spectrum of DS-1,4-DFB in D_2O	110
Figure 21. ^{19}F NMR spectrum of DS-1,4-DFB in D_2O	110

Figure 22. ^{13}C NMR spectrum of DS-1,4-DFB in D_2O	111
Figure 23. IR spectrum of DS-1,3-DFB	111
Figure 24. IR spectrum of DS-1,4-DFB	112
Figure 25. ^1H NMR spectrum of 2,5-dichloro-1,4-benzenedisulfonic acid showing minor impurities of 4,6-dichloro-1,3-benzenedisulfonic acid in D_2O	114
Figure 26. ^{13}C NMR spectrum of 2,5-dichloro-1,4-benzenedisulfonic acid showing minor impurities of 4,6-dichloro-1,3-benzenedisulfonic acid in D_2O	114
Figure 27. ^1H NMR spectrum of pure DS-1,3-DCB.....	115
Figure 28. ^{13}C NMR spectrum of pure DS-1,3-DCB	115
Figure 29. IR spectrum of the mixture of 2,5-dichlorobenzene-1,4-disulfonate and 2,5-dichlorobenzene-1,3-disulfonate	116
Figure 30. IR spectrum of DS-1,3-DCB	116
Figure 31. Distribution of sulfonated and non-sulfonated segments for sPPS-400 and DS-sPPS-400	117
Figure 32. Scheme of Fenton's test mechanism	119
Figure 33. Graph of weight, intrinsic viscosity and ion-exchange capacity retention (in %) values for sPPS-435, sPPS-435-CO and sPPS-435-O	120
Figure 34. Dissolution of sPPS from membrane surface due to low polymer entanglement	122
Figure 35. Graph of sPPS molecular weight dependence on lithium sulfide powder particle size	125
Figure 36. Leaching experiment on sPPS-240 + PBI-00 blend	127
Figure 37. Leaching experiment on sPPS-260 + PBI-00 blend	128
Figure 38. Water uptake of sPPSs and blends.....	129
Figure 39. Blends water uptakes into saturated water vapor and liquid water	130

Figure 40. Reaction kinetics graph for the synthesis of unoxidized precursor of sPPS-260	133
Figure 41. ^1H NMR spectrum of sPPS-240 in $\text{DMSO-}d_6$	134
Figure 42. ^{13}C NMR spectrum of sPPS-240 in $\text{DMSO-}d_6$	135
Figure 43. ^1H NMR spectrum of sPPS-260 in $\text{DMSO-}d_6$	135
Figure 44. ^{13}C NMR spectrum of sPPS-260 in $\text{DMSO-}d_6$	136
Figure 45. ^1H NMR spectrum of sPPS-275 in $\text{DMSO-}d_6$	136
Figure 46. ^{13}C NMR spectrum of sPPS-275 in $\text{DMSO-}d_6$	137
Figure 47. ^1H NMR spectrum of FDPS-Hex-FDPS in CDCl_3	145
Figure 48. ^{19}F NMR spectrum of FDPS-Hex-FDPS in CDCl_3	145
Figure 49. ^1H NMR spectrum of FDPS-Dec-FDPS in CDCl_3	146
Figure 50. ^{19}F NMR spectrum of FDPS-Dec-FDPS in CDCl_3	146
Figure 51. ^1H NMR spectrum of FDPS- $\text{CF}_2(4)$ -FDPS in CDCl_3	147
Figure 52. ^{19}F NMR spectrum of FDPS- $\text{CF}_2(4)$ -FDPS in CDCl_3	147
Figure 53. ^1H NMR spectrum of 1,4-dibromooctafluorobutane (1,4-DBOFB) in CDCl_3	148
Figure 54. ^{19}F NMR spectrum of 1,4-dibromooctafluorobutane (1,4-DBOFB) in CDCl_3	149
Figure 55. GPC chromatogram of sPPS-410-Hex-XXL before e-beam irradiation.....	156
Figure 56. GPC chromatogram of sPPS-410-Hex-XXL after e-beam irradiation (165 kGy)	157
Figure 57. GPC chromatogram of sPPS-410-Hex-XXL after e-beam irradiation (198 kGy)	157
Figure 58. ^1H NMR spectrum of FDPS-BP-FDPS in $\text{DMSO-}d_6$	161
Figure 59. ^{19}F NMR spectrum of FDPS-BP-FDPS in $\text{DMSO-}d_6$	161
Figure 60. ^1H NMR spectrum of sPPS-410- <i>p</i> -TP-XXL in $\text{DMSO-}d_6$	164
Figure 61. ^{13}C NMR spectrum of sPPS-410- <i>p</i> -TP-XXL in $\text{DMSO-}d_6$	164
Figure 62. ^1H NMR spectrum of sPPS-430- <i>p</i> -TP-XXL in $\text{DMSO-}d_6$	165

Figure 63. ^{13}C NMR spectrum of sPPS-430- <i>p</i> -TP-XXL in $\text{DMSO-}d_6$	165
Figure 64. ^1H NMR spectrum of sPPS-450- <i>p</i> -TP-XXL in $\text{DMSO-}d_6$	166
Figure 65. ^{13}C NMR spectrum of sPPS-450- <i>p</i> -TP-XXL in $\text{DMSO-}d_6$	166
Figure 66. ^1H NMR spectrum of FDPS-S-FDPS in CDCl_3	170
Figure 67. ^{19}F NMR spectrum of FDPS-S-FDPS in CDCl_3	170
Figure 68. ^1H NMR spectrum of FDPS-TBB-FDPS in CDCl_3	171
Figure 69. ^{19}F NMR spectrum of FDPS-TBB-FDPS in CDCl_3	171
Figure 70. ^1H NMR spectrum of sPPS-390-XXL in $\text{DMSO-}d_6$	175
Figure 71. ^{13}C NMR spectrum of sPPS-390-XXL in $\text{DMSO-}d_6$	175
Figure 72. Graph of proton conductivities of sPPS-390-XXL, sPPS-390-XXL-PE and sPPS-410- <i>p</i> -TP-XXL.....	178
Figure 73. Graph of dependence of voltage and current density.....	179
Figure 74. Graph of dependence of voltage (1 A/cm^2) and time	180
Figure 75. ^1H NMR spectrum of 1,3,5-FPS-PB in CDCl_3	182
Figure 76. ^{19}F NMR spectrum of 1,3,5-FPS-PB in CDCl_3	182

List of Schemes

Scheme 1. Chemical Structure of Nafion	3
Scheme 2. Chemical structure of sPPS-360	4
Scheme 3. Chemical structures of sPSS-312 and sPSO ₂ -430	6
Scheme 4. General synthesis scheme of poly(phenylene sulfone) copolymers	8
Scheme 5. Chemical structures of PFSA's.....	11
Scheme 6. Commercial Poly(arylene ether sulfone)s	14
Scheme 7. Mechanism of the Friedel-Crafts sulfonylation reaction	17
Scheme 8. Polycondensation reactions of the AB (I) and AA-BB (II) types through Friedel-Crafts sulfonylation	17
Scheme 9. Scheme of the reaction proceeding through the nucleophilic aromatic substitution (S _N Ar) mechanism.....	18
Scheme 10. Scheme depicting the synthesis of poly(arylene ether sulfone) using Bisphenol A	19
Scheme 11. Representations of poly(arylene ether sulfone)s synthesis through ring-opening polymerization [56].....	20
Scheme 12. Scheme of post-sulfonation of poly(arylene ether sulfone) [58]	20
Scheme 13. Schematic representation of the metalation-sulfination-oxidation post-sulfonation process in poly(arylene ether sulfone)s [67]	21
Scheme 14. Products obtained by post-sulfonation and direct copolymerization	22
Scheme 15. Scheme illustrating the synthesis of 3,3'-disulfonated 4,4'-dichlorodiphenylsulfone (SDCDPS) [68].....	23
Scheme 16. Scheme of the optimized synthesis approach for SDCDPS	23
Scheme 17. Synthesis scheme of BPSH copolymer	24

Scheme 18. Different functional groups involved in the structure of poly(arylene ether sulfone)s.....	25
Scheme 19. General structure of polyimide.....	25
Scheme 20. Two different types of monomers necessary for the synthesis of sulfonated polyimides.....	27
Scheme 21. Comparison scheme of hydrolytic stabilities of polyimides synthesized from different types of monomers.....	28
Scheme 22. Chemical structures of polyimides containing bulky pendant groups.....	29
Scheme 23. Chemical structures of polyimides containing flexible ether and sulfonic acid groups.....	29
Scheme 24. Chemical structures of multiblock copolymers containing hydrophilic segments of disulfonated poly(arylene ether sulfone)s.....	32
Scheme 25. SPSF- <i>b</i> -PVDF block copolymer synthesis scheme [99].....	33
Scheme 26. Synthetic scheme of segmented sulfonated polyimides [76].....	35
Scheme 27. General structure of PBI.....	36
Scheme 28. Chemical structure of Celazole — poly 2,2'- <i>m</i> -(phenylene)-5,5'-bibenzimidazole [101].....	37
Scheme 29. Synthesis scheme of high molecular weight PBI using a flexible monomer.....	37
Scheme 30. Introduction of a compound containing a sulfonic acid group into the main chain of PBI through activation of the N-H bond [104].....	38
Scheme 31. Synthesis scheme of PPO [106].....	39
Scheme 32. PPO modified with bromine and sulfonic acid group.....	39
Scheme 33. Synthesis scheme of post-sulfonation of PEK [66].....	41
Scheme 34. A low-temperature synthesis approach proposed by Lee: I. Synthesis of the hydrophobic block and introduction of hexafluorobenzene, II. Synthesis of the hydrophilic block, III. Coupling reaction of hydrophilic and hydrophobic blocks [118].....	43

Scheme 35. Incorporation of a bulk group to reduce the semi-crystallinity of PAEK; I. Synthesis of hydrophilic blocks, II. Synthesis of hydrophobic blocks, III. Synthesis of block copolymers [119]	45
Scheme 36. Synthesis scheme of sulfonated poly(<i>p</i> -phenylene)s, according to the findings by M. Litt and collaborators	48
Scheme 37. Chemical structures of PPDSA, PBPDSA and BXPY	48
Scheme 38. Chemical structures of diblock copolymer SP1-P2	49
Scheme 39. Synthesis scheme of SPP-QP	50
Scheme 40. Chemical structure of sPP-BP	51
Scheme 41. Chemical structures of different types of side-chain sulfonated poly(phenylene)s	51
Scheme 42. Synthesis scheme of sPPP by post-sulfonation of PPP	53
Scheme 43. Synthesis scheme of sPPP-H ⁺	55
Scheme 44. Synthesis scheme of SDFDPS by conventional and optimized method.....	99
Scheme 45. Mechanism of the sulfonation reaction of DFDPS	103
Scheme 46. Synthesis scheme of SBFPPPO	104
Scheme 47. Synthesis scheme of DS-1,3-DFB and DS-1,4-DFB.....	107
Scheme 48. Synthesis scheme of DS-1,3-DCB and DS-1,4-DCB	113
Scheme 49. Synthesis scheme of sPPSs with different linking units in the main chain.....	118
Scheme 50. General synthesis scheme of water-insoluble, statistical sPPSs	124
Scheme 51. I step of the nucleophilic aromatic substitution reaction between SDFDPS and Li ₂ S	124
Scheme 52. II step of the nucleophilic aromatic substitution reaction between SDFDPS and Li ₂ S	125

Scheme 53. A general comparative scheme of sulfonated poly(phenylene sulfone)s with "regular" statistical and microblock segments.....	142
Scheme 54. Synthesis scheme of FDPS-Hex-FDPS, FDPS-Dec-FDPS and FDPS-CF ₂ (4)-FDPS	144
Scheme 55. General synthesis scheme of polymers containing alkyl (C6 and C10) microblock segments	150
Scheme 56. General synthesis scheme of polymers containing perfluorinated segments..	151
Scheme 57. I step of the nucleophilic aromatic substitution reaction between SDFDPS and TBBT.....	151
Scheme 58. II step of the nucleophilic aromatic substitution reaction between SDFDPS and TBBT.....	152
Scheme 59. Proposed mechanism of cross-linking for alkyl microblock containing sPPS by E-beam irradiation	156
Scheme 60. Synthesis scheme of FDPS-BP-FDPS and FDPS- <i>p</i> -TP-FDPS.....	159
Scheme 61. Mechanism of the Friedel-Crafts sulfonylation reaction on the example of the synthesis of FDPS-BP-FDPS	160
Scheme 62. General synthesis scheme of microblock copolymers containing biphenyl fragments	162
Scheme 63. General synthesis scheme of microblock copolymers containing <i>p</i> -terphenyl fragments	163
Scheme 64. Synthesis scheme of FDPS-S-FDPS and FDPS-TBB-FDPS.....	169
Scheme 65. General synthesis scheme of microblock copolymers containing merely sulfone units (using FDPS-S-FDPS as microblock monomer)	172
Scheme 66. General synthesis scheme of microblock copolymers containing merely sulfone units (using FDPS-TBB-FDPS as microblock monomer).....	173
Scheme 67. Synthesis scheme of the branching monomer (1,3,5-FPS-PB).....	181

Scheme 68. General synthesis scheme of branched microblock copolymers containing merely sulfone units.....184

List of Pictures

Picture 1. Film made from sPPS-410-Hex-XXL.....	154
Picture 2. Precipitate of the unoxidized precursor of sPPS-390-XXL in <i>i</i> -PrOH.....	174
Picture 3. Films of the unoxidized precursor of sPPS-390-XXL	174
Picture 4. Film of sPPS-390-XXL	176

List of Abbreviations

AFM	atomic force microscopy
BDA	4,4'-diamino-2,2'-biphenyldisulfonic acid
CCM	catalyst coated membrane
CHP	<i>N</i> -cyclohexylpyrrolidone
DCDPS	4,4'-dichlorodiphenyl sulfone
DFDPS	4,4'-difluorodiphenyl sulfone
DMAc	dimethylacetamide
DMF	dimethylformamide
DMFC	direct methanol fuel cell
DMSO	dimethyl sulfoxide
DPS	diphenyl sulfone
DS-1,3-DCB	disulfonated-1,3-dichlorobenzene
DS-1,3-DFB	disulfonated-1,3-difluorobenzene
DS-1,4-DCB	disulfonated-1,4-dichlorobenzene
DS-1,4-DFB	disulfonated-1,4-difluorobenzene
DSC	differential scanning calorimetry
EIS	electrochemical impedance spectroscopy
EW	equivalent weight
GPC	gel permeation chromatography
IEC	ion-exchange capacity
IPA	isophthalic acid

MEA	membrane electrode assembly
MS	mass spectroscopy
NDA	naphthalene-1,4,5,8-tetracarboxylic dianhydride
NEP	<i>N</i> -ethyl-2-pyrrolidone
NMP	<i>N</i> -methyl-2-pyrrolidone
NMR	nuclear magnetic resonance
OBBT	4,4'-oxybisbenzenethiol
ODA	oxydianiline
<i>o</i> -DCB	<i>o</i> -dichlorobenzene
PAEK	poly(arylene ether ketone)
PBI	polybenzimidazole
PDA	perylene-3,4,9,10-tetracarboxylic dianhydride
PEEK	poly(ether ether ketone)
PEEKK	poly(ether ether ketone ketone)
PEK	poly(ether ketone)
PEKK	poly(ether ketone ketone)
PEM	proton-exchange membrane
PEMEL	proton-exchange membrane electrolyzer
PEMFC	polymer electrolyte membrane/proton-exchange membrane fuel cell
PES	poly(ether sulfone)
PFSA	perfluorosulfonic acid
PMMA	poly(methyl methacrylate)

PPO	poly(2,6-dimethyl-1,4-phenylene oxide)
PPP	phenylated polyphenylene
PPSNa	poly(sodium styrenesulfonate) macromonomer
PS	polystyrene
PSEPVE	perfluoro(4-methyl-3,6-dioxaoct-7-ene)sulfonyl fluoride
PSU	polysulfone
PVDF	polyvinylidene fluoride
RH	relative humidity
SAXS	small-angle X-ray scattering
SBFPPO	sulfonated bis(4-fluorophenyl)phenyl phosphine oxide
SDAPP	sulfonated Diels-Alder polyphenylene
SDCDPS	3,3'-disulfonated 4,4'-dichlorodiphenylsulfone
SDFDPS	disodium 3,3'-disulfonate-4,4'-difluorodiphenylsulfone
SPEEK	sulfonated poly(ether ether ketone)
sPEEK	sulfonated poly(ether ether ketone)
SPI	sulfonated copolyimide
sPPP	sulfonated phenylated polyphenylene
sPPS	sulfonated poly(phenylene sulfone)
sPPSS	sulfonated poly(phenylene sulfide sulfone)
TBA	tetraaminobiphenyl
TBBT	4,4'-thiobisbenzenethiol
TEM	transmission electron microscopy

TFE	tetrafluoroethylene
TGA	thermogravimetric analysis
UV-Vis	ultraviolet-visible spectroscopy
WAXD	wide-angle X-ray diffraction
WU	water uptake
dL	deciliter (100 mL)
meq	milliequivalent
M_n	number average molecular weight
M_w	weight average molecular weight
T_g	glass transition temperature
η	efficiency
λ	number of water molecules per sulfonic acid group of ionomer
η_{inh}	inherent viscosity
η_{int}	intrinsic viscosity
η_{rel}	relative viscosity
η_{sp}	specific viscosity

Introduction

With increasing global energy consumption and consequent greenhouse gas emissions, there is an increasing demand for renewable energy technologies in response to climate change (the development of green technologies has been accelerated by the United Nations 2015 Paris Agreement to combat climate change) [1, 2]. Among them, proton exchange membrane fuel cells (PEMFCs) are one of the most promising electrochemical energy conversion devices due to their high efficiency and zero-pollution emission for transportation and portable applications [3, 4].

PEMFC converts the chemical energy of the reactants directly into electricity with byproducts of water and heat. The key component of the device is the proton exchange membrane (PEM), which serves as the electrolyte to transport the protons from anode to cathode and separates the fuel and oxidant [3]. When the hydrogen is used as the fuel, the charge carrier is hydrogen ion (proton). At the anode, the hydrogen molecule is divided into protons and electrons ($\text{H}_2 \rightarrow 2\text{H}^+ + 2\text{e}^-$). Hydrogen ions pass through the electrolyte to the cathode, and the electrons move in the outer circle and produce electrical energy. Oxygen, which is taken from the air, is fed to the cathode and interacts with electrons and protons to form water ($\frac{1}{2}\text{O}_2 + 2\text{H}^+ + 2\text{e}^- \rightarrow \text{H}_2\text{O}$).

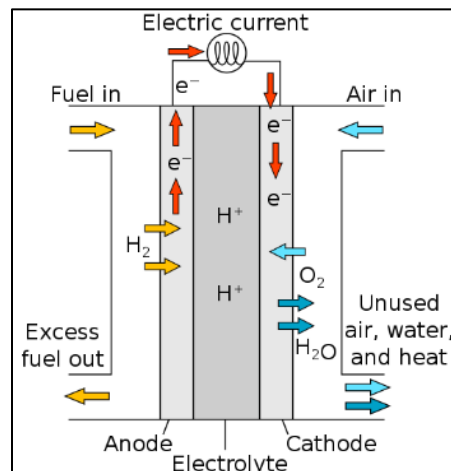


Figure 1. Proton-Exchange Membrane Fuel Cell (PEMFC) [5]

In addition to their application in PEMFCs, PEMs play a pivotal role in proton-exchange membrane water electrolyzers (PEMWEs). In these systems, electrical energy is utilized to drive the electrolysis of water, generating hydrogen and oxygen gas. The principle of operation mirrors that of PEMFCs: PEM is facilitating the transport of protons (H^+) from the anode to the cathode while preventing the mixing of hydrogen and oxygen gases. At the anode, water molecules undergo oxidation to produce protons, electrons, and oxygen ions according to the reaction: $H_2O(l) \rightarrow 1/2O_2(g) + 2H^+(aq) + 2e^-$. Meanwhile, at the cathode, protons and electrons combine to form hydrogen gas in the reduction reaction: $2H^+(aq) + 2e^- \rightarrow H_2(g)$. Overall, the PEMWE enables the conversion of electrical energy into chemical energy stored in the form of hydrogen gas, offering a promising avenue for sustainable energy storage and conversion.

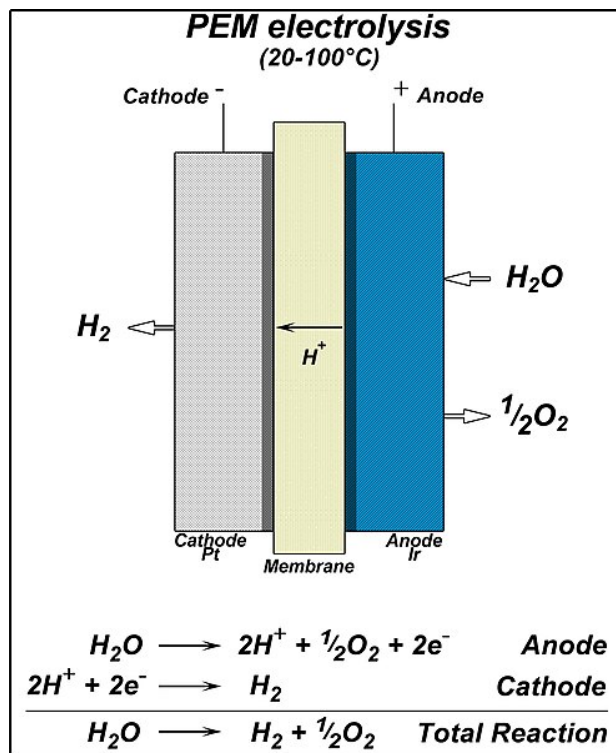
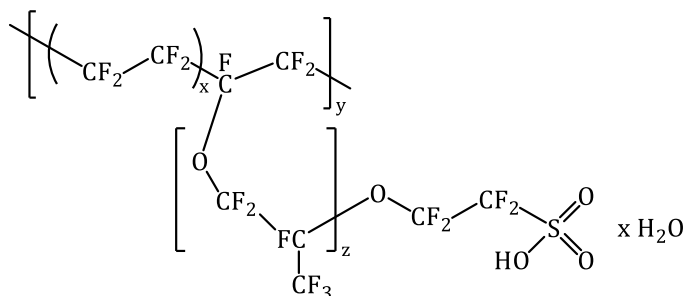


Figure 2. Proton-Exchange Membrane Electrolyzer (PEMWE) [6]

An ideal PEM should possess the combined properties of high proton conductivity, good mechanical, thermal and chemical stability, low swelling and gas permeability, and low cost [4, 7]. Currently, perfluorosulfonic acid (PFSA) ionomers, such as Nafion (Scheme 1) are

used as a commercial benchmark membrane due to their balanced properties, including high proton conductivity and mechanical stability. However, PFSA suffer from several drawbacks, such as loss of mechanical strength at elevated temperature [8], non-negligible hydrogen permeability [9], high electro-osmotic water drag [10], complicated synthesis and consequently high production cost [11], questionable environmental compatibility [12] and insufficient stability under OCV conditions [13].



Scheme 1. Chemical Structure of Nafion

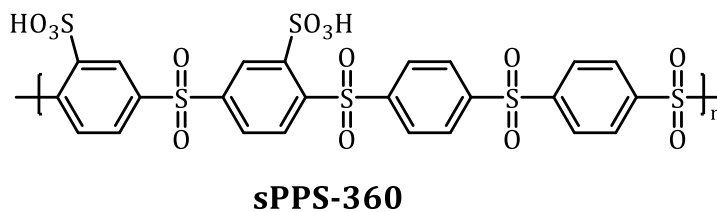
These drawbacks triggered the quest for alternative membrane materials and among them, sulfonated hydrocarbon-based polymers are considered as most promising candidates to substitute PFSA ionomers due to their relatively low cost, low fuel permeability, high mechanical and thermal stability. Extensive efforts have been made to develop sulfonated hydrocarbon-based polymers and a great number of polymer materials have been prepared. Among these materials sulfonated poly(phenylene sulfone)s (sPPS) with a backbone consisting of merely phenyl rings connected with electron-accepting sulfone units (-SO₂-) deserve special interest due to the several advantages over frequently reported sulfonated poly(arylene)s containing electron-donating units in the main chain:

- a. higher oxidative and hydrolytic stability caused by the presence of electron-withdrawing groups (-SO₂-) in the *ortho*-position to the sulfonic acid groups (Figure 3) [14]. Latter is an extremely important requirement for membrane application because of the harsh conditions in operating fuel cells (high temperatures, high water activities, formation of radicals);
- b. higher acidity of sulfonic acid groups caused by electron-deficiency of the aromatic rings;

- c. rigidity of backbone allowing preparation of water-insoluble ionomers with high ion-exchange capacity.

In 2007, the research group in the Max Planck Institute for Solid State Research, under the supervision of Dr. Klaus-Dieter Kreuer, started the study of poly(phenylene sulfone)s. Their work focused on synthesizing polymers with varying ion-exchange capacities and examining their properties. The findings revealed that both molecular weight and ion-exchange capacity significantly affect the membrane's film-forming ability. Specifically, an increase in ion-exchange capacity leads to greater swelling, which can render the membrane water-soluble. Conversely, a higher molecular weight reduces swelling, thereby enhancing the mechanical properties and improving the membrane's film-forming ability [14].

Among the sulfonated poly(phenylene sulfone)s (sPPSs) synthesized to date, sPPS-360 occupies a unique position. It is water-insoluble polymer with highest IEC, which is reported in the literature, exhibiting exceptional film-forming ability and an IEC surpassing that of Nafion. However, as noted in the literature [14], the relatively low molecular weight of sPPS-360 results in insufficient mechanical strength, which led to significant swelling ($\lambda \approx 37$) and decomposition at 80 °C. Additionally, the low molecular weight contributes to its reduced Young's modulus. The chemical structure of sPPS-360 is illustrated on Scheme 2.



Scheme 2. Chemical structure of sPPS-360

Thermogravimetric analysis (TGA) was conducted to evaluate the stability of sulfonated polymers under high humidity and elevated temperature conditions, which are critical for assessing their practical performance in real-world applications. By performing TGA in a controlled water atmosphere with a water vapor pressure of $p(\text{H}_2\text{O}) = 10^5$ Pa, high humidity environments were simulated to better understand how these polymers behave when exposed to conditions that mimic their operational use. The measurement, conducted

between 110 and 180 °C, allowed to observe reversible weight changes during heating and cooling cycles, providing insights into the polymers' hydrolytic stability and their ability to maintain structural integrity under thermal and water stress. This analysis was essential for distinguishing the performance of different sulfonated polymers, such as sPSO₂-430 and sPSS-312, by revealing their susceptibility to water uptake and associated stability issues.

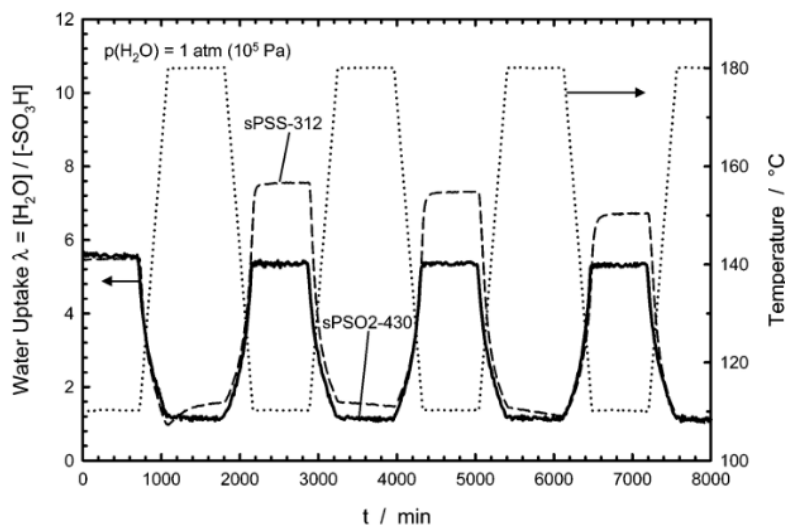
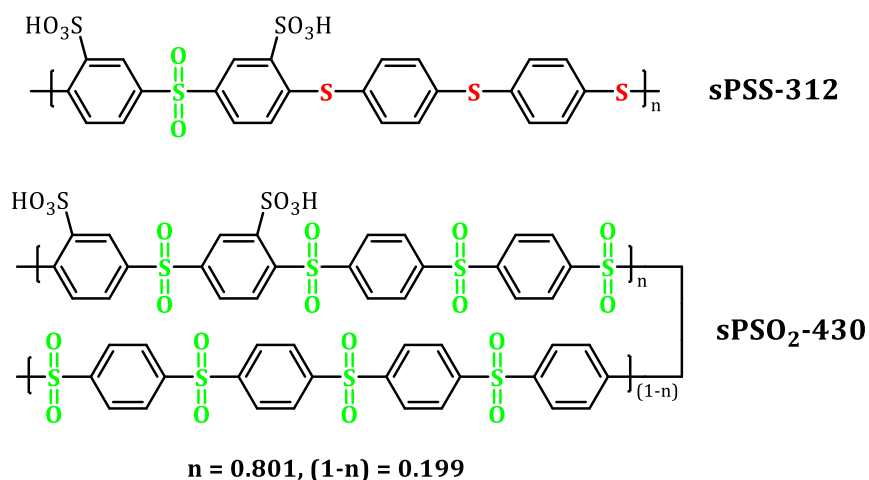


Figure 3. TGA analysis of sPSSs [14]

1. **TGA Behavior of Sulfonated Poly(Phenylene Sulfone) (sPSO₂-430):** The TGA graph shows that sPSO₂-430 maintains a constant weight throughout the temperature range and under high water vapor conditions. This stability indicates that sPSO₂-430 is not significantly affected by the high temperature and water activity, showing good hydrolytic stability;
2. **TGA Behavior of Sulfonated Poly(Phenylene Sulfide Sulfone) (sPSS-312):** sPSS-312 shows an ascending weight baseline during the first cycle in contrast to sPSO₂-430. This suggests that these polymers absorb more water and are affected by the possible formation of sulfuric acid, which increases their hygroscopicity and impacts stability.



Scheme 3. Chemical structures of sPSS-312 and sPSO₂-430

Thus, the stability of sulfonated poly(phenylene sulfone) in high temperature and high water activity conditions is highlighted by its consistent weight in the TGA graph, while sulfide-containing polymer showed instability due to increased water uptake.

sPPSs are obtained via a two-step process:

- a. step-growth polymerization;
- b. subsequent oxidation of poly(phenylene sulfide sulfone) to poly(phenylene sulfone).

Synthesis of sPPS were reported either by polymerization of sulfonated dihalidediphenyl sulfones with (1) organic dithiols [14] or with (2) metal sulfides [15].

Approach (1) enables the synthesis of water-insoluble sPPS copolymer with the IEC = 2.78 meq/g (sPPS-360) [14, 16].

Approach (2) was used to obtain sPPS homopolymer with IEC = 4.5 meq/g (sPPS-220) [15, 17].

Together with high oxidative and hydrolytic stability both sPPS-360 and sPPS-220 reveal high proton conduction (Figure 4).

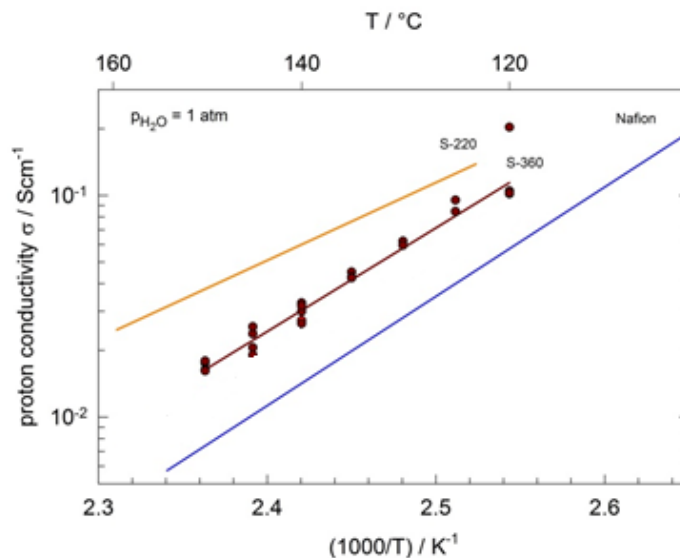


Figure 4. Proton conductivities of sPPS-360, sPPS-220 and Nafion

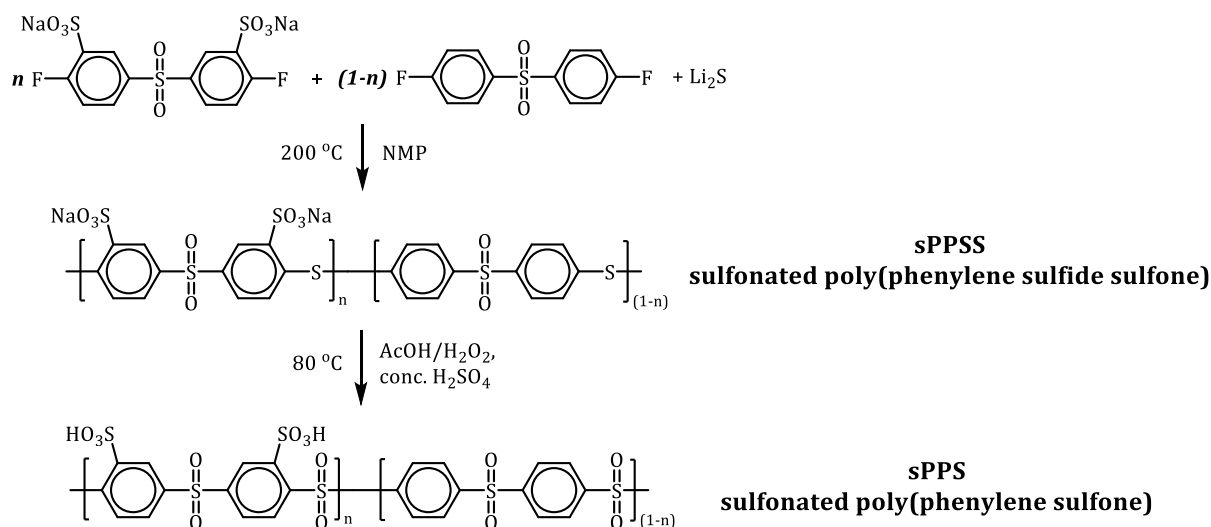
However, both ionomers suffer from significant drawbacks, sPPS-220 films are brittle and water-soluble and thus can't be used in a pure form, while sPPS-360 is characterized by excessive swelling under high humidity conditions and brittleness at very low RHs. Thus, their application in pure form remains questionable.

At the first stage the mechanical reinforcement of sPPS was done by the synthesis of multiblock copolymers, where the unique transport and stability properties of sPPS could be retained while the introduction of a well phase-separating hydrophobic block led to improved viscoelastic properties [18]. Water uptake (WU) in these block copolymers was successfully reduced, however, the brittleness issue in dry state was not fully resolved. In addition, the complex synthetic pathway used in preparation of block copolymers hindered the further development of this approach.

At the second stage, an acid-base blending strategy was applied to improve the viscoelastic properties and suppress the swelling. As a base polymer polybenzimidazole – PBI-O and PBI-OO were selected. Acid-base blend membranes exhibited significant improvement in viscoelastic properties [19]. However, polybenzimidazole blend composition has limitations, as acid-base interaction consumes protons lowering IEC, also here must be mentioned that IEC of blends is decreased by the volumetric addition of a non-conductive component as well (“dilution” of sulfonated ionomer). Coming from this, sPPS-

220 with IEC = 4.5 meq/g was found suitable for this approach. The sPPS-220/PBI-O blend with 75/25 ratio showed proton conductivity matching this of Nafion and also showed similar performance in a hydrogen-air fuel cell. Under accelerated stress conditions (OCV-hold on in hydrogen-air) sPPS-220/PBI-O blend showed higher durability than pure Nafion at low relative humidity (RH = 30 %).

In spite of very promising results, sPPS-220/PBI-O blend suffers from the drawback, as water-soluble sPPS-220 can be washed out during the conditioning step (sPPS-220 blends are prepared from neutral ionomers and only after that are conditioned with acid solution), or by condensed water. This led us to develop water-insoluble sPPSs with high IECs by copolymerization of sulfonated difluorodiphenyl sulfone, difluorodiphenyl sulfone and lithium sulfide (Scheme 4) [20]. We have found that sPPS-240 with IEC = 4.1 mequiv/g is already water insoluble at RT and such a high IEC allows to set blend ratio, where PBI-O content is sufficient to keep high mechanical stability of the membrane. With an increase of Equivalent Weight (EW) (e.g. sPPS-260), solubility in water decreases also at elevated temperatures, but the decrease of IEC at the same time leads to the decrease of PBI-O content, which is reflected in the worsening of mechanical properties. In addition, excessive swelling still remains an issue and needs to be lowered.



Scheme 4. General synthesis scheme of poly(phenylene sulfone) copolymers

In the presented doctoral work, we have developed novel high-molecular-weight sPPS copolymers having long unsulfonated segments, which allowed to prepare water insoluble sPPSs with higher IECs and in addition, such type of polymers revealed lower water uptake. For this purpose, we have followed two different strategies:

1. Synthesis of different unsulfonated long-chain difluoro-monomers, which were used further in polymerization leading to sPPS having defined unsulfonated microblock segments, which in turn decreased WU due to the strong interaction between hydrophobic microblocks;
2. Synthesis of new sulfonated monomers, where the sulfonation degree was higher compared to the sulfonated difluorodiphenyl sulfone. Such monomers allow to increase the molar content of unsulfonated difluorodiphenyl sulfone in polymerization and thus increase the length of statistical hydrophobic segments, which is likely to lead to the decrease of WU.

On the basis of sPPS copolymers synthesized via Li_2S route (sPPS-240, sPPS-260), PBI-OO blend membranes were prepared and studied. sPPS copolymers with lower WU and higher IEC allowed to increase as IEC of the blend membranes, as well as the content of polybenzimidazoles in them, which leads as to the increased proton conductivity, as well as to the increased mechanical properties.

At the same time, the lithium sulfide powder particle size effect on the polymerization process was studied in terms of polymerization optimization.

This thesis comprises the following chapters:

- Introduction, which briefly addresses the research problem, outlines the relevance of the research, discusses scientific novelty and presents the purpose and main objectives of the thesis;
- Literature Review, wherein detailed descriptions of published works, existing problems and contemporary challenges related to alternative membrane materials are provided. The publications discussed belong to leading scientists who have made significant contributions to the study of these scientific issues;

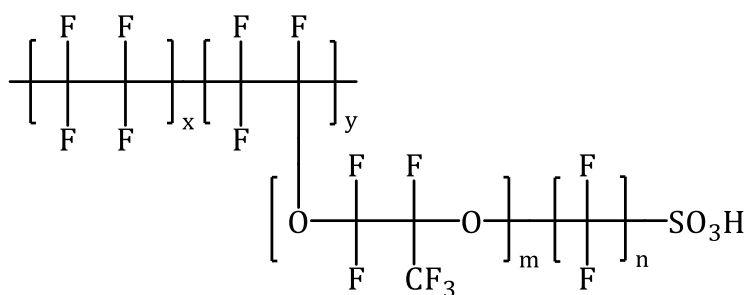
- Materials and Methods, where the materials utilized in the research are presented and the methodology for synthesizing monomers and polymers, characterizing them, and preparing and characterizing membranes is described;
- Results and Discussion, presenting the data obtained from the research and providing an interpretation of the results;
- Conclusions, where the findings of the dissertation work are summarized and the main conclusions are clearly formulated.

1. Literature Review

1.1. Main candidates for proton-exchange membranes

1.1.1. Nafion and other perfluorinated copolymers

Nafion, which is a product of DuPont, meets a number of requirements for ensuring good performance of fuel cells and is currently the reference polyelectrolyte membrane. It is a copolymer of tetrafluoroethylene (TFE) and perfluoro(4-methyl-3,6-dioxaoct-7-ene)sulfonyl fluoride (PSEPVE). Its chemical structure is shown on Scheme 5. Nafion is prepared by free radical copolymerization of TFE and PSEPVE monomers, resulting in a perfluorinated copolymer.



Nafion: $m = 1, n = 2$

Flemion: $m = 0, 1; n = 1-5$

Aciplex: $m = 0, 3; n = 2-5$

Dow membrane: $m = 0$

Scheme 5. Chemical structures of PFSA's

Conventional methods such as light scattering and gel permeation chromatography (GPC) cannot be used to determine the molecular weight of this polymer, since this latter does not form true solutions. To obtain the dispersion of Nafion, the polymer is heated in an autoclave under pressure in a mixture of water and alcohol at 240 °C. Nafion dispersions are used to coat the structure of the electrode in the preparation of the Membrane Electrode Assembly (MEA) and are also very important for the manufacture of the catalyst ink.

Nafion in both reducing and oxidizing atmospheres has good chemical and thermal stability, since its chemical structure contains a Teflon molecular backbone. Extruded Nafion membranes contain semi-crystalline domains that are responsible for good mechanical strength and the sulfonic acid groups in the structure of Nafion make this latter proton-conducting.

The concentration of ionic groups in Nafion can be controlled by changing the ratios of TFE and PSEPVE monomers. Currently, Nafion, which has an Equivalent Weight (EW) = 1100 is widely used and studied. These include Nafion 112, 115, 117 and 1110 (the first two digits indicate the equivalent weight and the last digit indicates the thickness in mil, which is equal to 25.4 μm). Nafion is also available in equivalent weights of 900 and 1200 $\text{g} \cdot \text{mol}^{-1}$. Nafion (EW = 1100) under hydrated conditions has a high proton conductivity. With a decrease in equivalent weight (EW < 900), polymers become soluble in many polar solvents [21].

Water uptake is one of the most important parameters for a polyelectrolyte material, as it affects as proton conductivity, as well as the mechanical properties of the membrane [22]. Nafion absorbs water from both liquid water and saturated steam. When the relative humidity (RH) is 100 %, the Nafion (EW = 1100) absorbs ~ 14 water molecules per acid group [23], while ~ 22 water molecules per sulfonate group are taken from liquid water [24].

The most important parameter of a polyelectrolyte material is proton conductivity. The proton conductivity depends on the IEC, polymer structure and morphology and also on the water content in the membrane, as the latter affects the mobility of protons. Additionally, the proton conductivity of Nafion is affected by temperature and concentration of ion-conducting sites, etc.

Other companies [25] have developed some perfluorosulfonic acid copolymers with structures similar to Nafion:

- Dow Chemical has developed a material with an equivalent weight of 800 $\text{g} \cdot \text{mol}^{-1}$ that has a shorter side chain than Nafion;

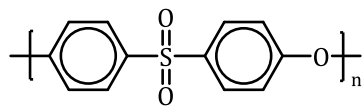
- AGC Inc. has developed membranes with an equivalent weight of $1000 \text{ g} \cdot \text{mol}^{-1}$, the name of which is Flemion;
- Asahi Kasei Corporation has developed polymers with an equivalent weight of 1000-1200 $\text{g} \cdot \text{mol}^{-1}$, the name of which is Aciplex;
- Solvay Solexis has developed polymers [26, 27] with an equivalent weight of 700-900 $\text{g} \cdot \text{mol}^{-1}$, the name of which is Hyflon and Aquivion (EW = 800-1100 $\text{g} \cdot \text{mol}^{-1}$).

However, PFSA materials have crucial disadvantages such as low operation temperature (this is due to the low glass transition temperature: $T_g \approx 90 \text{ }^\circ\text{C}$) which leads to the poisoning of the catalyst, environmental incompatibility, high gas permeability, high fuel crossover (especially in DMFCs [28, 29]), high cost [30], high electroosmotic drag of water [31, 32] from the anode to the cathode and deterioration of mechanical properties at high temperature and low humidity.

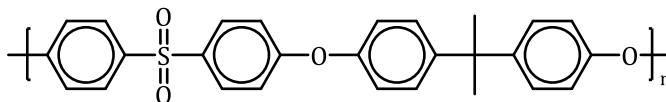
1.1.2. Poly(arylene ether sulfone)-based proton-exchange membranes

1.1.2.1. Overview of Poly(arylene ether sulfone)s

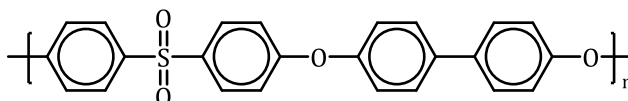
Over the past 40 years, certain chemical companies have conducted research on high-performance thermoplastics known as poly(arylene ether sulfone)s. These polymers exhibit distinctive properties, including a high glass transition temperature (T_g), excellent mechanical strength and thermal and oxidative stability. Consequently, they have been applied in various market sectors [33-36]. Scheme 6 below illustrates some commercial poly(arylene ether sulfone)s.



PES



PSU



PPSU

Scheme 6. Commercial Poly(arylene ether sulfone)s

The high thermal and oxidative stability of poly(arylene ether sulfone)s enables their processing in the molten state [37]. These polymers can be formed from melts at high temperatures (400 °C) [38] because the sulfur atom in the main chain of the polymer is fully oxidized and formed sulfone groups exhibit an enhanced resonance structure. Additionally, the high oxidative stability allows for the long-term use of these materials at elevated temperatures (150-190 °C).

Strong dipole-dipole interactions between neighboring chains of poly(arylene ether sulfone)s result from the interactions between rigid phenyl rings and sulfone groups [39, 40]. However, flexible ether linkages reduce interchain interactions due to increased conformational freedom. These factors collectively influence the glass transition temperatures of poly(arylene ether sulfone)s, which typically vary in the range of 180-250 °C. The glass transition temperatures of specific poly(arylene ether sulfone)s synthesized using 4,4'-dichlorodiphenylsulfone (DCDPS) and various biphenols are provided in Table 1 below [33].

Table 1. Glass transition temperatures of poly(arylene ether sulfone)s produced using DCDPS and diverse biphenols

Bisphenol	Chemical Structure	T _g (°C)
4,4'-dihydroxydiphenyl oxide		170
4,4'-dihydroxydiphenyl sulfide		175
4,4'-dihydroxydiphenyl methane		180
2,2'-bis(hydroxyphenyl)propane		185
Hydroquinone		200
4,4'-dihydroxydiphenyl phenone		205
2,2'-bis(hydroxyphenyl)perfluoropropane		205
4,4'-dihydroxydiphenyl sulfone		220
4,4'-dihydroxydiphenyl sulfone		220
1,4-bis(4-hydroxyphenyl)benzene		250
4,4'-bis(4''-hydroxybenzenesulfonyl)diphenyl		265

Additionally, poly(arylene ether sulfone)s exhibit relatively higher hydrolytic stability in comparison to other engineering plastics like polyetherimides, polycarbonates, and

polyesters [41]. Moreover, poly(arylene ether sulfone)s demonstrate stability to non-oxidizing acids, alkalis and salts [42].

Due to the aforementioned advantages, poly(arylene ether sulfone)s have found widespread applications [43-46].

1.1.2.2. Synthesis of poly(arylene ether sulfone)s

Poly(arylene ether sulfone)s can be synthesized using four distinct methods:

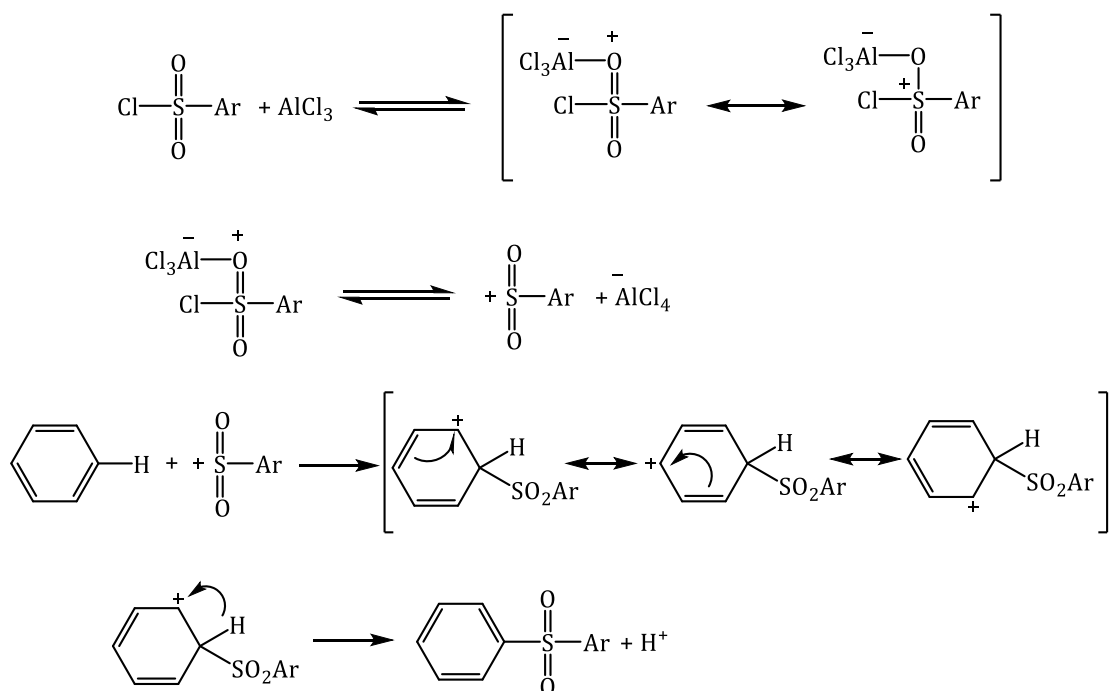
1. Step-growth polymerization involving electrophilic substitution of aromatic compounds;
2. Step-growth polymerization through a nucleophilic aromatic substitution mechanism, employing fluoro-, chloro-, and nitroaromatic compounds with an activating sulfone group in the para-position;
3. Modification of precursor polymers;
4. Ring-opening polymerization with the involvement of oligo(ether sulfone)s.

Each synthesis route will be discussed in detail below.

1.1.2.2.1. Electrophilic aromatic substitution pathway

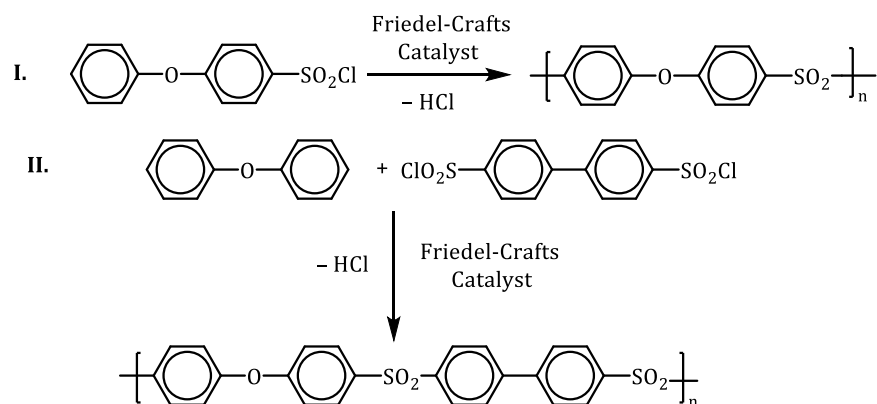
Historically, the oldest method employed for the synthesis of poly(arylene ether sulfone)s involves polycondensation with electrophilic substitution of the phenyl ether group by aromatic sulfonyl chloride [47]. This process is known as Friedel-Crafts sulfonylation, utilizing robust Lewis acids such as BF_3 , AlCl_3 and FeCl_3 as catalysts [33].

The reaction mechanism unfolds as depicted in Scheme 7: initially, the formation of an attacking reagent, arylsulfonylium cation, takes place through the interaction of sulfonyl chloride and a Lewis acid. Subsequently, the arylsulfonylium cation attacks the aromatic nucleus, leading to the formation of an intermediate. Upon deprotonation of this intermediate, the final product is obtained.



Scheme 7. Mechanism of the Friedel-Crafts sulfonylation reaction

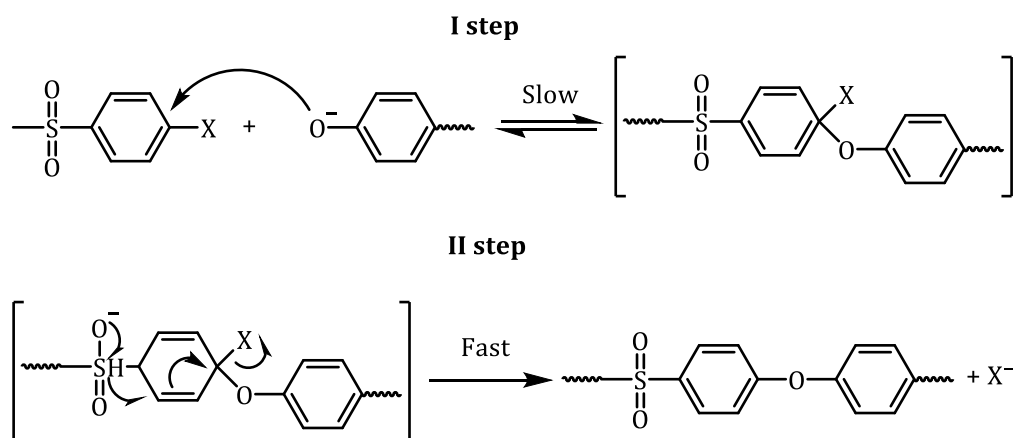
Via Friedel-Crafts sulfonylation, polymers can be synthesized through the self-condensation of AB-type monomers, where such monomers possess both functional groups within a single molecule. Additionally, the interaction of electrophilic and nucleophilic monomers allows for the condensation of AA and BB monomers [48-50]. Scheme 8 illustrates an example of each reaction type.



Scheme 8. Polycondensation reactions of the AB (I) and AA-BB (II) types through Friedel-Crafts sulfonylation

1.1.2.2.2. Nucleophilic aromatic substitution pathway

The most widely used method for synthesizing poly(arylene ether sulfone)s involves the nucleophilic aromatic substitution (S_NAr) reaction. This reaction is based on the interaction between aromatic dichloro-/difluorosulfones and bisphenols in the presence of an aqueous sodium alkali solution or dry K_2CO_3 . The latter is present either in equimolar amounts or in slight excess and the reaction occurs in polar aprotic solvents such as dimethylsulfoxide (DMSO), dimethylacetamide (DMAc) and *N*-Methylpyrrolidone (NMP) [35, 36, 41]. The general scheme of the reaction, occurring through the mechanism of nucleophilic aromatic substitution (S_NAr) is illustrated on Scheme 9 [51].

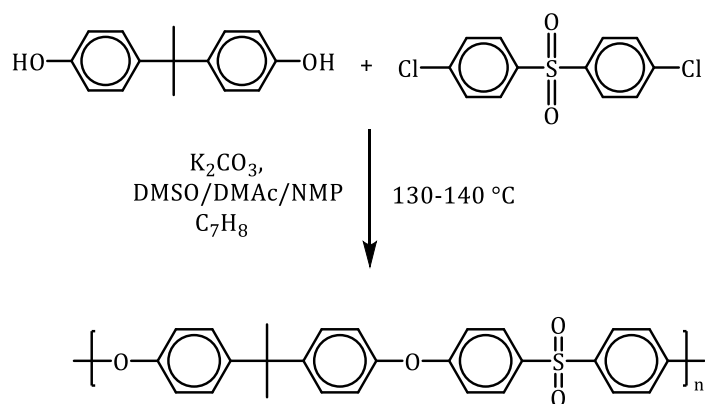


Scheme 9. Scheme of the reaction proceeding through the nucleophilic aromatic substitution (S_NAr) mechanism

In reactions of this nature, the reaction rate is depended on the basicity of bisphenol, the reaction area and the electron-acceptor capabilities of the activating group in the dihalide. The reaction rate achieves satisfaction only when dipolar aprotic solvents are selected [52, 53]. Solvents of this category stabilize the Meisenheimer intermediate and concurrently elevate the active concentration of the attacking nucleophile.

To expedite the reaction, the initial halogen groups should be positioned in the ortho- or para-position to the electron-withdrawing activating groups, as the latter strongly stabilize the Meisenheimer complex. Furthermore, the type of dihalide (containing fluorine or chlorine) significantly influences the reaction rate. Experimental evidence indicates that

difluorides exhibit much higher reactivity than dichlorides, although their relatively elevated cost somewhat restricts their commercial usage [54]. Scheme 10 illustrates a typical polycondensation reaction for the synthesis of bisphenol A-based polysulfone [36].

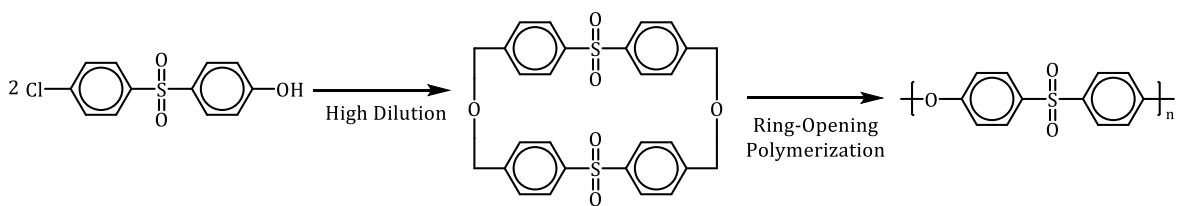


Scheme 10. Scheme depicting the synthesis of poly(arylene ether sulfone) using Bisphenol A

1.1.2.2.3. Synthesis of poly(arylene ether sulfone)s via ring-opening polymerization

Brunelle et al. employed the ring-opening polymerization method in the synthesis of polycarbonates, leading to an increased interest in this synthetic approach. A few years ago, a novel method for synthesizing poly(arylene ether sulfone)s based on the ring-opening polymerization of cyclic oligo(ether sulfone)s was developed [55-57]. The primary drawback of this approach lies in the limited availability of cyclic macromonomers required for synthesis, as only a few representatives of such monomers essential for poly(arylene ether sulfone)s synthesis are commercially accessible.

It's worth noting that this reaction does not yield side products. Furthermore, polymerization can be conducted in bulk, given that the low viscosity of the cyclic oligomer enables it to function as a reactive solvent simultaneously. By employing monomers with high cyclic tension, it becomes possible to produce polymers with substantial molecular weights ($M_n > 100$ kDa). Additionally, the synthesis of block copolymers is achievable through subsequent copolymerization with cyclic monomers. The synthesis of poly(arylene ether sulfone)s by ring-opening polymerization is depicted on Scheme 11.

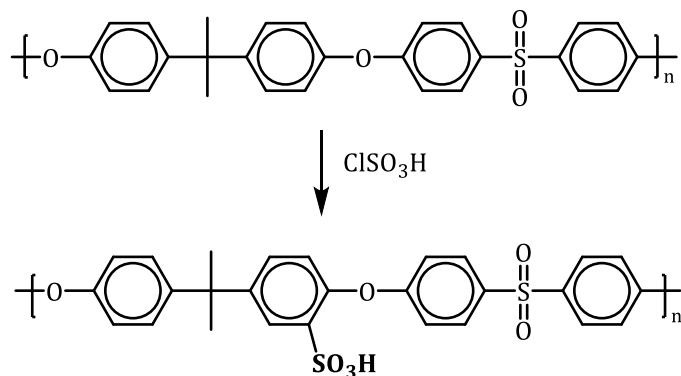


Scheme 11. Representations of poly(arylene ether sulfone)s synthesis through ring-opening polymerization [56]

1.1.2.3. Post-sulfonation of poly(arylene ether sulfone)s

Quentin et al. first conducted the post-sulfonation of bisphenol A-based poly(arylene ether sulfone)s using chlorosulfonic acid, a process proceeding through an electrophilic aromatic substitution mechanism. The simplicity of the post-sulfonation process stems from the ease of obtaining sulfonated polymers using readily available polymers and sulfonation agents such as sulfuric acid, chlorosulfonic acid, acetyl sulfate, oleum, etc. [58-62].

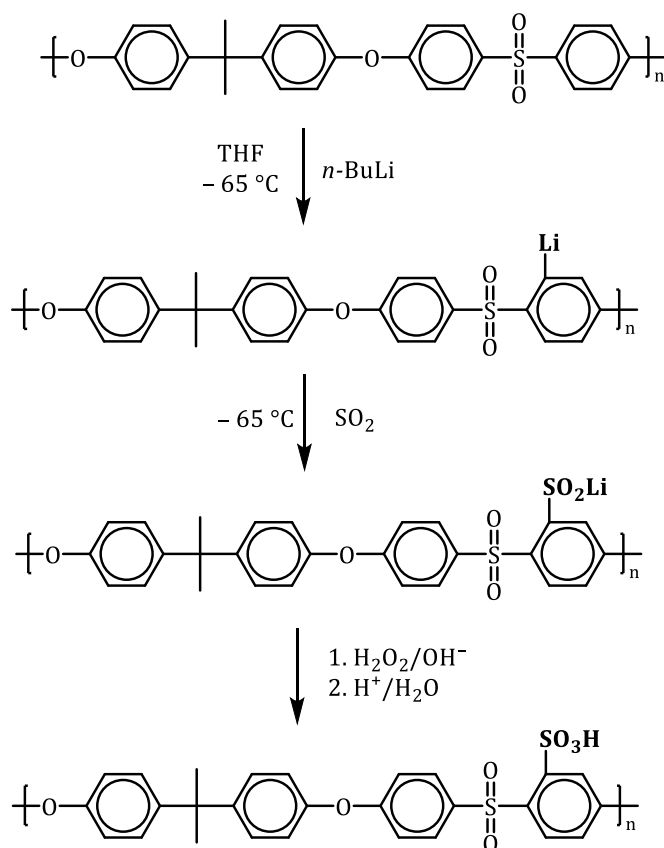
The polymer resulting from post-sulfonation gains the ability to conduct protons [63-65]. Bishop et al. achieved polymers with varying degrees of modification (30-100 %), achieved by adjusting the acid concentration and reaction time [66]. Typically, with an increase in the degree of sulfonation, the proton conductivity and water uptake of polyelectrolytes rise. However, beyond a certain threshold value, the polymer loses a mechanical strength due to excessive swelling. Therefore, finding a compromise becomes crucial and the compromise value for the degree of sulfonation typically falls within the range of 60-80 %. Scheme 12 provides an example of a post-sulfonation reaction.



Scheme 12. Scheme of post-sulfonation of poly(arylene ether sulfone) [58]

In this manner, sulfonation occurs under relatively harsh conditions, potentially leading to side reactions such as cross-linking and degradation of the polymer's main chain. To address these issues, Noshai and Robson suggested an alternative post-sulfonation pathway using a complex of SO_3 and triethylphosphate in a molar ratio of 2:1 [61]. However, the challenges associated with handling the chemicals and controlling the degree of sulfonation have outweighed any potential advantages of this route.

Furthermore, the introduction of sulfonic acid groups into the polymer's main chain can be achieved through metalation, subsequent sulfination and oxidation as proposed by Kerres et al. (Scheme 13) [67]. Despite the promising results demonstrated by polymers synthesized using this approach, the complexity of the synthesis process and challenges in reaction control have posed significant obstacles thus far.

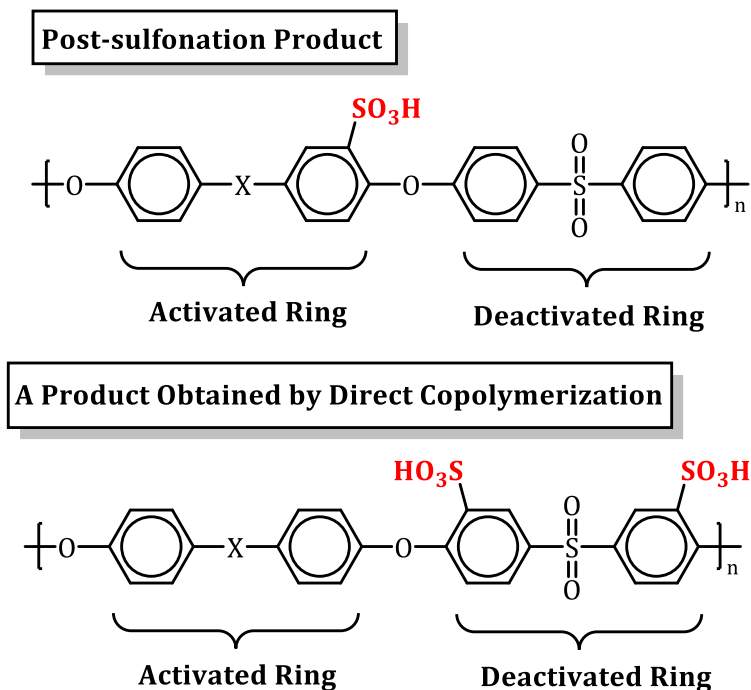


Scheme 13. Schematic representation of the metalation-sulfination-oxidation post-sulfonation process in poly(arylene ether sulfone)s [67]

1.1.2.4. Synthesis of disulfonated poly(arylene ether sulfone) copolymers through direct statistical copolymerization

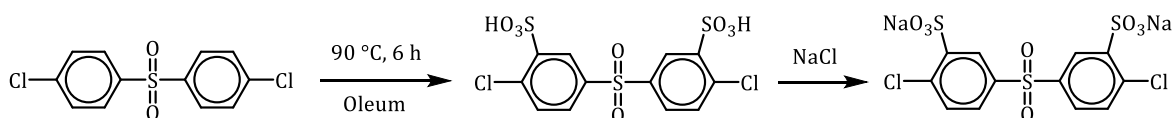
The primary drawback of post-sulfonation lies in the process's tendency to induce sulfonation in an electron-rich active ring. This reduces the electron density of the ring, making the bond between the aromatic carbon and oxygen more susceptible to hydrolysis [3]. To address this issue, researchers sought to develop a synthetic route where sulfonation would occur in the electron-poor deactivated ring (Scheme 14). Sulfonation of the deactivated ring enhances the hydrolytic stability of the polymer. Moreover, influenced by the electron-accepting sulfone group, the sulfonic acid fragment exhibits elevated acidity.

Sulfonation of the deactivated ring can be achieved through two methods: (1) the metalation-sulfination-oxidation method, as discussed earlier and developed by Kerres et al. [67], and (2) direct copolymerization of sulfonated monomers [68]. The first method may involve side reactions and difficulties in controlling the degree of sulfonation, thus drawing particular attention to the second method.



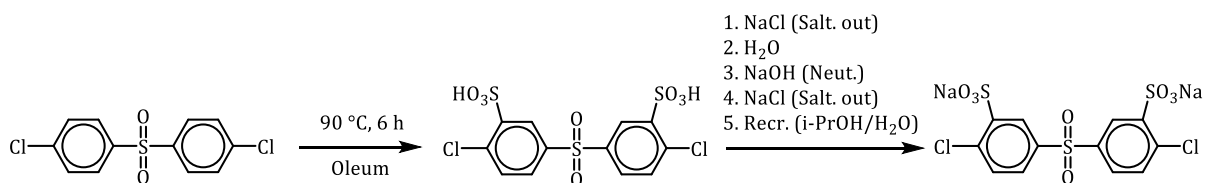
Scheme 14. Products obtained by post-sulfonation and direct copolymerization

Through the direct copolymerization of monomers, it becomes possible to achieve a more precise control over the degree of sulfonation. Ueda et al. synthesized 3,3'-disulfonated 4,4'-dichlorodiphenylsulfone (SDCDPS), which, in combination with bisphenol A and DCDPS, was employed to produce sulfonated poly(arylene ether sulfone)s with a sulfonation degree of 30 mol % [68]. The synthesis scheme for the sulfonated monomer by Ueda's group is illustrated on Scheme 15.

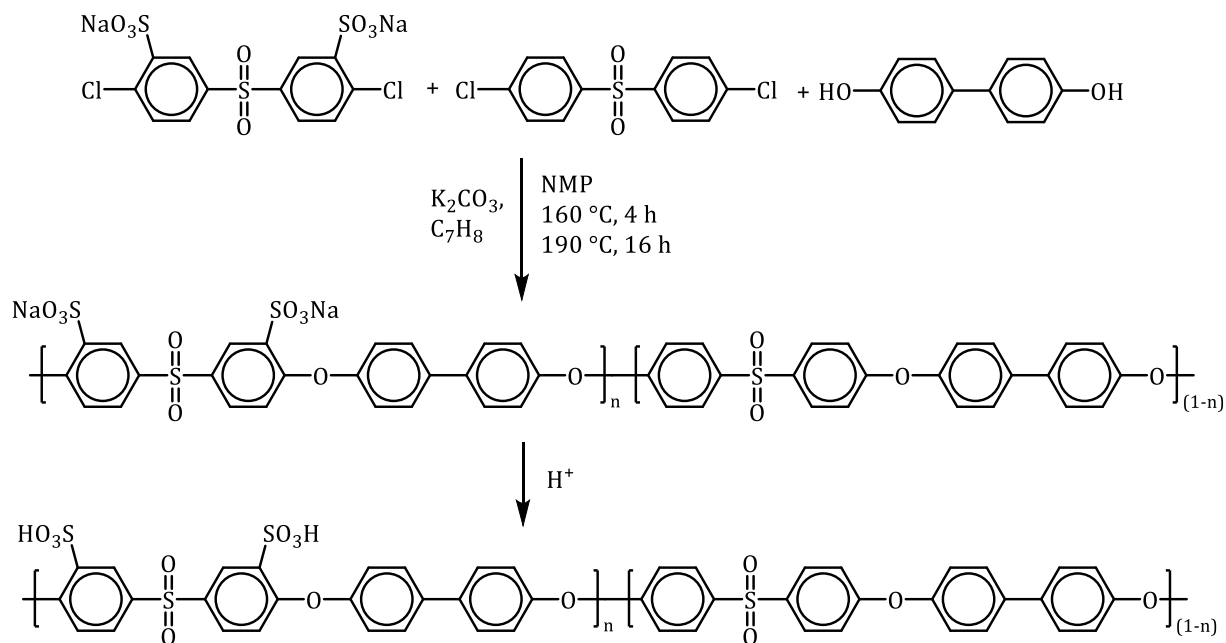


Scheme 15. Scheme illustrating the synthesis of 3,3'-disulfonated 4,4'-dichlorodiphenylsulfone (SDCDPS) [68]

McGrath et al. successfully conducted direct copolymerization syntheses to achieve fully aromatic sulfonated poly(arylene ether sulfone)s [69]. Additionally, they optimized the synthesis of SDCDPS, enhancing its purity and yield. Utilizing SDCDPS, DCDPS, and 4,4'-biphenol, they synthesized various types of polymers. Schematics illustrating the optimized synthesis of SDCDPS and the BPSH polymers synthesized by McGrath's group are presented below (Scheme 16 and Scheme 17).

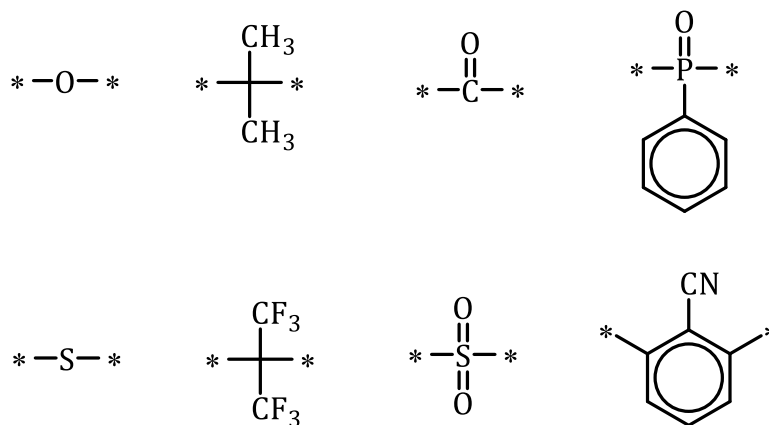


Scheme 16. Scheme of the optimized synthesis approach for SDCDPS



Scheme 17. Synthesis scheme of BPSH copolymer

A polymer with a sulfonation degree ranging from 35-40 % exhibited elevated proton conductivity, approximately equivalent to Nafion. However, when the sulfonation degree increased up to 60 %, there was a substantial rise in water uptake and polymer swelling, which led to the deterioration of the mechanical properties. This worsening in mechanical properties is attributed to the semi-continuous morphology of the hydrophilic domains [70-72]. The research group continued its investigations by introducing various functional groups into the same polymer, as illustrated on Scheme 18 [73].

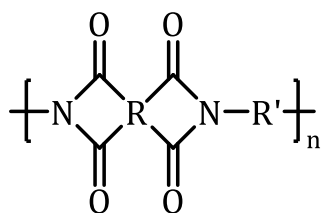


Scheme 18. Different functional groups involved in the structure of poly(arylene ether sulfone)s

1.1.3. Polyimide-based proton-exchange membranes

1.1.3.1. Overview of Polyimides

Polyimides are predominantly synthesized through the condensation of tetracarboxylic acid derivatives with diamines [74, 75]. These polymers incorporate an imide heterocyclic fragment within their main chain. The general structure of polyimides is depicted on Scheme 19.



R = cycloaliphatic/cycloaromatic
R' = aliphatic/aromatic

Scheme 19. General structure of polyimide

1.1.3.2. Polyimide-based PEMs

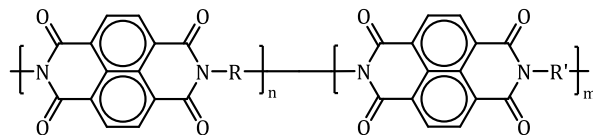
Polyimides, prized for their exceptional properties including excellent film-forming ability, thermal and chemical stability, and high mechanical strength, have been investigated

for their suitability as proton-exchange membranes (PEMs). Extensive research has been conducted to explore the characteristics of sulfonated polyimides. Initially, polyimides incorporating a sulfonated five-membered ring were synthesized using phthalic anhydride. However, these proved unsuccessful due to the hydrolytic instability of the anhydride in acidic fuel cell environments, leading to a significant reduction in molecular weight [76]. Subsequent studies suggested a potential solution by utilizing polyimides containing a six-membered ring, known for their increased stability against hydrolysis owing to lower cyclic strain. Genies et al. conducted a systematic investigation on sulfonated polyimides incorporating both five-membered and six-membered rings [76]. Model compounds synthesized were subjected to water at 80 °C, revealing notable differences in chemical stability. NMR analysis indicated that the sulfonated polyimide with a five-membered ring began decomposing within 1 hour and completed transformation in 10 hours. In contrast, the sulfonated polyimide with a six-membered ring exhibited structural changes after 120 hours, highlighting its comparatively high hydrolytic stability.

In recent decades, diverse sulfonated polyimides containing a six-membered ring have been synthesized and extensively studied [77, 78]. Various research groups employ commercially available naphthalene tetracarboxylic dianhydride (NTDA) along with sulfonated or non-sulfonated diamines for polyimide synthesis. Depending on the sulfonated diamine type, they are categorized into two groups:

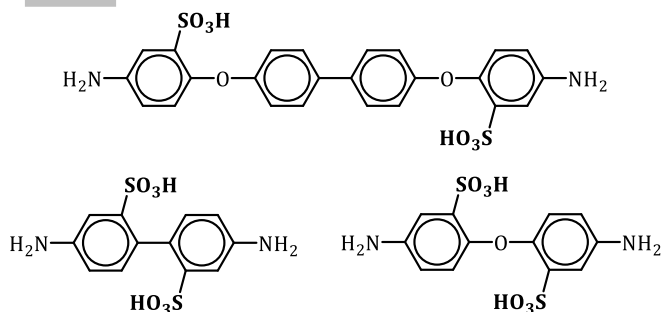
- Type I diamines, where the sulfonic acid and amine fragments are in the same aromatic ring;
- Type II diamines, where these fragments are located in different aromatic rings.

The chemical structures of some representative examples are illustrated on Scheme 20 below.

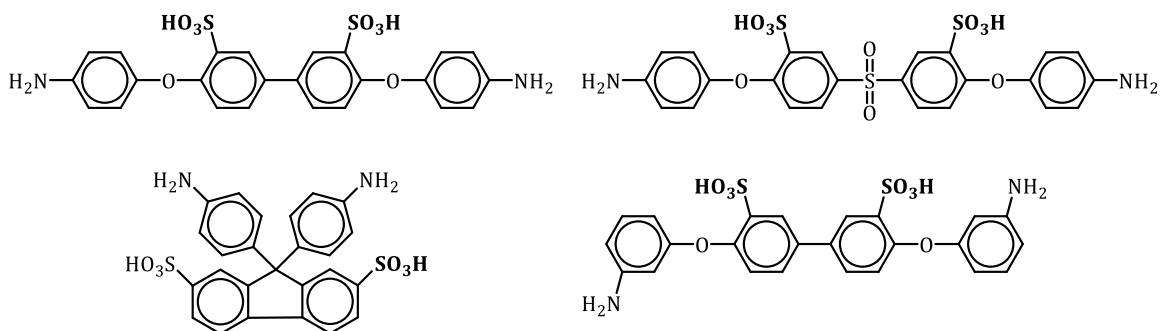


R = Sulfonated Diamines

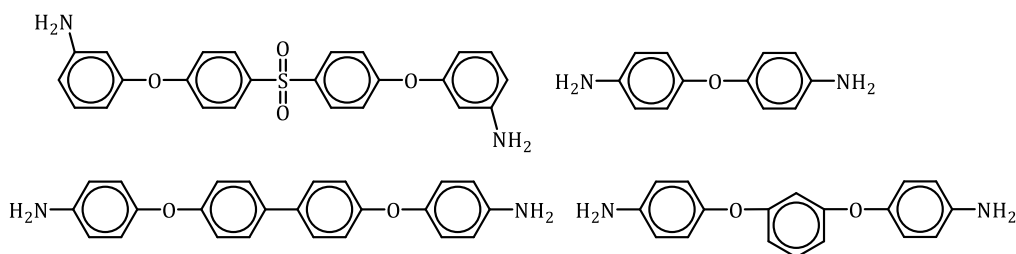
I Type



II Type



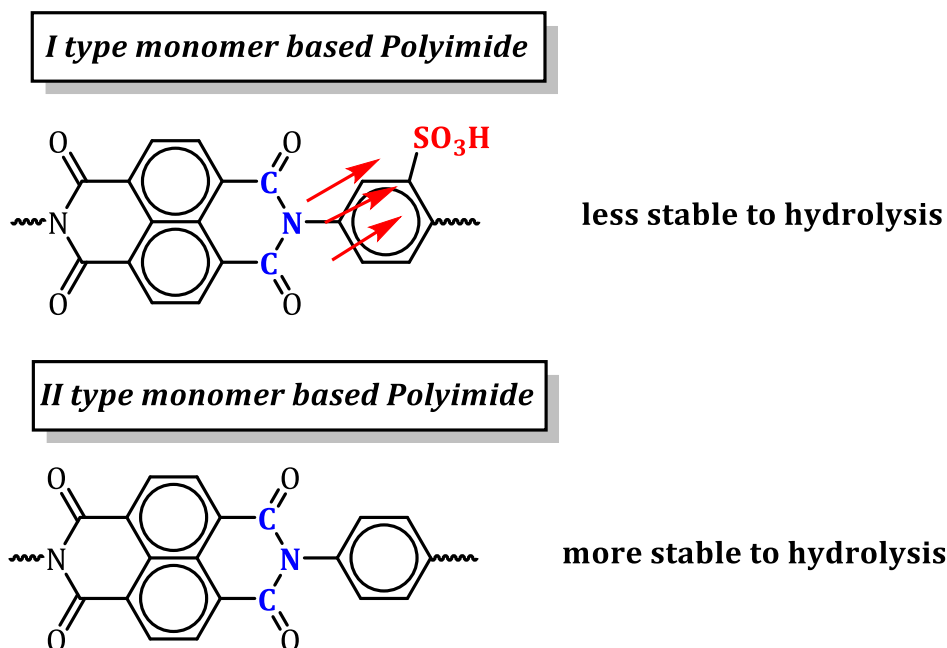
R' = Nonsulfonated Diamines



Scheme 20. Two different types of monomers necessary for the synthesis of sulfonated polyimides

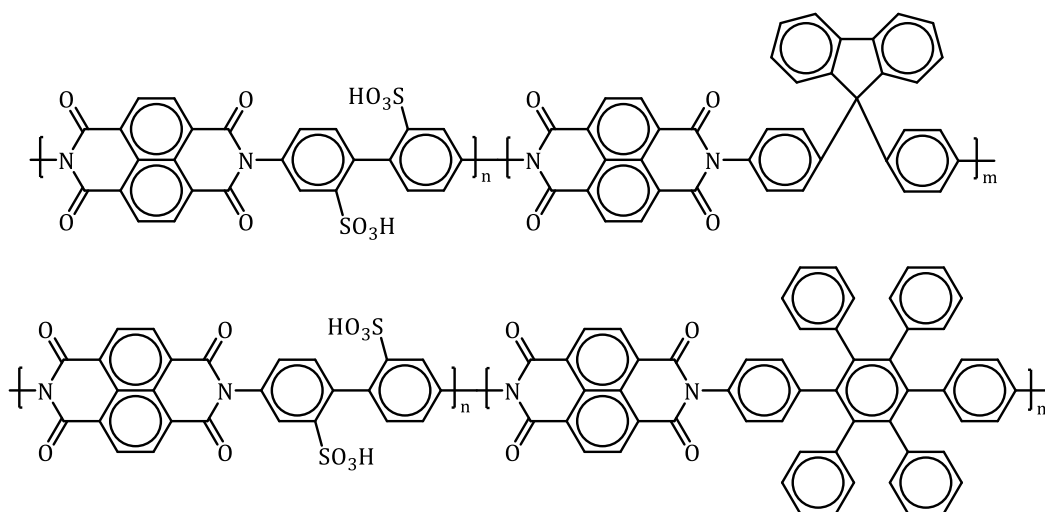
Polyimides derived from type I and type II monomers were thought to exhibit different hydrolytic stabilities. In the instance of type I monomers, the highly electron-withdrawing sulfonic acid group and the amine group are situated on the same aromatic ring, leading to electron deficiency in the nitrogen and carbon atoms, making them more

susceptible to water attack. In contrast, polyimides obtained from type II monomers, where the amine group and the sulfonic acid group are on different aromatic rings, experience a diminished impact on the electron impoverishment of nitrogen and carbon atoms. Consequently, they are characterized by relatively high hydrolytic stability (Scheme 21).



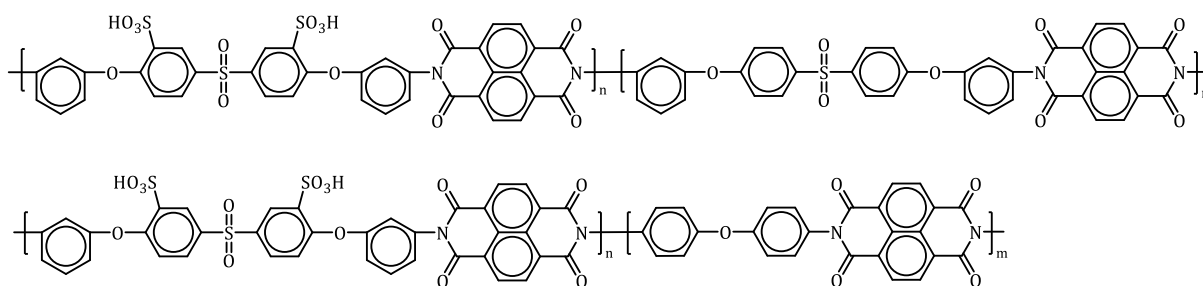
Scheme 21. Comparison scheme of hydrolytic stabilities of polyimides synthesized from different types of monomers

Watanabe et al. introduced bulky hydrophobic segments into the polyimides, preventing the packing of the main polyimide chains and creating space between the chains [79-81]. The chemical structures of these polyimides are depicted on Scheme 22. By generating similar spaces in proton-conducting membranes, it becomes possible to retain more water, resulting in significantly enhanced proton conductivity. Polyimides of this type exhibited proton conductivity approximately one order of magnitude higher than Nafion 112 at elevated relative humidities. However, this conductivity sharply decreased at lower relative humidities and remained lower than Nafion.



Scheme 22. Chemical structures of polyimides containing bulky pendant groups

Einsla et al. [82] proposed a novel method to enhance the hydrolytic stability of polyimides. They synthesized polyimides using a new type of sulfonated diamine containing flexible ether and sulfonic acid groups (Scheme 23). Although these polymers demonstrated acceptable values of proton conductivity and low fuel permeability, their hydrolytic stability remained somewhat limited.



Scheme 23. Chemical structures of polyimides containing flexible ether and sulfonic acid groups

1.1.4. Block copolymer-based proton-exchange membranes

1.1.4.1. Ionomer membrane morphological characteristics

Over the past few decades, various models explaining the transfer of ions in Nafion and similar membranes have been proposed. Wide-angle X-ray diffraction (WAXD) and small-angle X-ray scattering (SAXS) analyses have been conducted to investigate the sulfonic

acid groups in dry Nafion membranes, revealing their ability to aggregate and form ionic clusters. Building on these findings, Gierke developed the cluster-network model to elucidate the mechanism of proton transport in water-swollen membranes [83, 84]. In this model, the displacement of water in the membrane leads to the formation of ion channels, facilitating ion transport (Figure 5).

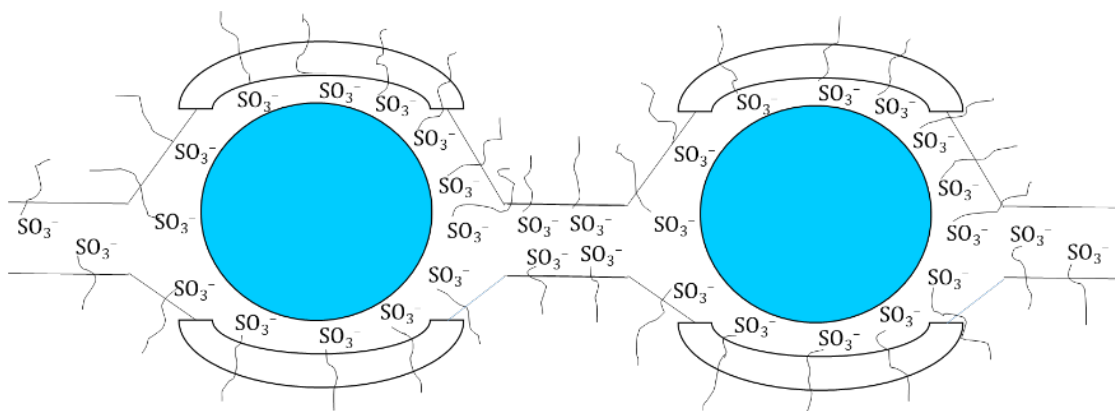


Figure 5. Figure of the ion-network model of hydrated Nafion

Moreover, various models of ion transport have been proposed by different researchers, including the lamellar model, depleted-zone core-shell model and modified hard sphere model [85, 86]. Although the morphology of Nafion has not been precisely determined, the most widely accepted model in the literature is the ion-network model, which effectively explains the correlation between the structure and properties of ion-conducting membranes. The nanophase-separated morphology of ion-conducting membranes is considered crucial for their ion-conducting properties.

The morphology of Nafion plays a critical role when used as a proton-conducting membrane. To achieve high proton conductivity, it is essential for the ion clusters to be easily interconnected through ion channels. Specific treatments can alter the locations of ionic and crystalline sites in Nafion [87]. For instance, placing extruded Nafion in an alcohol/water mixture and dispersing it results in a film known as "recast" Nafion, which exhibits different proton conductivity and mechanical strength compared to extruded Nafion. Moore et al. discovered that recast Nafion was brittle and yielded a thin dispersion in certain polar organic solvents, a characteristic not observed in extruded Nafion. WAXS and SAXS analyses

revealed that extruded Nafion was semi-crystalline, while recast Nafion was nearly amorphous.

1.1.4.2. Characteristics of self-assembly in block copolymers

Given the crucial role of morphology in ion transport, numerous studies have been undertaken with the primary aim of synthesizing block copolymers that exhibit nanophase separation, incorporating both hydrophilic and hydrophobic segments. Block copolymers are composed of two or more homopolymers (blocks) linked by covalent bonds [88]. Broadly, block copolymers fall into three main categories: diblock copolymers, triblock copolymers and multiblock copolymers. Additionally, there are star block copolymers and ABC-type block copolymers (Figure 6).

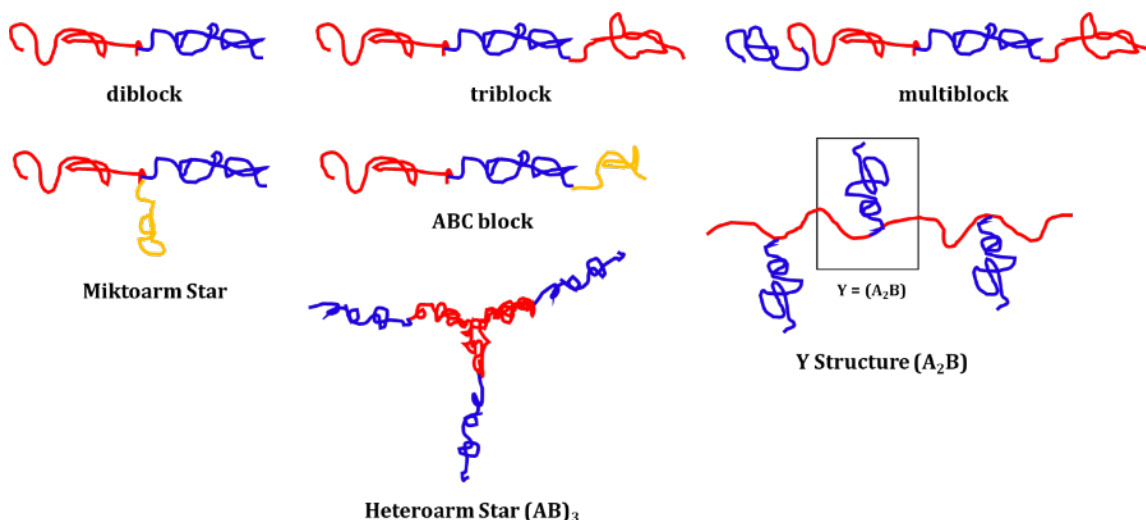
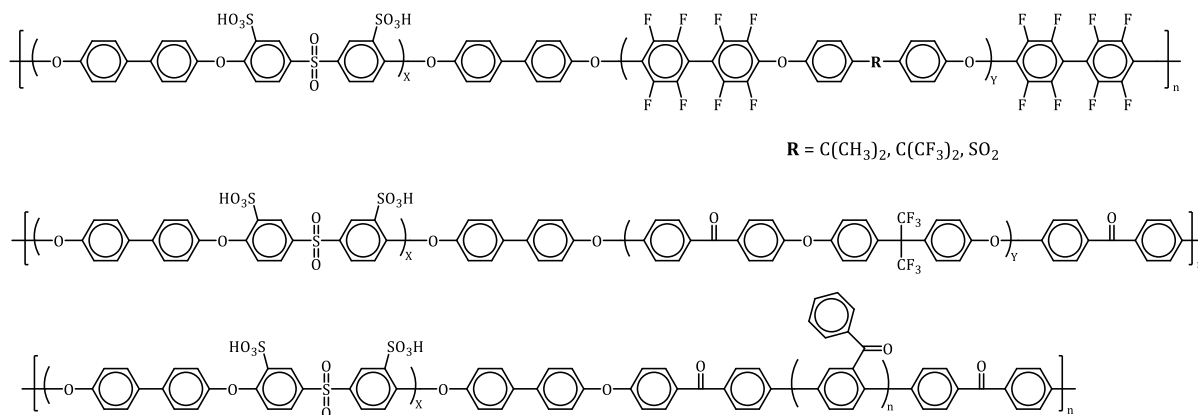


Figure 6. Different types of block copolymers

Block and graft copolymers exhibit the capability to develop various morphologies with distinct microphase distributions [89, 90]. Symmetrical diblock copolymers (AB) can exhibit bicontinuous gyroid, body-centered cubic arrays, lamellar, or hexagonally packed cylinders structures.

1.1.4.3. Research developments in the utilization of block copolymers PEMs

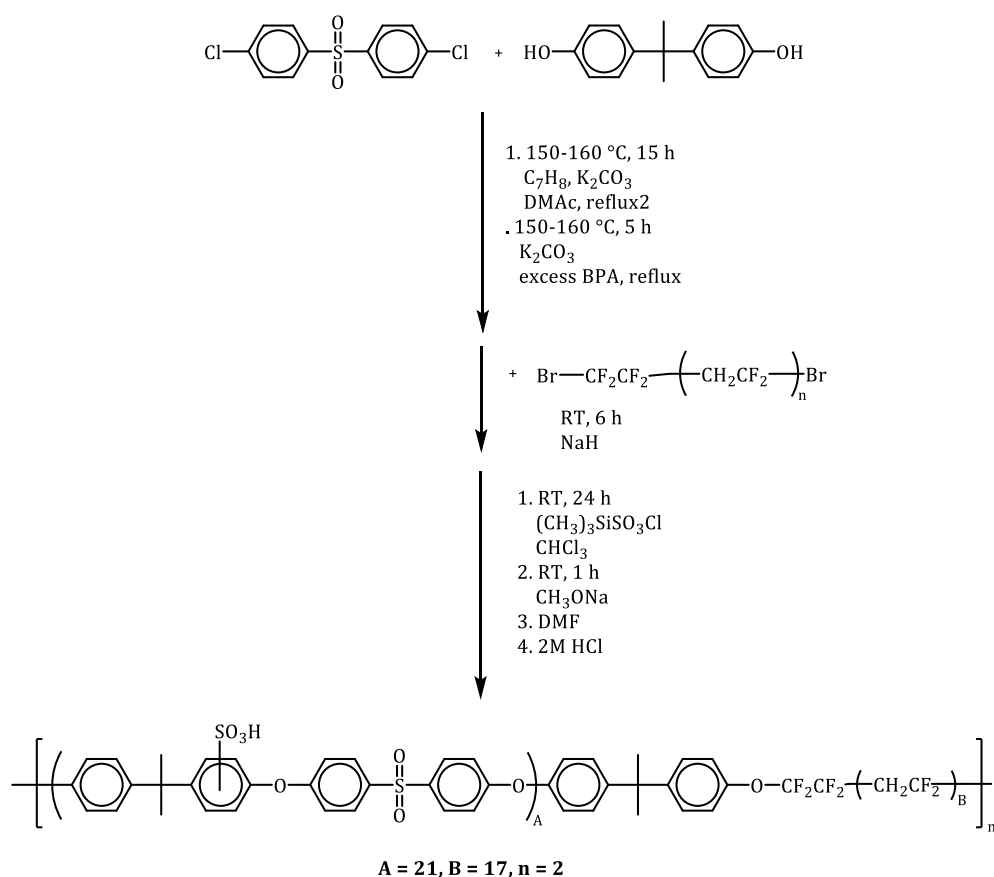
Among the multiblock copolymers, those derived from disulfide poly(arylene ether sulfone)s have been extensively investigated. As mentioned earlier, statistical copolymers (BPSH) based on poly(arylene ether sulfone)s exhibit excellent proton conductivity under fully hydrated conditions, along with impressive mechanical strength and chemical stability. However, a significant drawback of these systems is the decrease in proton conductivity at low relative humidity. To address this issue, McGrath et al. attempted to enhance performance by synthesizing multiblock copolymers [91-94]. By incorporating fully disulfonated poly(arylene ether sulfone)s as a hydrophilic block and introducing various hydrophobic blocks, they produced diverse types of multiblock copolymers (Scheme 24).



Scheme 24. Chemical structures of multiblock copolymers containing hydrophilic segments of disulfonated poly(arylene ether sulfone)s

In the case of the first three multiblock copolymers presented in the scheme above [93, 95], decafluorobiphenyl is employed to enhance phase separation for the synthesis of hydrophobic segments. Additionally, monomers containing isopropylidene, hexafluoroisopropylene and sulfone units are utilized for the synthesis of the hydrophobic segment. Structure-property correlation analysis revealed that the length of hydrophilic and hydrophobic blocks plays a crucial role in proton transport. The self-diffusion coefficient of water, explaining proton transport properties, increased with the lengthening of the blocks. However, proton conductivity values increased with longer hydrophilic blocks [96].

Another synthesis method for multiblock copolymers was investigated by Holdcroft et al. [97-100]. Through step-growth polymerization of bisphenol A poly(arylene ether sulfone) with phenoxide end groups was synthesized. These oligomers were combined with oligomers containing poly(vinylidene fluoride) (PVDF) bromine end groups to synthesize multiblock copolymers. Sulfonic acid groups responsible for proton conduction were introduced through post-sulfonation using trimethylsilyl chlorosulfonate. The synthesis scheme of the multiblock copolymer (SPSF-*b*-PVDF), obtained using poly(vinylidene fluoride) and polysulfone, is shown on Scheme 25.

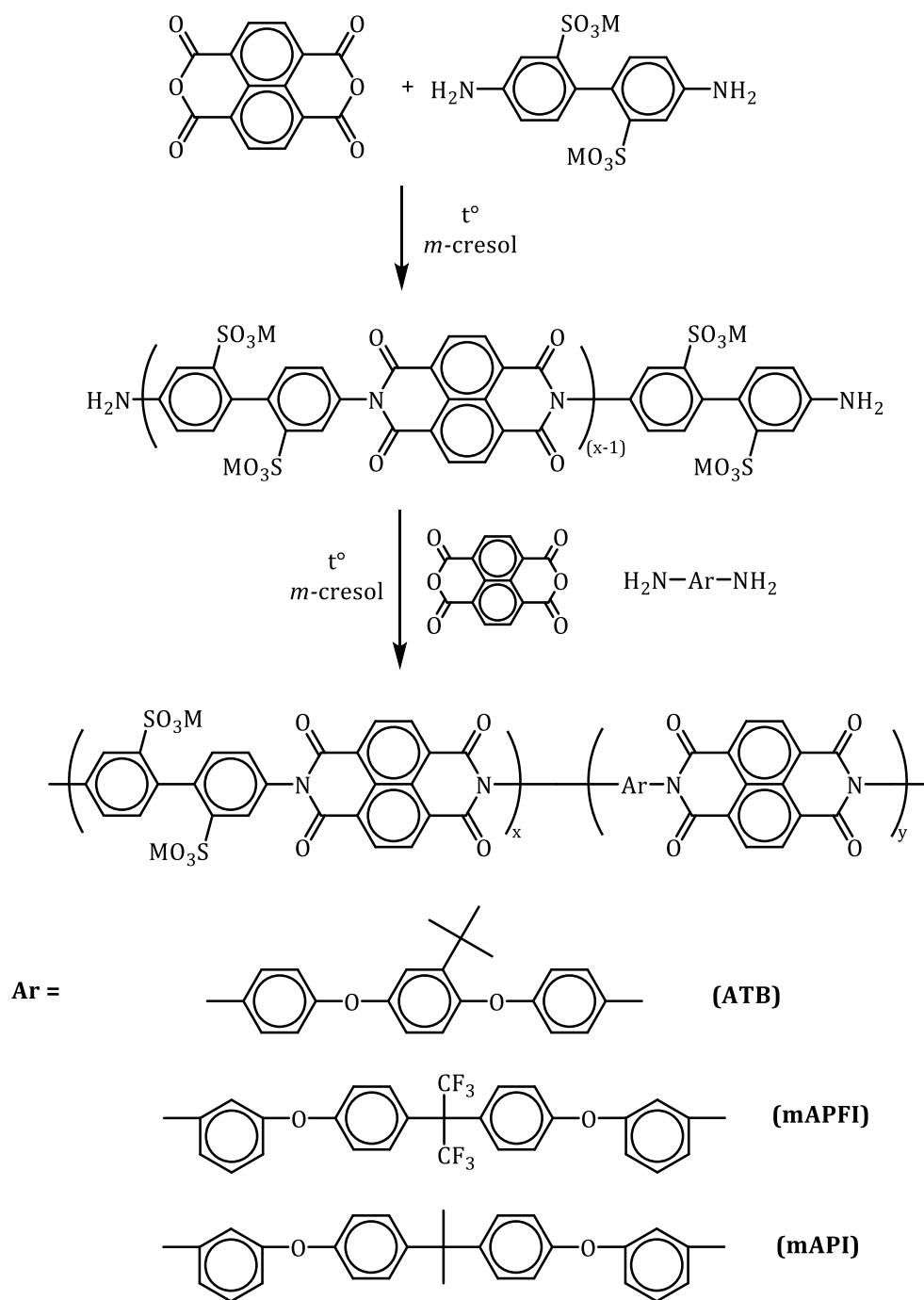


Scheme 25. SPSF-*b*-PVDF block copolymer synthesis scheme [99]

The multiblock copolymer SPSF-*b*-PVDF was compared with the sulfonated bisphenol A-based statistical copolymer, polysulfone (SPSF). Proton conductivity analysis revealed that in the low ion-exchange capacity region (< 1.0 meq/g), SPSF-*b*-PVDF exhibited four orders of magnitude higher proton conductivities than the statistical copolymer SPSF.

However, the difference in proton conductivities was completely reduced in cases of IEC > 1.5 meq/g. The high proton conductivity of multiblock copolymers with low ion-exchange capacity was explained with the help of fluorocopolymer, which promotes the formation of ion channels and aggregates.

In addition to sulfonated polysulfones, there is also interest in studying block copolymers derived from sulfonated polyimides. Genies et al. conducted a comprehensive study on a series of sequenced naphthalene polyimides [76]. A scheme for the synthesis of segmented sulfonated polyimide copolymers is shown on Scheme 26.



Scheme 26. Synthetic scheme of segmented sulfonated polyimides [76]

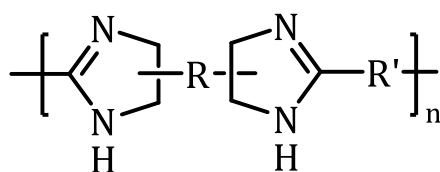
In the first step of polymerization, oligomeric sulfonated polyimide is obtained through step-growth polymerization of 1,4,5,8-tetracarboxylic dianhydride (NDA) and 4,4'-diamino-2,2'-biphenyldisulfonic acid (BDA). The molecular weight of the resulting product was controlled by the feed ratio of the two monomers. NDA and other non-sulfonated

diamines were introduced to the oligomeric blocks obtained in the second stage of polymerization. The ion-exchange capacity of the copolymers was regulated by varying the molar ratio of BDA to non-sulfonated diamines.

Proton conductivity and water uptake parameters of sulfonated naphthalene block copolymers were investigated. IEC ranging from 0.5 to 1.9 meq/g for copolymers exhibited variations within the range of 14-47 %. The degree of hydration (λ [H₂O/SO₃H]) increased linearly with the augmentation of the hydrophilic block, although the proton conductivity, typically correlated with IEC and λ , did not display such a trend. Proton conductivity decreased with an increase in the ionic block, attributed to the percolation of ionic domains. At low IEC, there are insufficient ionic groups to form continuous ionic domains and proton conductivity is proportionate to IEC. As IEC values reach the percolation threshold, proton conductivities are no longer determined by IEC, while water uptake continues to increase with growing IEC.

1.1.5. Polybenzimidazoles

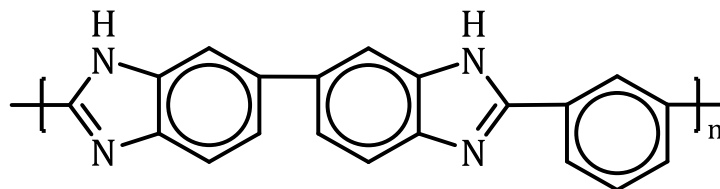
Polybenzimidazoles (PBIs) are thermoplastic and amorphous aromatic heterocyclic copolymers with repeating benzimidazole units. The general structure of PBI is depicted on Scheme 27.



Scheme 27. General structure of PBI

One of the widely used PBI is Celazole - poly 2,2'-m-(phenylene)-5,5'-bibenzimidazole, which was formerly produced by Celanese. Celazole is employed in various applications such as ultrafiltration, gas separation membranes, fibers, reverse osmosis, etc., owing to its stability under atmospheric pressure and at elevated temperatures [101]. While pure polybenzimidazoles exhibit low proton conductivities, the incorporation of different types of proton donor or acceptor acids, such as phosphoric acid, can enhance proton

conductivities. Consequently, these materials become more suitable for applications in fuel cells and water electrolyzers.

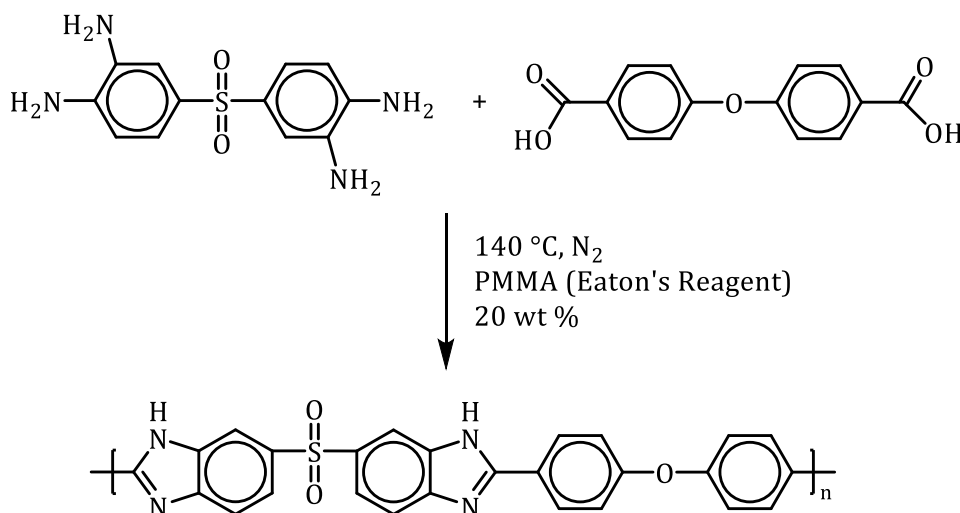


Scheme 28. Chemical structure of Celazole — poly 2,2'-*m*-(phenylene)-5,5'-bibenzimidazole [101]

Two primary methods are employed for the synthesis of high-molecular-weight PBI:

1. Utilizing monomers with functional groups and/or flexible linkages [102];
2. Post-modification of polymers by incorporating monomers containing acidic groups.

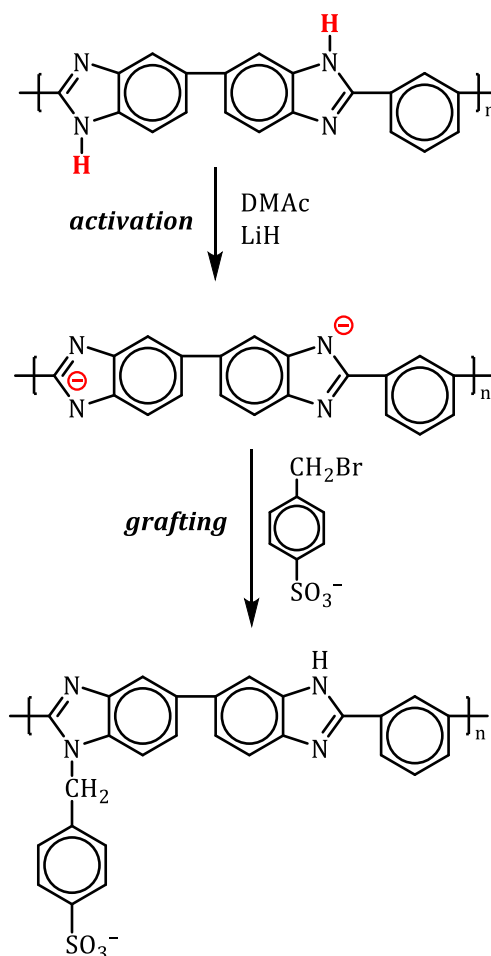
High molecular weight PBI suitable for gas separation can also be obtained using Eton's reagent (Scheme 29). Conversely, PBI synthesized in PPA is more suitable for use as a PEM [103].



Scheme 29. Synthesis scheme of high molecular weight PBI using a flexible monomer

The polymer can be modified by replacing different groups in the reactive N-H bond (Scheme 30). Following this, it is possible to synthesize membranes with higher proton conductivity for use in fuel cells and water electrolyzers [101]. Alkali metal hydrides are

employed for deprotonation in this reaction, enabling the subsequent reaction of the obtained product with various sulfonated reagents, such as arylsulfonates [104, 105].

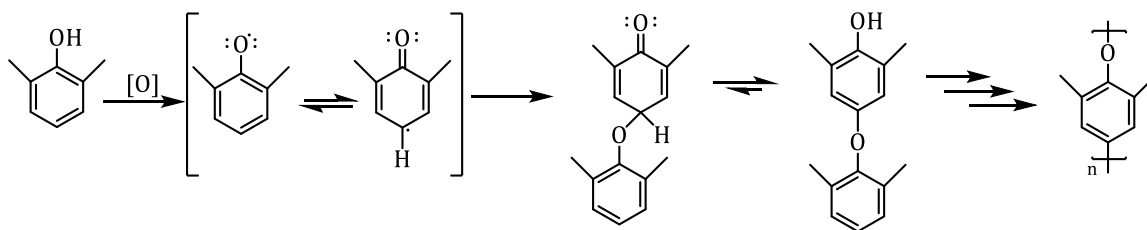


Scheme 30. Introduction of a compound containing a sulfonic acid group into the main chain of PBI through activation of the N-H bond [104]

1.1.6. Poly(2,6-dimethyl-1,4-phenylene oxide) — PPO

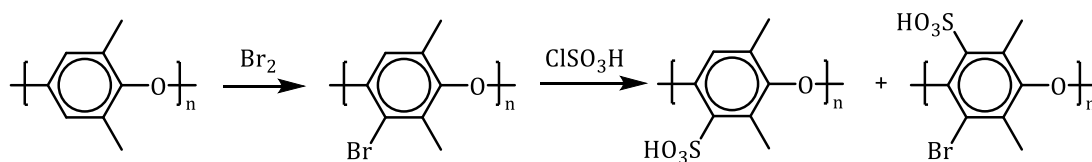
PPO is a fully aromatic copolymer synthesized primarily through oxidative coupling copolymerization, as illustrated on Scheme 31. This method is typically applied to monomers due to the absence of reactive halogens and the use of moderate reaction temperatures [106]. Despite being categorized as a free radical polymerization, the polymerization of phenolic rings follows a step-growth mechanism.

During this reaction, phenolic rings undergo oxidation, leading to the formation of an aryloxy radical, which subsequently undergoes further enolization. A potential drawback of this synthesis method is the potential for molecular dimerization, which can impede the attainment of a high molecular weight polymer. Hence, there is a need to optimize the synthesis conditions for PPO.



Scheme 31. Synthesis scheme of PPO [106]

If a hydrophobic co-monomer, such as fluorine or bromine, is incorporated into PPO, its properties, including ion-exchange capacity and water uptake, undergo changes [107-109]. These alterations directly impact the transport properties of the membrane. Yu et al. introduced controlled amounts of bromine and sulfonic acid groups into PPO, as depicted on Scheme 32 [109].



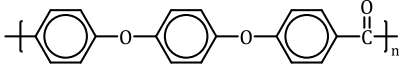
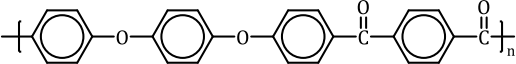
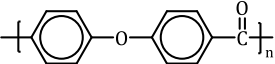
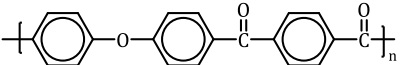
Scheme 32. PPO modified with bromine and sulfonic acid group

1.1.7. Poly(arylene ether ketone)s

PEK, PEKK, PEEK and PEEKK belong to the poly(arylene ether ketone) family. All these copolymers incorporate ether (E) and ketone (K) linkages in their main chain. These polymers exhibit semi-crystalline characteristics, featuring a broad range of glass transition (T_g) and melting (T_m) temperatures [110]. Their limited solubility in common solvents is attributed to their semi-crystalline nature. The key distinction among PAEK structures arises

from the quantity and placement of ether and ketone linkages, resulting in variations in T_g and T_m [106]. Table 2 outlines the properties of selected copolymers of this category.

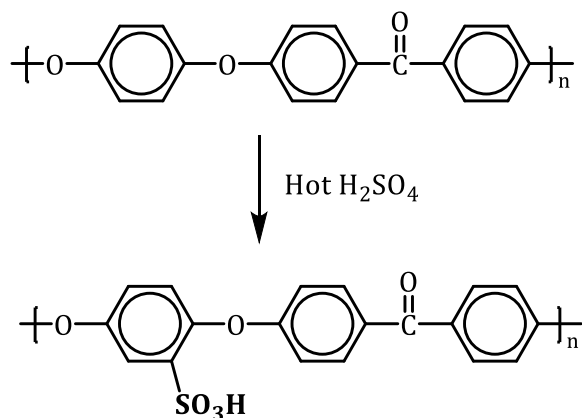
Table 2. Thermal properties of some representatives of the PAEK family [106, 111]

	Name	T_g , °C	T_m , °C
	PEEK	143	335
	PEEKK	154	358-365
	PEK	154	365
	PEKK	165-175	384

The synthesis of poly(arylene ether ketone)s can be achieved through the reaction of electrophilic aromatic substitutions, employing Friedel-Crafts catalysts. This type of reaction offers the advantage of being conducted at low temperatures and is economically efficient. However, the applicability of this method for PAEK synthesis is restricted to electron-rich monomers, which contain groups such as naphthalene sulfides and amines. Despite its benefits, this reaction method presents challenges, including the proper utilization of reaction co-products, limited solvent choices and the precipitation of catalyst complexes and/or low molecular weight oligomers [106, 112, 113].

Numerous scientific articles have addressed strategies to enhance the reaction conditions of PAEK synthesis via Friedel-Crafts polymerization, aiming to achieve polymers with improved solubility and higher T_g [113-115]. Cai et al. utilized this polymerization method to enhance both the mechanical and thermal properties of PAEK. Additionally, the synthesis of PAEK with various new monomers has resulted in products exhibiting significantly increased solubility in common polar aprotic solvents, such as DMAc, DMSO and NMP.

Sulfonated statistical copolymers (SPEK) were derived from PEK through post-sulfonation. In this approach, the non-sulfonated polymer is dissolved in a concentrated acid (e.g., sulfuric acid, acetyl sulfate, chlorosulfonic acid, etc.). After sulfonation is complete, the copolymer is precipitated in an antisolvent (e.g., isopropanol). Scheme 33 illustrates an example of the postsulfonation of PEK.

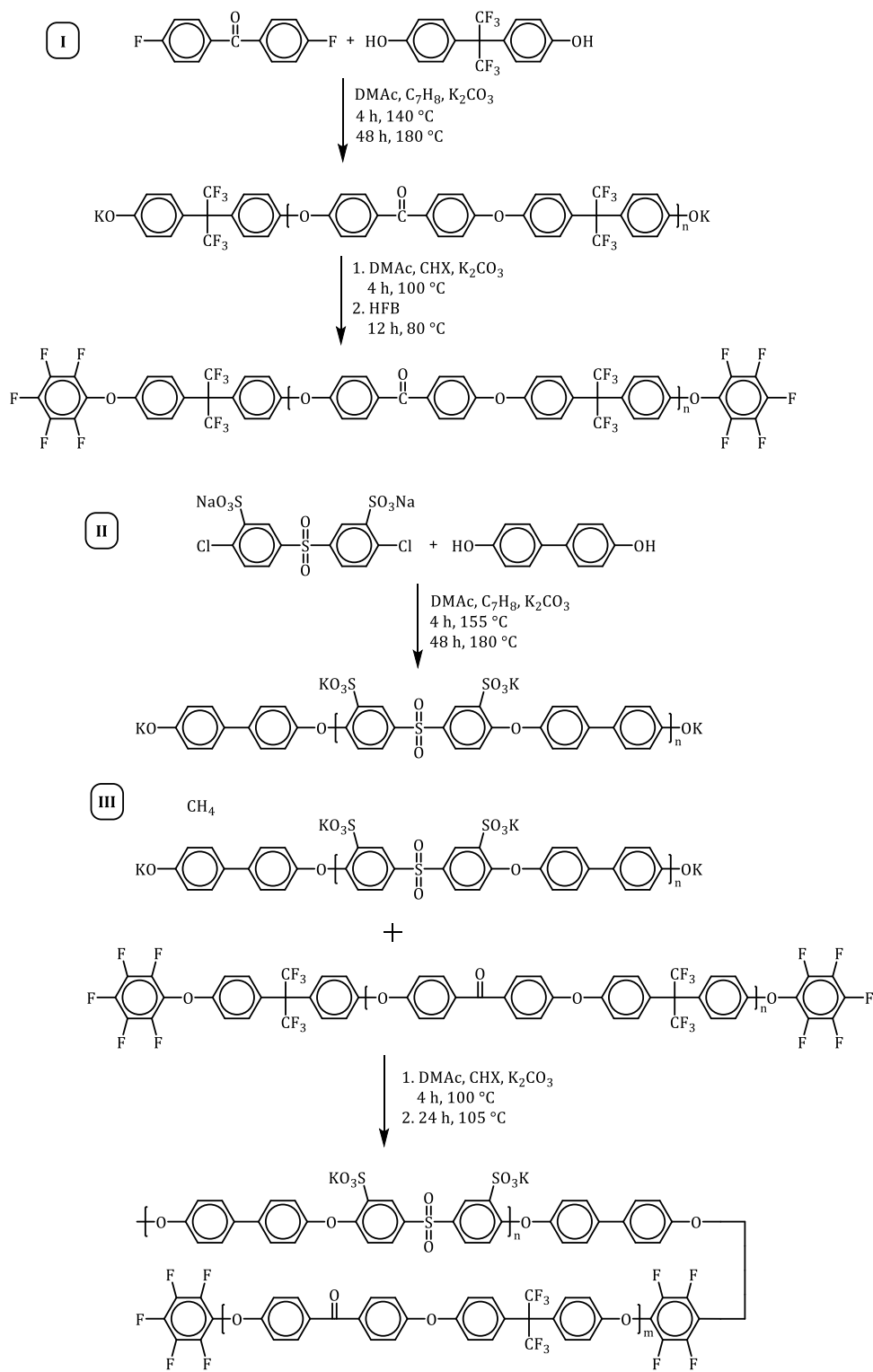


Scheme 33. Synthesis scheme of post-sulfonation of PEK [66]

Despite the potential for achieving favorable polymer properties at high molecular weights, highly converted sulfonated polyether ether ketone (SPEEK) has exhibited several drawbacks [116]. Morphological analyses of high-molecular-weight SPEEK have revealed the formation of a significant number of dead-end hydrophilic channels, leading to reduced proton conductivity [116, 117]. To address the low proton conductivities observed in statistical SPEEK, copolymerization with different polymers and the synthesis of block copolymers have been explored as potential solutions.

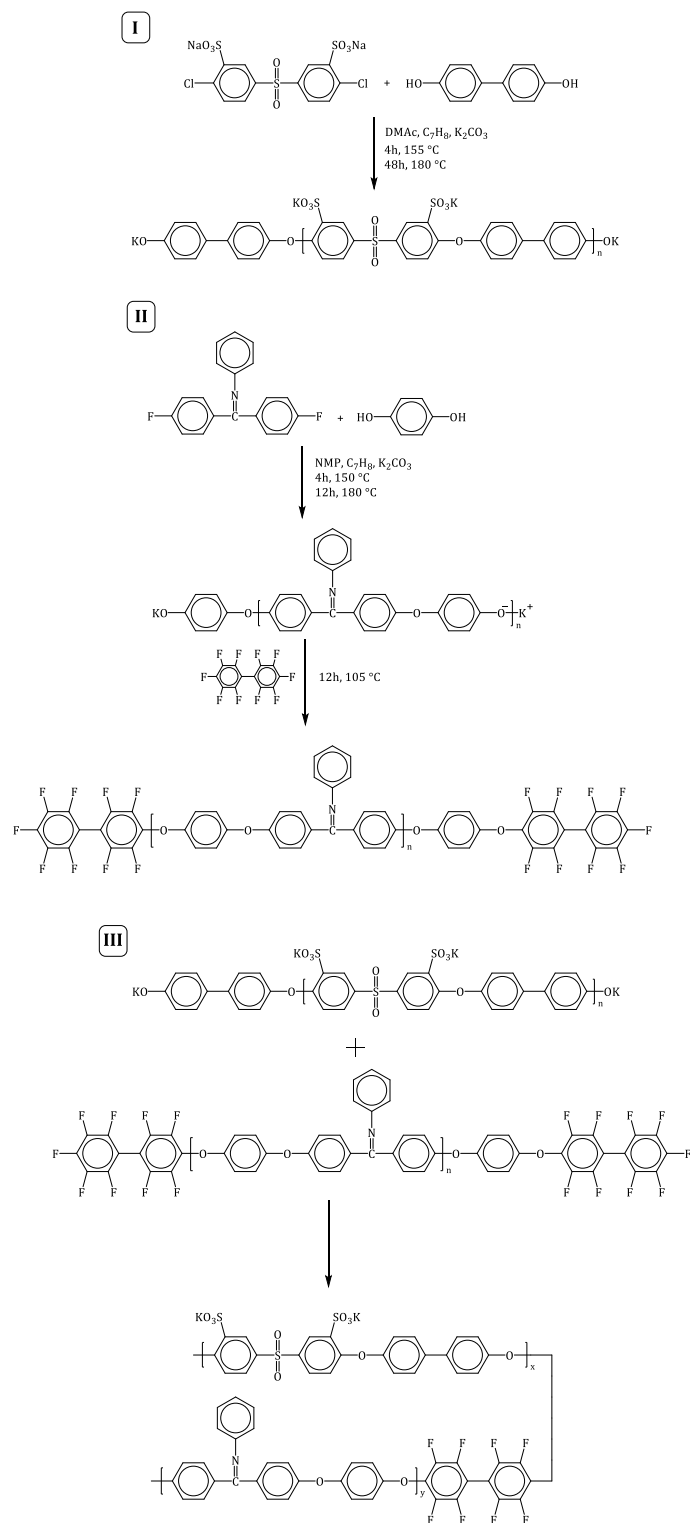
Lee et al. successfully obtained the block copolymer PEK-SPAES by copolymerizing SPEEK with the hydrophilic block of sulfonated polysulfone and the hydrophobic segment of polyether ether ketone (PEK) [118]. The coupling reaction (Scheme 34, I-III) involved the interaction of the two phenoxide end groups of the hydrophobic segment with the linking group of highly fluorinated hexafluorobenzene. Due to the high reactivity of hexafluorobenzene, it is crucial to conduct the coupling reaction at low temperatures. Additionally, the use of fluorinated monomers, such as 6F-bisphenols, disrupts the crystallinity of PEK and

enhances the stability of the final product during fuel cell operation under challenging conditions.



Scheme 34. A low-temperature synthesis approach proposed by Lee: I. Synthesis of the hydrophobic block and introduction of hexafluorobenzene, II. Synthesis of the hydrophilic block, III. Coupling reaction of hydrophilic and hydrophobic blocks [118]

Chen et al. aimed to reduce the crystallinity of poly(arylene ether ketone)s (PAEKs) by introducing ketamine groups into the main chain of the polymer (Scheme 35) [119]. In the synthesis of this multiblock copolymer, difluorobenzophenone (DFK) was modified into ketimine to introduce a bulky group into the hydrophobic oligomer. Decafluorobiphenyl was used as the end group, incorporated into the hydrophobic segment to enhance its reactivity with the hydrophilic blocks.



Scheme 35. Incorporation of a bulk group to reduce the semi-crystallinity of PAEK; I. Synthesis of hydrophilic blocks, II. Synthesis of hydrophobic blocks, III. Synthesis of block copolymers [119]

The resulting block copolymers exhibited significant improvements, including reduced water uptake, enhanced thermal and mechanical stability, and increased proton conductivity. TEM micrographs and AFM analyses indicated that increasing the block length of the copolymers improved interconnected hydrophilic channels, thereby enhancing proton conductivity [118, 119].

1.1.8. Poly(phenylene)s

1.1.8.1. General information about poly(phenylene)s

In previous chapters we have discussed sulfonated aromatic polymers containing hetero-atoms in the main backbone prepared via various synthetic strategies, including poly(arylene ether ketone)s [120], poly(arylene ether sulfone)s [121], poly(benzimidazole)s [120, 122], poly(arylene sulfide sulfone)s [123, 124] and poly(phenylene)s [125-128]. However, despite these significant advances, hydrocarbon-based polymer membranes faced ongoing criticism due to their insufficient oxidative stability compared to stabilized PFSA.

Polyphenylenes are a class of aromatic polymers characterized by a backbone made entirely of phenylene rings, distinguishing them from other aromatic polymers that incorporate heteroatoms like oxygen or sulfur. This structure endows polyphenylenes with exceptional thermal stability, chemical resistance, and mechanical strength. These properties make them highly suitable for various high-performance applications, particularly in environments requiring robust materials. Due to their unique molecular architecture, polyphenylenes have gained significant attention in recent years, especially in the field of proton-exchange membranes for fuel cells and water electrolyzers, where their enhanced oxidative stability and durability offer advantages over traditional hydrocarbon-based polymers. Consequently, research efforts were intensified on polyphenylenes – aromatic polymers consisting solely of phenylene rings in the main chain.

The journey towards commercialization of sulfonated polyphenylenes (SPPs) spans several decades, commencing with the early research efforts of G. Goldfinger on linear poly(*p*-phenylene)s and W. Ried, as well as J. K. Stille, on phenylated polyphenylenes during the late 1940s to early 1970s [129-134]. Subsequent milestones include the pioneering post-

sulfonation of a phenylated polyphenylene in 1972 and the recent development of reinforced SPPs by Ionomr Innovations, Inc., as reported in 2020 [135, 136].

There are various types of polyphenylenes depending on their composition and architecture.

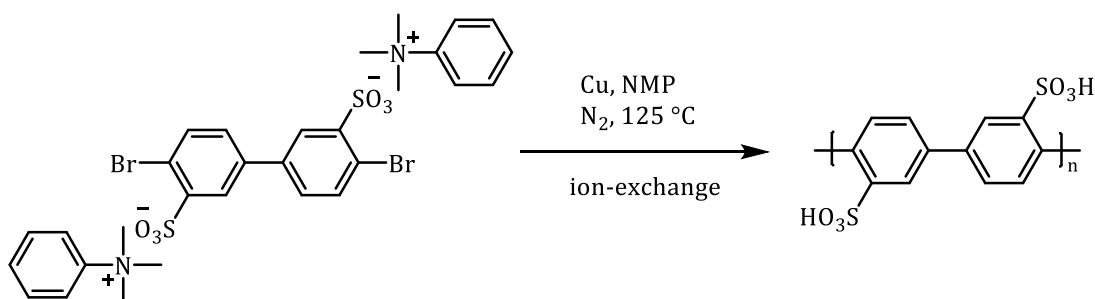
1.1.8.2. Linear poly(phenylene)s

Various approaches are employed to prepare oligo and poly(phenylene)s, with transition metal-catalyzed cross-coupling reactions being an excellent method to form aryl-aryl bonds [137]. This technique offers precise control over the resulting polymer backbone's regiochemistry. For example, coupling para-functionalized aromatic monomers yields a strictly para-functionalized polymer backbone, known as poly(*p*-phenylene). However, polyphenylenes consisting solely of para linkages are insoluble in common organic solvents due to their rigid-rod nature [138, 139]. The direct preparation of pristine poly(*p*-phenylene)s using transition metal-catalyzed methods faces challenges, as they precipitate at low molecular weights, terminating polymerization [138, 140, 141].

To enhance solubility, researchers have adopted strategies such as functionalizing phenylene monomers with solubility-enhancing groups. For instance, poly(*p*-phenylene)s were prepared via Suzuki cross-coupling of monomers substituted with hexyl chains, yielding soluble polymers with up to 18 phenylene repeat units [141]. An alternative approach involving a Ni- and Zn-mediated homocoupling of 2',3'-disubstituted poly(*p*-terphenylene) dichlorides was reported, resulting in partially phenylated poly(*p*-phenylene)s with improved solubility [142].

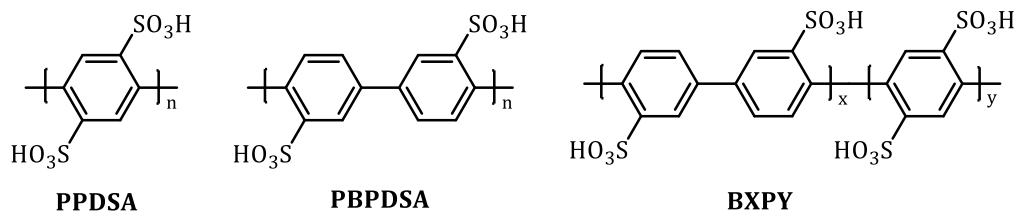
Recently, a feasible approach to the preparation of pristine poly(*p*-phenylene) was reported. It involved polymerizing a non-aromatic precursor to yield initially soluble, non-aromatic polymer, from which pristine poly(*p*-phenylene) was thermally generated in a solvent-free environment [140]. However, post-functionalization of poly(*p*-phenylene) to its sulfonated analogue has not been reported due to the aforementioned challenges [143, 144].

Sulfonated poly(*p*-phenylene)s have been prepared by M. Litt and coworkers using a pre-functionalization approach. Biphenyl monomers containing sulfonic acid-ammonium salts were first synthesized, followed by polymerization using the copper-catalyzed Ullman reaction, resulting in main-chain functionalized acid-bearing poly(*p*-phenylene)s with improved solubility [145-147].



Scheme 36. Synthesis scheme of sulfonated poly(*p*-phenylene)s, according to the findings by M. Litt and collaborators

M. Litt et al. used their synthetic approach to report various other poly(*p*-phenylene)s as proton-exchange membranes for PEMFCs. The sulfonated polymers PPDSA, PBPDSA and BXPY were prepared through copper-mediated Ullman coupling reactions between prefunctionalized acid-bearing monomers. Pre-functionalization of monomer units increased the solubility of the growing polymer chains in polar solvents [145, 148]. An additional series of copolymers based on PPDSA and PBPDSA incorporated cross-linkable aryl groups to some extent of the sulfonic acid moieties on the polymer main chain, yielding insoluble membranes with proton conductivities approaching 200 mS/cm [145, 148].

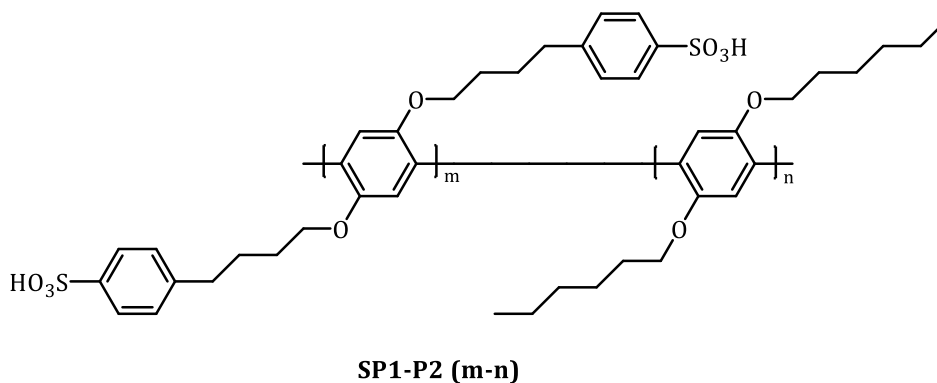


Scheme 37. Chemical structures of PPDSA, PBPDSA and BXPY

To manage water content and proton conductivity, grafts were incorporated into poly(*p*-phenylene)s. Various grafting moieties, including biphenyl, 2,6-di-*t*-butylphenyl, *t*-

butylbenzene, neopentyl benzene, *n*-octylbenzene, and *n*-dodecylbenzene, were utilized. Some grafted and crosslinked poly(*p*-phenylene)s exhibited proton conductivities up to 10 times greater than Nafion under both high and low humidity conditions [149-151]. Unfortunately, poor mechanical properties limited their practical application [145, 150].

M. Rikukawa et al. reported a series of side-chain sulfonated poly(*p*-phenylene) diblock copolymers with ion-exchange capacities ranging from 0.96–2.42 meq/g. Micro-phase separation depended on the hydrophobic and hydrophilic block length, as well as their unit ratios. The high ion-exchange capacity block copolymers displayed proton conductivity values comparable to Nafion [152].



Scheme 38. Chemical structures of diblock copolymer SP1-P2

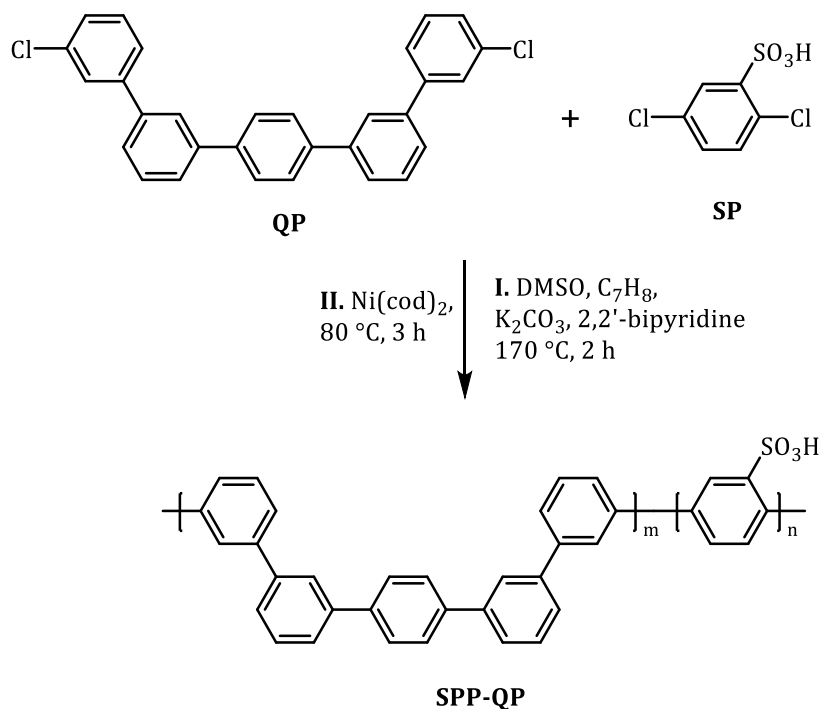
In conclusion, sulfonated polyphenylenes, particularly linear poly(*p*-phenylene)s, have attracted significant attention as promising materials for proton-exchange membranes in PEMFCs. Transition metal-catalyzed cross-coupling reactions offer precise control over their regiochemistry and functionalization strategies have been employed to enhance solubility. Challenges remain in terms of membrane integrity and mechanical strength due to the rigid-rod-like nature of the poly(*p*-phenylene) backbone. However, the properties can be changed by incorporating various co-monomers [140, 141, 145, 149, 150].

1.1.8.3. Kinked, sulfonated poly(phenylene)s

In the realm of proton-exchange membranes (PEMs), kinked sulfonated polyphenylenes have emerged as a promising materials with enhanced performance and

tunable properties. Miyatake et al. (2017) reported on a series of sulfonated polyphenylenes containing a mixture of *meta* and *para*-linkages throughout the polymer backbone, resulting in flexible coil-like structures with improved membrane forming capability and high in situ wet-dry cycle durability [128].

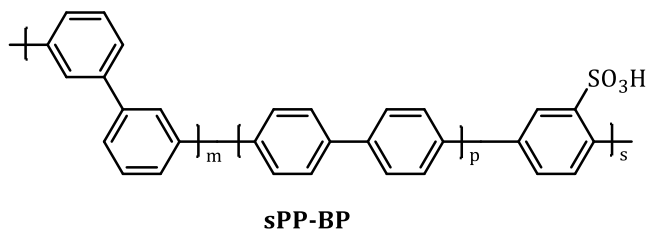
Shimizu et al. (2019) investigated the oxidative stability and stress durability of SPP-QP, a sulfonated polyphenylene synthesized using a Ni-mediated cross-coupling reaction. The results showed that SPP-QP outlived other heteroatomic linkage-containing polyaromatics and demonstrated excellent resistance to oxidative degradation [153]. To address membrane brittleness, the authors modified MEA and fuel cell components with softer variants, leading to improved mechanical durability [153].



Scheme 39. Synthesis scheme of SPP-QP

A next-generation sulfonated polyphenylene, SPP-BP, containing a mixture of *meta*- and *para*-phenylene groups, was synthesized without the need for a multistep monomer synthesis, reducing material cost and simplifying the overall polymerization process [154]. By adjusting the monomer feed ratio, the authors achieved tunable polymer backbones with varying ion-exchange capacities and *meta*-phenylene content. SPP-BP, with an 88 : 22 *meta*-

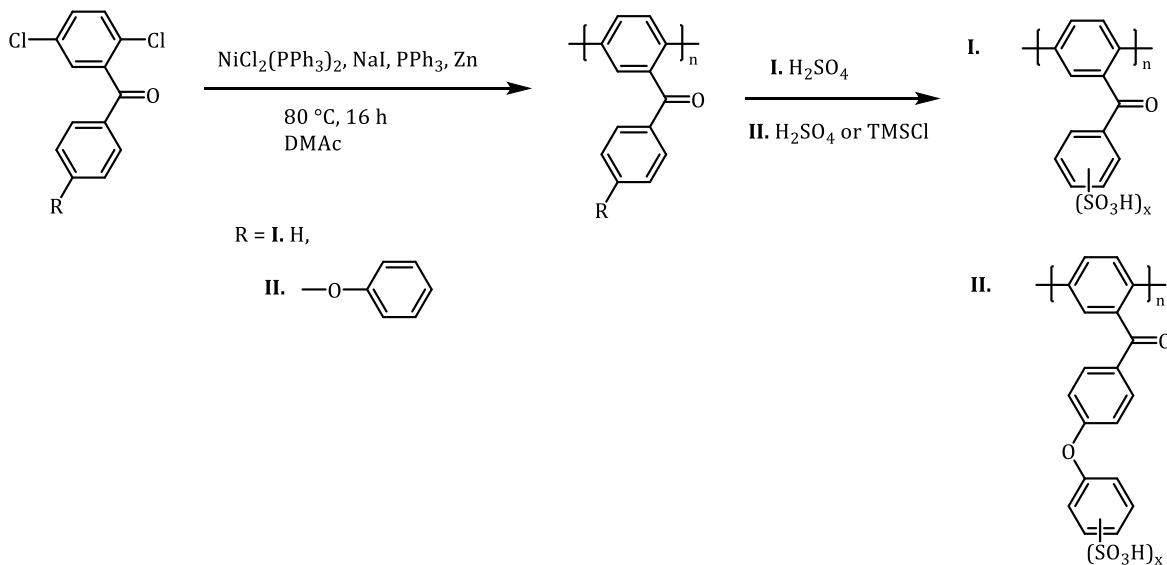
phenylene to *para*-phenylene ratio, exhibited proton conductivity and oxidative stability comparable to SPP-QP [154].



Scheme 40. Chemical structure of sPP-BP

1.1.8.4. Side chain sulfonated Poly(phenylene)s

The synthesis of sterically-encumbered polyphenylene backbones via coupling of dichlorobenzophenones has been extensively studied by various research groups [155, 156]. The resulting postsulfonated poly(benzophenone)s, such as poly(benzoyl-1,4-phenylene) and poly(*p*-phenoxybenzoyl-1,4-phenylene), exhibit excellent thermal stability and lower methanol permeability than Nafion in direct methanol fuel cells [157].



Scheme 41. Chemical structures of different types of side-chain sulfonated poly(phenylene)s

To improve control over ion-exchange capacity, pre-sulfonated poly(benzophenone)s have been developed, allowing precise tuning of proton conductivity

and water uptake [158]. Additionally, the introduction of partially fluorinated poly(benzophenone)s has been explored, although their electrochemical performance as PEMs remains unsatisfactory [159].

Notably, W. Kim and co-workers have investigated various side-chain sulfonated polyphenylene variants for PEMFC applications [160-163]. These polymers, prepared through Ni-catalyzed cross-coupling reactions, incorporate tetraphenylethylene and/or benzoyl moieties, including branched and alkyl-chain-grafted derivatives. Their proton conductivities are generally comparable to Nafion or even exceeding it [160-163].

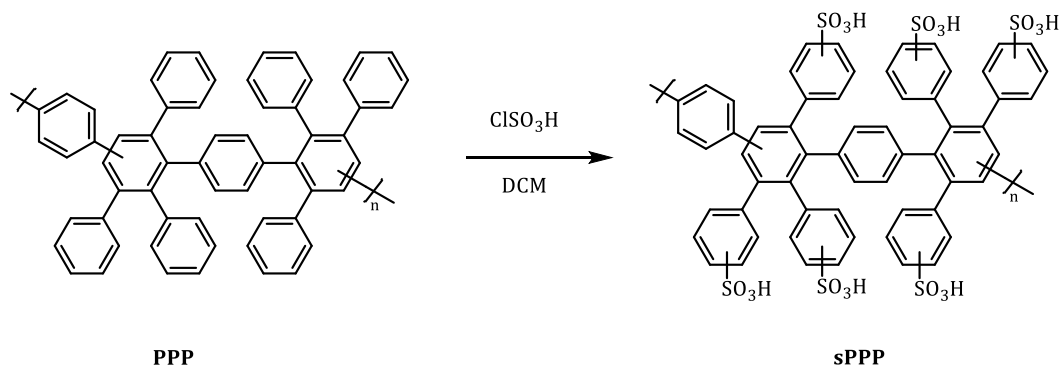
The flexible sulfonic acid alkyl side-chains in one of the variants promoted hydrophobic/hydrophilic phase separation, leading to enhanced proton conductivity. However, in situ fuel cell performance was not evaluated for this specific polymer. Another variant demonstrated high proton conductivity due to the greater acidity of the sulfonyl imide group compared to sulfonic acid groups [160-163].

While the polyphenylene backbone contributes to the membranes' chemical stability, their dimensional stability varies with IEC values, resulting in different water uptake [160-163]. Nonetheless, a comprehensive assessment of mechanical properties and in situ electrochemical characterization is needed for further improvement in electrochemical device applications [160-163].

1.1.8.5. Post-sulfonated phenylated poly(phenylene)s

In 2005, C. H. Fujimoto and colleagues introduced a new class of polyphenylene materials functionalized with sulfonic acid groups, termed as sulfonated phenylated polyphenylenes (sPPPs) or sulfonated Diels–Alder polyphenylenes (SDAPP) [164]. These acronyms, sPPP and SDAPP, represent the same materials synthesized through Diels–Alder polycondensation, featuring entirely aryl–aryl linkages devoid of heteroatoms and containing side-chain sulfonation with benzenesulfonic acid moieties. Unlike other polymer electrolyte membranes (PEMs) typically synthesized with additives and catalysts, the approach used here to produce these polyelectrolyte materials did not require such additives to form the base non-functionalized phenylated polyphenylene (PPP) backbone. Although an

earlier study by VanKerckhoven et al. had achieved post-functionalization of a similar PPP backbone using sulfuric acid to enhance hydrophobic polymer solubility, no details were provided about acid content, sulfonic acid group positions, or further research on the materials [135].



Scheme 42. Synthesis scheme of sPPP by post-sulfonation of PPP

Fujimoto et al. reported the controlled post-functionalization of PPP with chlorosulfonic acid to create sPPP, which was then investigated as a proton-exchange membrane for the first time [164]. This process rendered the polymer soluble in polar aprotic solvents like DMSO, yet it remained insoluble in water. It was hypothesized that sulfonation primarily occurred at the *para*- position of the pendant phenyl rings due to steric constraints, though definitive structural evidence was lacking.

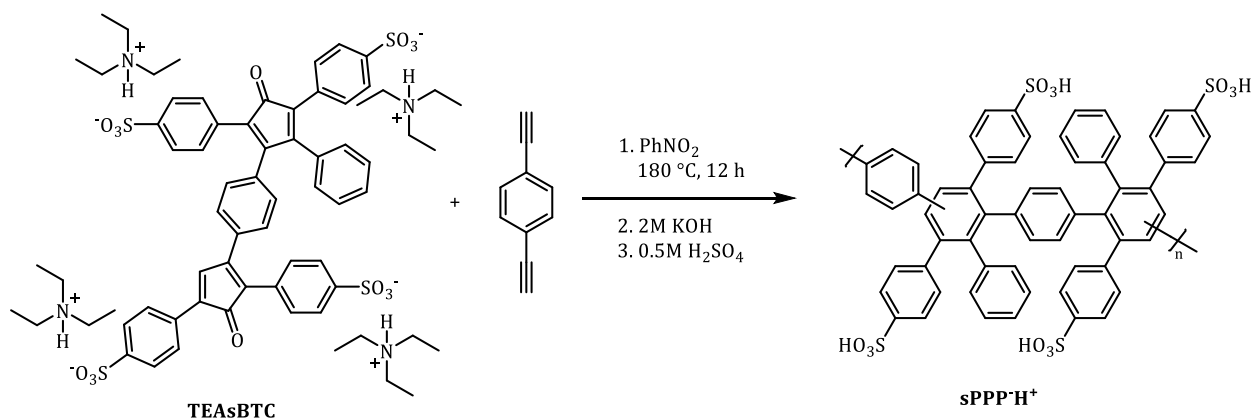
An alternative method for post-functionalization of phenylated polyphenylene was explored using Friedel–Crafts chemistry, as demonstrated by S. M. Budy and D. A. Loy [165]. In this process, PPP in a diluted solution reacted with 1,3,5-benzenetrisulfonyl chloride and FeCl₃ Lewis acid, yielding a sulfonylated branch phenylated polyphenylene with 1 or 2 pendant aryl sulfones. Hydrolyzing these polymers produced materials with 2 or 4 sulfonic acid moieties per repeat unit, exhibiting ion-exchange capacity values of 1.87 and 2.90 meq/g, respectively [165]. High IEC membranes were no longer water-soluble, an improvement over prior postsulfonated sPPPs that formed hydrogels at high degrees of sulfonation (42.1 acid groups per repeat unit) [164]. The decreased water solubility was attributed to significant segregation of the hydrophilic acid groups from the hydrophobic polymer backbone [165].

M. Hickner and coauthors investigated the water uptake and proton conductivity of post-sulfonated phenylated polyphenylenes, evaluating sPPPs (SDAPP) with various levels of acid functionalization (0.8 to 2.1 sulfonic acid groups per repeat unit) [166]. Their comparison with a Nafion 117 reference revealed a connection between polymer ion-exchange capacity, water uptake, hydration number (λ), and proton conductivity (σ_{H^+}). These membranes demonstrated substantial proton conductivity (up to 123 mS/cm) at higher IEC, surpassing the Nafion reference, but with greater water uptake. E. G. Sorte et al. explored a wider range of post-sulfonated phenylated polyphenylenes with varying sulfonation degrees, finding that water content and mass increased with humidity and sulfonation [167]. They discovered non-linear water adsorption and related it to morphological changes within hydrating samples. At 98 % relative humidity (RH), the number of water molecules per sulfonic acid moiety decreased with increasing IEC, affecting proton conductivity, which ranged from 30 mS/cm to 169 mS/cm. Activation energy decreased with higher sulfonation degrees, linked to enhanced Grötthuss ion conduction. L. He et al. explored ultrathin post-sulfonated phenylated polyphenylenes and observed non-uniform water distributions within films due to interfacial forces [168]. Water's impact on diffusion and the presence of dual nature surfaces with hydrophilic and hydrophobic components were highlighted [168].

1.1.8.6. Pre-sulfonated phenylated poly(phenylene)s

In the past 6 years, substantial advancements have been made in developing structurally-defined sulfo-phenylated polyphenylenes. T. Skalski et al. introduced a novel prefunctionalization strategy for creating sPPPs in 2015 [127]. This method involved modifying the cyclopentadienone diene monomer, resulting in a precisely functionalized analogue (TEAsBTC) with 4 sulfonate moieties attached para to its exterior pendant phenyl rings. A proof-of-concept pre-functionalized polymer (sPPP-H⁺) was prepared, revealing the presence of 4 sulfonate groups per polymer repeat unit through NMR integration ratios. The IEC was determined to be 3.47 meq/g, close to the theoretical and ¹H NMR-measured IEC (3.70 meq/g), the highest value reported for sPPPs thus far. These pre-sulfonated membranes displayed substantial proton conductivity (8.65 to 106 mS/cm), surpassing a

Nafion 211 reference across a humidity range of 40 to 95 % RH, except in liquid water where lower acid concentrations led to reduced conductivity. The introduction of sPPP-H⁺ as an ionomer in the catalyst layer of a fuel cell MEA exhibited promising performance relative to Nafion D520 at both high and low humidity levels, yet comprehensive in situ testing was limited due to swelling and mechanical constraints.



Scheme 43. Synthesis scheme of sPPP-H⁺

To address the challenges associated with excessive water uptake by sPPP-H⁺ membranes, M. Adamski et al. developed larger dienophile monomers based on naphthyl, biphenyl and terphenyl structures [169]. These led to polymers with reduced hydrophilicity (sPPN-H⁺, sPPB-H⁺, and sPPT-H⁺), each possessing 4 sulfonate moieties per repeat unit. The resultant membranes displayed varying mechanical properties, with sPPN-H⁺ and sPPB-H⁺ being robust and flexible, while sPPT-H⁺ was fragile due to poor solubility during polymerization. Mechanical measurements showed improved tensile strength and Young's modulus compared to Nafion 211, though elongation at break was lower. Water uptake and volumetric expansion decreased as polymer hydrophobicity increased, with sPPN-H⁺ > sPPB-H⁺ > sPPP-H⁺ > sPPT-H⁺. After exposure to Fenton's reagent, sPPN-H⁺ and sPPB-H⁺ membranes demonstrated no mass loss, no structural changes, and preserved mechanical integrity. Ex situ proton conductivities were on par with or exceeded a Nafion 211 reference under varying humidity conditions. In situ fuel cell performance showed promising results, with sPPB-H⁺ membranes closely matching Nafion 211, and sPPN-H⁺ outperforming a Nafion 212 reference. These findings emphasize the chemical and mechanical resilience of pre-

sulfonated sPPPs, highlighting their potential as effective and tunable PEMs for electrochemical energy conversion, such as fuel cells.

Sulfonated poly(phenylene)s (sPPs) and sulfonated poly(phenylene sulfone)s (sPPSs) are promising materials for proton-exchange membranes in fuel cells, each with its own advantages and disadvantages driven by their distinct chemical structures.

Hydrolytic Stability and Acidity: sPPS membranes generally offer superior hydrolytic stability compared to sPPs [170]. This advantage stems from the stronger electron-withdrawing effect of the sulfone group in sPPSs, which stabilizes the sulfonic acid groups against hydrolytic degradation. Moreover, the acidity of the sulfonic acid group in sPPSs is higher than in sPPs, again due to the sulfone group's ability to stabilize the negative charge on the sulfonate ion after proton dissociation. This higher acidity typically results in better proton conductivity in sPPS membranes under certain conditions.

Mechanical Stability and Water Uptake: While sPPS membranes excel in chemical stability, they tend to have higher water uptake compared to sPPs, which can lead to excessive swelling and compromise mechanical integrity. This high water uptake is advantageous for proton conductivity but can make sPPS membranes brittle when dry, particularly those with a high ion-exchange capacity. On the other hand, sPPs typically exhibit lower water uptake, which helps maintain better mechanical stability and reduces swelling under hydrated conditions, making them less prone to mechanical failure despite their lower hydrolytic stability.

In conclusion, sulfonated sPPS membranes offer significant advantages, including superior hydrolytic stability, thermal resistance, and higher sulfonic acid group acidity. However, their high water uptake can lead to swelling and reduced mechanical integrity, particularly in dry conditions. Reducing water uptake is therefore critical to enhance the performance and durability of sPPS membranes.

Conversely, sPPs while beneficial for their lower water uptake and better mechanical stability, suffer from poorer hydrolytic stability and lower proton conductivity compared to sPPSs.

Addressing the water uptake challenge in sPPSs through innovative research is essential to harness their full potential. The main target of this research was to overcome the sPPSs' disadvantages. By bridging these gaps, the advancements will contribute to more effective and reliable proton-exchange membranes in fuel cells, water electrolyzers and other advanced energy technologies.

2. Materials and Methods

2.1. Materials

Disulfonated 4,4'-difluorodiphenylsulfone (SDFDPS) was provided by FuMaTech GmbH and also was prepared according to the method we have developed and is described in detail below [171]. Before use it was dried at 150 °C in vacuum. Lithium sulfide (99.9 %, Alfa Aesar) was used as received without further purification or drying. Dialysis was carried out using SERVAPOR® dialysis tubing cellulose membrane (MWCO 12.000-14.000, pore diameter 25 Å). 4,4'-difluorodiphenylsulfone (DFDPS) was provided by FuMaTech GmbH, 4,4'-thiobisbenzenethiol (TBBT), 4,4'-oxybisbenzenethiol (OBBT) and PBI's® were received from FuMaTech GmbH. Ion-exchange was carried out using Amberlyst™ 15(H), ion-exchange resin (Alfa Aesar). Fuming sulfuric acid (20-30 % free SO₃ basis, Thermo Scientific), *N*-methyl-2-pyrrolidone (NMP) (≥ 99.8 %, extra dry stored over molecular sieve (4 Å), Carl Roth GmbH), 1,3-difluorobenzene (99 %, Alfa Aesar), 1,4-difluorobenzene (99+ %, Thermo Scientific), 1,3-dichlorobenzene (98 %, Thermo Fischer), 1,4-dichlorobenzene (99+ %, Thermo Scientific), Dimethylsulfoxide (DMSO) (≥ 99.5 %, Carl Roth), 4-fluorothiophenol (97 %, Thermo Scientific), 1,6-dibromohexane (97+%, Thermo Scientific), 1,10-dibromodecane (97 %, Thermo Scientific), Cyclohexane (≥ 99.5 %, Carl Roth GmbH), 1,2-dichloroethane (≥ 99 %, Carl Roth GmbH), Aluminum chloride (99 %, anhydrous, Alfa Aesar), *p*-terphenyl (99+%, pure, Thermo Scientific), Dimethylformamide (DMF) (≥ 99.5 %, Carl Roth GmbH), Lithium hydride (99.4 %, metals basis, Alfa Aesar), Dimethylacetamide (≥ 99 %, Carl Roth GmbH), 1,3,5-triphenylbenzene (95 %, Apollo Scientific), Dichloromethane (≥ 99.5 %, Carl Roth GmbH), Chloroform (≥ 99 %, Carl Roth GmbH), Methanol (≥ 99 %, Carl Roth GmbH), *n*-hexane (≥ 99 %, Carl Roth GmbH), Ethyl acetate (≥ 99 %, Sigma Aldrich), 1,4-dibromooctafluorobutane (98 %, Apollo Scientific), 4-fluorobenzenesulfonyl chloride (98 %, Thermo Scientific), Biphenyl (≥ 99 %, Sigma Aldrich), Potassium carbonate (≥ 99 %, Hatkim, Istanbul, Turkey), Sodium chloride (≥ 99 %, Hatkim, Istanbul, Turkey), Iron(III) chloride (98 %, anhydrous, Thermo Scientific), Silica gel (Chemapol), Glacial acetic acid (≥ 99 %, Hatkim, Istanbul, Turkey), Isopropanol (≥ 99 %, Hatkim, Istanbul, Turkey), 50 % hydrogen peroxide (GEOJEMI), Hydrochloric acid, 28-36 %, (Champion Technologies), Barium carbonate and

sulfuric acid, 97 % (Champion Technologies) were used without further purification. Bis(4-fluorophenyl)phenyl phosphine oxide (BFPPPO) was synthesized according to the reported procedure [172].

2.2. Characterization of monomers and polymers

Nuclear Magnetic Resonance (NMR) spectra were taken using a Benchtop Magritek Spinsolve 60 MHz, Bruker Avance II 250 and 300 MHz NMR spectrometers. 10-40 mg samples were dissolved in DMSO-*d*₆ or D₂O.

Infrared spectra were recorded on a Bruker Alpha II FT-IR spectrophotometer with ZnSe-ATR.

The melting temperatures of the prepared monomers and starting materials were determined on the device MPM-H3 melting point measuring unit.

To test the solubility, pre-vacuum dried (at 120 °C for 48 h) polymer samples were taken and solutions with a concentration of 1 % were prepared.

Membranes were prepared on the petri dishes by solution casting (1, 2.5, 5 or 10 wt %) using different solvents (DMAc, DMSO). All solutions were filtered with a disposable syringe filter CHROMAFIL Xtra GF 100/25 (pore size: nom. 1.0 or 2.7 μm, Filter - Ø: 25 mm).

Oxidative stability test was performed with Fenton's reagent (3 % H₂O₂, 2 ppm Fe²⁺) [128, 173]. The polymer film sample was placed in Fenton's reagent solution at 80 °C for 1 h, after which it was transferred in distilled water for 1 h to wash. After that, the sample was dried in a vacuum oven at 120 °C for 48 h. The differences in weight, intrinsic viscosities and ion-exchange capacities of the samples were measured before and after the test.

Proton conductivities of prepared membranes were measured by ac-impedance spectroscopy (HP-ac-impedance analyzer 4192A LF) in the frequency range from 10 Hz to 10 MHz with oscillating voltage of 0.1 V. The measurements were performed in a closed cell with preequilibrated samples (10-30 stacked slices of membranes with preadjusted water content, diameter ~ 6 mm, thickness 2-5 mm) with gold electrodes. Conductivity measurements in pure water vapor ($p(\text{H}_2\text{O}) = 10^5$ Pa) were carried out in a double-wall

temperature-controlled glass chamber with an open outlet at temperatures between 110 and 160 °C. Liquid water was continuously evaporated by a heater and injected into the chamber with a constant flow rate using a digital peristaltic pump (Ismatec). Inside the chamber membranes (10-20 stacked slices of membranes with diameter 8 mm and total thickness 2-4 mm) were placed in a porous cylindrical tube with a gold electrode at the bottom. The second gold electrode was pressed from the top onto the stack of membranes by a screw in order to ensure optimum contact. Conductivities were calculated from complex impedance spectra.

Leaching of sulfonated copolymers from blend membranes was studied by monitoring of IEC using automatic titrator (SI Analytics Titrator Titroline® 5000).

High-resolution NMR (Bruker Avance II 250 and 300 MHz NMR Spectrometer), GPC (1260 Infinity II, Agilent Technologies) and proton conductivity measurements were carried out at our collaborator institutes Max Planck Institute for Solid State Research (Stuttgart, Germany) and Hahn-Schickard (Freiburg, Germany).

For GPC measurements, solution of LiBr (0.5 %) in dimethylsulfoxide (DMSO) was used as an eluent. The polymer sample volume was 50 µl with a polymer content of 0.5 g/L in the solution, the elution rate — 1.0 mL/min, the temperature — 70 °C and polymethyl methacrylate (PMMA) was used as a standard.

The water uptake (WU) values were obtained by measuring the differences in the weight under different humidification. Prior to the measurements the films were thoroughly dried at 120 °C for 24 h and subsequently stored at an atmosphere of fixed RH until a constant weight was obtained. Different relative humidities were adjusted using different salt solutions [174]. Typically, the WU equilibrated within 48 h. The WU was calculated according to following equation:

$$\text{WU (\%)} = \frac{M_{\text{RH}} - M_{\text{dry}}}{M_{\text{dry}}} \times 100$$

where M_{RH} is the weight of the membrane at a specific RH and M_{dry} is the weight in the dry state. Water content λ (number of water molecules per sulfonic-acid group of ionomer) was calculated by the following equation [175, 176] to examine the WU of sPPSs:

$$\lambda = \frac{(M_w - M_0)/M_{H_2O}}{M_i/EW}$$

where M_0 and M_w are the initial weight of dried sample and the weight of humidified sample, respectively. M_{H_2O} is the molar weight of water ($18 \text{ g} \cdot \text{mol}^{-1}$), M_i is the dry weight of the sPPS ionomer in the sample, and EW is the equivalent weight of the ionomer.

Inherent viscosity was measured at $40 \text{ }^\circ\text{C}$ in DMSO (sample volume – 13 mL) at a polymer concentration $0.5 \text{ g} \cdot \text{dL}^{-1}$, using a Pinkevitch viscometer, and the resulting values were obtained by calculating specific viscosity $\eta_{sp} = t/t_0 - 1$, relative viscosity $\eta_{rel} = t/t_0$ and inherent viscosity $\eta_{inh} = (\ln\eta_{rel})/c$. The corresponding intrinsic viscosity was obtained by one-point method (Solomon-Ciuta equation [177]) as follows:

$$\eta_{int} = \frac{\sqrt{2(\eta_{sp} - \ln\eta_{rel})}}{c}$$

2.3. Synthesis of monomers with high sulfonation degree

2.3.1. Synthesis of SDFDPS

4,4'-difluorodiphenylsulfone DFDPS (0.0198 mol, 5.04 g) was placed in a 50 mL round-bottom flask, after which fuming sulfuric acid (11 mL) was added to it. The mixture was stirred for 24 hours at $140 \text{ }^\circ\text{C}$. To avoid loss of SO_3 , the system was connected to gas-bubbler filled with silicon oil.

After completion of sulfonation process, the solution was slowly poured into ice-water and BaCO_3 was added to precipitate BaSO_4 and neutralize the solution. Interestingly SDFDPS (Ba-form) does not precipitate in water in contrast to its chloride analogue — SDCDPS (Ba-form). Solution was concentrated using rotary evaporator, after which this concentrated aqueous solution of SDFDPS (Ba-form) was converted into Na-form using ion-exchange resin. Distilled water was fully removed using rotary evaporator, after which

SDFDPS (Na-form) was dried in vacuum at 150 °C several days. The product (7.64 g) was obtained by ~ 84 % yield.

2.3.2. Synthesis of SBFPPPO

Sulfonated bis(4-fluorophenyl)phenyl phosphine oxide SBFPPPO was prepared according to the procedure described above. The yield was 61.3 %.

2.3.3. Synthesis of DS-1,3-DFB

1,3-difluorobenzene 1,3-DFB (0.0439 mol, 5.01 g) was placed in a 50 mL round-bottom flask and fuming sulfuric acid (20 mL) was added to it. The mixture was slowly heated up to 80 °C and kept for 1 hour at this temperature to prevent evaporation of 1,3-DFB, then it was heated at 160 °C for 15 h.

After completion of sulfonation process, the solution was slowly poured into ice-water and BaCO₃ was added to precipitate BaSO₄ and neutralize the solution. Solution was concentrated on rotary evaporator and then concentrated aqueous solution of DS-1,3-DFB (Ba-form) was converted into Na-form using ion-exchange resin. Distilled water was fully removed using rotary evaporator, after which DS-1,3-DFB (sodium 4,6-difluorobenzene-1,3-disulfonate) was dried in vacuum at 150 °C several days. The product (11.31 g) was obtained in ~ 81 % yield.

2.3.4. Synthesis of DS-1,4-DFB

1,4-difluorobenzene 1,4-DFB (0.0447 mol, 5.10 g) was placed in a 50 mL round-bottom flask and fuming sulfuric acid (25 mL) was added to it. The reaction was carried out in an oil bath at 200 °C for 48 h with stirring.

After completion of sulfonation process, the solution was slowly poured into ice-water. After that, BaCO₃ was added to precipitate BaSO₄ and neutralize the solution. The solution was concentrated using rotary evaporator and this concentrated aqueous solution of DS-1,4-DFB (Ba-form) was converted into Na-form using ion-exchange resin. After ion-

exchange, the mixture consisted of two isomers: 2,5-difluorobenzene-1,3-disulfonate and 2,5-difluorobenzene-1,4-disulfonate with a ratio of 0.56 : 0.44. To separate the isomers, we carried out recrystallization from an *i*-PrOH/H₂O mixture (8 : 1), which yielded pure 2,5-difluorobenzene-1,3-disulfonate with a ~ 54 % yield (7.65 g).

2.3.5. Synthesis of DS-1,3-DCB

4,6-dichlorobenzene-1,3-disulfonate (DS-1,3-DCB) was prepared following the procedure described above. After ion-exchange no further purification was needed. The yield was 80.6 %.

2.3.6. Synthesis of DS-1,4-DCB

2,5-dichlorobenzene-1,4-disulfonate (DS-1,4-DCB) was prepared following the procedure described above. After ion-exchange, there was a mixture of 1,4-sulfonated and 1,3-sulfonated products with a ratio of 0.91 : 0.09. No additional separation of the mixture was undertaken. The yield of isomer mixture was 73.1 %.

2.4. Synthesis of poly(phenylene sulfone) based statistical copolymers with different linking groups via TBBT route

2.4.1. Synthesis of sPPS-435

2.4.1.1. Synthesis of sPPSS precursor of sPPS-435

The polymerization was conducted in a dried and nitrogen-filled 100 mL round-bottom flask equipped with a nitrogen gas inlet, magnetic stirrer and condenser. The flask was charged with disodium 3,3'-disulfonate-4,4'-difluorodiphenylsulfone SDFDPS (0.0113 mol, 5.1668 g), 4,4'-difluorodiphenylsulfone DFDPS (0.0030 mol, 0.7669 g; it is taken into account 99.5 % purity of DFDPS), 4,4'-thiobisbenzenethiol TBBT (0.0143 mol, 3.5742 g), K₂CO₃ (1.5 equiv, 0.0214 mol, 2.9592 g), cyclohexane (7 mL) and NMP (14 mL). Azeotropic distillation was carried out at 125 °C for 4 h, after which the reaction was carried out at 200 °C for 8 h. After cooling to room temperature, NMP (35 mL) was added to dilute the mixture. Finally, the the product was precipitated by pouring into isopropanol (1 L). The precipitate

was separated by filtration, washed with isopropanol and dried at 80 °C. In order to remove all by- and low-molecular products, the polymer was purified by dialysis against distilled water for 72 h (SERVAPOR® dialysis tubing cellulose membrane, MWCO 12.000-14.000, pore diameter 25 Å). The water was removed with a rotary evaporator and the product was dried at 110 °C. Sulfonated poly(phenylene sulfide sulfone) — sPPSS (8.75 g, Na-form) was obtained in ~ 98 % yield.

2.4.1.2. Synthesis of sPPS-435

Dried precursor was oxidized following the same procedure as described by Schuster et. al. [14]. Dried sPPSS was oxidized by 50 % H₂O₂ in glacial acetic acid (200 L) and concentrated sulfuric acid (15 mL) mixture at 80 °C. Oxidation was carried out for 2 days. Product precipitates from the solution and is separated by filtration once the reaction is complete. The polymer was converted to H-form using a 10 % HCl solution. In order to remove all byproducts, the aqueous polymer solution was dialyzed for 72 h (SERVAPOR® dialysis tubing cellulose membrane, MWCO 12.000-14.000, pore diameter 25 Å). The water was removed using a rotary evaporator and the product was dried at 80 °C in vacuo. Sulfonated poly(phenylene sulfone) — sPPS-435 (9.41 g, H-form) was obtained in ~ 96 % yield.

2.4.2. Synthesis of sPPS-435-CO

2.4.2.1. Synthesis of sPPSS precursor of sPPS-435-CO

The polymerization was conducted in a dried and nitrogen-filled 50 mL round-bottom flask equipped with a nitrogen gas inlet, magnetic stirrer and condenser. The flask was charged with disodium 3,3'-disulfonate-4,4'-difluorodiphenylsulfone SDFDPS-Na (0.0062 mol, 2.8568 g), 4,4'-difluorodiphenylketone DFDPK (0.0018 mol, 0.3949 g; calculation takes into account 98 % purity of DFDPK), 4,4'-thiobisbenzenethiol TBBT (0.0080 mol, 2.0048 g), K₂CO₃ (1.5 equiv, 0.0120 mol, 1.6598 g), cyclohexane (4 mL) and NMP (8 mL). Azeotropic distillation was carried out at 125 °C for 4 h, after which the reaction was carried out at 200 °C for 8 h. After cooling to room temperature, NMP (20 mL) was added

to dilute the mixture. Finally, the dark reaction mixture was precipitated in isopropanol (700 mL). The precipitate was separated by filtration, washed with isopropanol and dried at 80 °C. In order to remove all by- and low-molecular products, the polymer was purified by dialysis against distilled water for 72 h (SERVAPOR® dialysis tubing cellulose membrane, MWCO 12.000-14.000, pore diameter 25 Å). The water was removed with a rotary evaporator and the product was dried at 110 °C. Sulfonated poly(phenylene sulfide sulfone) — sPPSS-CO (4.53 g, Na-form) was obtained in ~ 92 % yield.

2.4.2.2. Synthesis of sPPS-435-CO

Dried sPPSS-CO was oxidized by 50 % H₂O₂ in glacial acetic acid (150 L) and concentrated sulfuric acid (8 mL) mixture at 80 °C. Oxidation lasted 2 days. Product precipitates from the solution and is separated by filtration once the reaction is complete. The polymer was converted to H-form using a 10 % HCl solution. In order to remove all byproducts, the aqueous polymer solution was dialyzed for 72 h (SERVAPOR® dialysis tubing cellulose membrane, MWCO 12.000-14.000, pore diameter 25 Å). The water was removed using a rotary evaporator and the product was dried at 80 °C in vacuo. Sulfonated poly(phenylene sulfone) — sPPS-435-CO (4.77 g, H-form) was obtained in ~ 88 % yield.

2.4.3. Synthesis of sPPS-435-O

2.4.3.1. Synthesis of sPPSS precursor of sPPS-435-O

The polymerization was conducted in a dried and nitrogen-filled 50 mL round-bottom flask equipped with a nitrogen gas inlet, magnetic stirrer and condenser. The flask was charged with disodium 3,3'-disulfonate-4,4'-difluorodiphenylsulfone SDFDPS-Na (0.0062 mol, 2.8286 g), 4,4'-difluorodiphenylsulfone DFDPS (0.0024 mol, 0.6071 g; calculation takes into account 99.5 % purity of DFDPS), 4,4'-oxybisbenzenethiol OBBT (0.0085 mol, 2.0029 g), K₂CO₃ (1.5 equiv, 0.0128 mol, 1.7719 g), cyclohexane (4 mL) and NMP (8 mL). Azeotropic distillation was carried out at 125 °C for 4 h, after which the reaction was carried out at 200 °C for 8 h. After cooling to room temperature, NMP (20 mL) was added to dilute the mixture. Finally, the dark reaction mixture was precipitated in isopropanol (700

mL). The precipitate was separated by filtration, washed with isopropanol and dried at 80 °C. In order to remove all by- and low-molecular products, the polymer was purified by dialysis against distilled water for 72 h (SERVAPOR® dialysis tubing cellulose membrane, MWCO 12.000-14.000, pore diameter 25 Å). The water was removed with a rotary evaporator and the product was dried at 110 °C. Sulfonated poly(phenylene sulfide sulfone) — sPPSS (4.48 g, Na-form) was obtained in ~ 88 % yield.

2.4.3.2. Synthesis of sPPS-435-O

Dried sPPSS was oxidized by 50 % H₂O₂ in glacial acetic acid (150 L) and concentrated sulfuric acid (8 mL) mixture at 80 °C. Oxidation lasted 2 days. Product precipitates from the solution and is separated by filtration once the reaction is complete. The polymer was converted to H-form using a 10 % HCl solution. In order to remove all byproducts, the aqueous polymer solution was dialyzed for 72 h (SERVAPOR® dialysis tubing cellulose membrane, MWCO 12.000-14.000, pore diameter 25 Å). The water was removed using a rotary evaporator and the product was dried at 80 °C in vacuo. Sulfonated poly(phenylene sulfone) — sPPS-435-O (4.35 g, H-form) was obtained in ~ 81 % yield.

2.5. Synthesis of poly(phenylene sulfone) based statistical copolymers with different equivalent weights via Li₂S route

2.5.1. Synthesis of sPPS-240

2.5.1.1. Synthesis of sPPSS precursor of sPPS-240

The polymerization was conducted in a dried and nitrogen-filled 500 mL round-bottom flask equipped with a nitrogen gas inlet, mechanical stirrer and condenser. The flask was charged with disodium 3,3'-disulfonate-4,4'-difluorodiphenylsulfone SDFDPS-Na (0.1914 mol, 87.7059 g), 4,4'-difluorodiphenylsulfone DFDPS (0.0270 mol, 6.9033 g; calculation takes into account 99.5 % purity of DFDPS), lithium sulfide (0.2184 mol, 10.0272 g; calculation takes into account 99.95 % purity of Li₂S) and NMP (102 mL). The reaction was carried out at 200 °C for 8 h. After cooling to room temperature, NMP (250 mL) was added to dilute the mixture. Finally, the dark reaction mixture was precipitated in isopropanol (3

L). The precipitate was separated by filtration, washed with isopropanol and dried at 80 °C. In order to remove all by- and low-molecular products, the polymer was purified by dialysis against distilled water for 72 h (SERVAPOR® dialysis tubing cellulose membrane, MWCO 12.000-14.000, pore diameter 25 Å). The water was removed with a rotary evaporator and the product was dried at 110 °C. Sulfonated poly(phenylene sulfide sulfone) — sPPSS(85.6 g, Na-form) was obtained in ~ 92 % yield.

2.5.1.2. Synthesis of sPPS-240

sPPSS was suspended in a glacial acetic acid (1.5 L) and concentrated sulfuric acid (130 mL) mixture at 80 °C, after which 50 % H₂O₂ was dropwise added. Oxidation was carried out 4 days. Product precipitates from the solution and is separated by filtration once the reaction is complete. The polymer was converted to H-form using a 15 % HCl solution. In order to remove all byproducts, the aqueous polymer solution was dialyzed for 72 h (SERVAPOR® dialysis tubing cellulose membrane, MWCO 12.000-14.000, pore diameter 25 Å). The water was removed using a rotary evaporator and the product was dried at 80 °C in vacuo. Sulfonated poly(phenylene sulfone) — sPPS-240 (74.4 g, H-form) was obtained in ~ 81 % yield.

2.5.2. Synthesis of sPPS-253.5

2.5.2.1. Synthesis of sPPSS precursor of sPPS-253.5

The polymerization was conducted in a dried and nitrogen-filled 500 mL round-bottom flask equipped with a nitrogen gas inlet, mechanical stirrer and condenser. The flask was charged with disodium 3,3'-disulfonate-4,4'-difluorodiphenylsulfone SDFDPS-Na (0.1543 mol, 70.7267 g), 4,4'-difluorodiphenylsulfone DFDPS (0.0366 mol, 9.3650 g; calculation takes into account 99.5 % purity of DFDPS), lithium sulfide (0.1910 mol, 8.7685 g; calculation takes into account 99.95 % purity of Li₂S) and NMP (87 mL). The reaction was carried out at 200 °C for 8 h. After cooling to room temperature, NMP (200 mL) was added to dilute the mixture. Finally, the dark reaction mixture was precipitated in isopropanol (2.5 L). The precipitate was separated by filtration, washed with isopropanol and dried at 80 °C.

In order to remove all by- and low-molecular products, the polymer was purified by dialysis against distilled water for 72 h (SERVAPOR® dialysis tubing cellulose membrane, MWCO 12.000-14.000, pore diameter 25 Å). The water was removed with a rotary evaporator and the product was dried at 110 °C. Sulfonated poly(phenylene sulfide sulfone) — sPPSS (74.6 g, Na-form) was obtained in ~ 95 % yield.

2.5.2.2. Synthesis of sPPS-253.5

Dried sPPSS was oxidized by 50 % H₂O₂ in glacial acetic acid (1.2 L) and concentrated sulfuric acid (112 mL) mixture at 80 °C. Oxidation was carried out for 4 days. Product precipitates from the solution and is separated by filtration once the reaction is complete. The polymer was converted to H-form using a 15 % HCl solution. In order to remove all byproducts, the aqueous polymer solution was dialyzed for 72 h (SERVAPOR® dialysis tubing cellulose membrane, MWCO 12.000-14.000, pore diameter 25 Å). The water was removed using a rotary evaporator and the product was dried at 80 °C in vacuo. Sulfonated poly(phenylene sulfone) — sPPS-253.5 (66.5 g, H-form) was obtained in ~ 85 % yield.

2.5.3. Synthesis of sPPS-260

2.5.3.1. Synthesis of sPPSS precursor of sPPS-260

The polymerization was conducted in a dried and nitrogen-filled 1000 mL round-bottom flask equipped with a nitrogen gas inlet, mechanical stirrer and condenser. The flask was charged with disodium 3,3'-disulfonate-4,4'-difluorodiphenylsulfone SDFDPS-Na (0.2748 mol, 125.9280 g), 4,4'-difluorodiphenylsulfone DFDPS (0.0780 mol, 19.9303 g; calculation takes into account 99.5 % purity of DFDPS), lithium sulfide (0.3528 mol, 16.1973 g; calculation takes into account 99.95 % purity of Li₂S) and NMP (158 mL). The reaction was carried out at 200 °C for 8 h. After cooling to room temperature, NMP (390 mL) was added to dilute the mixture. Finally, the dark reaction mixture was precipitated in isopropanol (3.5 L). The precipitate was separated by filtration, washed with isopropanol and dried at 80 °C. In order to remove all by- and low-molecular products, the polymer was purified by dialysis against distilled water for 72 h (SERVAPOR® dialysis tubing cellulose membrane, MWCO

12.000-14.000, pore diameter 25 Å). The water was removed with a rotary evaporator and the product was dried at 110 °C. Sulfonated poly(phenylene sulfide sulfone) — sPPSS (139.3 g, Na-form) was obtained in ~ 97 % yield.

2.5.3.2. Synthesis of sPPS-260

Dried sPPSS was oxidized by 50 % H₂O₂ in glacial acetic acid (2.5 L) and concentrated sulfuric acid (208 mL) mixture at 80 °C. Oxidation was carried out for 4 days. Product precipitates from the solution and is separated by filtration once the reaction is complete. The polymer was converted to H-form using a 15 % HCl solution. In order to remove all byproducts, the aqueous polymer solution was dialyzed for 72 h (SERVAPOR® dialysis tubing cellulose membrane, MWCO 12.000-14.000, pore diameter 25 Å). The water was removed using a rotary evaporator and the product was dried at 80 °C in vacuo. Sulfonated poly(phenylene sulfone) — sPPS-260 (133.1 g, H-form) was obtained in ~ 93 % yield.

2.5.4. Synthesis of sPPS-275

2.5.4.1. Synthesis of sPPSS precursor of sPPS-275

The polymerization was conducted in a dried and nitrogen-filled 500 mL round-bottom flask equipped with a nitrogen gas inlet, magnetic stirrer and condenser. The flask was charged with disodium 3,3'-disulfonate-4,4'-difluorodiphenylsulfone SDFDPS-Na (0.1901 mol, 87.1230 g), 4,4'-difluorodiphenylsulfone DFDPS (0.0743 mol, 18.9872 g; calculation takes into account 99.5 % purity of DFDPS), lithium sulfide (0.2644 mol, 12.1402 g; calculation takes into account 99.95 % purity of Li₂S) and NMP (115 mL). The reaction was carried out at 200 °C for 8 h. After cooling to room temperature, NMP (250 mL) was added to dilute the mixture. Finally, the dark reaction mixture was precipitated in isopropanol (2.5 L). The precipitate was separated by filtration, washed with isopropanol and dried at 80 °C. In order to remove all by- and low-molecular products, the polymer was purified by dialysis against distilled water for 72 h (SERVAPOR® dialysis tubing cellulose membrane, MWCO 12.000-14.000, pore diameter 25 Å). The water was removed with a rotary evaporator and

the product was dried at 110 °C. Sulfonated poly(phenylene sulfide sulfone) — sPPSS (102.4 g, Na-form) was obtained in ~ 98 % yield.

2.5.4.2. Synthesis of sPPS-275

Dried sPPSS was oxidized by 50 % H₂O₂ in glacial acetic acid (2 L) and concentrated sulfuric acid (150 mL) mixture at 80 °C. Oxidation was carried out for 4 days. Product precipitates from the solution and is separated by filtration once the reaction is complete. The polymer was converted to H-form using a 15 % HCl solution. In order to remove all byproducts, the aqueous polymer solution was dialyzed for 72 h (SERVAPOR® dialysis tubing cellulose membrane, MWCO 12.000-14.000, pore diameter 25 Å). The water was removed using a rotary evaporator and the product was dried at 80 °C in vacuo. Sulfonated poly(phenylene sulfone) — sPPS-275 (100.2 g, H-form) was obtained in ~ 96 % yield.

2.5.5. Synthesis of sPPS-280

2.5.5.1. Synthesis of sPPSS precursor of sPPS-280

The polymerization was conducted in a dried and nitrogen-filled 50 mL round-bottom flask equipped with a nitrogen gas inlet, magnetic stirrer and condenser. The flask was charged with disodium 3,3'-disulfonate-4,4'-difluorodiphenylsulfone SDFDPS-Na (0.0108 mol, 4.9664 g), 4,4'-difluorodiphenylsulfone DFDPs (0.0046 mol, 1.1811 g; calculation takes into account 99.5 % purity of DFDPs), lithium sulfide (0.0155 mol, 0.7098 g; calculation takes into account 99.95 % purity of Li₂S) and NMP (7 mL). The reaction was carried out at 200 °C for 8 h. After cooling to room temperature, NMP (20 mL) was added to dilute the mixture. Finally, the dark reaction mixture was precipitated in isopropanol (500 mL). The precipitate was separated by filtration, washed with isopropanol and dried at 80 °C. In order to remove all by- and low-molecular products, the polymer was purified by dialysis against distilled water for 72 h (SERVAPOR® dialysis tubing cellulose membrane, MWCO 12.000-14.000, pore diameter 25 Å). The water was removed with a rotary evaporator and the product was dried at 110 °C. Sulfonated poly(phenylene sulfide sulfone) — sPPSS (5.8 g, Na-form) was obtained in ~ 96 % yield.

2.5.5.2. Synthesis of sPPS-280

Dried sPPSS was oxidized by 50 % H₂O₂ in glacial acetic acid (100 mL) and concentrated sulfuric acid (8 mL) mixture at 80 °C. Oxidation was carried out for 4 days. Product precipitates from the solution and is separated by filtration once the reaction is complete. The polymer was converted to H-form using a 15 % HCl solution. In order to remove all byproducts, the aqueous polymer solution was dialyzed for 72 h (SERVAPOR® dialysis tubing cellulose membrane, MWCO 12.000-14.000, pore diameter 25 Å). The water was removed using a rotary evaporator and the product was dried at 80 °C in vacuo. Sulfonated poly(phenylene sulfone) — sPPS-280 (5.6 g, H-form) was obtained in ~ 92 % yield.

2.5.6. Synthesis of sPPS-300

2.5.6.1. Synthesis of sPPSS precursor of sPPS-300

The polymerization was conducted in a dried and nitrogen-filled 50 mL round-bottom flask equipped with a nitrogen gas inlet, magnetic stirrer and condenser. The flask was charged with disodium 3,3'-disulfonate-4,4'-difluorodiphenylsulfone SDFDPS-Na (0.0069 mol, 3.1829 g), 4,4'-difluorodiphenylsulfone DFDPs (0.0040 mol, 1.0102 g; calculation takes into account 99.5 % purity of DFDPs), lithium sulfide (0.0109 mol, 0.5004 g; calculation takes into account 99.95 % purity of Li₂S) and NMP (4.6 mL). The reaction was carried out at 200 °C for 8 h. After cooling to room temperature, NMP (12 mL) was added to dilute the mixture. Finally, the dark reaction mixture was precipitated in isopropanol (400 mL). The precipitate was separated by filtration, washed with isopropanol and dried at 80 °C. In order to remove all by- and low-molecular products, the polymer was purified by dialysis against distilled water for 72 h (SERVAPOR® dialysis tubing cellulose membrane, MWCO 12.000-14.000, pore diameter 25 Å). The water was removed with a rotary evaporator and the product was dried at 110 °C. Sulfonated poly(phenylene sulfide sulfone) — sPPSS (3.9 g, Na-form) was obtained in ~ 95 % yield.

2.5.6.2. Synthesis of sPPS-300

Dried sPPSS was oxidized by 50 % H₂O₂ in glacial acetic acid (100 mL) and concentrated sulfuric acid (8 mL) mixture at 80 °C. Oxidation was carried out for 3 days. Product precipitates from the solution and is separated by filtration once the reaction is complete. The polymer was converted to H-form using a 15 % HCl solution. In order to remove all byproducts, the aqueous polymer solution was dialyzed for 72 h (SERVAPOR® dialysis tubing cellulose membrane, MWCO 12.000-14.000, pore diameter 25 Å). The water was removed using a rotary evaporator and the product was dried at 80 °C in vacuo. Sulfonated poly(phenylene sulfone) — sPPS-300 (3.8 g, H-form) was obtained in ~ 92 % yield.

2.5.7. Synthesis of statistical sPPS-360

2.5.7.1. Synthesis of sPPSS precursor of statistical sPPS-360

The polymerization was conducted in a dried and nitrogen-filled 50 mL round-bottom flask equipped with a nitrogen gas inlet, magnetic stirrer and condenser. The flask was charged with disodium 3,3'-disulfonate-4,4'-difluorodiphenylsulfone SDFDPS-Na (0.0146 mol, 6.6913 g), 4,4'-difluorodiphenylsulfone DFDPS (0.0146 mol, 3.7207 g; calculation takes into account 99.5 % purity of DFDPS), lithium sulfide (0.0292 mol, 1.3403 g; calculation takes into account 99.95 % purity of Li₂S) and NMP (11.5 mL). The reaction was carried out at 200 °C for 8 h. After cooling to room temperature, NMP (30 mL) was added to dilute the mixture. Finally, the dark reaction mixture was precipitated in isopropanol (500 mL). The precipitate was separated by filtration, washed with isopropanol and dried at 80 °C. In order to remove all by- and low-molecular products, the polymer was purified by dialysis against distilled water for 72 h (SERVAPOR® dialysis tubing cellulose membrane, MWCO 12.000-14.000, pore diameter 25 Å). The water was removed with a rotary evaporator and the product was dried at 110 °C. Sulfonated poly(phenylene sulfide sulfone) — sPPSS (9.42 g, Na-form) was obtained in ~ 92 % yield.

2.5.7.2. Synthesis of statistical sPPS-360

Dried sPPSS was oxidized by 50 % H₂O₂ in glacial acetic acid (200 mL) and concentrated sulfuric acid (15 mL) mixture at 80 °C. Oxidation was carried out for 2 days. Product precipitates from the solution and is separated by filtration once the reaction is complete. The polymer was converted to H-form using a 15 % HCl solution. In order to remove all byproducts, the aqueous polymer solution was dialyzed for 72 h (SERVAPOR® dialysis tubing cellulose membrane, MWCO 12.000-14.000, pore diameter 25 Å). The water was removed using a rotary evaporator and the product was dried at 80 °C in vacuo. Sulfonated poly(phenylene sulfone) — statistical sPPS-360 (9.21 g, H-form) was obtained in ~ 95 % yield.

2.6. Experimental study of polymer leaching from polymer blends

2.6.1. Preparation of the blends of sPPS-240 and sPPS-260 with PBI-00

Solutions of the sPPS polymers in DMSO (5 wt %) were first neutralized with Et₃N and then mixed with the appropriate amount of PBI-00 dissolved in the same solvent (5 wt %), to obtain blends with IEC_{theor.} = 2.21 meq/g.

2.6.2. Leaching experiments on sPPS-240 and sPPS-260 blends with PBI-00

The blend was divided into several portions and the samples were placed in a 250 mL single-necked round-bottomed flask filled with distilled water. The samples were heated in water at 80 °C under stirring conditions. The samples were removed after 24, 60 and 168 h, washed with distilled water and then placed in a vacuum oven at 120 °C for 48 h to dry. After drying and treatment with a concentrated solution of NaCl, the ion-exchange capacity was determined using an automatic titrator.

2.7. Synthesis of microblock copolymers containing an alkyl and perfluoroalkyl main chains

2.7.1. Synthesis of microblock monomers containing an alkyl and perfluoroalkyl main chains

2.7.1.1. Synthesis of FDPS-Hex-FDPS

2.7.1.1.1. Synthesis of precursor of FDPS-Hex-FDPS

3.0040 g (0.0234 mol) of 4-fluorothiophenol was weighed under nitrogen in a 250 mL two-necked round-bottomed flask placed in a glove box. 125 mL of DMF was poured onto it and the resulting mixture was cooled using an ice bath. After 20 minutes of cooling, 0.2235 g (0.0281 mol) of LiH, weighed under nitrogen, was also added to the reaction mixture; After 30 min, 2.5992 g (0.0107 mol) of 1,6-dibromohexane was added, after which a white precipitate was formed. The reaction was left for 19 h.

After completion of the reaction, the reaction mixture was concentrated to dryness on a rotary evaporator; In order to isolate the product, the residue was dissolved in ethyl acetate. The ethyl acetate-insoluble phase was removed by filtration. The resulting filtrate was concentrated to a dry residue, after which the latter was dried in a vacuum oven at 65 °C for 24 h.

After drying, the resulting residue was dissolved in hot *n*-hexane, after which the obtained product began to crystallize intensively in the form of white needle-like crystals. After crystallization, the resulting precipitate was filtered, washed with a small amount of cold *n*-hexane. The precursor 1,6-bis((4-fluorophenyl)thio)hexane was obtained with a yield of ~ 71 % (2.56 g). mp 89-90 °C.

2.7.1.1.2. Synthesis of FDPS-Hex-FDPS

The dry residue was transferred to a 250 mL single-necked round-bottomed flask, on which 125 mL of glacial acetic acid was poured. The reaction mixture was heated in an oil bath at 80 °C, after which 5 mL of 50 % H₂O₂ was added to the latter for oxidation. After 15

h, 3 mL of 50 % H₂O₂ was added. The oxidation was considered complete when the reaction mixture became colorless.

To remove excess 50 % H₂O₂, the reaction mixture was heated to 100 °C for 1 h. The resulting clear solution was concentrated on a rotary evaporator, after which the flask was placed in a refrigerator to crystallize the product. The desired product crystallized as white lustrous crystals. FDPS-Hex-FDPS (1,6-bis((4-fluorophenyl)sulfonyl)hexane) was obtained with a yield of ~ 94 % (2.86 g). mp 140-141 °C.

2.7.1.2. Synthesis of FDPS-Dec-FDPS

4.000 g (0.0312 mol) of 4-fluorothiophenol was weighed under nitrogen in a 250 mL two-necked round-bottomed flask placed in a glove box. 166 mL of DMF was poured onto it and the resulting mixture was cooled using an ice bath. After 20 minutes of cooling, 0.3000 g (0.0375 mol) of LiH, weighed under nitrogen, was also added to the reaction mixture; After 30 min, 4.2570 g (0.0142 mol) of 1,10-dibromodecane was added, after which a white precipitate was formed. The reaction was left for 19 h.

After completion of the reaction, the reaction mixture was concentrated to dryness on a rotary evaporator; In order to isolate the product, the residue was dissolved in ethyl acetate. The ethyl acetate-insoluble phase was removed by filtration. The resulting filtrate was concentrated to a dry residue, after which the latter was dried in a vacuum oven at 60 °C for 24 h.

The dry residue was transferred to a 250 mL single-necked round-bottomed flask, on which 150 mL of glacial acetic acid was poured. The reaction mixture was heated in an oil bath at 80 °C, after which 10 mL of 50 % H₂O₂ was added to the latter for oxidation. After 15 h, 5 mL of 50 % H₂O₂ was added. The oxidation was considered complete when the reaction mixture completely lost its color.

To remove excess 50 % H₂O₂, the reaction mixture was heated to 100 °C for 1 h. The resulting clear solution was concentrated on a rotary evaporator, after which the flask was placed in a refrigerator to crystallize the product. The desired product crystallized as white

lustrous crystals. FDPS-Dec-FDPS (1,10-bis((4-fluorophenyl)sulfonyl)decane) was obtained with a yield of ~ 61 % (3.98 g). mp 135-136 °C.

2.7.1.3. Synthesis of FDPS-CF₂(4)-FDPS

5.0000 g (0.0390 mol) of 4-fluorothiophenol was weighed under nitrogen in a 500 mL three-necked round-bottomed flask placed in a glove box. 250 mL of DMF was poured onto it and the resulting mixture was cooled using an ice bath. After 20 minutes of cooling, 0.3721 g (0.0468 mol) of LiH, weighed under nitrogen, was also added to the reaction mixture; After 30 min, 6.3810 g (0.0177 mol) of 1,4-dibromooctafluorobutane was added, after which the solution turned yellow. The reaction was left for 19 h.

After completion of the reaction, the reaction mixture was concentrated to dryness on a rotary evaporator; In order to isolate the product, the resulting dry residue was dissolved in dichloromethane; The insoluble part was removed by filtration. The obtained filtrate was washed 3 times with concentrated NaCl (292 g/800 mL) solution, and finally 1 time with distilled water. The dichloromethane fraction was dried using anhydrous Na₂SO₄ for 2 h.

The dichloromethane fraction was separated by filtration, after which the product was obtained after solvent removal. Thin layer chromatographic analysis of the product (eluent: dichloromethane) showed that it contained 3 different compounds with close *R_f* values. The procedure described in 2.7.1.1. and 2.7.1.2. was carried out on the obtained dry residue.

The dry residue was transferred to a 250 mL single-necked round-bottomed flask, on which 125 mL of glacial acetic acid was poured. The reaction mixture was heated in an oil bath at 80 °C, after which 5 mL of 50 % H₂O₂ was added to the latter for oxidation. The next day, 3 mL of 50 % H₂O₂ was added. The oxidation was considered complete when the reaction mixture turned completely white.

To remove excess 50 % H₂O₂, the reaction mixture was heated to 100 °C for 1 h. The resulting precipitate was filtered on a glass filter, after which the latter was washed several

times with distilled water to neutral pH until the acetic acid was completely removed. The resulting precipitate was dried in a vacuum oven at 80 °C for 24 h. FDPS-CF₂(4)-FDPS (4,4'-(perfluorobutane-1,4-diyl)disulfonyl)bis(fluorobenzene)) was obtained with a yield of ~ 58 % (5.33 g).

2.7.2. Synthesis of poly(phenylene sulfone)s containing alkyl and perfluoroalkyl main chains

2.7.2.1. Synthesis of sPPS-400-Hex-XXL

2.7.2.1.1. Synthesis of sPPSS precursor of sPPS-400-Hex-XXL

Into a 100-mL one-necked round-bottom flask equipped with a dean-stark and reflux condenser was placed 6.1146 g (0.0244 mol) 4,4'-thiobisbenzenethiol (TBBT), 3.7125 g (0.0269 mol, 1.1x excess) K₂CO₃, 10.0668 g (0.0220 mol) sodium 5,5'-sulfonylbis(2-fluorobenzenesulfonate) (SDFDPS), 0.9885 g (0.0025 mol) 1,6-bis((4-fluorophenyl)sulfonyl)hexane FDPS-Hex-FDPS, 12.5 mL cyclohexane and 25 mL of *N*-methylpyrrolidone.

Azeotropic distillation under nitrogen was carried out for 4 h. After 4 h, a cyclohexane/water layer was removed, after which the temperature was increased up to 200 °C. Polymerization was carried out for 8 h.

After completion of reaction, reaction mixture was precipitated in 500 mL of isopropanol. Obtained precipitate was washed several times with isopropyl alcohol and then the obtained dry residue was dialyzed against water using a dialysis membrane (SERVAPOR[®] dialysis tubing cellulose membrane, MWCO 12000-14000, pore diameter 25 Å). Dialysis was performed for 72 h.

In order to obtain a dry residue, water was distilled on a rotary evaporator and the obtained dry residue was dried in a vacuum oven at 100 °C for 24 h. sPPSS 15.71 g, Na-form) was obtained in ~ 97 % yield.

2.7.2.1.2. Synthesis of sPPS-400-Hex-XXL

sPPSS precursor was placed in a 500 mL one-necked round-bottomed flask, onto which was poured 300 mL of glacial acetic acid, 22 mL conc. sulfuric acid and 15 mL of 50 % hydrogen peroxide was added dropwise. After 15 h, addition of hydrogen peroxide was continued until the reaction mixture became completely white. Oxidation was carried out at 80 °C for 48 h. Oxidized polymer precipitated in acetic acid was collected by filtration, after which the obtained residue was dialyzed against water using a dialysis membrane (SERVAPOR® dialysis tubing cellulose membrane, MWCO 12000-14000, pore diameter 25 Å), until the pH of dialysis water became neutral.

In order to obtain the desired product, the obtained aqueous solution was concentrated to a dry residue, after which the latter was transferred to a 1000 mL beaker in a pre-filled 10 % hydrochloric acid solution, in order to convert the polymer into its acidic form. After several acid exchanges, the obtained product was collected by filtration, washed with distilled water until neutral pH, after which it was dried in a vacuum oven at 80 °C for 24 h. sPPS-400-Hex-XXL (16.22 g, H-form) was obtained in ~ 95 % yield.

2.7.2.2. Synthesis of sPPS-390-Dec-XXL

2.7.2.2.1. Synthesis of sPPSS precursor of sPPS-390-Dec-XXL

Into a 100-mL one-necked round-bottom flask equipped with a dean-stark and reflux condenser was placed 6.000 g (0.0240 mol) 4,4'-thiobisbenzenethiol (TBBT), 3.6429 g (0.0264 mol, 1.1x excess) K₂CO₃, 10.1930 g (0.0222 mol) sodium 5,5'-sulfonylbis(2-fluorobenzenesulfonate) (SDFDPS), 0.7901 g (0.0017 mol) 1,10-bis((4-fluorophenyl)sulfonyl)-decane FDPS-Dec-FDPS, 12.5 mL cyclohexane and 25 mL of *N*-methylpyrrolidone.

Azeotropic distillation under nitrogen was carried out for 4 h. After 4 h, a cyclohexane/water layer was removed, after which the temperature was increased up to 200 °C. Polymerization was carried out for 8 h.

After completion of reaction, reaction mixture was precipitated in 500 mL of isopropanol. Obtained precipitate was washed several times with isopropyl alcohol and then

the obtained dry residue was dialyzed against water using a dialysis membrane (SERVAPOR® dialysis tubing cellulose membrane, MWCO 12000-14000, pore diameter 25 Å). Dialysis was performed for 72 h.

In order to obtain a dry residue, water was distilled on a rotary evaporator and the obtained dry residue was dried in a vacuum oven at 100 °C for 24 h. sPPSS (15.68 g, Na-form) was obtained in ~ 98 % yield.

2.7.2.2.2. Synthesis of sPPS-390-Dec-XXL

sPPSS precursor was placed in a 500 mL one-necked round-bottomed flask, onto which was poured 300 mL of glacial acetic acid, 22 mL conc. sulfuric acid and 15 mL of 50 % hydrogen peroxide was added dropwise. After 15 h, addition of hydrogen peroxide was continued until the reaction mixture became completely white. Oxidation was carried out at 80 °C for 48 h. Oxidized polymer precipitated in acetic acid was collected by filtration, after which the obtained residue was dialyzed against water using a dialysis membrane (SERVAPOR® dialysis tubing cellulose membrane, MWCO 12000-14000, pore diameter 25 Å), until the pH of dialysis water became neutral.

In order to obtain the desired product, the obtained aqueous solution was concentrated to a dry residue, after which the latter was transferred to a 1000 mL beaker in a pre-filled 10 % hydrochloric acid solution, in order to convert the polymer into its acidic form. After several acid exchanges, the obtained product was collected by filtration, washed with distilled water until neutral pH, after which it was dried in a vacuum oven at 80 °C for 24 h. sPPS-390-Dec-XXL (16.15 g, H-form) was obtained in ~ 95 % yield.

2.7.2.3. Synthesis of sPPS-410-CF₂(4)-XXL

2.7.2.3.1. Synthesis of sPPSS precursor of sPPS-410-CF₂(4)-XXL

Into a 50-mL one-necked round-bottom flask equipped with a dean-stark and reflux condenser was placed 2.0119 g (0.0080 mol) 4,4'-thiobisbenzenethiol (TBBT), 1.6657 g

(0.0121 mol) K_2CO_3 , 3.2870 g (0.0072 mol) sodium 5,5'-sulfonylbis(2-fluorobenzene-sulfonate) (SDFDPS), 0.4519 g (0.0009 mol) 4,4'-perfluorobutane-1,4-diyl-disulfonyl-bis-(fluorobenzene) FDPS-(CF_2)₄-FDPS, 4 mL cyclohexane and 8.5 mL of *N*-methylpyrrolidone.

Azeotropic distillation under nitrogen was carried out for 4 h. After 4 h, a cyclohexane/water layer was removed, after which the temperature was increased up to 200 °C. Polymerization was carried out for 8 h.

After completion of reaction, reaction mixture was precipitated in 250 mL of isopropanol. Obtained precipitate was washed several times with isopropyl alcohol and then the obtained dry residue was dialyzed against water using a dialysis membrane (SERVAPOR® dialysis tubing cellulose membrane, MWCO 12000-14000, pore diameter 25 Å). Dialysis was performed for 72 h.

In order to obtain a dry residue, water was distilled on a rotary evaporator and the obtained dry residue was dried in a vacuum oven at 100 °C for 24 h. sPPSS (4.51 g, Na-form) was obtained in ~ 83 % yield.

2.7.2.3.2. Synthesis of sPPS-410-CF₂(4)-XXL

sPPSS precursor was placed in a 250 mL one-necked round-bottomed flask, onto which was poured 100 mL of glacial acetic acid, 8 mL conc. sulfuric acid and 5 mL of 50 % hydrogen peroxide was added dropwise. After 15 h, addition of hydrogen peroxide was continued until the reaction mixture became completely white. Oxidation was carried out at 80 °C for 48 h. Oxidized polymer precipitated in acetic acid was collected by filtration, after which the obtained residue was dialyzed against water using a dialysis membrane (SERVAPOR® dialysis tubing cellulose membrane, MWCO 12000-14000, pore diameter 25 Å), until the pH of dialysis water became neutral.

in order to obtain the desired product, the obtained aqueous solution was concentrated to a dry residue, after which the latter was transferred to a 1000 mL beaker in a pre-filled 10 % hydrochloric acid solution, in order to convert the polymer into its acidic form. after several acid exchanges, the obtained product was collected by filtration, washed

with distilled water until neutral pH, after which it was dried in a vacuum oven at 80 °C for 24 h. sPPS-410-CF₂(4)-XXL (4.31 g, H-form) was obtained in ~ 88 % yield.

2.7.2.4. Synthesis of sPPS-430-CF₂(4)-XXL

2.7.2.4.1. Synthesis of sPPSS precursor of sPPS-430-CF₂(4)-XXL

Into a 50-mL one-necked round-bottom flask equipped with a dean-stark and reflux condenser was placed 1.3118 g (0.0052 mol) 4,4'-thiobisbenzenethiol (TBBT), 1.0861 g (0.0079 mol) K₂CO₃, 2.0543 g (0.0045 mol) sodium 5,5'-sulfonylbis(2-fluorobenzene-sulfonate) (SDFDPS), 0.3963 g (0.0008 mol) 4,4'-perfluorobutane-1,4-diyldisulfonyl)bis-(fluorobenzene) FDPS-(CF₂)₄-FDPS, 3 mL cyclohexane and 5.5 mL of *N*-methylpyrrolidone.

Azeotropic distillation under nitrogen was carried out for 4 h. After 4 h, a cyclohexane/water layer was removed, after which the temperature was increased up to 200 °C. Polymerization was carried out for 8 h.

After completion of reaction, reaction mixture was precipitated in 250 mL of isopropanol. Obtained precipitate was washed several times with isopropyl alcohol and then the obtained dry residue was dialyzed against water using a dialysis membrane (SERVAPOR® dialysis tubing cellulose membrane, MWCO 12000-14000, pore diameter 25 Å). Dialysis was performed for 72 h.

In order to obtain a dry residue, water was distilled on a rotary evaporator and the obtained dry residue was dried in a vacuum oven at 100 °C for 24 h. sPPSS (3.06 g, Na-form) was obtained in ~ 86 % yield.

2.7.2.4.2. Synthesis of sPPS-430-CF₂(4)-XXL

sPPSS precursor was placed in a 250 mL one-necked round-bottomed flask, onto which was poured 60 mL of glacial acetic acid, 4 mL conc. sulfuric acid and 4 mL of 50 % hydrogen peroxide was added dropwise. After 15 h, addition of hydrogen peroxide was continued until the reaction mixture became completely white. Oxidation was carried out at 80 °C for 48 h. Oxidized polymer precipitated in acetic acid was collected by filtration, after

which the obtained residue was dialyzed against water using a dialysis membrane (SERVAPOR® dialysis tubing cellulose membrane, MWCO 12000-14000, pore diameter 25 Å), until the pH of dialysis water became neutral.

in order to obtain the desired product, the obtained aqueous solution was concentrated to a dry residue, after which the latter was transferred to a 1000 mL beaker in a pre-filled 10 % hydrochloric acid solution, in order to convert the polymer into its acidic form. after several acid exchanges, the obtained product was collected by filtration, washed with distilled water until neutral pH, after which it was dried in a vacuum oven at 80 °C for 24 h. sPPS-430-CF₂(4)-XXL (2.99 g, H-form) was obtained in ~ 90 % yield.

2.8. Synthesis of microblock copolymers containing phenylene moieties

2.8.1. Synthesis of microblock monomers containing phenylene moieties

2.8.1.1. Synthesis of FDPS-BP-FDPS

The synthesis of FDPS-BP-FDPS was carried out following the procedure described in the patent [178].

Into a 250 mL 3-necked round-bottom flask equipped with a mechanical stirrer and condenser was placed 23 mL of 1,2-dichloroethane, after which 11.6332 g (0.0873 mol) of AlCl₃ was placed in the flask under nitrogen. Then, 15.6731 g (0.0805 mol, 7 % excess) of 4-fluorobenzenesulfonyl chloride 4-FBSC and 6.0000 g (0.0389 mol) of biphenyl were added to the reaction mixture. The reaction mixture soon acquired a dark purple color. The reaction was carried out under reflux conditions for 4 h, after which the reaction mixture was cooled for about 30 min and 70 mL of a 2/1 (v/v) MeOH/H₂O mixture was added dropwise over 10 min. Brownish-white precipitate was formed in the solution, after which reflux was continued for 1 hour. The obtained solid residue was transferred to 2 % HCl solution, after which it was washed several times with distilled water and finally with methanol. For purification, the obtained product was recrystallized from chloroform. FDPS-BP-FDPS (4,4'-bis((4-fluorophenyl)sulfonyl)-1,1'-biphenyl) was obtained by ~ 68 % yield (12.47 g). mp 267-268 °C.

2.8.1.2. Synthesis of FDPS-*p*-TP-FDPS

The synthesis of FDPS-*p*-TP-FDPS was carried out following the procedure described in the patent [178].

Into a 250 mL 3-necked round-bottom flask equipped with a mechanical stirrer and condenser was placed 23 mL of 1,2-dichloroethane, after which 7.7894 g (0.0584 mol) of AlCl₃ was placed in the flask under nitrogen. Then, 10.4945 g (0.0539 mol, 7 % excess) of 4-fluorobenzenesulfonyl chloride 4-FBSC and 6.0000 g (0.0261 mol) of *p*-terphenyl were added to the reaction mixture. The reaction mixture soon acquired a dark burgundy color. The reaction was carried out under reflux conditions for 4 h, after which the reaction mixture was cooled for about 30 min and 70 mL of a 2/1 (v/v) MeOH/H₂O mixture was added dropwise over 10 min. Brownish-white precipitate was formed in the solution, after which reflux was carried out for 1 hour. The obtained solid residue was transferred to 2 % HCl solution, after which it was washed several times with distilled water and finally with methanol. Due to the insolubility of the obtained product, it was not possible to characterize it by NMR spectroscopy. Its purification was carried out by washing with different solvents (ethyl acetate, acetone, 1,2-dichloroethane) through Soxhlet. The resulting compound was dissolved only in hot NMP and TLC was performed with the latter, where only one spot appeared, indicating the purity of the product.

2.8.2. Synthesis of poly(phenylene sulfone)s containing phenylene moieties

2.8.2.1. Synthesis of sPPS-400-BP-XXL

2.8.2.1.1. Synthesis of sPPSS precursor of sPPS-400-BP-XXL

Into a 100-mL one-necked round-bottom flask equipped with a dean-stark and reflux condenser was placed 3.5106 g (0.0140 mol) 4,4'-thiobisbenzenethiol (TBBT), 2.1315 g (0.0154 mol, 1.1x excess) K₂CO₃, 5.8310 g (0.0127 mol) sodium 5,5'-sulfonylbis(2-fluorobenzenesulfonate) (SDFDPS), 0.6107 g (0.0013 mol) 4,4'-bis((4-fluorophenyl)sulfonyl)-1,1'-biphenyl FDPS-BP-FDPS, 8 mL cyclohexane and 14.5 mL of *N*-methylpyrrolidone.

Azeotropic distillation under nitrogen was carried out for 4 h. After 4 h, a cyclohexane/water layer was removed, after which the temperature was increased up to 200 °C. Polymerization was carried out for 8 h.

After completion of reaction, reaction mixture was precipitated in 500 mL of isopropanol. Obtained precipitate was washed several times with isopropyl alcohol and then the obtained dry residue was dialyzed against water using a dialysis membrane (SERVAPOR® dialysis tubing cellulose membrane, MWCO 12000-14000, pore diameter 25 Å). Dialysis was performed for 72 h.

In order to obtain a dry residue, water was distilled on a rotary evaporator and the obtained dry residue was dried in a vacuum oven at 100 °C for 24 h. sPPSS (9.11 g, Na-form) was obtained in ~ 97 % yield.

2.8.2.1.2. Synthesis of sPPS-400-BP-XXL

sPPSS precursor was placed in a 250 mL one-necked round-bottomed flask, onto which was poured 180 mL of glacial acetic acid, 15 mL conc. sulfuric acid and 10 mL of 50 % hydrogen peroxide was added dropwise. After 15 h, addition of hydrogen peroxide was continued until the reaction mixture completely became white. Oxidation was carried out at 80 °C for 48 h. Oxidized polymer precipitated in acetic acid was collected by filtration, after which the obtained residue was dialyzed against water using a dialysis membrane (SERVAPOR® dialysis tubing cellulose membrane, MWCO 12000-14000, pore diameter 25 Å), until the pH of dialysis water became neutral.

In order to obtain the desired product, the obtained aqueous solution was concentrated to a dry residue, after which the latter was transferred to a 1000 mL beaker in a pre-filled 10 % hydrochloric acid solution, in order to convert the polymer into its acidic form. After several acid exchanges, the obtained product was collected by filtration, washed with distilled water until neutral pH, after which it was dried in a vacuum oven at 80 °C for 24 h. sPPS-400-BP-XXL (9.60 g, H-form) was obtained in ~ 97 % yield.

2.8.2.2. Synthesis of sPPS-410-*p*-TP-XXL

2.8.2.2.1. Synthesis of sPPSS precursor of sPPS-410-*p*-TP-XXL

Into a 100-mL one-necked round-bottom flask equipped with a dean-stark, magnetic stirrer and reflux condenser, was placed 2.5591 g (0.0102 mol) 4,4'-thiobisbenzenethiol (TBBT), 2.1188 g (0.0153 mol, 1.5x excess) K₂CO₃, 4.1960 g (0.0092 mol) sodium 5,5'-sulfonylbis(2-fluorobenzenesulfonate) (SDFDPS), 0.5942 g (0.0011 mol, the calculation takes into account 98 % purity of FDPS-*p*-TP-FDPS) bis(4-((4-((4-fluorophenyl)sulfonyl)-phenyl)thio)phenyl)sulfane FDPS-*p*-TP-FDPS, 6 mL cyclohexane and 11 mL of *N*-methylpyrrolidone.

Azeotropic distillation under nitrogen was carried out for 4 h. After 4 h, a cyclohexane/water layer was removed, after which the temperature was increased up to 200 °C. Polymerization was carried out for 8 h.

After completion of reaction, reaction mixture was precipitated in 500 mL of isopropanol. Obtained precipitate was washed several times with isopropyl alcohol and then the obtained dry residue was dialyzed against water using a dialysis membrane (SERVAPOR® dialysis tubing cellulose membrane, MWCO 12000-14000, pore diameter 25 Å). Dialysis was performed for 72 h.

In order to obtain a dry residue, water was distilled on a rotary evaporator and the obtained dry residue was dried in a vacuum oven at 100 °C for 24 h. sPPSS (6.81 g, Na-form) was obtained in ~ 98 % yield.

2.8.2.2.2. Synthesis of sPPS-410-*p*-TP-XXL

sPPSS precursor was placed in a 250 mL one-necked round-bottomed flask, onto which was poured 140 mL of glacial acetic acid, 10 mL conc. sulfuric acid and 8 mL of 50 % hydrogen peroxide was added dropwise. After 15 h, addition of hydrogen peroxide was continued until the reaction mixture completely became white. Oxidation was carried out at 80 °C for 48 h. Oxidized polymer precipitated in acetic acid was collected by filtration, after which the obtained residue was dialyzed against water using a dialysis membrane

(SERVAPOR® dialysis tubing cellulose membrane, MWCO 12000-14000, pore diameter 25 Å), until the pH of dialysis water became neutral.

In order to obtain the desired product, the obtained aqueous solution was concentrated to a dry residue, after which the latter was transferred to a 1000 mL beaker in a pre-filled 10 % hydrochloric acid solution, in order to convert the polymer into its acidic form. After several acid exchanges, the obtained product was collected by filtration, washed with distilled water until neutral pH, after which it was dried in a vacuum oven at 80 °C for 24 h. sPPS-410-*p*-TP-XXL (7.16 g, H-form) was obtained in ~ 97 % yield.

2.8.2.3. Synthesis of sPPS-430-*p*-TP-XXL

2.8.2.3.1. Synthesis of sPPSS precursor of sPPS-430-*p*-TP-XXL

Into a 100-mL one-necked round-bottom flask equipped with a dean-stark, magnetic stirrer and reflux condenser, was placed 2.5545 g (0.0102 mol) 4,4'-thiobisbenzenethiol (TBBT), 2.1149 g (0.0153 mol, 1.5x excess) K₂CO₃, 4.0196 g (0.0088 mol) sodium 5,5'-sulfonylbis(2-fluorobenzenesulfonate) (SDFDPS), 0.7986 g (0.0014 mol, the calculation takes into account 98 % purity of FDPS-*p*-TP-FDPS) bis(4-((4-((4-fluorophenyl)sulfonyl)phenyl)thio)phenyl)sulfane FDPS-*p*-TP-FDPS, 6 mL cyclohexane and 11 mL of *N*-methylpyrrolidone.

Azeotropic distillation under nitrogen was carried out for 4 h. After 4 h, a cyclohexane/water layer was removed, after which the temperature was increased up to 200 °C. Polymerization was carried out for 8 h.

After completion of reaction, reaction mixture was precipitated in 500 mL of isopropanol. Obtained precipitate was washed several times with isopropyl alcohol and then the obtained dry residue was dialyzed against water using a dialysis membrane (SERVAPOR® dialysis tubing cellulose membrane, MWCO 12000-14000, pore diameter 25 Å). Dialysis was performed for 72 h.

In order to obtain a dry residue, water was distilled on a rotary evaporator and the obtained dry residue was dried in a vacuum oven at 100 °C for 24 h. sPPSS (6.86 g, Na-form) was obtained in ~ 99 % yield.

2.8.2.3.2. Synthesis of sPPS-430-*p*-TP-XXL

sPPSS precursor was placed in a 250 mL one-necked round-bottomed flask, onto which was poured 150 mL of glacial acetic acid, 10 mL conc. sulfuric acid and 8 mL of 50 % hydrogen peroxide was added dropwise. After 15 h, addition of hydrogen peroxide was continued until the reaction mixture became completely white. Oxidation was carried out at 80 °C for 48 h. Oxidized polymer precipitated in acetic acid was collected by filtration, after which the obtained residue was dialyzed against water using a dialysis membrane (SERVAPOR® dialysis tubing cellulose membrane, MWCO 12000-14000, pore diameter 25 Å), until the pH of dialysis water became neutral.

In order to obtain the desired product, the obtained aqueous solution was concentrated to a dry residue, after which the latter was transferred to a 1000 mL beaker in a pre-filled 10 % hydrochloric acid solution, in order to convert the polymer into its acidic form. After several acid exchanges, the obtained product was collected by filtration, washed with distilled water until neutral pH, after which it was dried in a vacuum oven at 80 °C for 24 h. sPPS-430-*p*-TP-XXL (7.35 g, H-form) was obtained in ~ 99 % yield.

2.8.2.4. Synthesis of sPPS-450-*p*-TP-XXL

2.8.2.4.1. Synthesis of sPPSS precursor of sPPS-450-*p*-TP-XXL

Into a 100-mL one-necked round-bottom flask equipped with a dean-stark, magnetic stirrer and reflux condenser, was placed 2.5662 g (0.0102 mol) 4,4'-thiobisbenzenethiol (TBBT), 2.1246 g (0.0154 mol, 1.5x excess) K₂CO₃, 3.8815 g (0.0085 mol) sodium 5,5'-sulfonylbis(2-fluorobenzenesulfonate) (SDFDPS), 0.9927 g (0.0018 mol, the calculation takes into account 98 % purity of FDPS-*p*-TP-FDPS) bis(4-((4-((4-fluorophenyl)sulfonyl)phenyl)thio)phenyl)sulfane FDPS-*p*-TP-FDPS, 6 mL cyclohexane and 11 mL of *N*-methylpyrrolidone.

Azeotropic distillation under nitrogen was carried out for 4 h. After 4 h, a cyclohexane/water layer was removed, after which the temperature was increased up to 200 °C. Polymerization was carried out for 8 h.

After completion of reaction, reaction mixture was precipitated in 500 mL of isopropanol. Obtained precipitate was washed several times with isopropyl alcohol and then the obtained dry residue was dialyzed against water using a dialysis membrane (SERVAPOR® dialysis tubing cellulose membrane, MWCO 12000-14000, pore diameter 25 Å). Dialysis was performed for 72 h.

In order to obtain a dry residue, water was distilled on a rotary evaporator and the obtained dry residue was dried in a vacuum oven at 100 °C for 24 h. sPPSS (6.92 g, Na-form) was obtained in ~ 99 % yield.

2.8.2.4.2. Synthesis of sPPS-450-*p*-TP-XXL

sPPSS precursor was placed in a 250 mL one-necked round-bottomed flask, onto which was poured 150 mL of glacial acetic acid, 10 mL conc. sulfuric acid and 8 mL of 50 % hydrogen peroxide was added dropwise. After 15 h, addition of hydrogen peroxide was continued until the reaction mixture became completely white. Oxidation was carried out at 80 °C for 48 h. Oxidized polymer precipitated in acetic acid was collected by filtration, after which the obtained residue was dialyzed against water using a dialysis membrane (SERVAPOR® dialysis tubing cellulose membrane, MWCO 12000-14000, pore diameter 25 Å), until the pH of dialysis water became neutral.

In order to obtain the desired product, the obtained aqueous solution was concentrated to a dry residue, after which the latter was transferred to a 1000 mL beaker in a pre-filled 10 % hydrochloric acid solution, in order to convert the polymer into its acidic form. After several acid exchanges, the obtained product was collected by filtration, washed with distilled water until neutral pH, after which it was dried in a vacuum oven at 80 °C for 24 h. sPPS-450-*p*-TP-XXL (7.37 g, H-form) was obtained in ~ 98 % yield.

2.9. Synthesis of microblock copolymers containing merely sulfone units

2.9.1. Synthesis of microblock monomers containing sulfur and sulfone units

2.9.1.1. Synthesis of FDPS-S-FDPS

Into a 100 mL three-necked round-bottom flask equipped with a reflux condenser and a magnetic stirrer was placed 0.5000 g (0.0109 mol) of lithium sulfide, 11.0688 g (0.0435 mol, ~2x excess) of 4,4'-difluorodiphenylsulfone DFDPS and 19 mL of DMAc. The temperature was increased up to 80 °C and the reaction was carried out under these conditions for 6 h, and then the temperature was increased up to 100 °C for 12 h.

To remove DMAc, the reaction mixture was concentrated on a rotary evaporator to a solid residue, after which the latter was washed several times first with hot water and then with hot isopropanol.

The solid residue was purified by column chromatography (silica gel, eluent: chloroform) to isolate the desired product. A white powder was obtained in ~ 32 % yield (1.75 g). mp 185-186 °C.

2.9.1.2. Synthesis of FDPS-TBB-FDPS

Into a 500 mL three-necked round-bottom flask equipped with a reflux condenser and a mechanical stirrer was placed 16.8526 g (0.0673 mol) of 4,4'-thiobisbenzenethiol TBBT, 10.2320 g (0.0740 mol, 1.1x excess) K₂CO₃, 68 mL of cyclohexane and 60 mL of DMAc. Azeotropic distillation was carried out at 125 °C for 4 h under nitrogen. After this process, the reaction mixture was cooled to 60 °C, after which a solution of 68.4493 g (0.2692 mol, ~2x excess) of 4,4'-difluorodiphenylsulfone DFDPS in 76 mL of DMAc was added under nitrogen. The temperature was increased up to 80 °C and the reaction was carried out under these conditions for 6 h, and then the temperature was increased up to 100 °C for 12 h.

To remove DMAc, the reaction mixture was concentrated on a rotary evaporator to a solid residue, after which the latter was washed several times first with hot water and then with hot isopropanol.

The solid residue was recrystallized from chloroform to isolate the desired product. A white powder was obtained in ~ 68 % yield (48.38 g). mp: 159-161 °C.

2.9.2. Synthesis of poly(phenylene sulfone)s with microblock segments containing merely sulfone units

2.9.2.1. Synthesis of sPPS-400-L

2.9.2.1.1. Synthesis of sPPSS precursor of sPPS-400-L

Into a 100-mL one-necked round-bottom flask equipped with a dean-stark, magnetic stirrer and reflux condenser, was placed 1.0257 g (0.0041 mol) 4,4'-thiobisbenzenethiol (TBBT), 0.6228 g (0.0045 mol, 1.1x excess) K₂CO₃, 1.7158 g (0.0085 mol) sodium 5,5'-sulfonylbis(2-fluorobenzenesulfonate) (SDFDPS), 0.9927 g bis(4-((4-fluorophenyl)-sulfonyl)phenyl)sulfane FDPS-S-FDPS, 3 mL cyclohexane and 4.5 mL of *N*-methylpyrrolidone.

Azeotropic distillation under nitrogen was carried out for 4 h. After 4 h, a cyclohexane/water layer was removed, after which the temperature was increased up to 200 °C. Polymerization was carried out for 8 h.

After completion of reaction, reaction mixture was precipitated in 500 mL of isopropanol. Obtained precipitate was washed several times with isopropyl alcohol and then the obtained dry residue was dialyzed against water using a dialysis membrane (SERVAPOR® dialysis tubing cellulose membrane, MWCO 12000-14000, pore diameter 25 Å). Dialysis was performed for 72 h.

In order to obtain a dry residue, water was distilled on a rotary evaporator and the obtained dry residue was dried in a vacuum oven at 100 °C for 24 h. sPPSS (2.65 g, Na-form) was obtained in ~ 96 % yield.

2.9.2.1.2 Synthesis of sPPS-400-L

sPPSS precursor was placed in a 100 mL one-necked round-bottomed flask, onto which was poured 60 mL of glacial acetic acid, 4 mL conc. sulfuric acid and 4 mL of 50 %

hydrogen peroxide was added dropwise. After 15 h, addition of hydrogen peroxide was continued until the reaction mixture became completely white. Oxidation was carried out at 80 °C for 48 h. Oxidized polymer precipitated in acetic acid was collected by filtration, after which the obtained residue was dialyzed against water using a dialysis membrane (SERVAPOR® dialysis tubing cellulose membrane, MWCO 12000-14000, pore diameter 25 Å), until the pH of dialysis water became neutral.

In order to obtain the desired product, the obtained aqueous solution was concentrated to a dry residue, after which the latter was transferred to a 1000 mL beaker in a pre-filled 10 % hydrochloric acid solution, in order to convert the polymer into its acidic form. After several acid exchanges, the obtained product was collected by filtration, washed with distilled water until neutral pH, after which it was dried in a vacuum oven at 80 °C for 24 h. sPPS-400-L (2.74 g, H-form) was obtained in ~ 95 % yield.

2.9.2.2. Synthesis of sPPS-390-XXL

2.9.2.2.1. Synthesis of sPPSS precursor of sPPS-390-XXL

Into a 500-mL three-necked round-bottom flask equipped with a dean-stark, mechanical stirrer and reflux condenser, was placed 47.9331 g (0.1914 mol) 4,4'-thiobisbenzenethiol (TBBT), 29.1025 g (0.2106 mol, 1.1x excess) K₂CO₃, 83.3343 g (0.1818 mol) sodium 5,5'-sulfonylbis(2-fluorobenzenesulfonate) (SDFDPS), 6.9782 g (0.0096 mol, the calculation takes into account 99 % purity of FDPS-TBB-FDPS) bis(4-((4-fluorophenyl)sulfonyl)phenyl)thio)phenyl)sulfane FDPS-TBB-FDPS, 101 mL cyclohexane and 202 mL of *N*-methylpyrrolidone.

Azeotropic distillation under nitrogen was carried out for 4 h. After 4 h, a cyclohexane/water layer was removed, after which the temperature was increased up to 200 °C. Polymerization was carried out for 8 h.

After completion of reaction, reaction mixture was precipitated in 500 mL of isopropanol. Obtained precipitate was washed several times with isopropyl alcohol and then the obtained dry residue was dialyzed against water using a dialysis membrane

(SERVAPOR® dialysis tubing cellulose membrane, MWCO 12000-14000, pore diameter 25 Å). Dialysis was performed for 72 h.

In order to obtain a dry residue, water was distilled on a rotary evaporator and the obtained dry residue was dried in a vacuum oven at 100 °C for 24 h. sPPSS (126.24 g, Na-form) was obtained in ~ 96 % yield.

2.9.2.2.2. Synthesis of sPPS-390-XXL

SPPSS precursor was placed in a 4 L four-necked round-bottomed reactor, onto which was poured 2.5 L of glacial acetic acid, 180 mL conc. sulfuric acid and 125 mL of 50 % hydrogen peroxide was added dropwise. After 15 h, addition of hydrogen peroxide was continued until the reaction mixture became completely white. Oxidation was carried out at 80 °C for 72 h. Oxidized polymer precipitated in acetic acid was collected by filtration, after which the obtained residue was dialyzed against water using a dialysis membrane (SERVAPOR® dialysis tubing cellulose membrane, MWCO 12000-14000, pore diameter 25 Å), until the pH of dialysis water became neutral.

In order to obtain the desired product, the obtained aqueous solution was concentrated to a dry residue, after which the latter was transferred to a 1000 mL beaker in a pre-filled 10 % hydrochloric acid solution, in order to convert the polymer into its acidic form. After several acid exchanges, the obtained product was collected by filtration, washed with distilled water until neutral pH, after which it was dried in a vacuum oven at 80 °C for 24 h. sPPS-390-XXL (132.44 g, H-form) was obtained in ~ 97 % yield.

2.10. Synthesis of microblock copolymers with different branching degree

2.10.1. Synthesis of the branching agent

2.10.1.1. Synthesis of 1,3,5-FPS-PB

The synthesis was carried out following the procedure reported in the literature [179].

Triphenylbenzene (2.718 g, 0.0089 mol) and 4-fluorobenzenesulfonyl chloride (11.975 g, 0.0617 mol, ~2.3x excess) were placed in a 100 mL three-necked round-bottom flask containing a magnetic stirrer, condenser, and N₂ inlet, all under a nitrogen atmosphere. After heating at 100 °C for 5 min, nitrobenzene (10 mL) was added into the mixture while stirring, followed by the slow addition of FeCl₃ (1.028 g, 0.0063 mol). The mixture was stirred at 100 °C for 3 h, then cooled and poured into a solution of MeOH (90 mL) and concentrated HCl (5 mL) with vigorous stirring. The resulting precipitate was filtered, washed with 3 % HCl aqueous solution, followed by distilled water and dried under vacuum at 50 °C overnight. The product was further purified by recrystallization from glacial acetic acid and then by column chromatography (silica gel, eluent: EtOAc/*n*-hexane = 5/1, v/v). 1,3,5-FPS-PB (1,3,5-tris(4-(4-fluorophenylsulfonyl)phenyl)benzene) was obtained in ~ 58 % yield (4.02 g).

2.10.2. Synthesis of branched poly(phenylene sulfone)s with microblock segments

2.10.2.1. Synthesis of sPPS-400-XXL (with 0.25 % branching agent)

2.10.2.1.1. Synthesis of sPPSS precursor of sPPS-400-XXL (with 0.25 % branching agent)

Into a 50-mL one-necked round-bottom flask equipped with a dean-stark, magnetic stirrer and reflux condenser, was placed 2.0519 g (0.0082 mol) 4,4'-thiobisbenzenethiol (TBBT), 1.2458 g (0.0090 mol, 1.1x excess) K₂CO₃, 3.5042 g (0.0076 mol) sodium 5,5'-sulfonylbis(2-fluorobenzenesulfonate) (SDFDPS), 0.3726 g (0.0005 mol) bis(4-((4-(4-fluorophenyl)sulfonyl)phenyl)thio)phenyl)sulfane FDPS-TBB-FDPS, 0.0160 g (0.00002 mol) 4,4''-bis((4-fluorophenyl)sulfonyl)-5'-(4-((4-fluorophenyl)sulfonyl)phenyl)-1,1':3',1''-terphenyl 1,3,5-FPS-PB, 5 mL cyclohexane and 9 mL of *N*-methylpyrrolidone.

Azeotropic distillation under nitrogen was carried out for 4 h. After 4 h, a cyclohexane/water layer was removed, after which the temperature was increased up to 200 °C. Polymerization was carried out for 8 h.

After completion of reaction, reaction mixture was precipitated in 300 mL of isopropanol. Obtained precipitate was washed several times with isopropyl alcohol and then the obtained dry residue was dialyzed against water using a dialysis membrane (SERVAPOR® dialysis tubing cellulose membrane, MWCO 12000-14000, pore diameter 25 Å). Dialysis was performed for 72 h.

In order to obtain a dry residue, water was distilled on a rotary evaporator and the obtained dry residue was dried in a vacuum oven at 100 °C for 24 h. sPPSS (5.56 g, Na-form) was obtained in ~ 98 % yield.

2.10.2.1.2. Synthesis of sPPS-400-XXL (with 0.25 % branching agent)

SPPSS precursor was placed in a 250 mL one-necked round-bottomed flask, onto which was poured 120 mL of glacial acetic acid, 8 mL conc. sulfuric acid and 6 mL of 50 % hydrogen peroxide was added dropwise. After 15 h, addition of hydrogen peroxide was continued until the reaction mixture became completely white. Oxidation was carried out at 80 °C for 48 h. Oxidized polymer precipitated in acetic acid was collected by filtration, after which the obtained residue was dialyzed against water using a dialysis membrane (SERVAPOR® dialysis tubing cellulose membrane, MWCO 12000-14000, pore diameter 25 Å), until the pH of dialysis water became neutral.

In order to obtain the desired product, the obtained aqueous solution was concentrated to a dry residue, after which the latter was transferred to a 1000 mL beaker in a pre-filled 10 % hydrochloric acid solution, in order to convert the polymer into its acidic form. After several acid exchanges, the obtained product was collected by filtration, washed with distilled water until neutral pH, after which it was dried in a vacuum oven at 80 °C for 24 h. sPPS-400-XXL (with 0.25 % branching agent) (5.77 g, H-form) was obtained in ~ 96 % yield.

2.10.2.2. Synthesis of sPPS-400-XXL (with 0.50 % branching agent)

2.10.2.2.1. Synthesis of sPPSS precursor of sPPS-400-XXL (with 0.50 % branching agent)

Into a 50-mL one-necked round-bottom flask equipped with a dean-stark, magnetic stirrer and reflux condenser, was placed 2.0113 g (0.0080 mol) 4,4'-thiobisbenzenethiol (TBBT), 1.2212 g (0.0088 mol, 1.1x excess) K₂CO₃, 3.4305 g (0.0075 mol) sodium 5,5'-sulfonylbis(2-fluorobenzenesulfonate) (SDFDPS), 0.3505 g (0.0005 mol) bis(4-((4-(4-fluorophenyl)sulfonyl)phenyl)thio)phenyl)sulfane FDPS-TBB-FDPS, 0.0314 g (0.00004 mol) 4,4''-bis((4-fluorophenyl)sulfonyl)-5'-(4-((4-fluorophenyl)sulfonyl)phenyl)-1,1':3',1''-terphenyl 1,3,5-FPS-PB, 5 mL cyclohexane and 9 mL of *N*-methylpyrrolidone.

Azeotropic distillation under nitrogen was carried out for 4 h. After 4 h, a cyclohexane/water layer was removed, after which the temperature was increased up to 200 °C. Polymerization was carried out for 8 h.

After completion of reaction, reaction mixture was precipitated in 300 mL of isopropanol. Obtained precipitate was washed several times with isopropyl alcohol and then the obtained dry residue was dialyzed against water using a dialysis membrane (SERVAPOR® dialysis tubing cellulose membrane, MWCO 12000-14000, pore diameter 25 Å). Dialysis was performed for 72 h.

In order to obtain a dry residue, water was distilled on a rotary evaporator and the obtained dry residue was dried in a vacuum oven at 100 °C for 24 h. sPPSS (5.35 g, Na-form) was obtained in ~ 96 % yield.

2.10.2.2.2. Synthesis of sPPS-400-XXL (with 0.50 % branching agent)

sPPSS precursor was placed in a 250 mL one-necked round-bottomed flask, onto which was poured 110 mL of glacial acetic acid, 8 mL conc. sulfuric acid and 6 mL of 50 % hydrogen peroxide was added dropwise. After 15 h, addition of hydrogen peroxide was continued until the reaction mixture was became completely white. Oxidation was carried out at 80 °C for 48 h. Oxidized polymer precipitated in acetic acid was collected by filtration,

after which the obtained residue was dialyzed against water using a dialysis membrane (SERVAPOR® dialysis tubing cellulose membrane, MWCO 12000-14000, pore diameter 25 Å), until the pH of dialysis water became neutral.

In order to obtain the desired product, the obtained aqueous solution was concentrated to a dry residue, after which the latter was transferred to a 1000 mL beaker in a pre-filled 10 % hydrochloric acid solution, in order to convert the polymer into its acidic form. After several acid exchanges, the obtained product was collected by filtration, washed with distilled water until neutral pH, after which it was dried in a vacuum oven at 80 °C for 24 h. sPPS-400-XXL (with 0.50 % branching agent) (5.46 g, H-form) was obtained in ~ 94 % yield.

2.10.2.3. Synthesis of sPPS-400-XXL (with 1.00 % branching agent)

2.10.2.3.1. Synthesis of sPPSS precursor of sPPS-400-XXL (with 1.00 % branching agent)

Into a 50-mL one-necked round-bottom flask equipped with a dean-stark, magnetic stirrer and reflux condenser, was placed 2.0136 g (0.0080 mol) 4,4'-thiobisbenzenethiol (TBBT), 1.2226 g (0.0088 mol, 1.1x excess) K₂CO₃, 3.4315 g (0.0075 mol) sodium 5,5'-sulfonylbis(2-fluorobenzenesulfonate) (SDFDPS), 0.3122 g (0.0004 mol) bis(4-((4-fluorophenyl)sulfonyl)phenyl)thio)phenyl)sulfane FDPS-TBB-FDPS, 0.0628 g (0.0001 mol) 4,4''-bis((4-fluorophenyl)sulfonyl)-5'-(4-((4-fluorophenyl)sulfonyl)phenyl)-1,1':3',1''-terphenyl 1,3,5-FPS-PB, 5 mL cyclohexane and 9 mL of *N*-methylpyrrolidone.

Azeotropic distillation under nitrogen was carried out for 4 h. After 4 h, the cyclohexane and water layers were removed and the temperature was increased up to 200 °C. Polymerization was carried out for 8 h.

After completion of reaction, the product was precipitated by pouring into 300 mL of isopropanol. Obtained precipitate was washed three times with isopropyl alcohol and then the obtained dry residue was dialyzed against water using a dialysis membrane (SERVAPOR® dialysis tubing cellulose membrane, MWCO 12000-14000, pore diameter 25 Å). Dialysis was performed for 72 h.

In order to obtain a dry residue, water was distilled on a rotary evaporator and the obtained dry residue was dried in a vacuum oven at 100 °C for 24 h. sPPSS (5.52 g, Na-form) was obtained in ~ 99 % yield.

2.10.2.3.2. Synthesis of sPPS-400-XXL (with 1.00 % branching agent)

SPPSS precursor was placed in a 250 mL one-necked round-bottomed flask, onto which was poured 110 mL of glacial acetic acid, 8 mL conc. sulfuric acid and 6 mL of 50 % hydrogen peroxide was added dropwise. On the next day, the addition of hydrogen peroxide was continued until the reaction mixture was completely become white in color. Oxidation was carried out at 80 °C for 48 h. Precipitated oxidized polymer was collected by filtration, after which the obtained residue was dialyzed against water using a dialysis membrane (SERVAPOR® dialysis tubing cellulose membrane, MWCO 12000-14000, pore diameter 25 Å), until the pH of dialysis water became neutral.

In order to obtain the desired product, the obtained aqueous solution was concentrated to a dry residue, after which the latter was transferred to a 1000 mL beaker in a pre-filled 10 % hydrochloric acid solution, in order to convert the polymer into its acidic form. After several acid changes, the obtained product was collected by filtration, washed with distilled water until neutral pH, after which it was dried in a vacuum oven at 80 °C for 24 h. sPPS-400-XXL (with 1.00 % branching agent) (5.81 g, H-form) was obtained in ~ 97 % yield.

3. Results and Discussion

3.1. Synthesis of monomers with high sulfonation degree

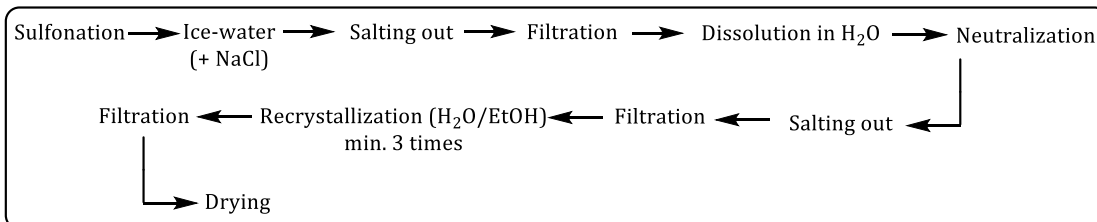
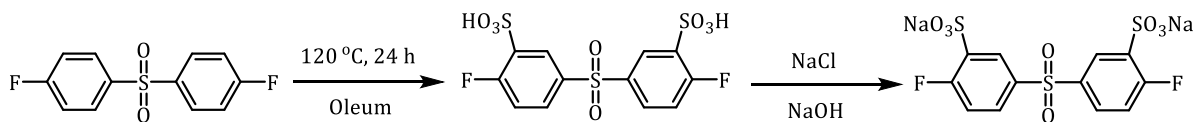
The synthesis of monomers with a high degree of sulfonation holds paramount importance in the development of polyelectrolytes with high ion-exchange capacity and proton conductivity. Proton conductivity is a critical parameter governing the efficiency of proton-exchange membrane fuel cells (PEMFCs) and proton-exchange membrane electrolyzers (PEMEs). Sulfonated aromatic polymers require high IEC values to achieve high effective proton conductivity, due to the lower acidity of sulfonic acid groups and the smaller hydrophilic/hydrophobic contrast compared to PFSA. Monomers with high degrees of sulfonation serve as building blocks for polyelectrolytes and can be used to increase overall IECs, as well as to enhance hydrophilic/hydrophobic contrast due to a local increase in sulfonic acid group density. Consequently, such monomers are of great importance in the design of appropriate polyelectrolytes.

In the IR spectra of all synthesized monomers, a new characteristic band at 1025–1041 cm^{-1} , assigned to O=S=O stretching, appeared, indicating successful sulfonation, along with the below discussed NMR spectral data.

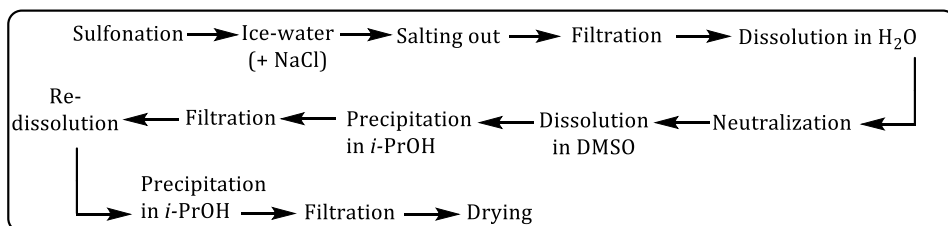
3.1.1. Optimized synthesis of SDFDPS

The synthesis and purification of SDFDPS are well-documented [180, 181, 182]. Despite extensive optimization over the years, the procedure involves multiple steps and at least three recrystallizations [180], resulting in a minimum of 10 steps (Scheme 44) and often leading to uncertain purity of the monomer. To achieve adequate purity for polycondensation reactions, the overall yield typically drops to around 55 % mol. In this work, we present a novel preparation route for SDFDPS and extend the same method to synthesize new highly sulfonated dihalo-monomers. We also developed a new purification process that leverages the solubility of sulfonated monomers in their barium form, a technique we previously used to detect sodium sulfate contamination in SDFDPS [16].

Synthesis pathway of SDFDPS by "conventional" method



Synthesis pathway of SDFDPS using DMSO



Optimized synthesis pathway of SDFDPS



Scheme 44. Synthesis scheme of SDFDPS by conventional and optimized method

Scheme 44 illustrates the conventional synthesis and purification steps for SDFDPS. Instead of multiple recrystallizations, the monomer can be separated from salts using an organic solvent like dimethyl sulfoxide (DMSO) [183, 184]. In this method, the salts are insoluble in DMSO, allowing them to be removed by simple filtration after dissolving the impure SDFDPS. However, the monomer obtained from the precipitation of the organic solution often suffers from DMSO contamination, which persists even after vacuum drying, necessitating additional re-precipitation. While DMSO contamination might be missed when analyzed in DMSO- d_6 , it becomes apparent in ^1H NMR spectrum recorded in D_2O . Although this method effectively eliminates inorganic salts without requiring recrystallization, it still

involves at least 12 steps and the use of organic solvents. The overall yield is improved to 65 %, which is about 10 % higher than the conventional method (Figure 7) [14].

The new method introduced here significantly streamlines the purification process while maintaining both the purity and yield of the sulfonated monomer. Following the conventional sulfonation of DFDPS, direct neutralization with BaCO₃ is performed. This carbonate reacts with excess H₂SO₄, forming BaSO₄ as a precipitate and releasing CO₂, while the filtrate contains water-soluble Ba-SDFDPS. After filtration, the monomer can be converted to the desired ion form by passing the solution through an ion-exchange resin before removing the water. The purity of the monomer obtained through this new method was confirmed by ¹H, ¹³C and ¹⁹F NMR spectroscopy (Figure 8-Figure 10) and meets the requirements for polycondensation reactions. Any potential incomplete exchange from Ba to Na or Li-forms was assessed by adding Na₂SO₄, which resulted in no precipitation.

Overall, this process shortens the work-up times and achieves a total yield of over 84 %. The benefits of this method include both time savings and increased yields, with no use of expensive chemicals. As for concerns about using Ba-salts, it is worth noting that barite is widely used in the petrochemical industry as an additive in well-drilling solutions [185].

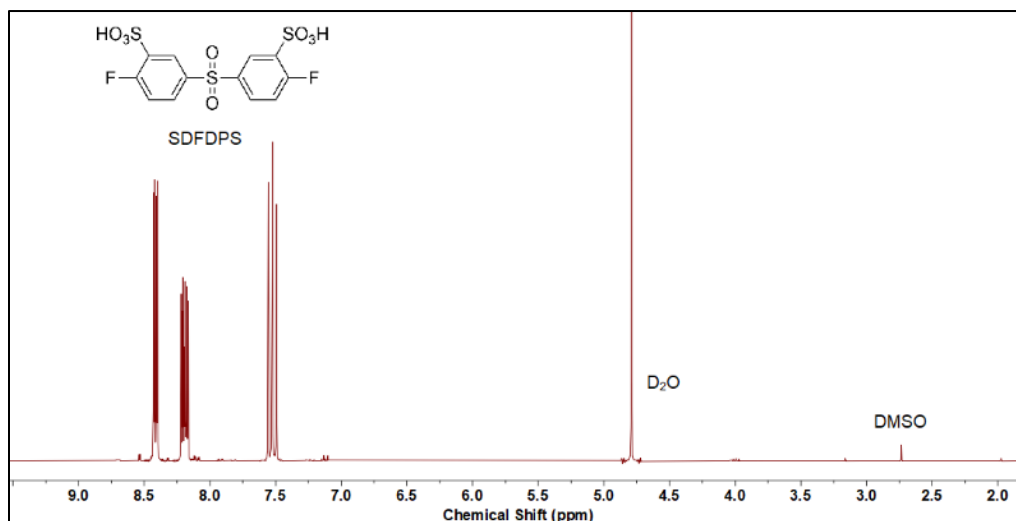


Figure 7. ¹H NMR spectrum of SDFDPS in D₂O showing DMSO contamination

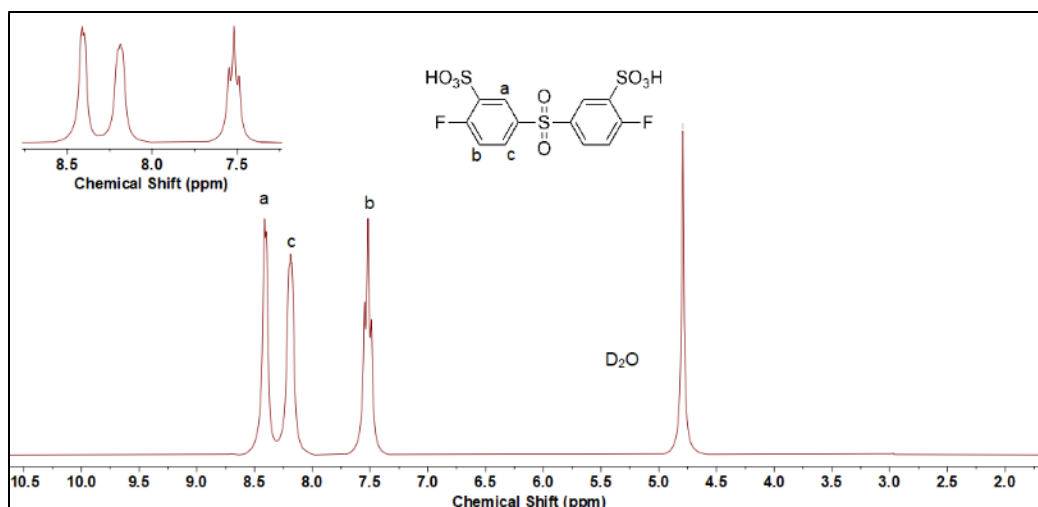


Figure 8. ¹H NMR spectrum of pure SFDPS in D₂O

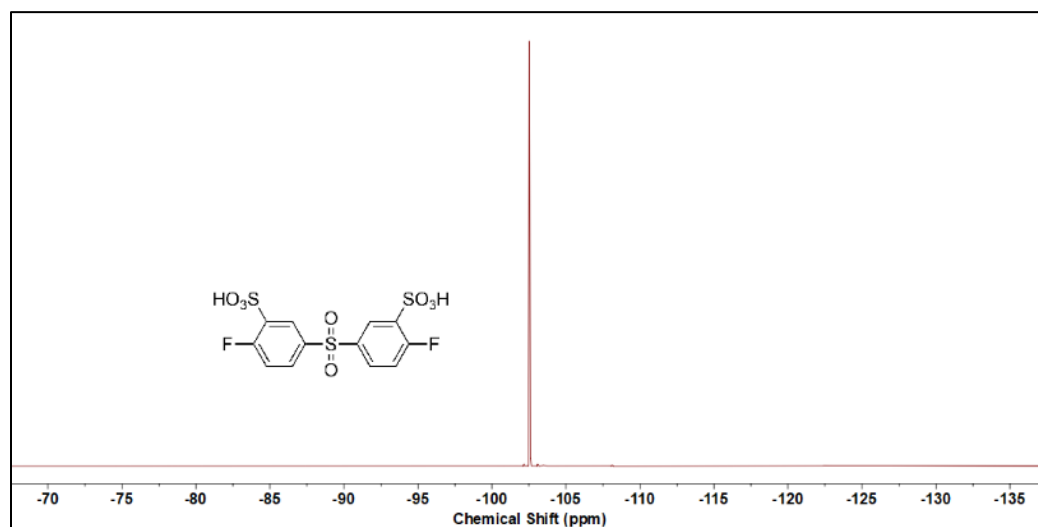


Figure 9. ¹⁹F NMR spectrum of pure SFDPS in D₂O

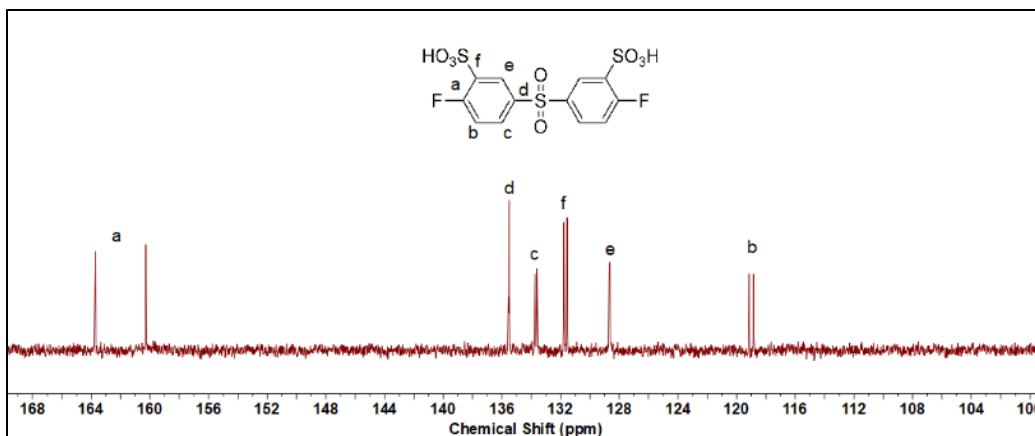


Figure 10. ^{13}C NMR spectrum of pure SDFDPS in D_2O

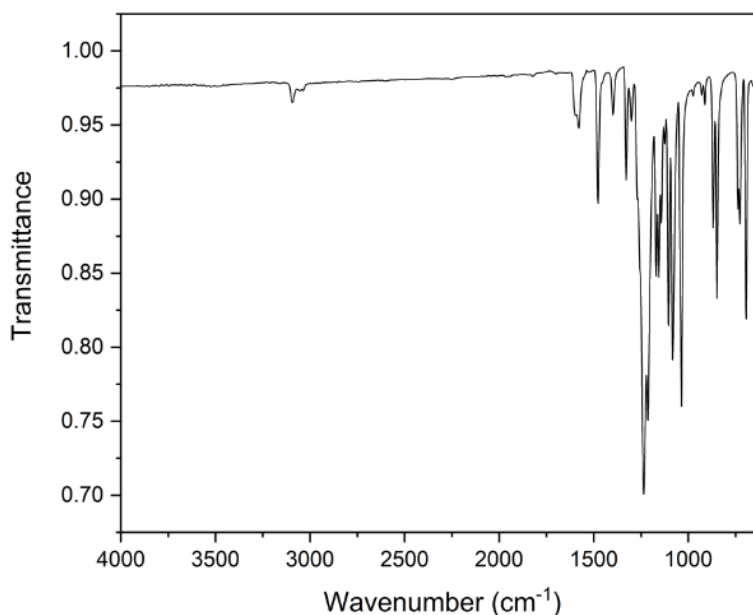
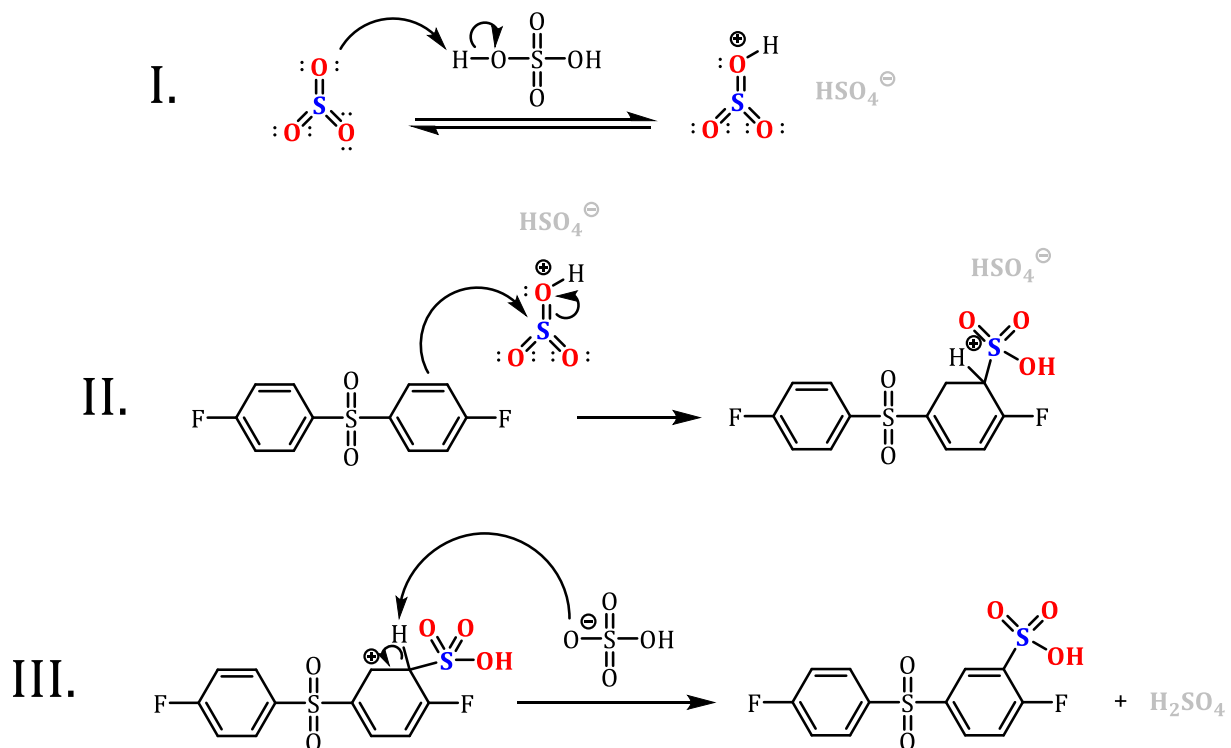


Figure 11. IR spectrum of SDFDPS

Sulfonation takes place using fuming sulfuric acid (also called oleum), which contains free SO_3 . As it is known, this reaction undergoes by the electrophilic aromatic substitution ($\text{S}_{\text{E}}\text{Ar}$) mechanism [186].

- I. Sulfur trioxide is “activated” by the addition of a proton from sulfuric acid;
- II. In the rate determining step, the highly electrophilic SO_3H^+ is then attacked by the aromatic ring to give the carbocation intermediate, forming C-S and breaking C-C (π);

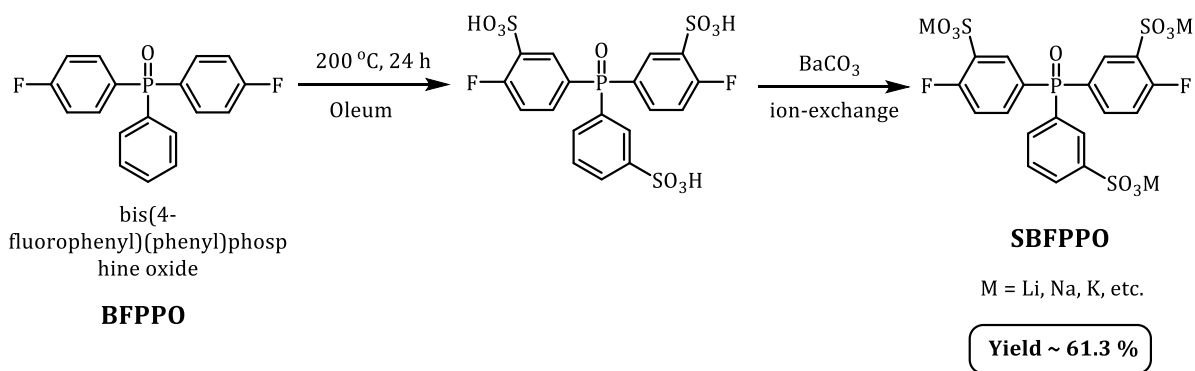
III. As with all electrophilic aromatic substitutions, the C-H bond is then deprotonated with a weak base to regenerate the C-C (π) bond and restore aromaticity, providing the sulfonic acid product:



Scheme 45. Mechanism of the sulfonation reaction of DFDPS

3.1.2. Optimized synthesis of SBFPPO

Another noteworthy monomer for the synthesis of sulfonated polyarylene is sulfonated bis(4-fluorophenyl)phenyl phosphine oxide (SBFPPO). The high degree of sulfonation and resulting increased water solubility make its purification more challenging than that of SDFDPS, necessitating the use of column chromatography [187, 188]. We utilized the previously described method to synthesize the SBFPPO monomer.



Scheme 46. Synthesis scheme of SBFPPO

The advantage of the proposed method lies in its adaptability to various sulfonated monomers produced via direct sulfonation and its higher yield compared to traditional methods. However, the purity of the final product can be influenced by the monomer's complexity and the number of rings undergoing sulfonation. In the case of SBFPPO, the presence of a phosphine oxide group instead of a sulfone group, along with an additional ring, led to a less pure product using the same method. As evidenced by ^1H , ^{13}C , and ^{19}F NMR spectra (Figure 12 – Figure 14), an almost pure product was obtained following the same purification process. Nevertheless, minor impurities (around 2 % according to ^{19}F NMR spectrum) were observed, likely due to partial sulfonation or sulfonation occurring at different sites of the monomer. Although these impurities are acceptable for condensation polymerization, they highlight the influence of the starting monomer on the final product's quality and may indicate the need for optimization of the sulfonation step. SBFPPO was obtained with a higher yield of 61.3 % compared to the previously reported 50 % yield after column chromatography [187, 188].

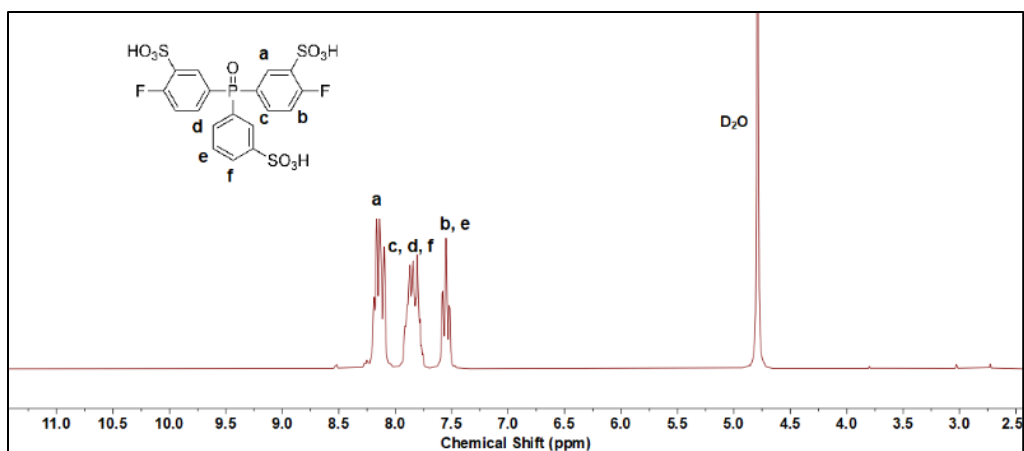


Figure 12. ^1H NMR spectrum of pure SBFPPO in D_2O

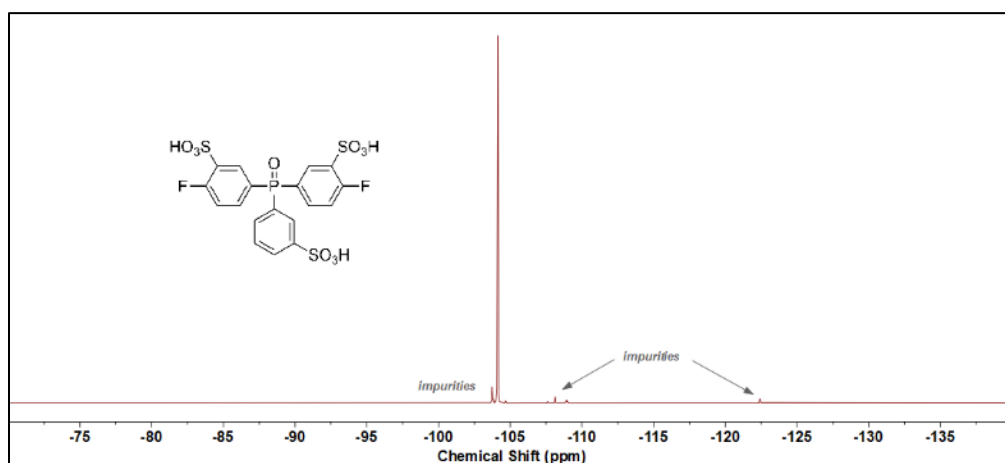


Figure 13. ^{19}F NMR spectrum of SBFPPO in D_2O showing the presence of traces impurities (ca. 2 % mol)

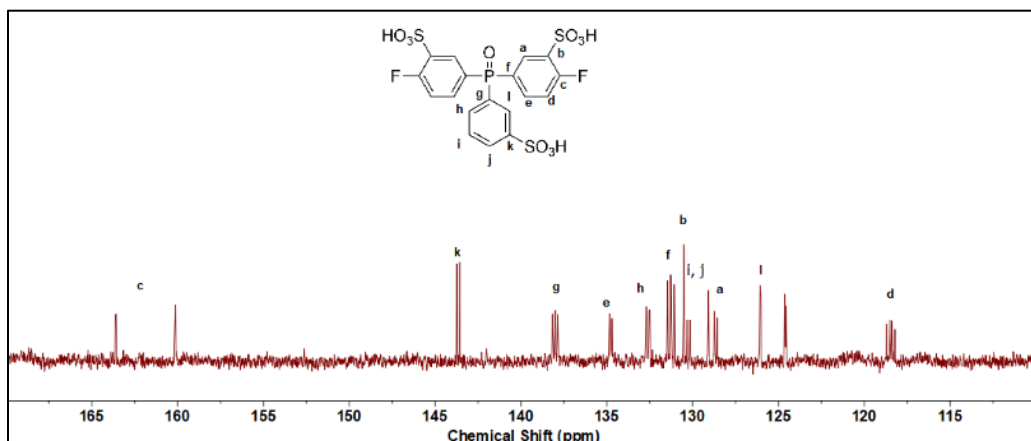


Figure 14. ^{13}C NMR spectrum of SBFPPO in D_2O

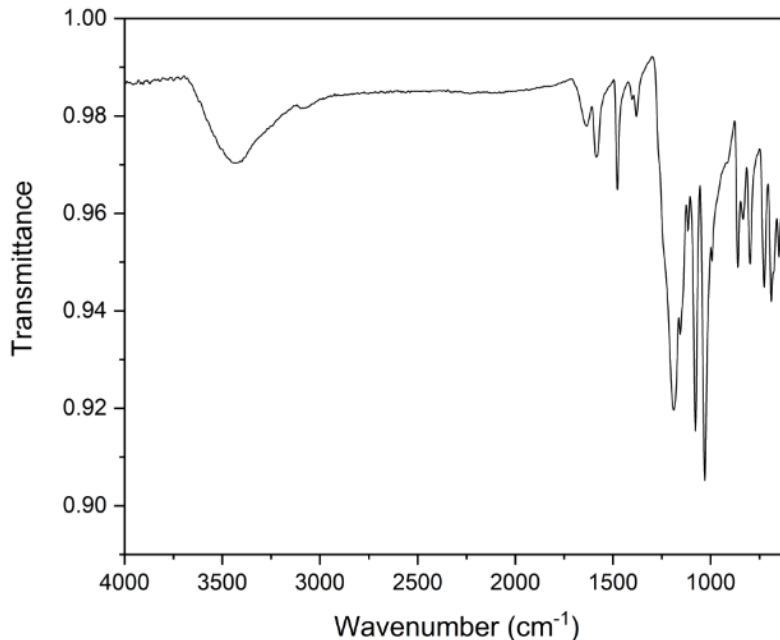


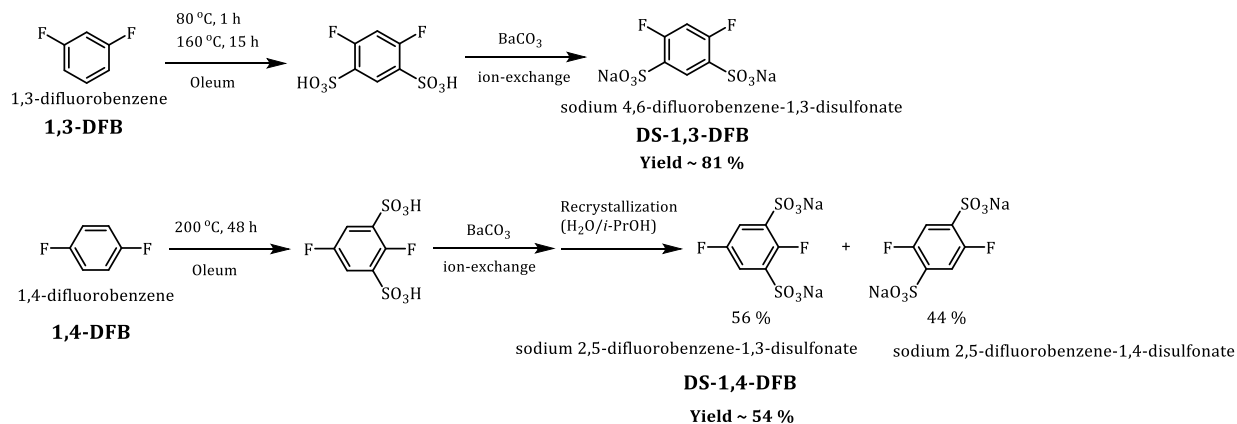
Figure 15. IR spectrum of SBFPPO

3.1.3. Synthesis of DS-1,3-DFB and DS-1,4-DFB

In an effort to expand the range of monomers available for synthesizing sulfonated polyarylenes, we applied our newly developed synthesis method to produce highly sulfonated difluorophenylenes, which could serve as promising new building blocks for polymers and block copolymers. A high degree of local sulfonation is advantageous for achieving high proton conductivity and nanophase separation, although it requires balancing with water solubility in the final polymers. Furthermore, it has been shown that 'hypersulfonated' units can be detrimental due to counterion condensation [189], which is why, in this study, we focused on disulfonated monomers without sulfonic groups in the ortho position.

Achieving double sulfonation on the same ring requires higher temperatures and longer reaction times compared to DFDPS or DCDPS. We followed the same synthetic steps outlined in Scheme 46. The resulting products and their relative compositions depend on the initial non-sulfonated monomer. For *p*-difluorobenzene, a mixture with a molar ratio of 0.56:0.44 of 2,5-difluorobenzene-1,3-disulfonate and 2,5-difluorobenzene-1,4-disulfonate, respectively, was obtained (Figure 16). To separate the isomers, we performed

recrystallization from an *i*-PrOH/H₂O mixture, which yielded pure 2,5-difluorobenzene-1,3-disulfonate (54 %), but we were unable to isolate pure 2,5-difluorobenzene-1,4-disulfonate. Conversely, in the case of *m*-difluorobenzene, only 4,6-difluorobenzene-1,3-disulfonate was obtained, with a high yield of 81 %.



Scheme 47. Synthesis scheme of DS-1,3-DFB and DS-1,4-DFB

The purity of the monomers was confirmed using ¹H, ¹³C, and ¹⁹F NMR spectra (Figure 17 –Figure 22). A single signal in the ¹⁹F NMR spectrum indicates symmetric substitution for 4,6-difluorobenzene-1,3-disulfonate (Figure 18), whereas two signals are observed in the ¹⁹F NMR spectrum of 2,5-difluorobenzene-1,3-disulfonate (Figure 21). Similar to SDFDPS, the complete exchange from Ba to Na or Li-form was confirmed by adding Na₂SO₄, which resulted in no precipitation.

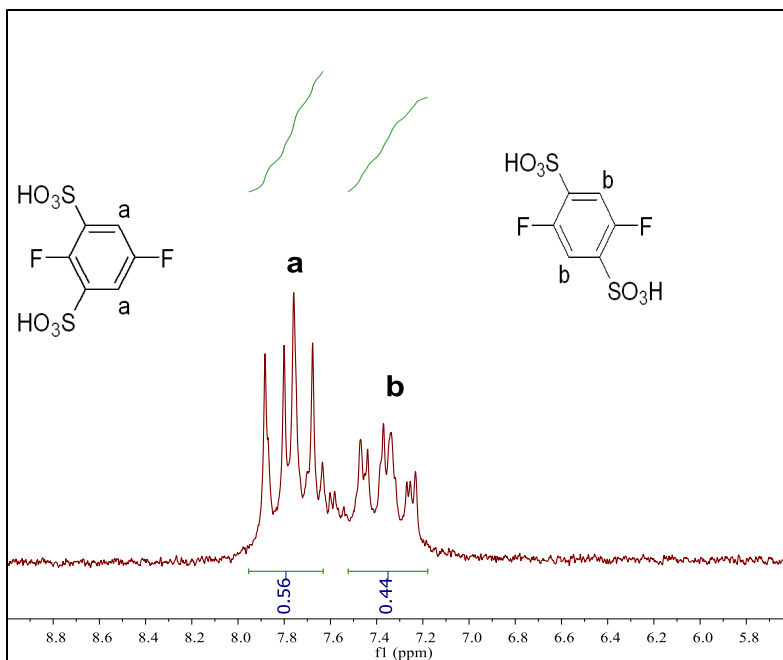


Figure 16. ^1H NMR spectrum of crude mixture of 2,5-difluorobenzene-1,3-disulfonate and 2,5-difluorobenzene-1,4-disulfonate obtained after sulfonation in D_2O

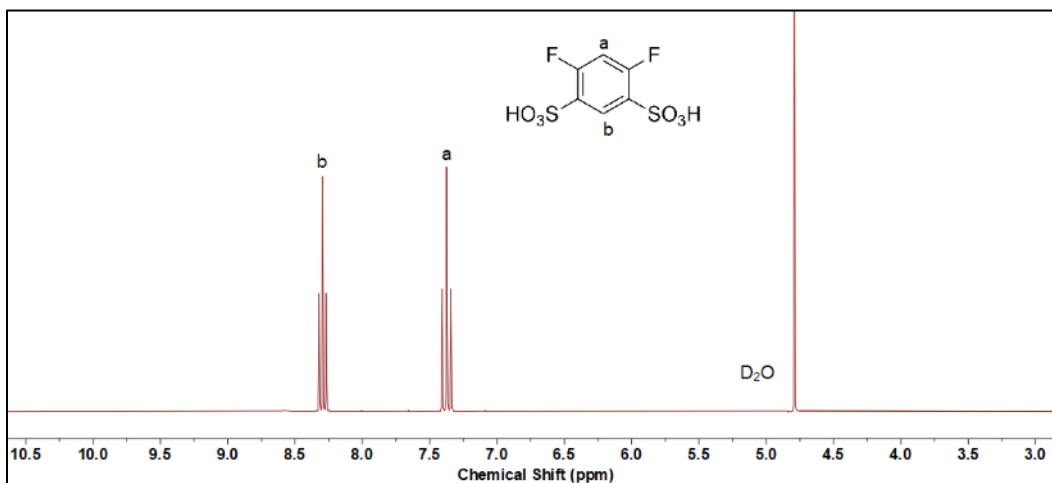


Figure 17. ^1H NMR spectrum of DS-1,3-DFB in D_2O

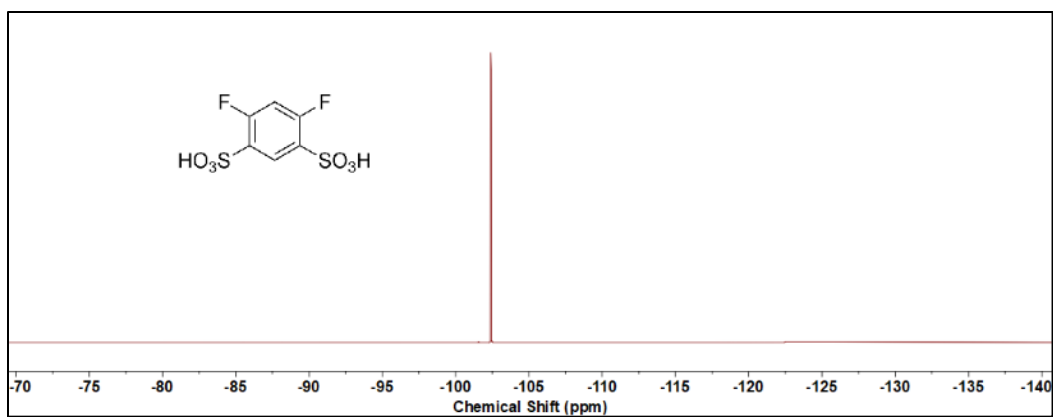


Figure 18. ¹⁹F NMR spectrum of DS-1,3-DFB in D₂O

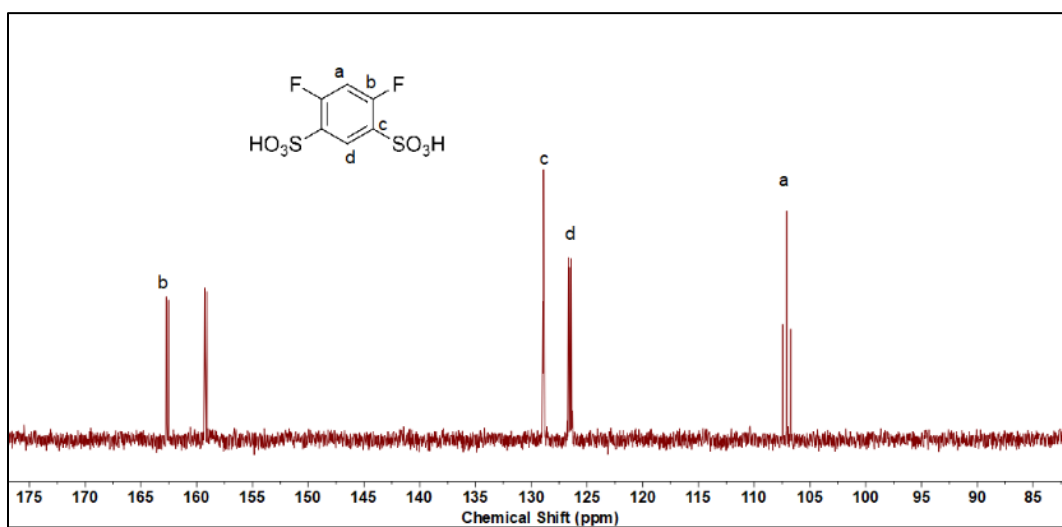


Figure 19. ¹³C NMR spectrum of DS-1,3-DFB in D₂O

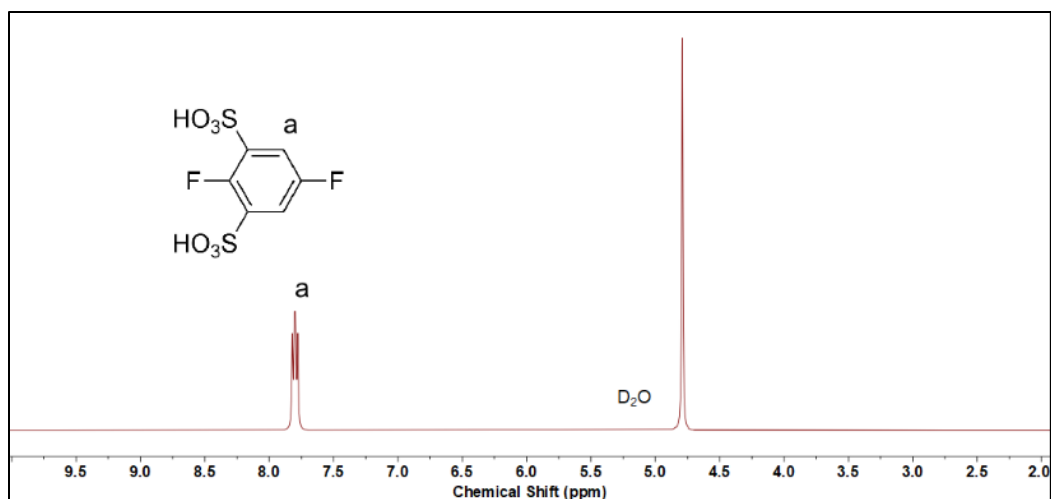


Figure 20. ¹H NMR spectrum of DS-1,4-DFB in D₂O

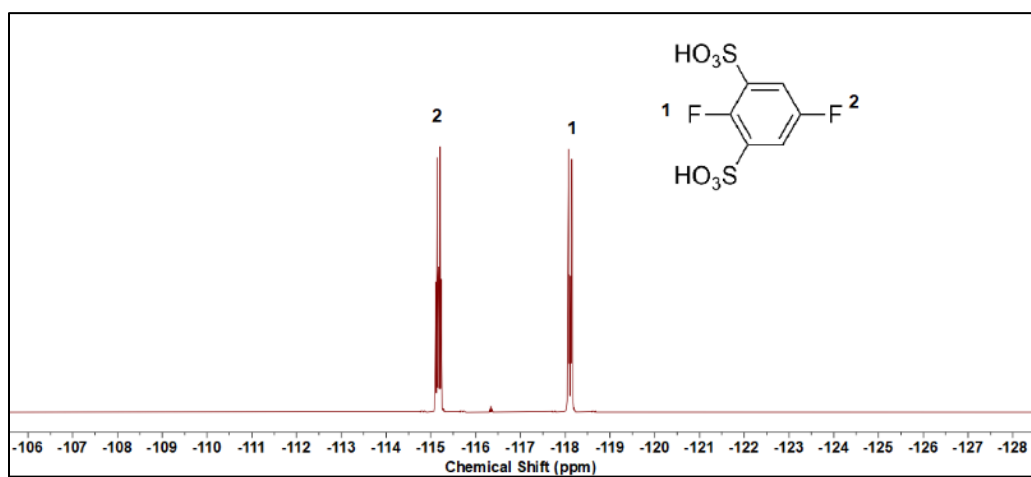


Figure 21. ¹⁹F NMR spectrum of DS-1,4-DFB in D₂O

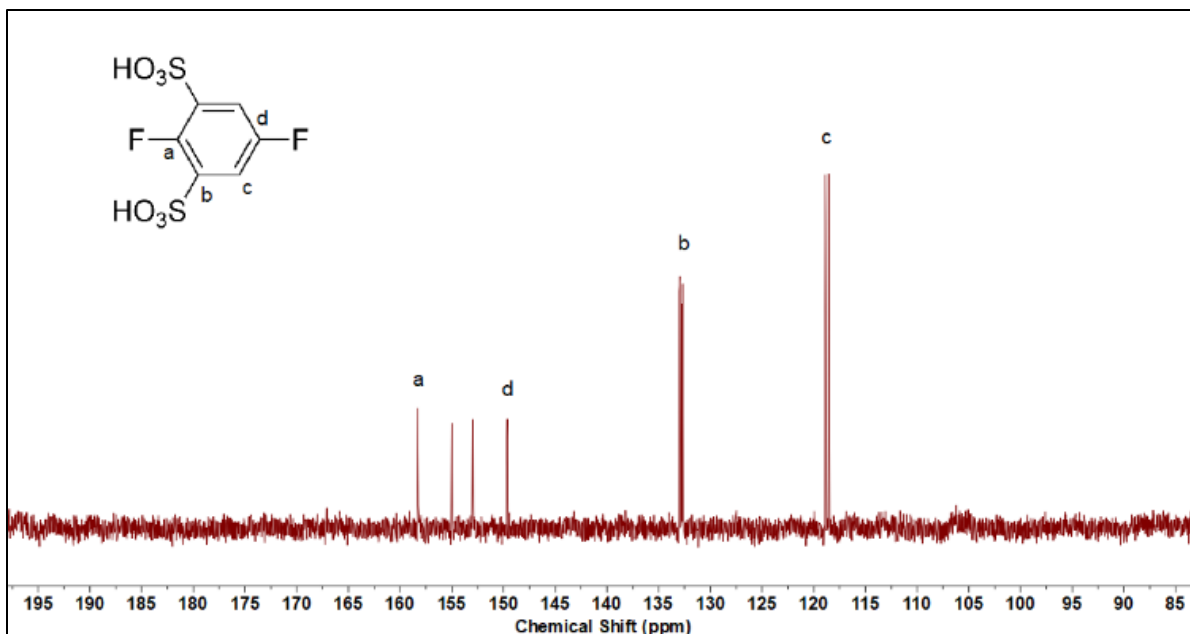


Figure 22. ^{13}C NMR spectrum of DS-1,4-DFB in D_2O

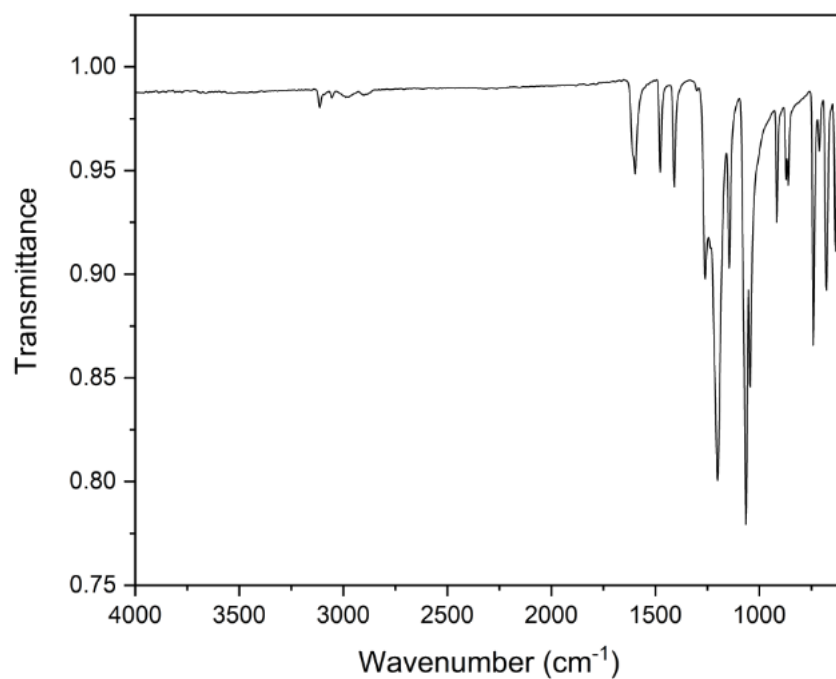


Figure 23. IR spectrum of DS-1,3-DFB

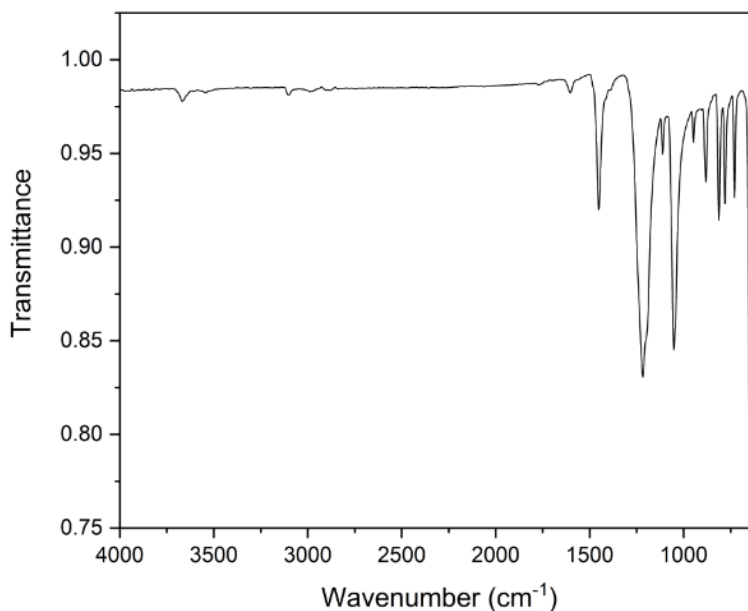


Figure 24. IR spectrum of DS-1,4-DFB

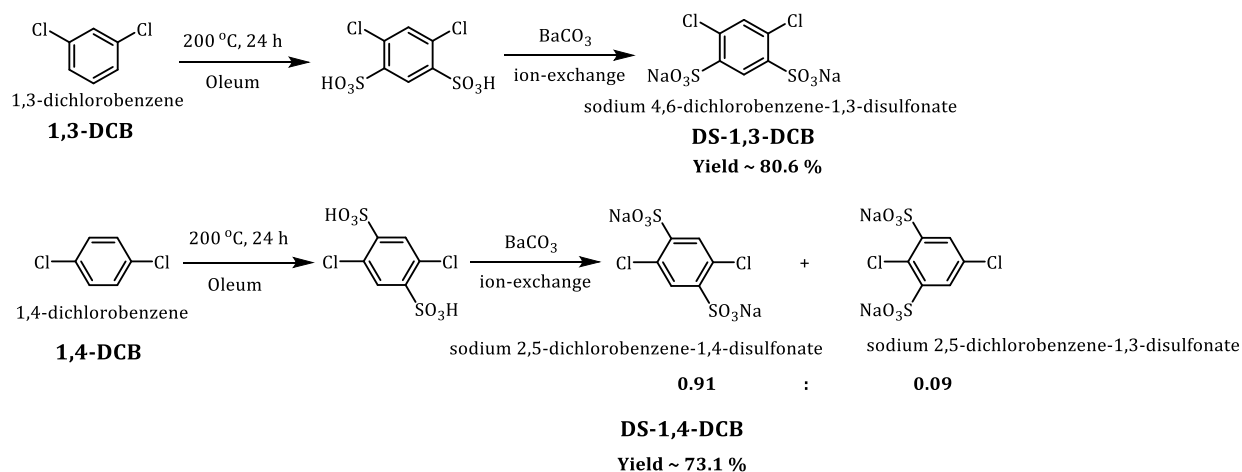
3.1.4. Synthesis of DS-1,3-DCB and DS-1,4-DCB

The synthesis of disulfonated 1,3-dichlorobenzene and 1,4-dichlorobenzene is particularly important because it addresses environmental concerns associated with the use of fluoride. Fluoride compounds, often used in similar chemical processes, are harmful to the environment due to their persistence and potential for bioaccumulation. Although dichloride analogues are less reactive to step-growth polymerization compared to difluorides, by switching to dichlorides, we can eliminate the use of fluoride, thereby reducing the environmental impact.

Unlike 2,5-dichlorobenzene sulfonic acid, its disulfonated analogue is not commercially available, likely due to the complexity of the purification process. The high water solubility of the monomer complicates the salting-out purification step after neutralization, which is sometimes skipped for this reason.

Considering the challenges associated with the synthesis and purification of disulfonated monomers, we applied the new synthetic approach also to single-ring dichlorobenzene compounds in this study.

Like their difluoro- analogues, the sulfonation of *p*- and *m*-dichlorobenzenes required high temperatures and relatively long reaction times (Scheme 48).



Scheme 48. Synthesis scheme of DS-1,3-DCB and DS-1,4-DCB

The purification of both monomers was conducted using the previously mentioned method. *p*-dichlorobenzene produced a mixture of 1,4-disulfonated and 1,3-disulfonated products with a ratio of 0.91 : 0.09, free from any additional impurities (Figure 25 – Figure 26). Further separation of the mixture was not performed. The yield of the isomer mixture was 73.1 %, which contrasts with its difluoro analogue, while *m*-dichlorobenzene yielded the 1,3-disulfonated product in high yield (80.6 %) (Figure 27 – Figure 28), similar to the difluoro analogue. No additional purification was required for either product. The purity of the monomers was confirmed by ¹H and ¹³C NMR spectra.

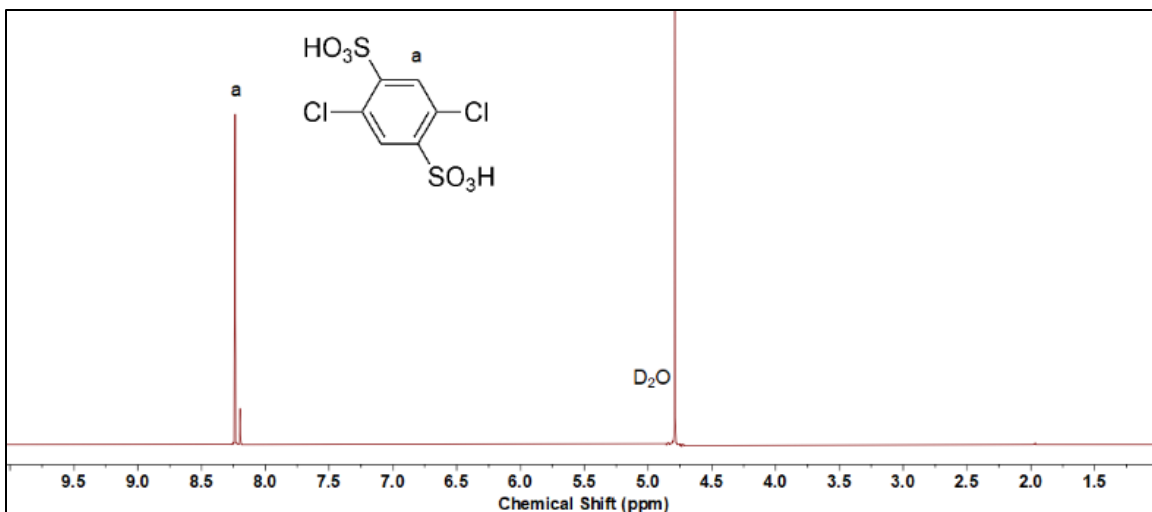


Figure 25. ^1H NMR spectrum of 2,5-dichloro-1,4-benzenedisulfonic acid showing minor impurities of 4,6-dichloro-1,3-benzenedisulfonic acid in D_2O

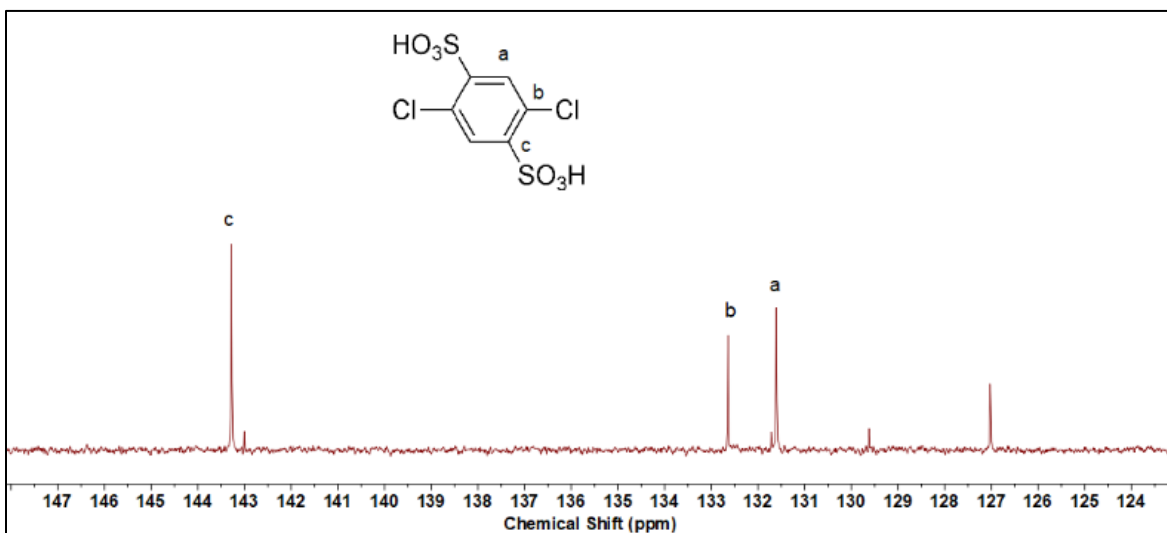


Figure 26. ^{13}C NMR spectrum of 2,5-dichloro-1,4-benzenedisulfonic acid showing minor impurities of 4,6-dichloro-1,3-benzenedisulfonic acid in D_2O

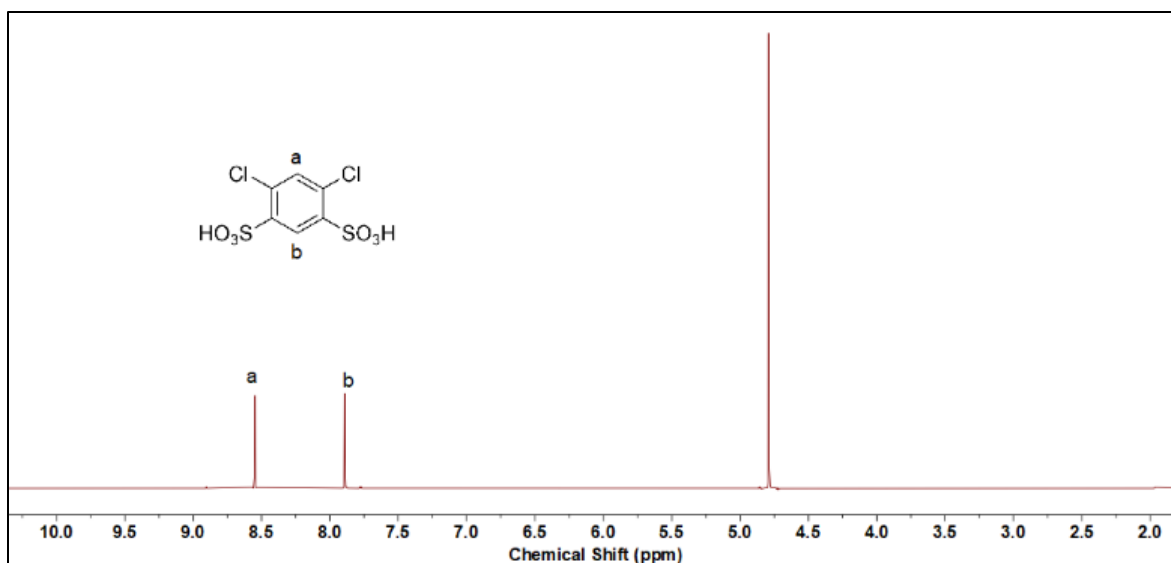


Figure 27. ¹H NMR spectrum of pure DS-1,3-DCB

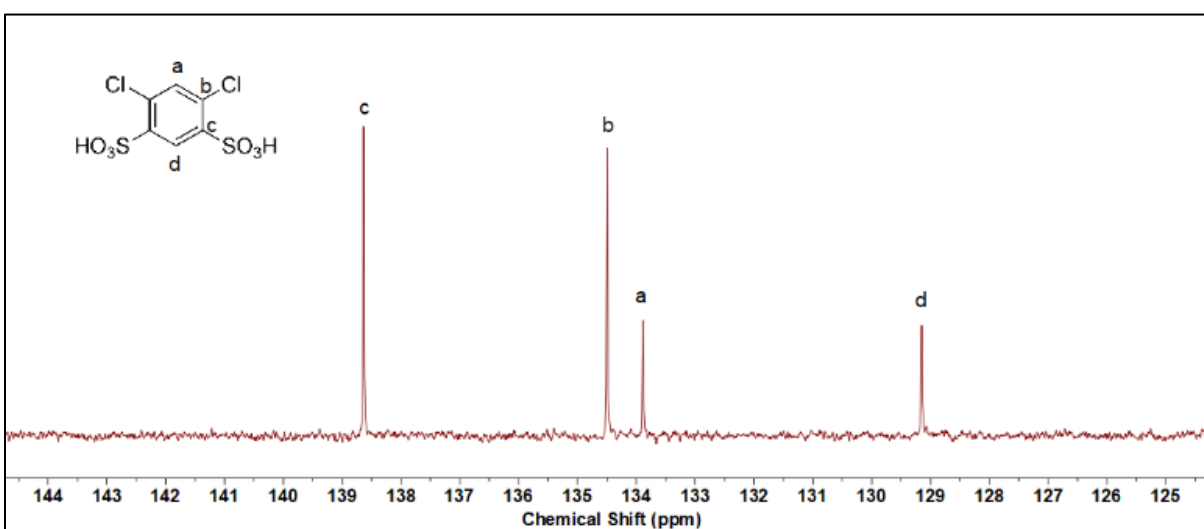


Figure 28. ¹³C NMR spectrum of pure DS-1,3-DCB

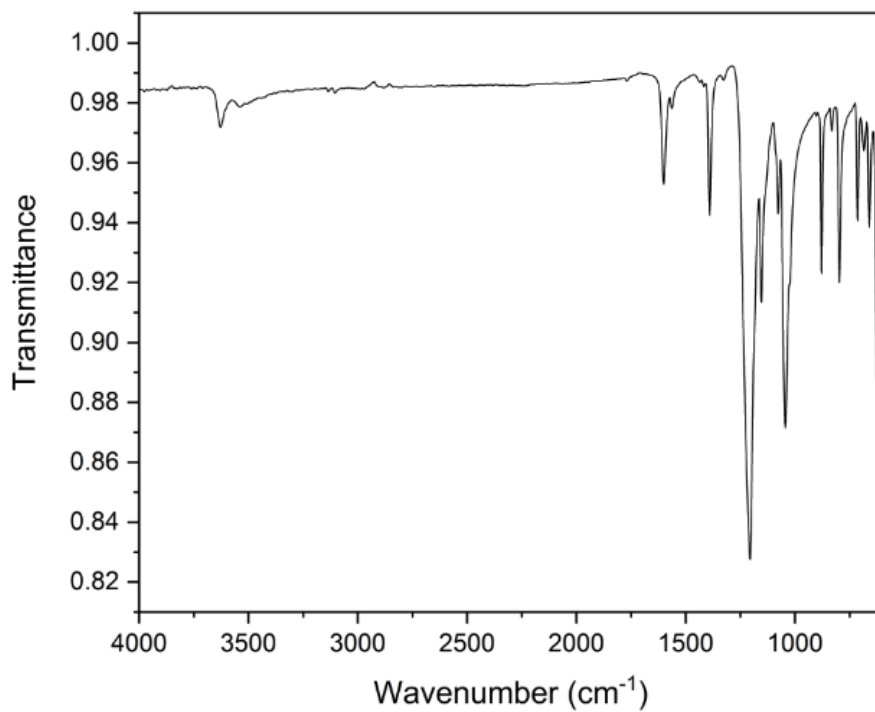


Figure 29. IR spectrum of the mixture of 2,5-dichlorobenzene-1,4-disulfonate and 2,5-dichlorobenzene-1,3-disulfonate

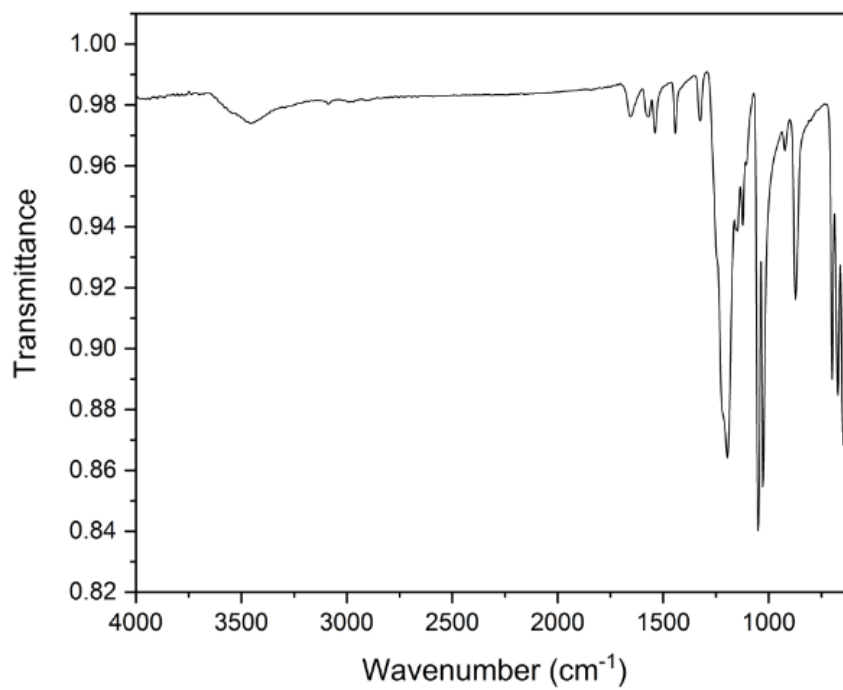


Figure 30. IR spectrum of DS-1,3-DCB

3.1.5. An outlook of the practical application of highly sulfonated monomers

AB-type polymers derived from sulfonated monomers generally exhibit high ion-exchange capacity and are either soluble in water or have significant water uptake. To address this issue, a co-polymerization strategy is often employed, where a non-sulfonated co-monomer is incorporated to reduce the IEC while still maintaining sufficient levels to achieve high proton conductivity. A monomer with a high degree of sulfonation allows for the incorporation of longer non-sulfonated segments within the main chain, as illustrated below.

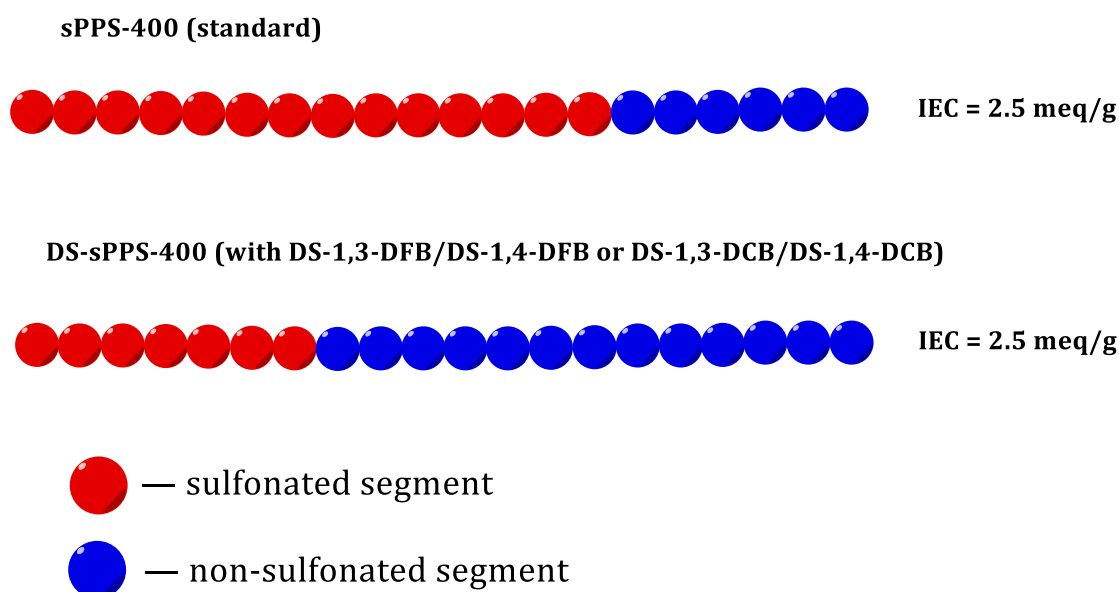


Figure 31. Distribution of sulfonated and non-sulfonated segments for sPPS-400 and DS-sPPS-400

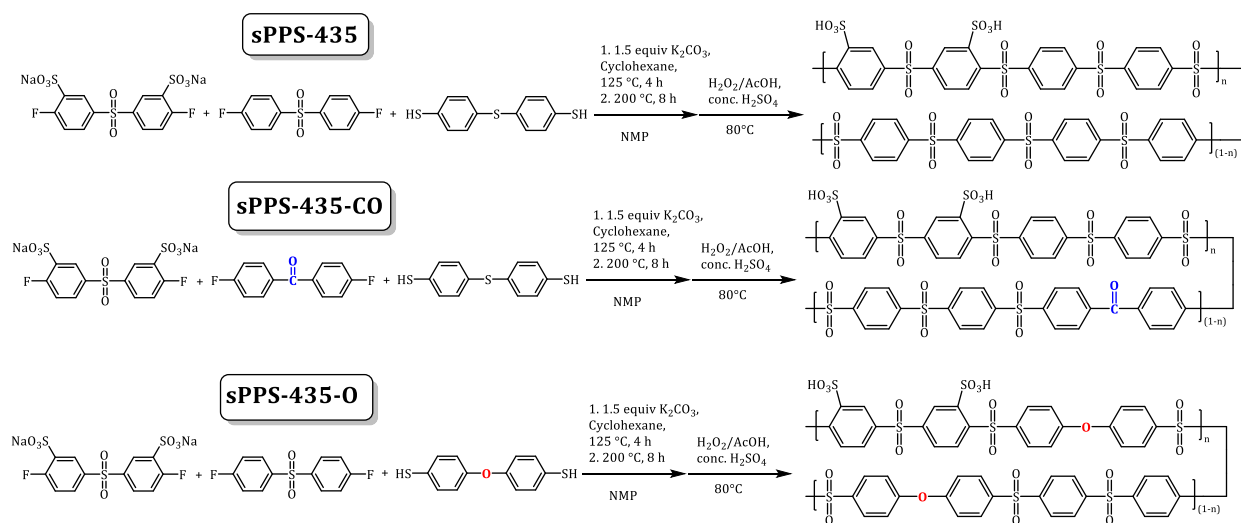
An increased fraction of non-sulfonated segments enhances the interactions among these segments, resulting in a decrease in water uptake. It is important to find a balance between ion-exchange capacity, proton conductivity and water uptake.

In summary, the increased content of non-sulfonated fragments into polymers on the expense of monomers with high sulfonation degrees represents a promising strategy for reducing water uptake in proton-conducting membranes. This approach enhances the mechanical and structural properties of the membrane, which in turn improves its durability and overall performance in demanding operating environments.

3.2. Evaluating the radical stability of sulfonated poly(phenylene sulfone)s with different heteroatoms in the main chain

There is ongoing discussion about the radical stability of the main backbone in aromatic polymers. Our group previously reported that sPPSS has lower stability compared to sPPS by Fenton's test [190]. However, this difference in stability may be influenced by the positioning of the sulfonic acid group in the *ortho*- position relative to either the electron-donating sulfide bridge or the electron-withdrawing sulfone bridge. To mitigate this effect, in the current study, we have designed polymers where the introduction of different groups does not occur in the *ortho*- positions relative to the sulfonic acid groups.

Polymers with the same equivalent weight (EW = 435) and different linking units in the main chain were synthesized. The stability of the mentioned polymers against radical attack was studied through the Fenton's test.



Scheme 49. Synthesis scheme of sPPSs with different linking units in the main chain

Fenton's reagent consists of a mixture of hydrogen peroxide (H₂O₂) and an iron catalyst, usually iron(II) sulfate (FeSO₄). Hydrogen peroxide oxidizes iron(II) to iron(III), generating a hydroxyl radical and a hydroxide ion. Iron(III) is subsequently reduced to iron(II) by another hydrogen peroxide molecule, producing a hydroperoxyl radical and a proton. Overall, this process leads to the conversion of hydrogen peroxide into two distinct oxygen-radical species, accompanied by the formation of water:

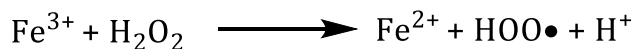


Figure 32. Scheme of Fenton's test mechanism

The oxidative stability of synthesized polymers is vital for PEMFCs and water electrolyzers due to the following reasons:

a. Durability in Harsh Operating Conditions:

- PEMFCs and water electrolyzers operate under conditions where oxidative stress can be significant, especially at elevated temperatures;
- Oxidative stability is essential to prevent the degradation of the PEM, which can lead to decreased fuel cell and water electrolyzer performance and a shortened lifespan.

b. Hydroxyl Radical Testing:

- Fenton's reagent is used to generate highly reactive hydroxyl radicals ($\cdot\text{OH}$), which simulate the oxidative environment that PEMs may encounter during fuel cell and water electrolyzer operation;
- By subjecting the polymer to Fenton's reagent, its resistance to radical-induced degradation can be assessed, a critical factor in long-term fuel cell and water electrolyzer durability.

c. Material Selection and Optimization:

- Assessing oxidation stability aids in the selection of suitable polymer materials for PEMs;
- It also guides to modify polymer structures or incorporate additives to enhance oxidative resistance.

d. Predicting PEM Lifespan:

- Results from oxidation stability tests can be used to estimate the expected lifespan of PEMs in practical fuel cell and water electrolyzer applications;

- This information is essential for assessing the economic viability of PEMFC and water electrolyzer technology and predicting maintenance needs.

The results of the Fenton's test are summarized in the Figure 33:

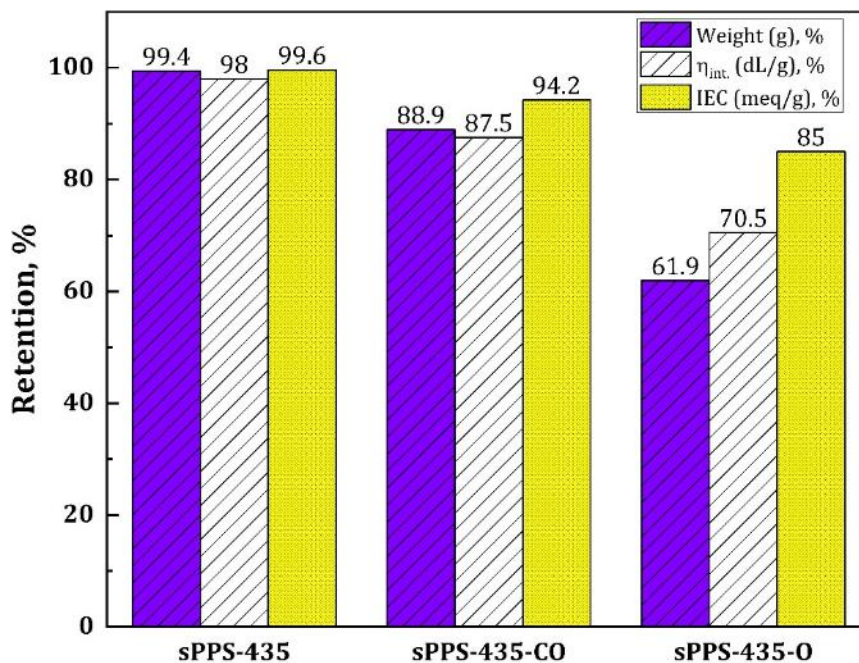


Figure 33. Graph of weight, intrinsic viscosity and ion-exchange capacity retention (in %) values for sPPS-435, sPPS-435-CO and sPPS-435-O

The stability of polymers with different linking groups in the main chain, as determined by Fenton's test, can be explained by considering the reactivity of these linking groups and their susceptibility to oxidative degradation.

sPPS-435:

- Polymers containing only sulfonyl ($-\text{SO}_2$) linkages show stability in Fenton's test. This stability can be attributed to the high electron-withdrawing nature of the $-\text{SO}_2$ group and the fact that sulfur is in its highest oxidation state.

sPPS-435-CO:

- Carbonyl groups are more susceptible to oxidation compared to sulfonyl groups; Thus, polymer with the combination of $-\text{SO}_2$ and $-\text{C}=\text{O}$ linking groups is more vulnerable to oxidative attack.

sPPS-435-O:

- The presence of oxygen atoms in the polymer backbone makes it more reactive towards reactive oxygen species (ROS) generated during Fenton's test. These ROS can easily attack and break the polymer chains at the oxygen sites, leading to degradation. Consequently, a main chain containing both $-\text{SO}_2$ and $-\text{O}$ linking groups is the least stable among the three cases.

Based on these results, we synthesized microblock monomers and subsequently their corresponding polymers, which did not contain vulnerable groups to radical attack.

3.3. Synthesis of poly(phenylene sulfone) based statistical copolymers with different equivalent weights via Li_2S route

One of the effective approaches for improving the properties of sulfonated aromatic polymer membrane materials is polymer blending, particularly through acid-base polymer blends. These blends typically comprise an ionomer containing sulfonic acid groups and a base polymer. Among base polymers, polybenzimidazoles are frequently utilized due to their notable mechanical strength and robust chemical and thermal stability. Our research group recently investigated a polymer blend consisting of fully sulfonated poly(phenylene sulfone) (sPPS-220) and polybenzimidazole (PBI-O), demonstrating favorable performance properties and remarkable stability against radical attack, which is crucial for these materials [191]. Nevertheless, the use of water-soluble sPPS was still considered as point for further optimization due to the possible leaching of the latter. Leaching of water-soluble polymer can occur during long-term operation by liquid water formed at the cathode during startup or condensed during fuel cell shutdown [192, 193]. Another drawback of the use of water-soluble polymer, can be sPPS leaching during conditioning step: acid-base blend membrane is prepared using neutralized form of sPPS, which has to be later acidified in order to transform the polymer in H-form. Compared to PVPA-PBI blend membranes [194], which

are known as free from acid leaching systems, and where ionic interaction is introduced during the casting process, sPPS-PBI blend membranes after casting do not contain ionic links between two components. Thus, lack of interaction between two components, may lead to the dissolution of water-soluble sPPS from the surface of the membrane due to the low polymer entanglement (Figure 34).

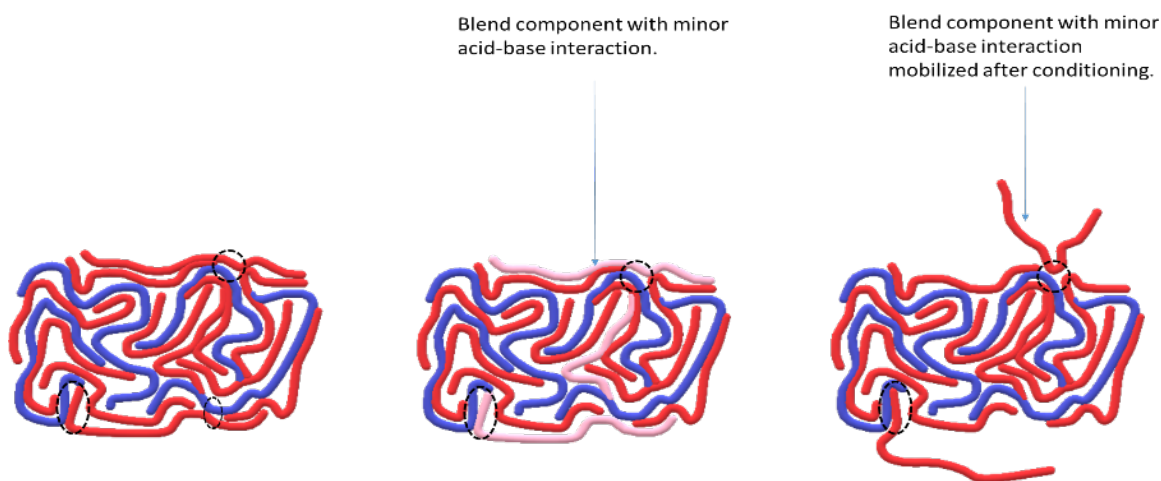


Figure 34. Dissolution of sPPS from membrane surface due to low polymer entanglement

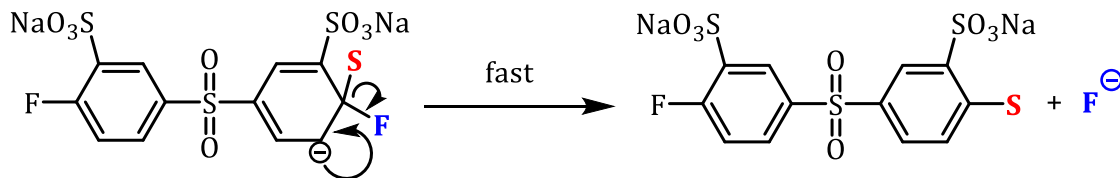
To address this need, we aimed to synthesize water-insoluble sulfonated poly(phenylene sulfone)s with high ion-exchange capacities by incorporating non-sulfonated segments. This was achieved using the Li_2S route, where the sulfonated monomer (SDFDPS) and the unsulfonated monomer (DFDPS) were copolymerized with lithium sulfide. Interestingly, Li_2S residue in the polymer structure is only the sulfide linkage (after oxidation – sulfone), which increases the possibility of obtaining longer random “blocks” as DFDPS molecules can be directly connected to each other. In contrast to sPPS-360, where the general structure of copolymer can be presented as $(\text{AA}-\text{BB})_n$, chosen strategy leads to the statistical copolymers with general structure of $(\text{AA})_m-(\text{BB})_n$. It should be noted, that before the current study, there was a gap between sPPS-220 and sPPS-360, which are obtained by different synthetic routes (Li_2S route versus dithiol route). By partial combination of these two methods, we have synthesized sPPS copolymers with IEC in the range of 2.78-4.5 meq/g. It was found that sPPS-240 with an ion-exchange capacity of 4.17 meq/g is already insoluble in water at room temperature [195], while sPPS with EW > 255 (IEC < 3.92 meq/g) are

insoluble in water even at elevated temperatures (autoclaving of 1 % sPPS-260 in water leads to the gel). Water insolubility results from the strong interactions between unsulfonated segments. For sPPSs with an equivalent weight (EW) greater than 290, this strong interaction also leads to insolubility in aprotic polar solvents such as DMSO, NMP, DMAc, and DMF.

Such a high ion-exchange capacity of water insoluble sPPS's enables to adjust the blend ratio, ensuring that the content of PBI-O remains sufficient to maintain the membrane's mechanical stability.

Since the acid-base interactions within polymer blends are dynamic and tend to weaken at elevated temperatures, the risk of polymer leaching becomes a significant concern, influenced by the molecular weight of the polymers. Mitigating this issue can be achieved by increasing the molecular weight of the polymer electrolyte, which in turn leads to greater entanglement and enhanced interaction with the base polymer. For this reason, we have optimized the synthesis of sPPS using the lithium sulfide route, with a particular focus on the particle size of Li_2S powder.

Preventing ionomer leaching from polymer blends is crucial for the optimal performance and longevity of fuel cells and water electrolyzers. Leaching can degrade the membrane's ion-exchange capacity, leading to diminished proton transport and, consequently, a reduction in overall cell efficiency and power output. Over time, the loss of sulfonated species not only affects the electrochemical performance but also compromises the physical integrity of the membrane leading to mechanical failure. This degradation poses risks not only to the device's operational lifespan but also to the environment, as leached contaminants can lead to pollution and complicate waste management. Therefore, ensuring the stability of the polymer blend against leaching is essential for both the device's performance and its environmental impact. General synthesis scheme of water-insoluble poly(phenylene sulfone)s with high IEC, synthesized via Li_2S route is shown on Scheme 50:



Scheme 52. II step of the nucleophilic aromatic substitution reaction between SDFDPS and Li_2S

3.3.1. Influence of Li_2S particle size on sPPSs molecular weights

Step-growth polymerizations were performed with different particle size (500, 50-75 and 5 μm) lithium sulfide and the latter's influence on the molecular weights of polymers was studied in case of sPPS-220, sPPS-240 and sPPS-260:

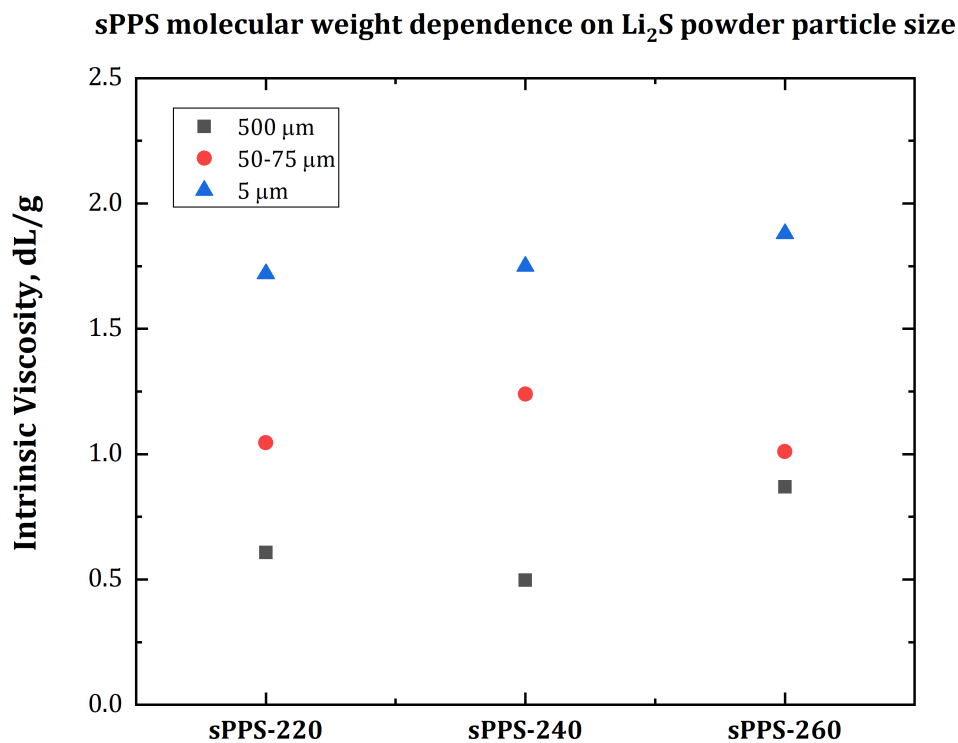


Figure 35. Graph of sPPS molecular weight dependence on lithium sulfide powder particle size

As shown in Figure 35, the highest molecular weights are obtained with smaller particle sizes due to their higher surface area.

High molecular weights are important not only for mitigating leaching out, but also for achieving good mechanical properties. Therefore, understanding factors that influence molecular weight control in polymer synthesis is essential for tailoring polymer properties to specific applications.

3.3.2. Preparation of the blends of sPPSs with PBI-OO

sPPSs with an equivalent weight (EW) in the range of 240-280 form brittle films with excessive swelling, making them unsuitable for use in pure form. However, their mechanical properties can be enhanced through acid-base blending. For ionic crosslinking, polybenzimidazole (PBI-OO) was chosen as base containing polymer for its excellent mechanical properties. Although polymer blending is a complex process, interactions via hydrogen bonding are believed to facilitate miscibility of the two polymers [196, 197].

Since direct mixing of DMSO solutions of sPPS polymers in their acidic form with PBI-OO solutions leads to immediate precipitation, the sPPS must be neutralized before mixing. Based on studies of sPPS-220/PBI-O blends, IEC of 2.21 meq/g was selected to achieve conductivity comparable to that of Nafion.

3.3.2.1. Leaching experiments on sPPS-240 and sPPS-260 blends with PBI-OO

➤ sPPS-240 + PBI-OO

First, the ion-exchange capacity of the blend was determined, which matched the theoretical value: $IEC_{\text{prac.}} = 2.21 \text{ meq/g}$.

The blend underwent hydrothermal treatment at 80 °C for varying durations (24, 60, and 168 hours). Following the treatment, the samples were dried and their ion-exchange capacity was determined. The analysis revealed that leaching was practically complete within the first 24 hours, as evidenced by the stabilization of the IEC, with no further decrease observed in the subsequent measurements. Intrinsic viscosity of sPPS-240 was 1.41 dL/g.

The results of the leaching experiment are shown in the Figure 36:

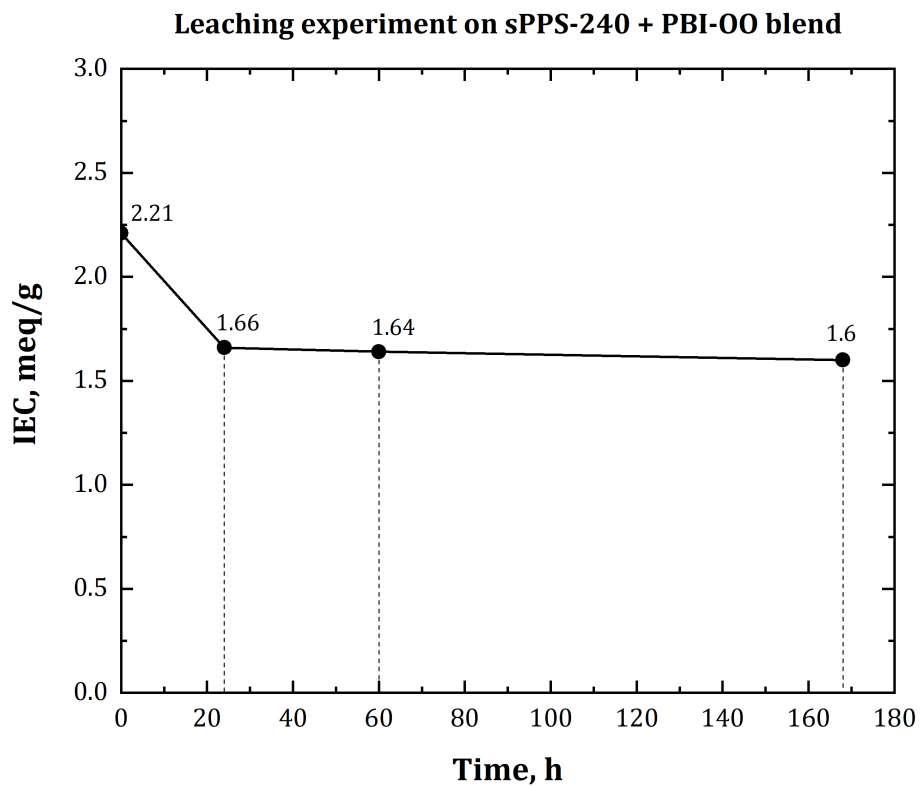


Figure 36. Leaching experiment on sPPS-240 + PBI-00 blend

➤ sPPS-260 + PBI-00

A similar procedure was performed on the sPPS-260 + PBI-00 blend.

Intrinsic viscosity of sPPS-260 was 1.42 dL/g.

The results are presented in Figure 37:

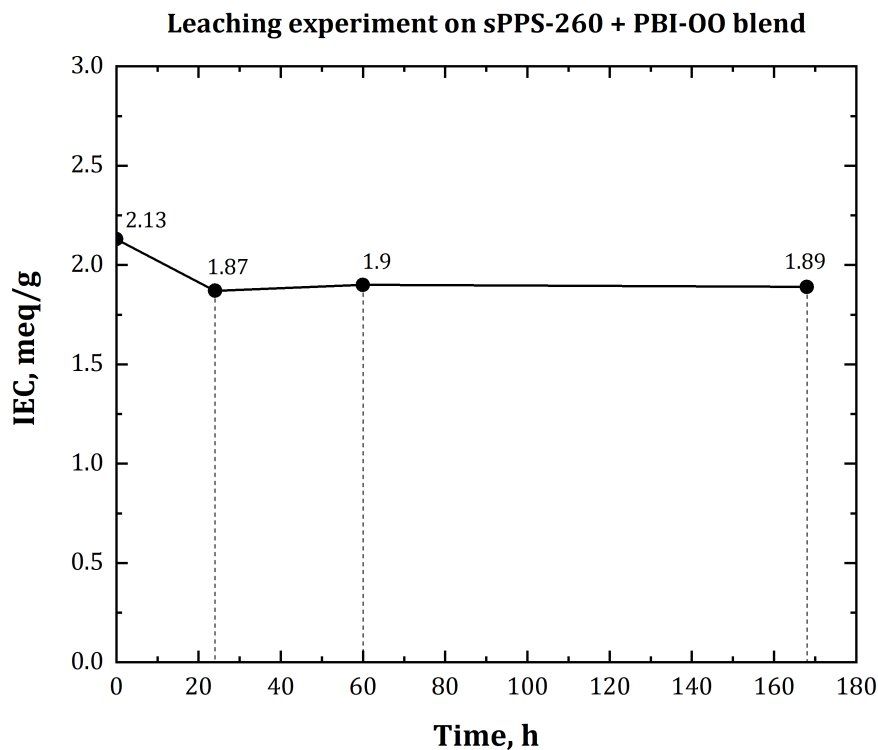


Figure 37. Leaching experiment on sPPS-260 + PBI-00 blend

According to the results, sPPS-240 with higher water mobility was washed out in relatively higher amounts (the decrease in ion-exchange capacity was $2.21 - 1.60 = 0.61$ meq/g) than the less mobile sPPS-260 (the decrease in ion-exchange capacity was $2.13 - 1.87 = 0.26$ meq/g). Since the intrinsic viscosities of sPPS-240 and sPPS-260 are almost the same, the effect of molecular weight can be neglected. Notably, the leaching of sPPS-240, with an intrinsic viscosity of 0.8 dL/g from the PBI-00 blend, was significantly high ($2.20 - 1.10 = 1.10$ meq/g). Thus, leaching is influenced not only by water mobility of sPPS, which is proportional to IEC, but also by molecular weight.

3.3.3. Water uptakes of sPPSs and their blends

The water uptake of sulfonated membranes plays an important role in proton conductivity as water acts as transport medium for protons; it also has a strong impact on the mechanical properties [198]. High WU leads to higher conductivities, but on the other hand causes critical dimensional changes and reduces the mechanical stability of the membranes. Therefore, a balanced WU is necessary for the application as PEMs. WU was

measured as a function of RH at 25 °C as described above. λ values of sPPSs are presented in Figure 38:

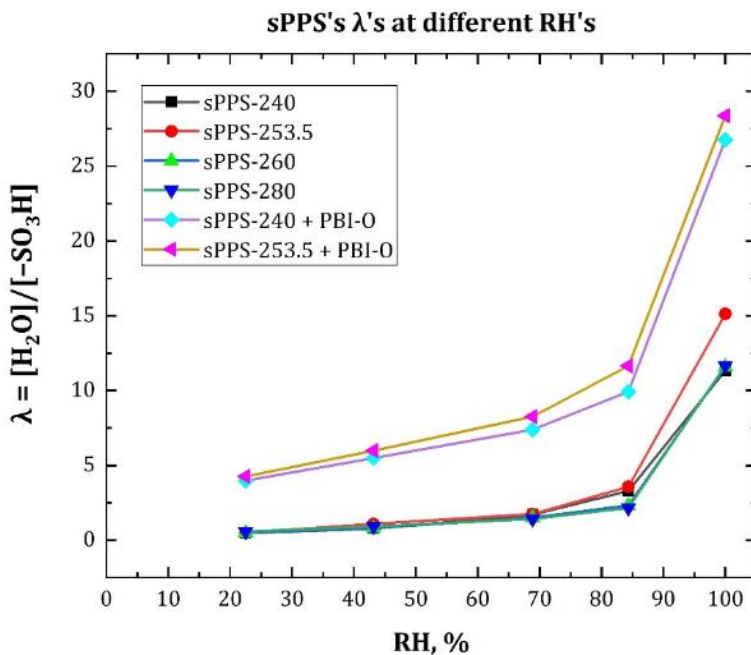


Figure 38. Water uptake of sPPSs and blends

There is a notable difference in the λ values between samples immersed in water and those stored at 100 % relative humidity, even though the water's chemical activity is the same in both conditions. The water uptake (WU) of samples in direct contact with liquid water was approximately 20 % higher than that of samples exposed to saturated water vapor. The phenomenon is known as the Schroeder's paradox and several explanations are reported on the basis of different WU kinetics [199-204]. However, since the data reported in Figure 39 have been obtained after "equilibration" of the samples, i.e. after waiting unless no weight change could be observed anymore, it remains a paradox in this case.

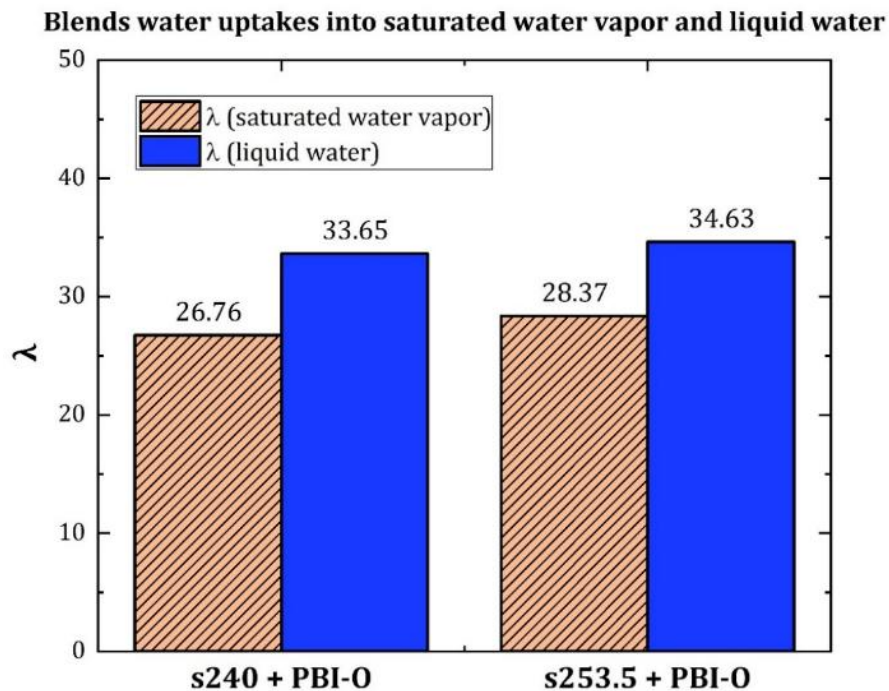


Figure 39. Blends water uptakes into saturated water vapor and liquid water

Both sPPS-240 + PBI-O and sPPS-253.5 + PBI-O polymer blends showed high water uptake in liquid water at room temperature, which is a serious problem for water electrolyzers and needs to be reduced. In order to eliminate this problem, we synthesized monomers with a microblock structure and subsequently polymers from them, in order to decrease the water uptake of the polymer by introducing non-sulfonated microblock segments into the polymer's main backbone. These issues will be discussed in the following chapters.

Reducing water uptake is critical not only in polymer blends but also in pure materials, particularly in the context of water electrolyzers. Here are several reasons why achieving low water uptake is important in both polymer blends and pure materials:

- **Electrochemical Efficiency:** In water electrolyzers, low water uptake is essential for maintaining efficient electrochemical reactions. Excessive water content can lead to flooding of the electrocatalyst sites, limiting the access of reactants to active sites and impeding the kinetics of electrochemical reactions. This reduces the overall efficiency of the electrolyzer, as a

significant portion of the catalyst surface becomes inactive due to water flooding;

- **Proton Conductivity:** Optimal water uptake is crucial for facilitating proton transport in proton-conducting membranes. While water is necessary for proton conduction, excessive water uptake can lead to swelling and structural deformation of the membrane, disrupting the proton-conducting pathways and hindering efficient proton transport. This ultimately reduces the overall proton conductivity of the membrane and compromises device performance;
- **Mechanical Stability:** Low water uptake is necessary to maintain the mechanical stability of the membrane in water electrolyzers. High water content can cause swelling and mechanical instability, leading to dimensional changes and loss of mechanical integrity. This can result in membrane delamination, cracking, or deformation, compromising the structural integrity of the electrolyzer and reducing its operational lifespan;
- **Corrosion and Degradation:** Reduced water uptake helps mitigate corrosion and degradation of electrode materials in water electrolyzers. Excessive water content can facilitate the migration of corrosive species to the electrode surfaces, accelerating degradation of electrode materials and overall system performance;
- **Energy Efficiency:** Minimizing water uptake contributes to improved energy efficiency of water electrolyzers by reducing the energy required for water transport and preventing energy losses associated with inefficient electrochemical reactions. This leads to lower energy consumption and improved overall system efficiency;
- **Long-Term Stability and Reliability:** Low water uptake in both polymer blends and pure materials ensures enhanced stability and reliability over extended periods of operation. This is crucial for maintaining consistent performance and longevity of water electrolyzers, particularly in industrial and commercial applications where reliability is paramount.

Thus, efforts to develop materials with lower water uptake are crucial for advancing the performance and viability of water electrolyzers in various applications such as hydrogen production for renewable energy storage and industrial processes.

3.3.4. Study of the kinetics on the sample of the unoxidized precursor of sPPS-260

The step-growth polymerization reaction is the fundamental process used to synthesize sulfonated aromatic polymers with heteroatoms in main backbone. Understanding its kinetics is essential for several reasons:

a. Control of Polymer Properties:

- Reaction kinetics dictate the rate of polymerization, which directly affects the molecular weight and structure of the polymer;

b. Reaction Efficiency and Yield:

- Studying kinetics helps to optimize the reaction conditions to maximize polymer yield and minimize undesirable byproducts;
- This ensures cost-effective and sustainable production of PEM materials, as efficient reactions reduce waste and resource consumption.

c. Monitoring Reaction Progress:

- Kinetics data provide insight into the reaction progress, enabling to track the formation of functional groups or cross-linking that may affect PEM properties;

d. Quality Control:

- Understanding reaction kinetics is crucial for quality control during PEM manufacturing;
- Deviations from expected kinetics can indicate batch-to-batch variations or the presence of impurities, ensuring consistent PEM quality.

Gel-permeation chromatography (GPC) analyses were conducted in order to study kinetics. During the step-growth polymerization reaction, samples were taken after 2, 4, 6, 8, 10, 12, and 24 hours, precipitated in isopropanol, acidified with concentrated HCl and dialyzed against distilled water for 2 days. After completion, the samples were dried in a vacuum oven at 100 °C for 48 h.

The resulting graph is shown in Figure 40:

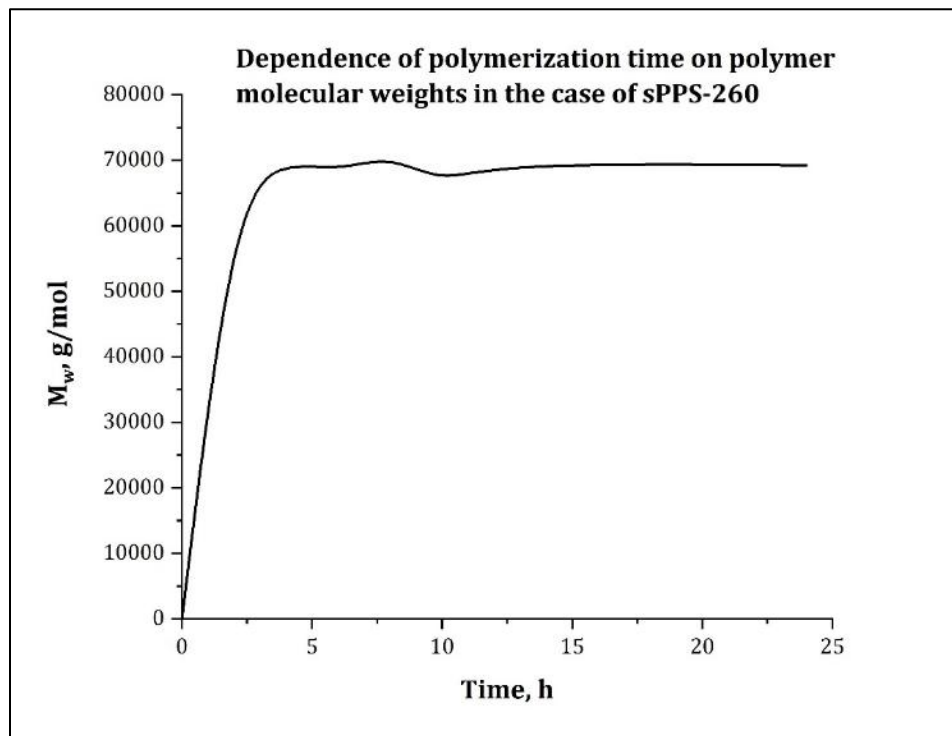


Figure 40. Reaction kinetics graph for the synthesis of unoxidized precursor of sPPS-260

The information provided from the GPC analysis and the kinetics of polymer synthesis has several significant implications and benefits:

1. **Efficient Production:** The plateau in molecular weight after 4 hours indicates a quick, efficient polymer synthesis process, saving time and resources;
2. **Commercial Viability:** Rapid synthesis of high molecular weight polymers supports large-scale production, enhancing cost-effectiveness;
3. **Sustainability:** Shorter reaction times reduce energy and resource consumption, aligning with eco-friendly practices;
4. **Quality Control:** Predictable molecular weight plateauing aids in consistent quality control during production.

3.3.5. NMR spectra of sPPSs

The chemical structure of synthesized polymers was confirmed by nuclear-magnetic resonance spectroscopic analysis.

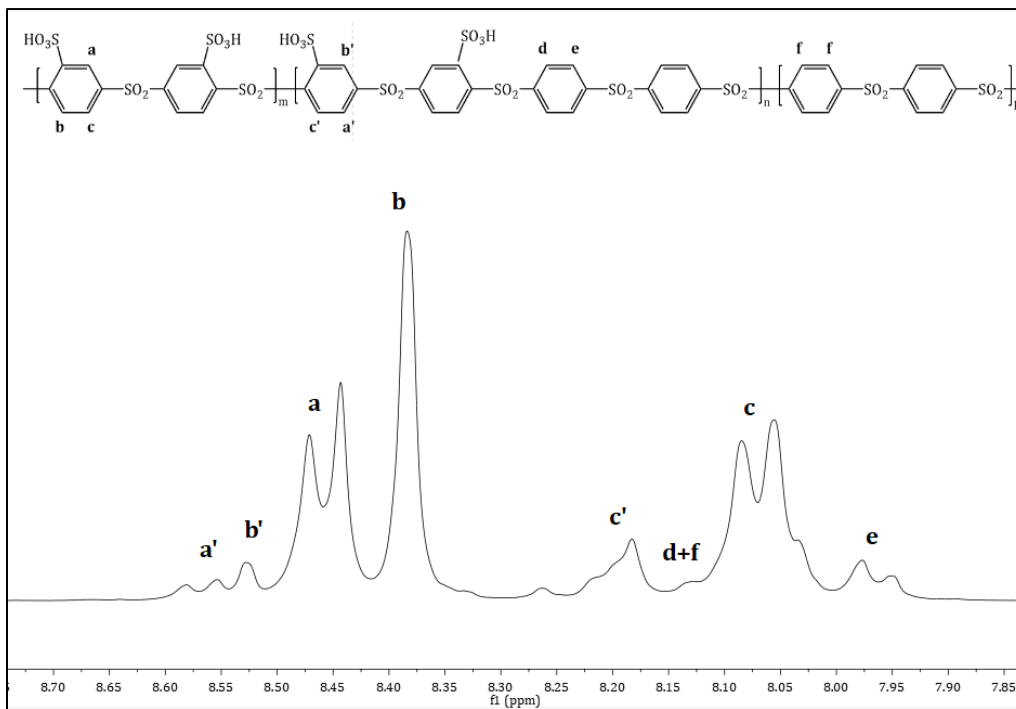


Figure 41. ^1H NMR spectrum of sPPS-240 in $\text{DMSO-}d_6$

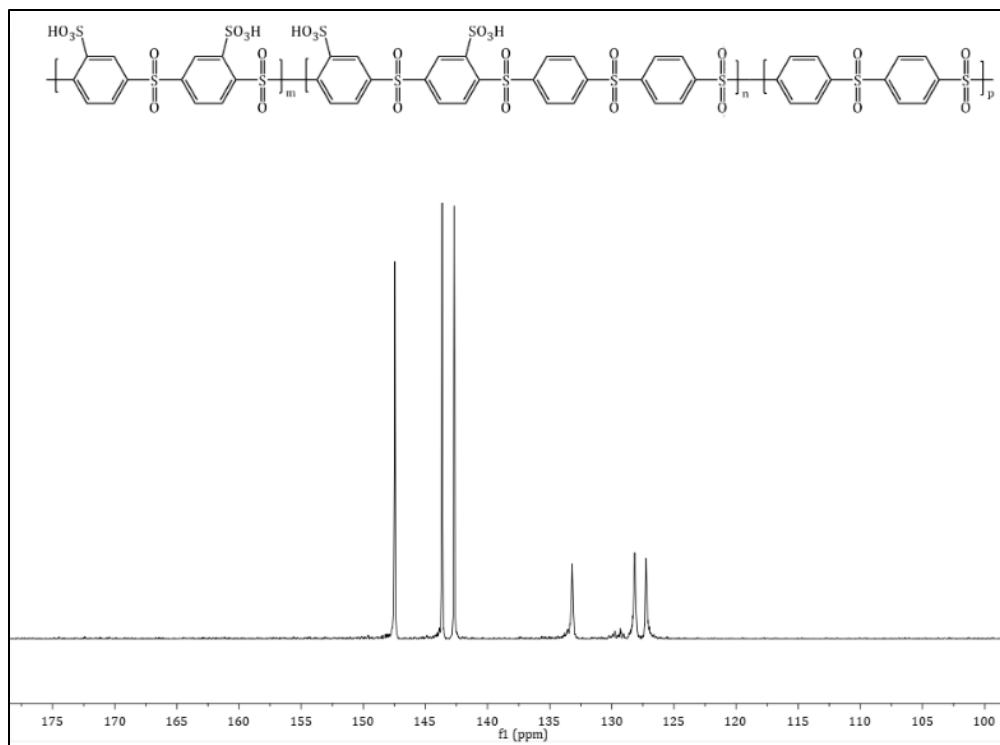


Figure 42. ¹³C NMR spectrum of sPPS-240 in DMSO-d₆

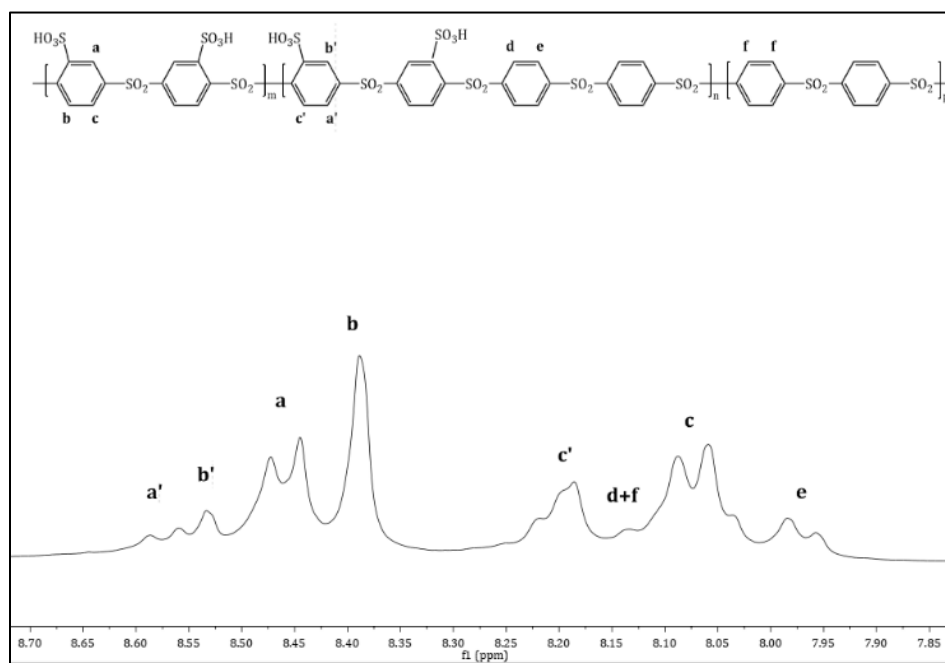


Figure 43. ¹H NMR spectrum of sPPS-260 in DMSO-d₆

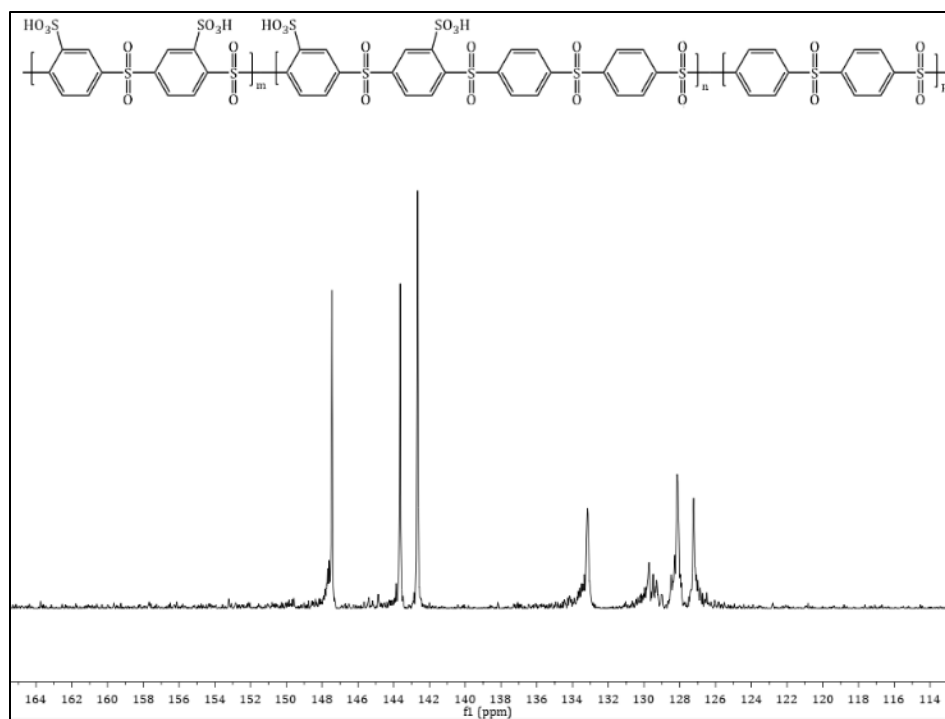


Figure 44. ^{13}C NMR spectrum of sPPS-260 in $\text{DMSO-}d_6$

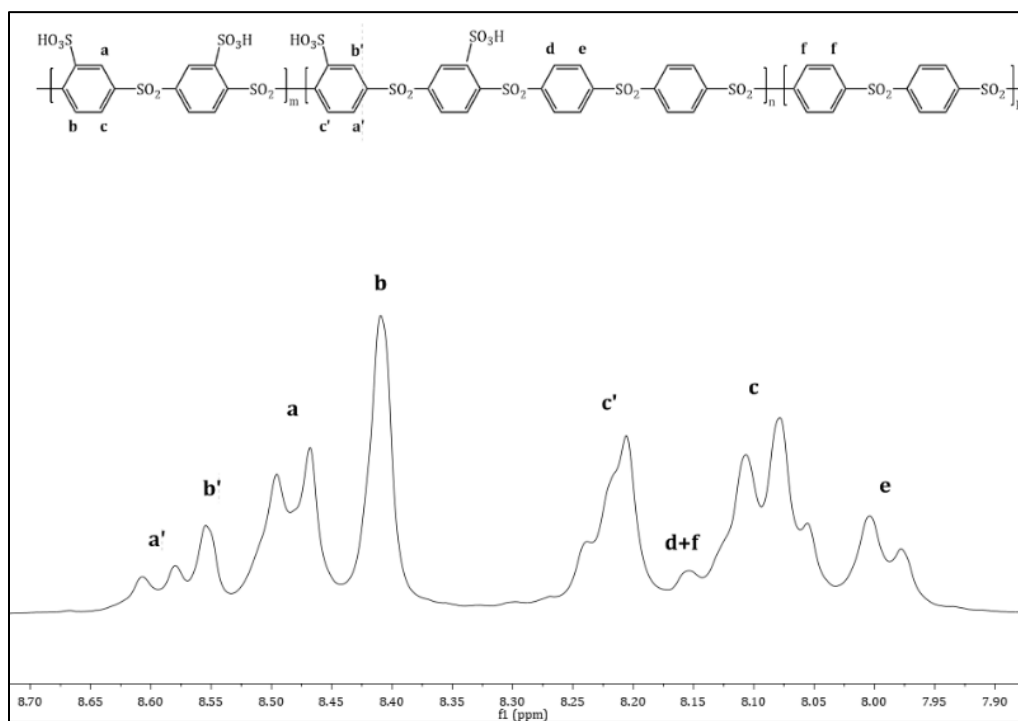


Figure 45. ^1H NMR spectrum of sPPS-275 in $\text{DMSO-}d_6$

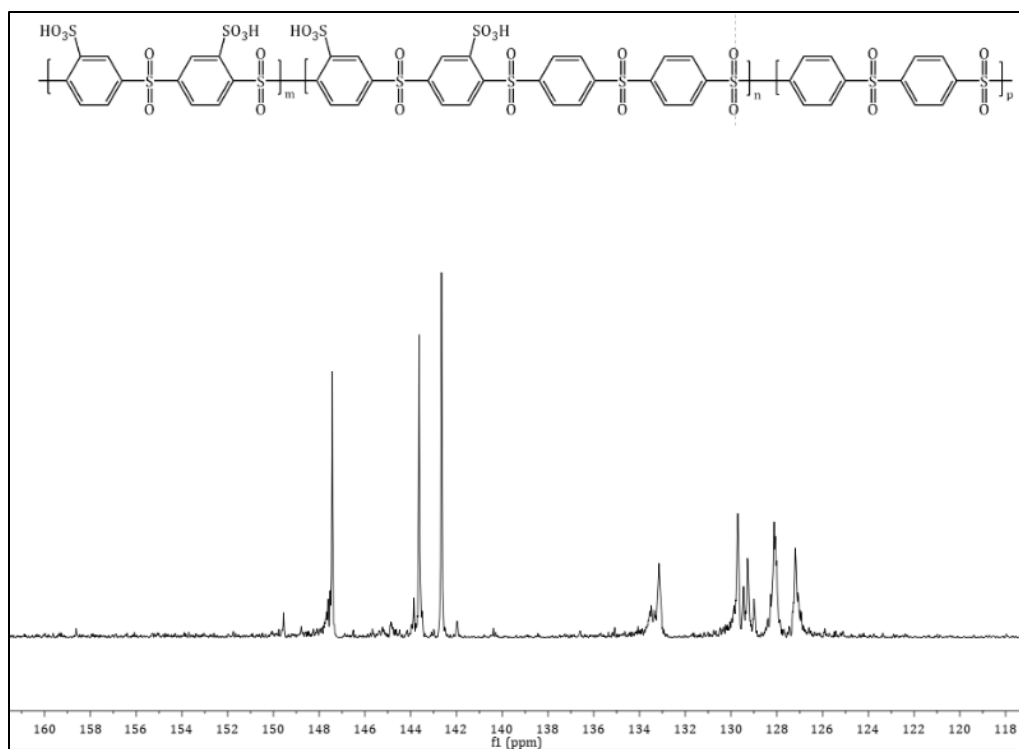


Figure 46. ^{13}C NMR spectrum of sPPS-275 in $\text{DMSO-}d_6$

3.3.6. Solubilities of statistical sPPSs with different equivalent weights

Solubility of polyelectrolytes in different solvents was studied, as it is an important parameter for film casting. The Table 3 summarizes the solubility results of statistical sPPSs with different equivalent weights (synthesized via Li_2S route):

Table 3. Solubilities of statistical sPPSs with different EW's in various common solvents

Sample (H-form)	H_2O (RT)*	DMAc	DMSO	DMF	NMP	NEP
sPPS-240	-	+	+	+	+	+
sPPS-253.5	-	+	+	+	+	+
sPPS-260	-	+	+	+	+	+
sPPS-275	-	+	+	+	+	+
sPPS-280	-	+	+	+	+	+
sPPS-300	-	-	-	-	-	-

Statistical sPPS-360	-	-	-	-	-	-
----------------------	---	---	---	---	---	---

* It should be noted that polyarylenes with ion-exchange capacity > 2.2-2.3 meq/g are soluble in water even at room temperature, highlighting the advantage of sPPS polymers.

As can be seen from the solubility table, the statistical sPPS-360 with blocky fragments obtained by the Li₂S route is insoluble in common organic solvents, unlike the AB-type sPPS-360 reported in the literature [14, 16], which is obtained by the step growth polymerization of SDFDPS and TBBT (4,4'-thiobisbenzenethiol) and does not contain blocky fragments.

Having blocky fragments in the main chain of the polymer has a serious effect on the solubility of the polymer, some reasons are discussed below:

- **Increased Interactions:** The presence of blocky fragments can enhance intermolecular interactions within the polymer matrix. These interactions may include van der Waals forces, hydrogen bonding, or π - π stacking interactions between aromatic groups. As a result, the polymer chains become more tightly packed, reducing the availability of free volume for solvent molecules to penetrate and dissolve the polymer;
- **Reduced Chain Mobility:** Blocky fragments can restrict the mobility of polymer chains, limiting the flexibility and conformational freedom of the polymer. This reduced chain mobility makes it more difficult for solvent molecules to effectively solvate and dissolve the polymer chains, further contributing to decreased solubility;

3.4. General introduction to the synthesis strategy of polymers with different non-sulfonated microblock segments

Sulfonated poly(phenylene sulfone) (sPPS) constitutes a category of hydrocarbon-based polymers with the capacity to conduct protons, holding significant promise as a substitute for perfluorosulfonic acid polymers in various energy applications due to:

1. Outstanding hydrolytic stability of -SO₃H group

Sulfonated poly(phenylene sulfone) (sPPS) exhibits remarkable hydrolytic stability, a critical attribute for materials intended for use in energy applications.

2. Higher acidity of sulfonic acid group compared to other sulfonated aromatic polymer electrolytes

In sPPS, the sulfonated aromatic rings are linked to strongly electron-withdrawing sulfone groups, resulting in their high electron deficiency, which subsequently lowers the pK_a of the sulfonic acid group.

3. Lower gas crossover compared to PFSA

Compared to perfluorosulfonic acid (PFSA) polymers, sPPS demonstrates lower gas crossover. Gas crossover is a phenomenon where hydrogen or other gases permeate through the polymer membrane, affecting the efficiency of electrochemical devices such as fuel cells. The reduced gas crossover in sPPS contributes to enhanced performance and longevity of fuel cells, as it minimizes undesired reactions.

4. Water insolubility at high Ion-Exchange Capacity

One of the notable features of sPPS is its water insolubility, even at high Ion-Exchange Capacity, which results from the strong interaction between macromolecules and the rigidity of the main backbone.

5. High oxidative stability

As discussed in paragraph 3.2, polysulfones containing only sulfone units exhibit the highest oxidative stability, which is crucial for the performance and lifespan of materials in oxidative environments, such as those encountered in fuel cells.

Main drawbacks of sPPS polymers are:

1. Rigid backbone affects film formation properties — strongly dependent on IEC

The rigidity of the backbone in sulfonated poly(phenylene sulfone) (sPPS) presents a notable drawback, particularly affecting its film formation properties. The rigid structure can

hinder the ability of sPPS to form uniform and continuous films, which are crucial for the performance of membranes in energy devices such as fuel cells. The film formation properties are strongly dependent on the Ion-Exchange Capacity of the polymer. This issue may be exacerbated at higher IECs, as increased sulfonation leads to the reduced polymer chain flexibility, making it challenging to achieve the desired film morphology.

2. Excessive Water Uptake (WU) at high IEC

In the development of proton-exchange membranes (PEMs) for fuel cells, balancing proton conductivity with structural integrity remains a significant challenge. Sulfonated poly(phenylene sulfone) (sPPS) has been identified as a promising material due to its thermal stability and proton conductivity. However, achieving the desired levels of proton conductivity often requires a high degree of sulfonation, leading to an elevated Ion-Exchange Capacity. While a higher IEC is advantageous for enhancing proton conductivity, it simultaneously induces excessive water uptake (WU) within the membrane. This excessive water uptake can lead to a series of detrimental effects that compromise the overall performance of the PEM. Below, the key issues associated with excessive WU at high IEC are outlined.

To match the proton conductivity of PFSA, sPPS needs almost double the IEC, which consequently leads to excessive swelling and resulting in following issues:

a. Low mechanical stability at high hydration level

The influx of water molecules into the polymer matrix may compromise its structural integrity, potentially resulting in decreased mechanical strength.

b. High gas crossover — higher oxidative radical formation

High hydrogen permeation in highly water-swollen PEM membranes is due to both increased diffusivity and the higher solubility of hydrogen in the water domains within the membrane. This affects the efficiency of energy conversion processes and leads to higher oxidative radical formation within the system.

We have implemented new strategic approach to address the existing challenges:

"μ-block" strategy

This strategy involves mimicking the structure of multiblock copolymers, which exhibit nano-phase-separated bicontinuous morphologies. This microstructure enhances proton conductivity within the hydrophilic phase and provides mechanical stability through the hydrophobic phase.

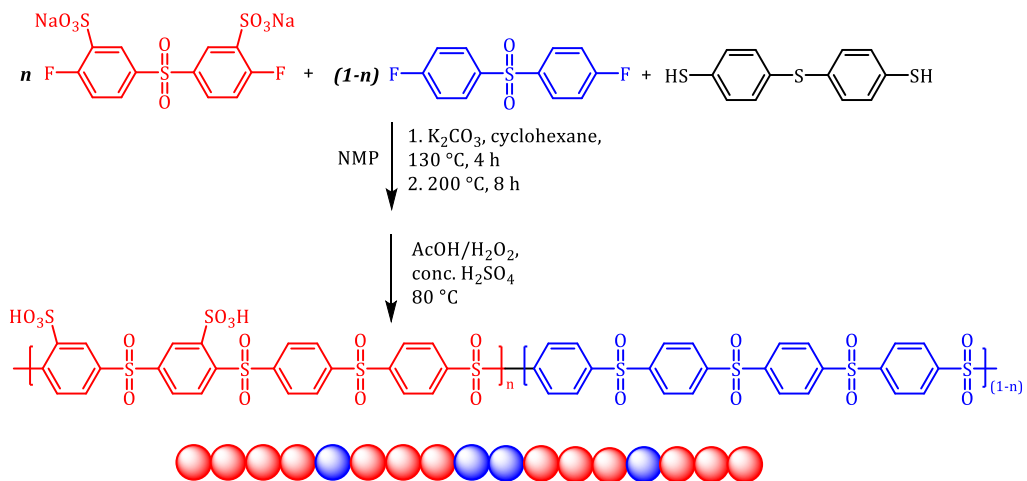
The incorporation of longer unsulfonated poly(phenylene sulfone) (PPS) fragments leads to stronger intermolecular interactions and promotes physical crosslinking. This leads to a decrease in water uptake and an increase in mechanical properties which can be attributed to the increased crystallinity resulting from the longer "blocks" [205].

Due to the relatively shorter block lengths in microblock sPPS, nano-phase separation similar to that in multiblock copolymers is not expected. Consequently, observing its effect on proton conductivity is challenging.

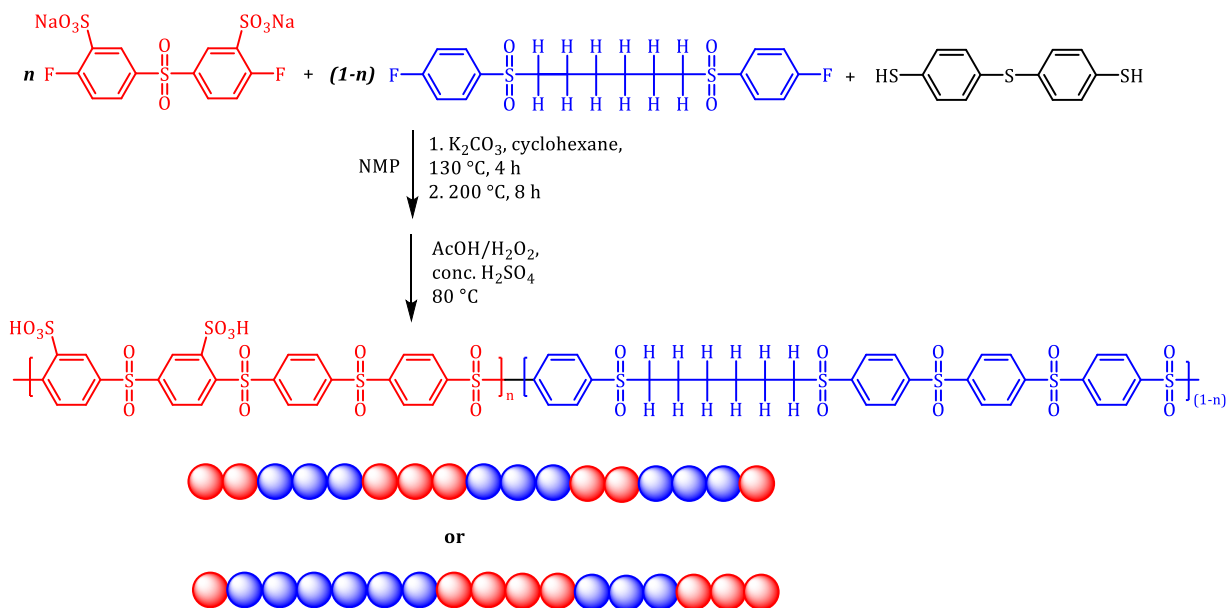
Microblock monomers allow to change the sulfonation sequence in the synthesized polymers (Scheme 53):

In contrast to multiblock copolymers, the microblock copolymers we developed using our strategy do not contain vulnerable electron-donating linking groups such as $-O-$, $-C(CH_3)_2-$, or $-S-$ within non-sulfonated fragments (discussed in 1.1.2–1.1.7).

Synthesis scheme of "regular" sPPS-410



Synthesis scheme of microblock sPPS-410-Hex-XXL



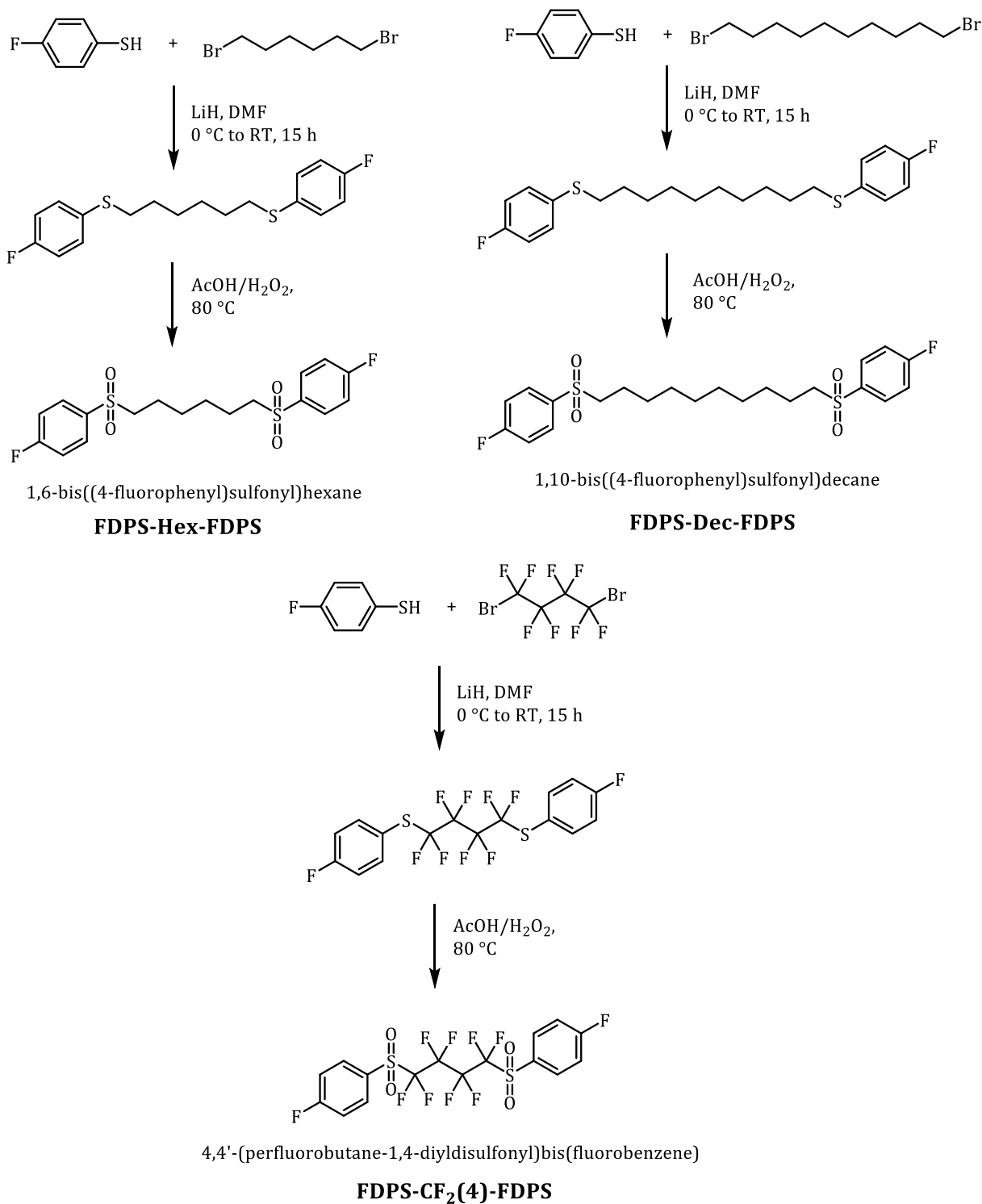
Scheme 53. A general comparative scheme of sulfonated poly(phenylene sulfone)s with "regular" statistical and microblock segments

3.4.1. Synthesis of microblock copolymers containing an alkyl and perfluoroalkyl main chains

In the first part, we will consider the synthesis of microblock monomers containing alkyl and perfluoroalkyl fragments, and then – their corresponding polymers. Perfluoroalkyl-containing microblock was synthesized for comparison with the alkyl-containing monomers but is not intended for application due to the reasons discussed in the introduction.

3.4.1.1. Synthesis of microblock monomers containing an alkyl and perfluoroalkyl main chains

Microblock monomers containing alkyl (*n*-hexyl and *n*-decyl) and perfluoroalkyl (*n*-perfluorobutyl) fragments were synthesized. The reaction proceeds via an S_N2 (bimolecular nucleophilic substitution) mechanism, where the thiolate anion, generated from 4-fluorobenzenethiol, nucleophilically attacks the carbon atoms of dibromides, displacing the bromide ions and forming appropriate products. The synthesis is a two-stage process involving initial nucleophilic substitution followed by oxidation (Scheme 54).



Scheme 54. Synthesis scheme of FDPS-Hex-FDPS, FDPS-Dec-FDPS and FDPS-CF₂(4)-FDPS

The chemical structure of the synthesized monomers was confirmed by nuclear magnetic resonance spectroscopic analysis.

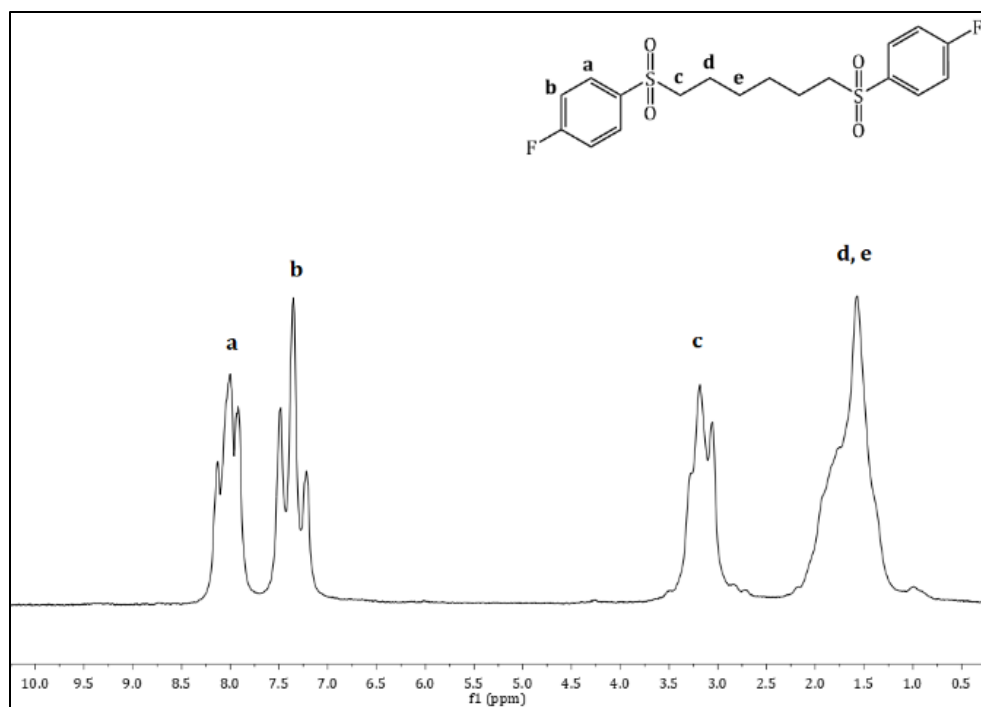


Figure 47. ^1H NMR spectrum of FDPS-Hex-FDPS in CDCl_3



Figure 48. ^{19}F NMR spectrum of FDPS-Hex-FDPS in CDCl_3

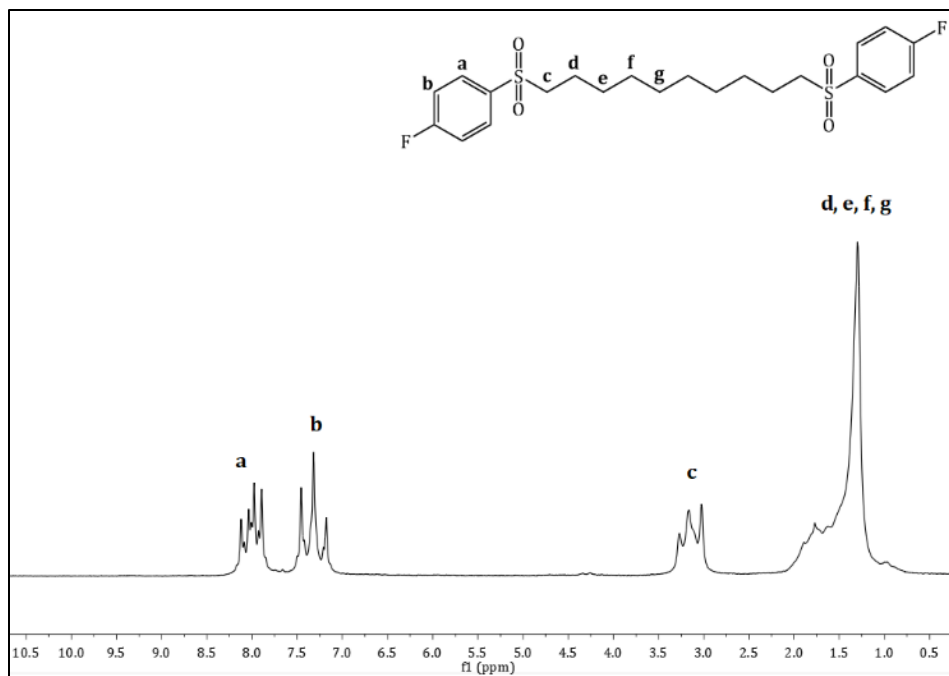


Figure 49. ^1H NMR spectrum of FDPS-Dec-FDPS in CDCl_3

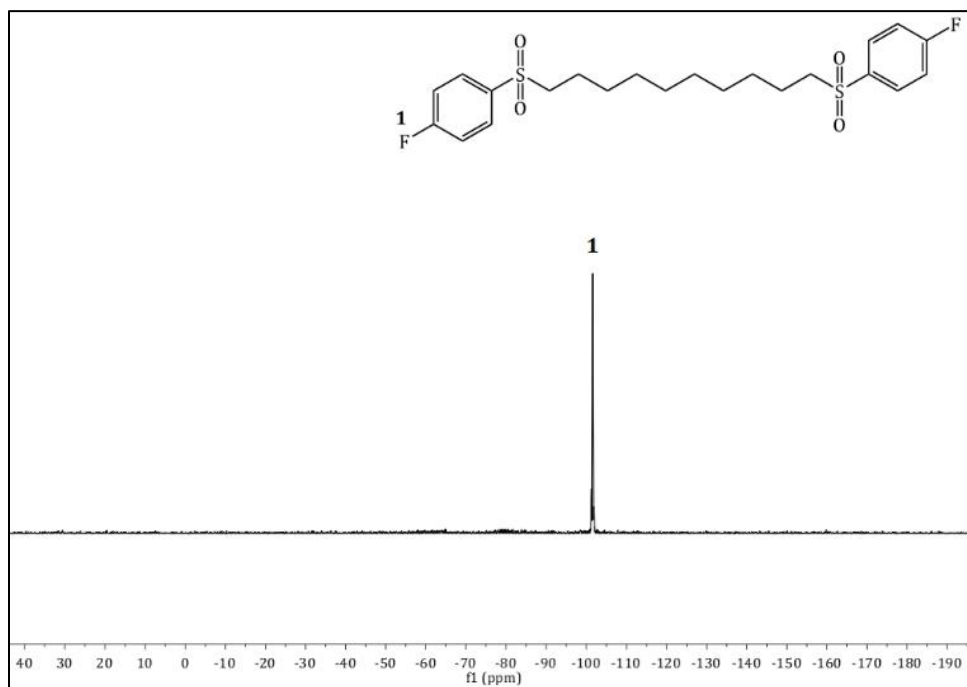


Figure 50. ^{19}F NMR spectrum of FDPS-Dec-FDPS in CDCl_3

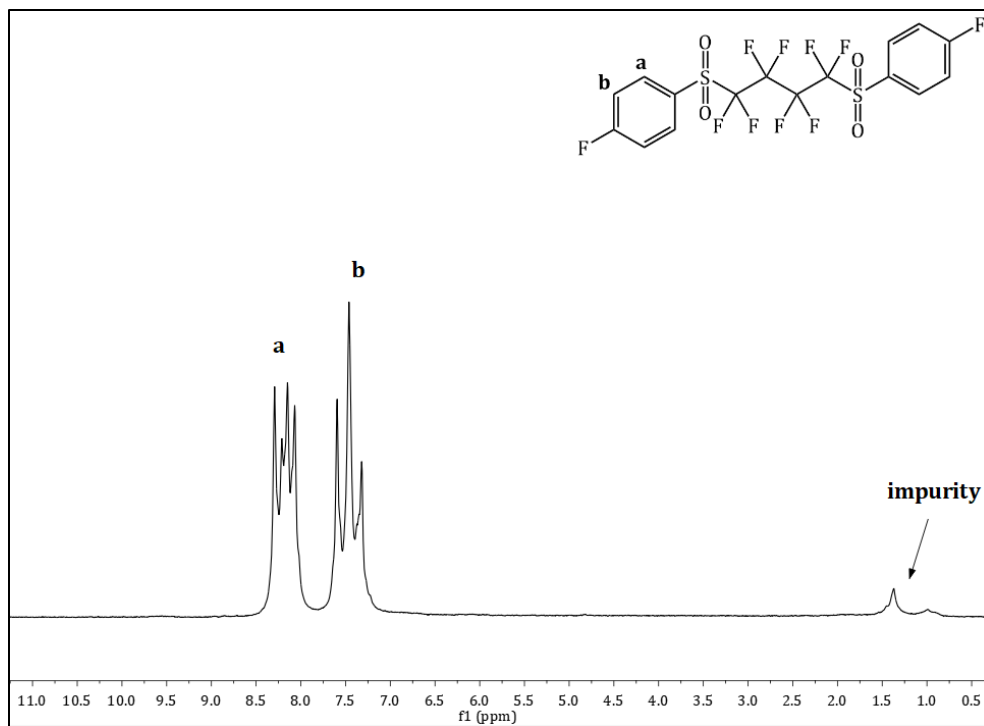


Figure 51. ^1H NMR spectrum of FDPS- $\text{CF}_2(4)$ -FDPS in CDCl_3

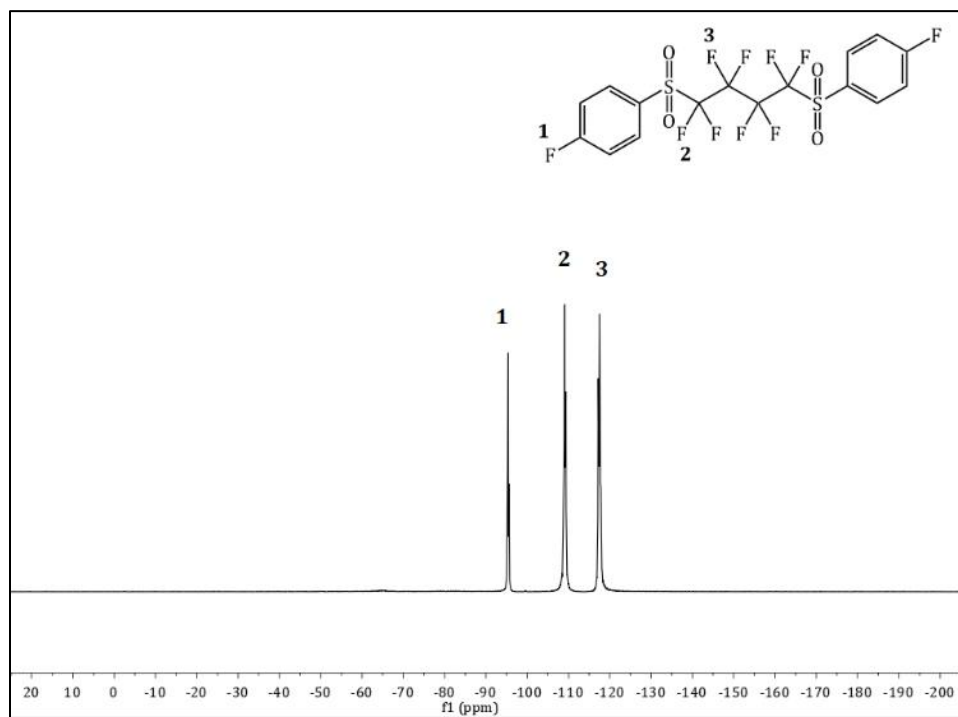


Figure 52. ^{19}F NMR spectrum of FDPS- $\text{CF}_2(4)$ -FDPS in CDCl_3

Despite repeated purification efforts, including recrystallization and column chromatography, additional signals in the 1-1.5 ppm range persisted in the NMR spectrum of the monomer, suggesting the presence of impurities. These impurities likely caused a stoichiometry imbalance during the copolymerization reaction, leading to the formation of low molecular weight polymers that were unable to form films. To further investigate, we analyzed the initial monomer, Br-(CF₂)₄-Br. Although the ¹⁹F NMR spectrum aligned with expectations, the ¹H NMR spectrum revealed unexpected signals, indicating that the compound might not be fully perfluorinated.

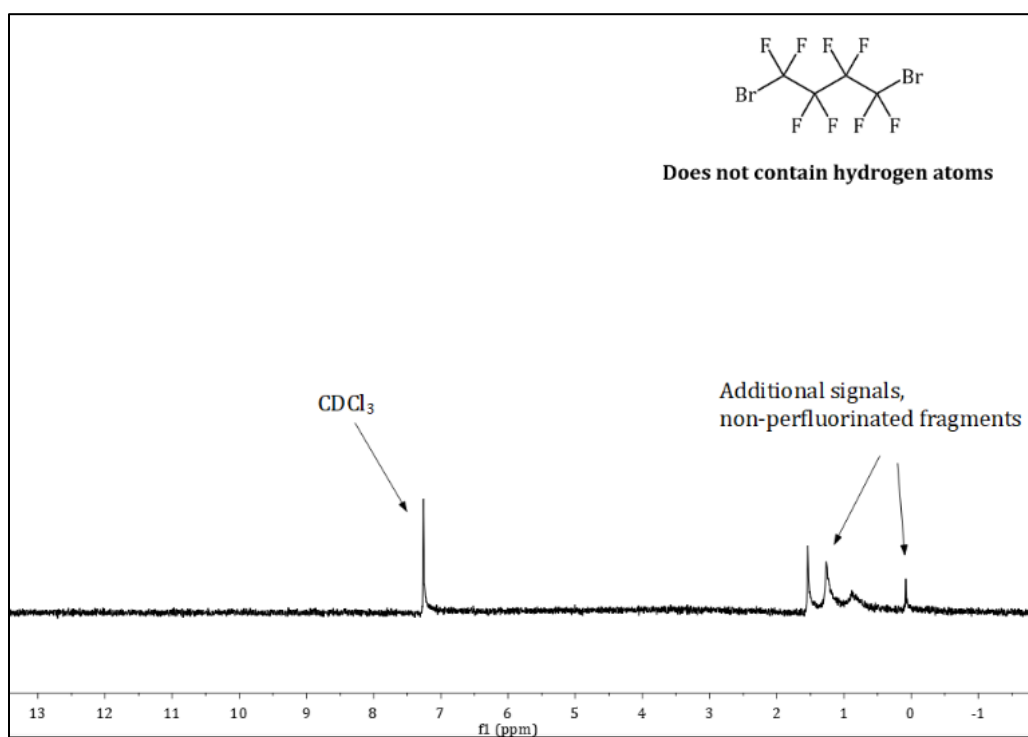


Figure 53. ¹H NMR spectrum of 1,4-dibromooctafluorobutane (1,4-DBOFB) in CDCl₃

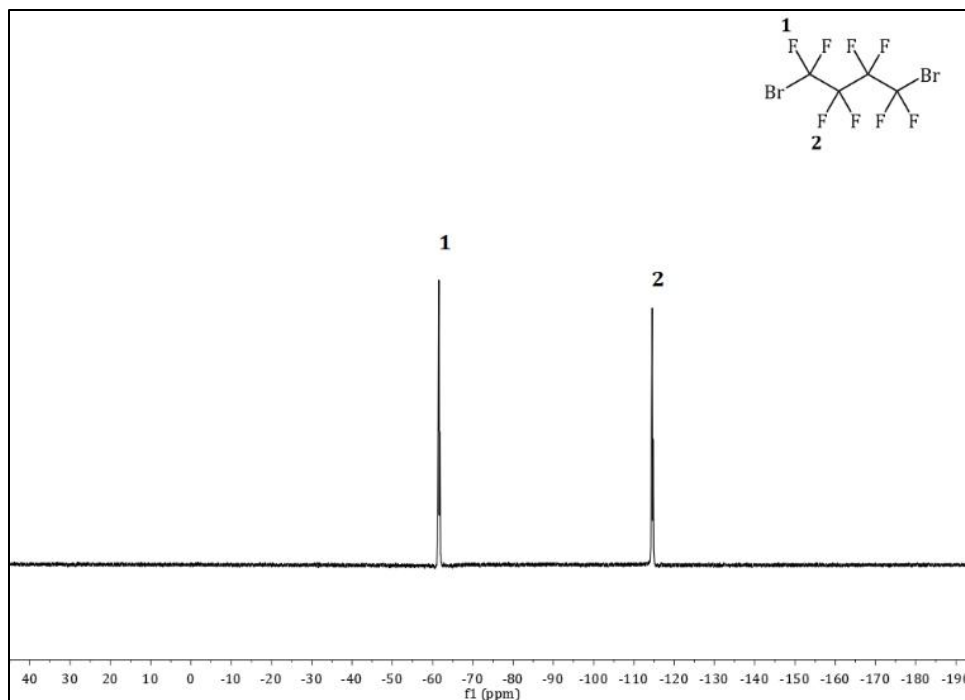
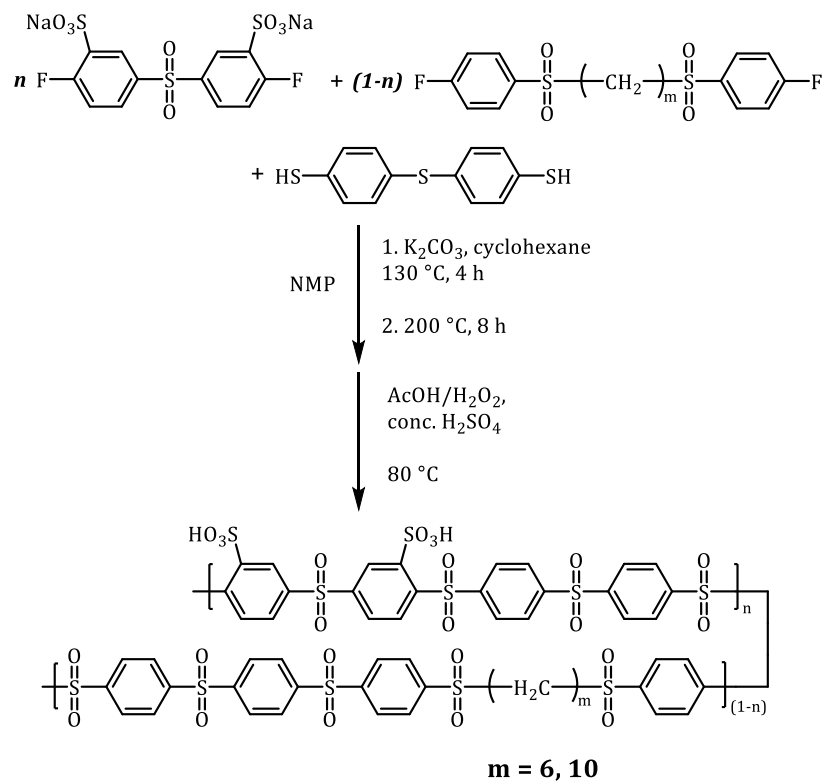


Figure 54. ^{19}F NMR spectrum of 1,4-dibromooctafluorobutane (1,4-DBOFB) in CDCl_3

The monomers FDPS-Hex-FDPS, FDPS-Dec-FDPS, and FDPS- $\text{CF}_2(4)$ -FDPS were synthesized in high yields. These monomers were purified through standard methods, such as recrystallization, ensuring the removal of impurities and enhancing product purity. Each monomer was subjected to specific purification processes appropriate to its chemical properties, leading to the isolation of the desired compounds as white crystalline solids.

3.4.1.2. Synthesis of poly(phenylene sulfone)s containing an alkyl and perfluorinated chains

By co-polymerization of the obtained monomers with TBBT and SDFDPS, oxidation and ion-exchange, polymers with different ion-exchange capacities (2.5-2.3 meq/g) were obtained.



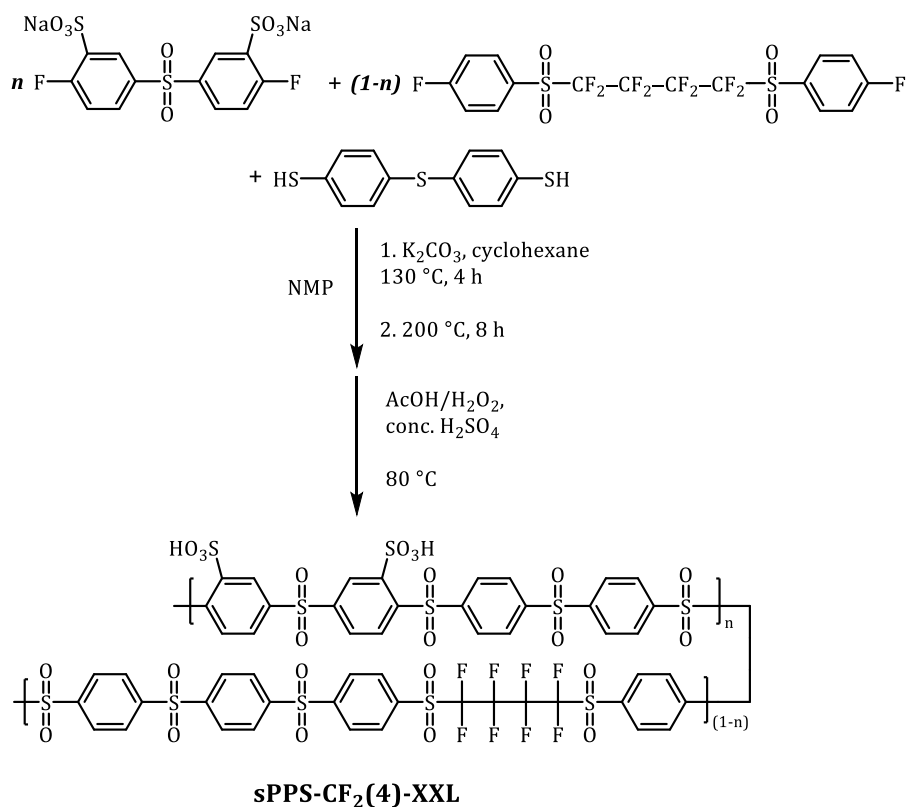
sPPS-Hex-XXL

EW = 410, when $n = 0.877$, $(1-n) = 0.123$.

sPPS-Dec-XXL

EW = 390, when $n = 0.928$, $(1-n) = 0.072$.

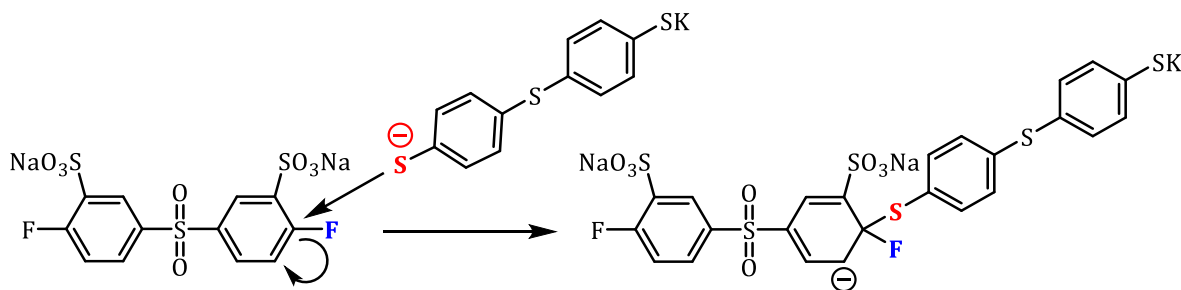
Scheme 55. General synthesis scheme of polymers containing alkyl (C6 and C10) microblock segments



EW = 410, when $n = 0.893$, $(1-n) = 0.107$;
EW = 430, when $n = 0.856$, $(1-n) = 0.144$.

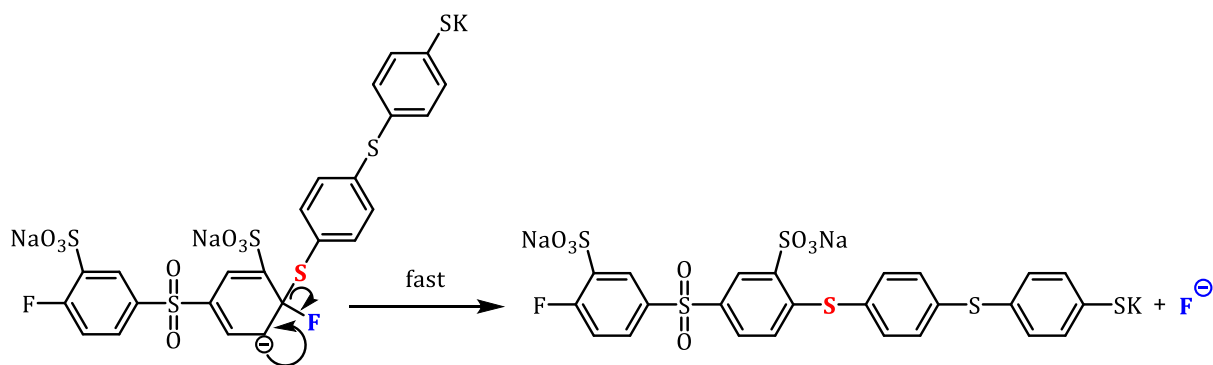
Scheme 56. General synthesis scheme of polymers containing perfluorinated segments

The reaction between SDFDPS and TBBT goes by the mechanism of nucleophilic aromatic substitution (S_NAr). On the first step, nucleophile is attacking electrophilic carbon atom of the aromatic ring (C-F), forming a negatively charged intermediate:



Scheme 57. 1 step of the nucleophilic aromatic substitution reaction between SDFDPS and TBBT

The second step of this reaction is the expulsion of leaving group:



Scheme 58. II step of the nucleophilic aromatic substitution reaction between SDFDPS and TBBT

The intrinsic viscosities of the synthesized polymers were determined and are summarized in the Table 4:

Table 4. Intrinsic viscosities of microblock copolymers containing alkyl and perfluorinated fragments

Sample (H-form)	Intrinsic Viscosity [η], dL/g
sPPS-410-CF ₂ (4)-XXL	0.21
sPPS-430-CF ₂ (4)-XXL	0.15
sPPS-410-Hex-XXL	1.26
sPPS-390-Dec-XXL	1.89

The obtained viscosities indicate that monomers containing alkyl fragments produced high molecular weight sPPS polymers, whereas monomers containing perfluoroalkyl fragments resulted in low molecular weight polymers in both cases. Low molecular weights are attributed to insufficient purity of perfluoroalkyl monomers, as discussed in section 3.4.1.1, leading to stoichiometric imbalance during step-growth polymerization, thus, polymers containing the perfluorinated segment failed to form a film.

In order to determine the film-forming ability of polymers, their solutions in DMSO were prepared, after which they were filtered with a syringe filter and poured onto a petri dish. The results are summarized in the table below:

Table 5. Film forming abilities of microblock copolymers containing alkyl and perfluorinated fragments

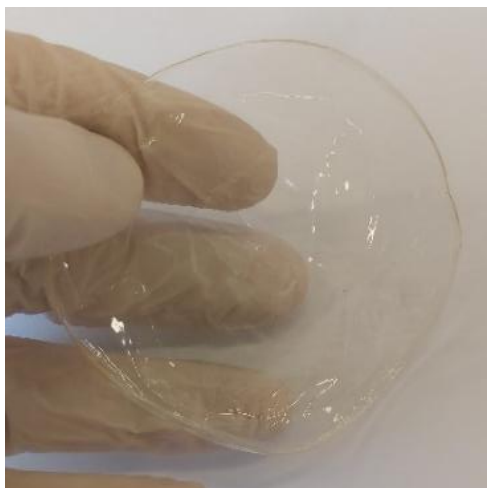
Sample (H-form)	Film formation ability
sPPS-410-CF ₂ (4)-XXL	-
sPPS-430-CF ₂ (4)-XXL	-
sPPS-410-Hex-XXL	+
sPPS-390-Dec-XXL	+

The lack of film-forming properties in sPPS polymers with perfluorinated fragments is attributed to their low molecular weights, rather than their chemical composition and will not be discussed further.

Solubility of polyelectrolytes in different solvents was studied. The table below summarizes the solubility results of microblock copolymers containing alkyl and perfluorinated segments:

Table 6. Solubilities of microblock copolymers containing alkyl and perfluorinated fragments in different solvents

Sample (H-form)	H ₂ O	DMAc	DMSO	DMF	NMP	NEP
sPPS-410-CF ₂ (4)-XXL	-	-	+	-	+	+
sPPS-430-CF ₂ (4)-XXL	-	-	+	-	+	+
sPPS-410-Hex-XXL	-	-	+	-	+	+
sPPS-390-Dec-XXL	-	-	+	-	+	+



Picture 1. Film made from sPPS-410-Hex-XXL

The water uptake of polymers in liquid water at 80 °C was determined. Determining the water uptake parameter of polymers at 80 °C is crucial for assessing their suitability for use in water electrolyzers for several reasons:

- ***Operating Conditions Alignment:*** Water electrolyzers commonly operate at elevated temperatures to enhance reaction kinetics and proton conductivity. The working temperature of 80 °C is often chosen to optimize performance while minimizing energy consumption. Therefore, assessing water uptake at this specific temperature ensures that the polymer's behavior aligns with the actual operating conditions of the electrolyzer;
- ***Thermal and Dimensional Stability Evaluation:*** Operating at elevated temperatures places additional demands on the materials used in water electrolyzers. Assessing water uptake at 80 °C provides valuable insights into the polymer's thermal stability and resistance to dimensional changes under operating conditions.

This parameter provides valuable information for the selection and development of polymer membranes that can withstand the demanding requirements of electrolyzer operation at elevated temperatures.

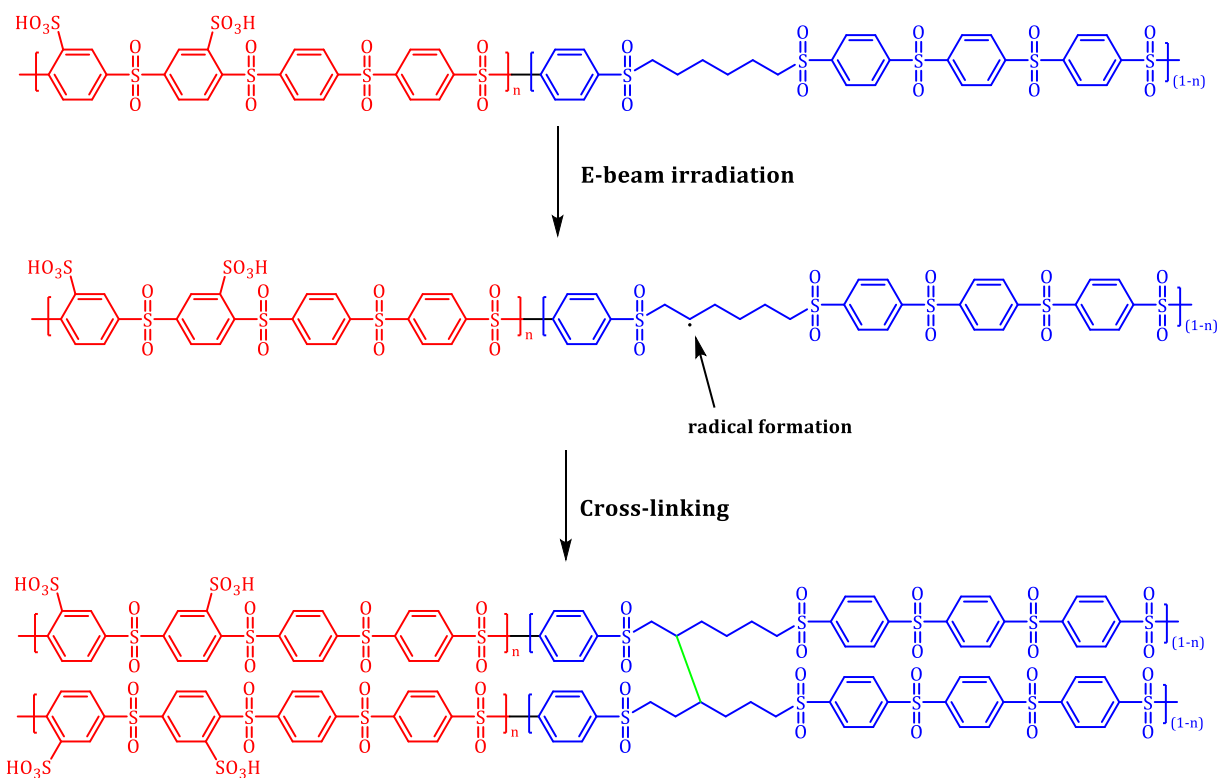
The results are summarized in the Table 7:

Table 7. λ values of microblock copolymers containing alkyl and perfluorinated segments at 80 °C

Sample (H-form)	$\lambda_{80\text{ }^\circ\text{C}} = [\text{H}_2\text{O}]/[-\text{SO}_3\text{H}]$
sPPS-410-CF ₂ (4)-XXL	No film formation ability
sPPS-430-CF ₂ (4)-XXL	No film formation ability
sPPS-410-Hex-XXL	26-30
sPPS-390-Dec-XXL	26-30

The λ values of co-polymers containing alkyl microblock segments is quite close to the target value, but still needs further reduction, which can be implemented by incorporating longer and hydrophobic, new type of microblock segments into the polymer main chain. The discussion on this issue will be continued in the following chapters.

In order to further decrease the water uptake, e-beam irradiation crosslinking trials were carried out on alkyl main chain containing copolymers. E-beam irradiation of membranes with the irradiation dosage of 165 and 198 kGy led to an increase of molecular weight (from M_n 17 kDa up to 46-48 kDa), resulting in a decrease of the water uptake (from $\lambda_{80\text{ }^\circ\text{C}} = 26-30$ to 24-25). The possible mechanism of the crosslinking is shown on Scheme 59:



Scheme 59. Proposed mechanism of cross-linking for alkyl microblock containing sPPS by E-beam irradiation

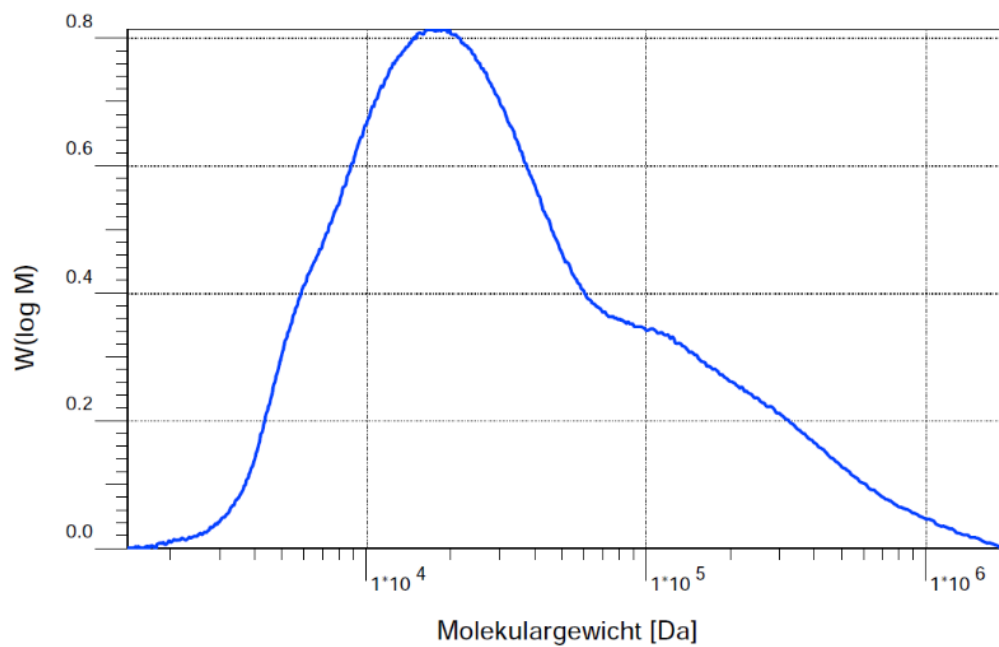


Figure 55. GPC chromatogram of sPPS-410-Hex-XXL before e-beam irradiation

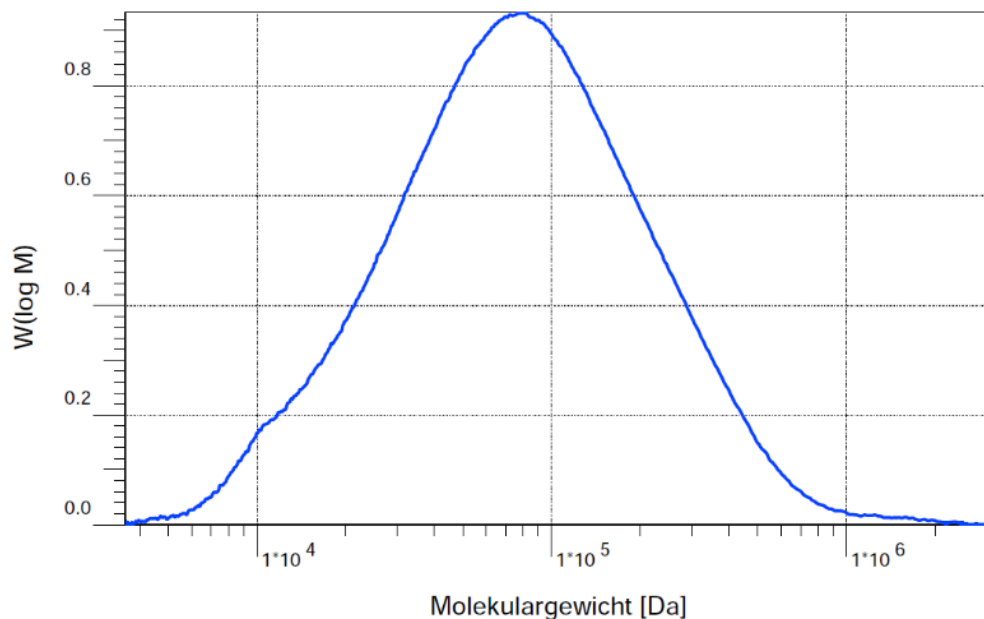


Figure 56. GPC chromatogram of sPPS-410-Hex-XXL after e-beam irradiation (165 kGy)

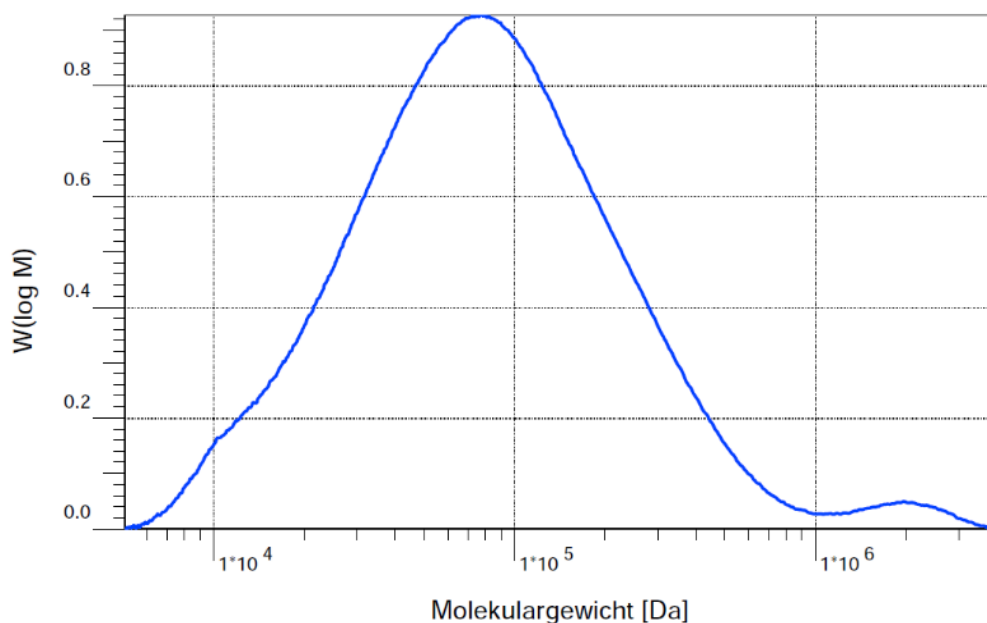


Figure 57. GPC chromatogram of sPPS-410-Hex-XXL after e-beam irradiation (198 kGy)

E-beam irradiation of polymers containing alkyl microblock segments can induce radical formation and subsequent cross-linking of polymer chains through a process known as radiation-induced cross-linking. The mechanism typically involves the following steps:

- **Generation of Free Radicals:** When the polymer is exposed to high-energy electron beams, it absorbs the energy, leading to the formation of free radicals within the polymer matrix. This occurs through the breaking of covalent bonds in the polymer backbone, resulting in the generation of polymer radicals;
- **Migration and Reaction of Radicals:** The free radicals generated within the polymer matrix are highly reactive and can migrate throughout the polymer chains. These radicals then undergo various chemical reactions, including addition reactions with neighboring polymer chains;
- **Cross-Linking:** As the radicals migrate and react with neighboring polymer chains, they can form covalent bonds between the polymer chains, resulting in the formation of cross-links. These cross-links connect different polymer chains together, thereby increasing the overall network density of the polymer matrix.

The cross-linking of polymer chains induced by E-beam irradiation can have several effects on water uptake:

- **Reduced Swelling:** Cross-linking increases the structural integrity and rigidity of the polymer matrix, making it less susceptible to swelling;
- **Enhanced Mechanical Strength:** Cross-linking improves the mechanical properties of the polymer, such as tensile strength and toughness. This can prevent excessive swelling-induced deformation and maintain the dimensional stability of the polymer matrix under aqueous conditions;
- **Improved Chemical Stability:** Cross-linking enhances the chemical stability of the polymer, making it more resistant to degradation by environmental factors such as heat, chemicals, and radiation. This increased stability can prolong the lifespan of the polymer and maintain its performance over time.

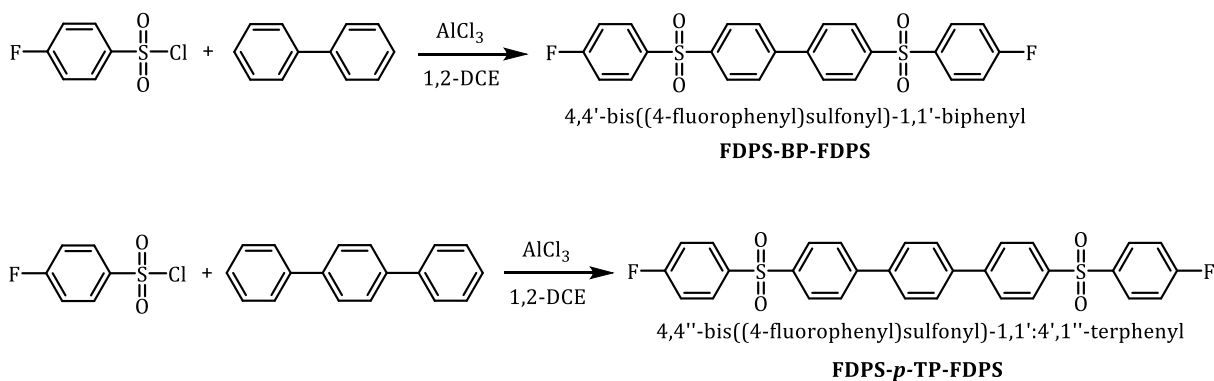
3.4.2. Synthesis of microblock copolymers containing phenylene moieties

In this part is discussed the synthesis of microblock monomers containing phenylene fragments, and then – their corresponding polymers. This approach is inspired by the advantageous properties of sulfonated polyphenylene (sPP), such as good mechanical

properties and lower water uptake, which are attributed to its hydrophobic backbone [128, 169]. Additionally, phenylene fragments are of interest because they can be further sulfonated and used for thermal crosslinking [206]. Thus, this approach is an attempt to combine the advantageous properties of sulfonated poly(phenylene sulfones) and polyphenylenes.

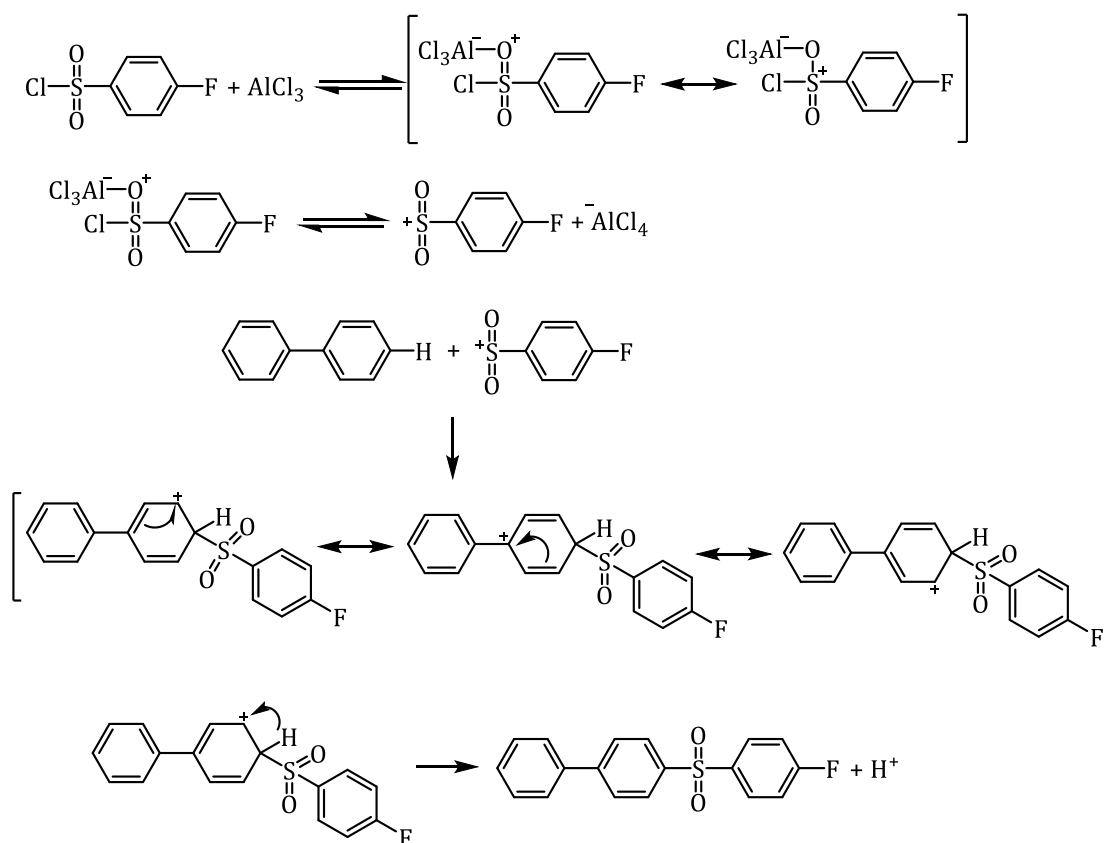
3.4.2.1. Synthesis of microblock monomers containing phenylene moieties

Microblock monomers containing phenylene moieties were synthesized according to the scheme below:



Scheme 60. Synthesis scheme of FDPS-BP-FDPS and FDPS-p-TP-FDPS

The reaction mechanism unfolds as depicted in scheme below: initially, the formation of an attacking reagent, arylsulfonylium cation, takes place through the interaction of sulfonyl chloride and AlCl_3 . Subsequently, the arylsulfonylium cation attacks the aromatic ring, leading to the formation of an intermediate. Upon deprotonation of this intermediate, the final product is obtained.



Scheme 61. Mechanism of the Friedel-Crafts sulfonylation reaction on the example of the synthesis of FDPS-BP-FDPS

In the synthesis of FDPS-BP-FDPS, the product was obtained with a yield of 68 %. After the reaction, the crude product was purified by washing with HCl, distilled water, and methanol, followed by recrystallization from chloroform to obtain the final product with a melting point of 267-268 °C. The chemical structure of FDPS-BP-FDPS was confirmed by NMR analysis.

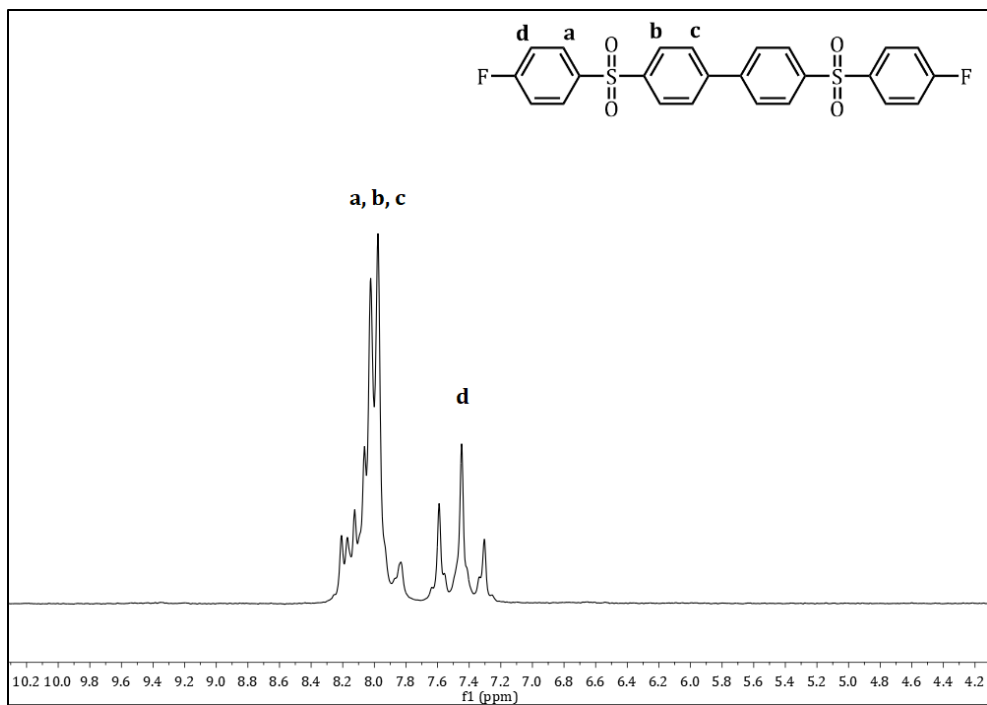


Figure 58. ^1H NMR spectrum of FDPS-BP-FDPS in $\text{DMSO-}d_6$

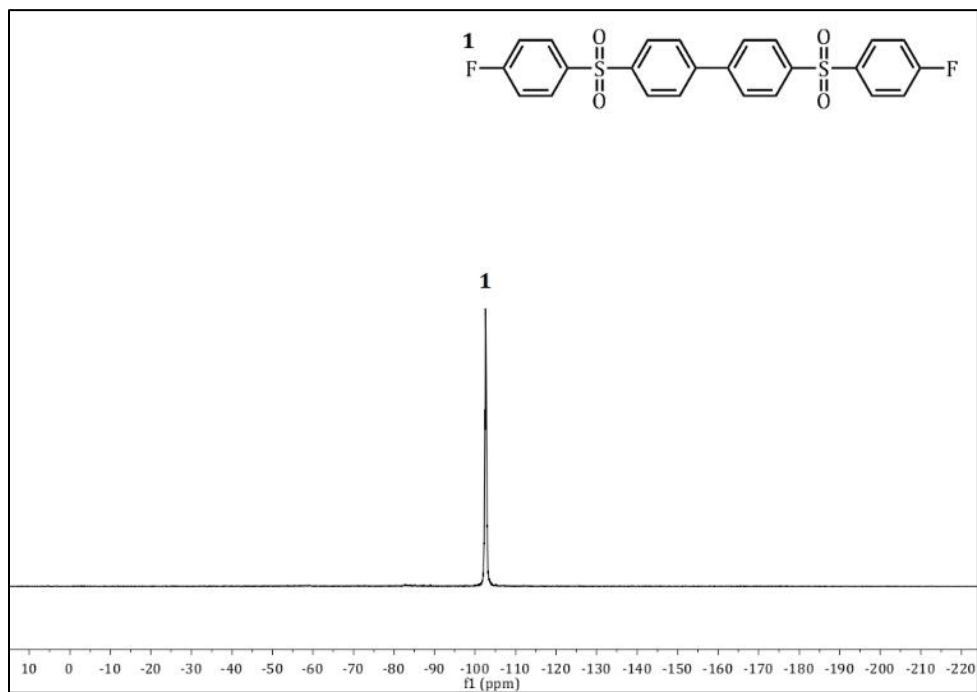


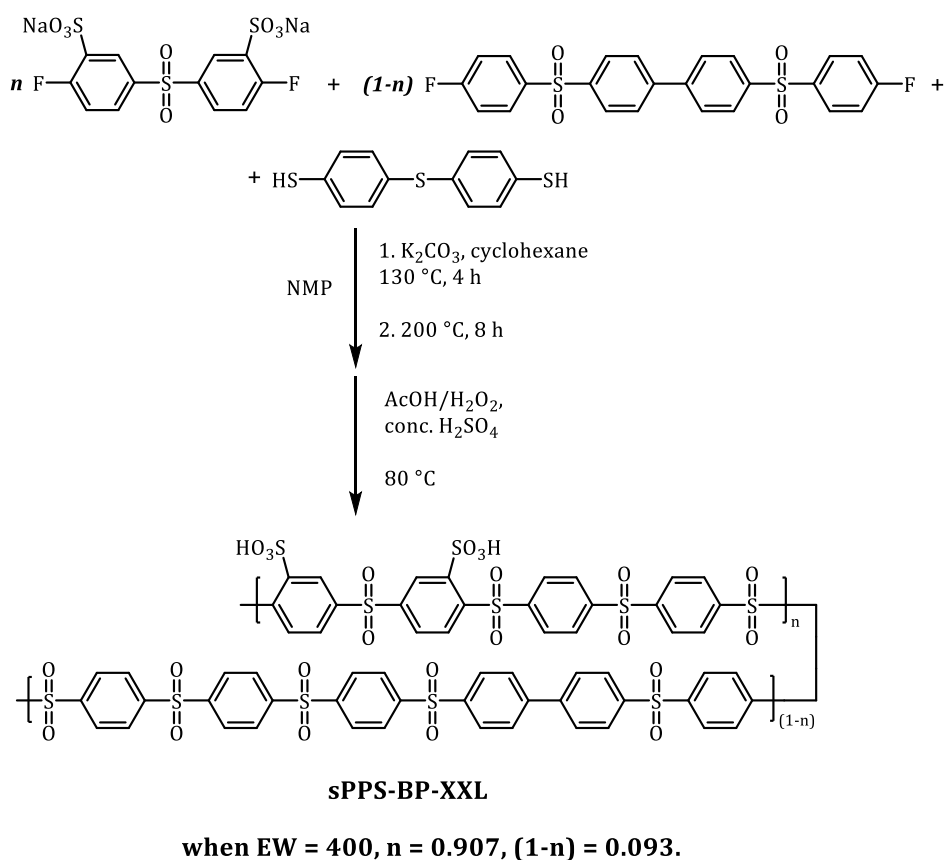
Figure 59. ^{19}F NMR spectrum of FDPS-BP-FDPS in $\text{DMSO-}d_6$

For FDPS-*p*-TP-FDPS, the only solvent in which this compound dissolves is NMP, however, only at high temperatures, therefore, it was not possible to record NMR spectra for

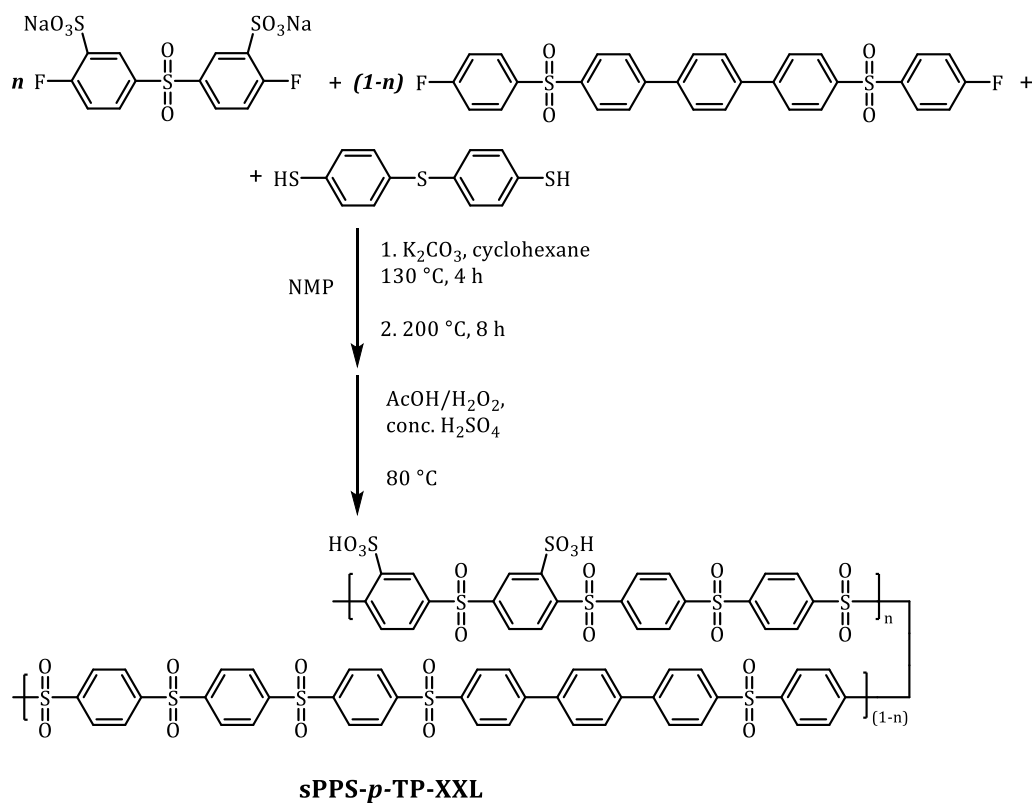
the mentioned compound. TLC analysis confirmed the purity, as indicated by the appearance of a single spot. Solubility in solvents such as acetone, ethyl acetate, dichloromethane, chloroform, 1,2-dichloroethane, acetonitrile, THF, DMSO, DMF, and DMAc was tested, but the compound is not soluble. However, one of the reasons for this may be a high crystallinity, increased π - π stacking and hydrophobicity resulting from the introduction of a *p*-terphenyl fragment.

3.5.2.2. Synthesis of poly(phenylene sulfone)s containing phenylene moieties

By co-polymerization of the obtained monomers with TBBT and SDFDPS, oxidation and ion-exchange, polymers with different ion-exchange capacities (2.5-2.2 meq/g) were obtained.



Scheme 62. General synthesis scheme of microblock copolymers containing biphenyl fragments



when EW = 410, $n = 0.896$, $(1-n) = 0.104$;
 when EW = 430, $n = 0.860$, $(1-n) = 0.140$;
 when EW = 450, $n = 0.826$, $(1-n) = 0.174$.

Scheme 63. General synthesis scheme of microblock copolymers containing *p*-terphenyl fragments

The chemical structure of synthesized polymers was confirmed by ^1H and ^{13}C NMR analysis.

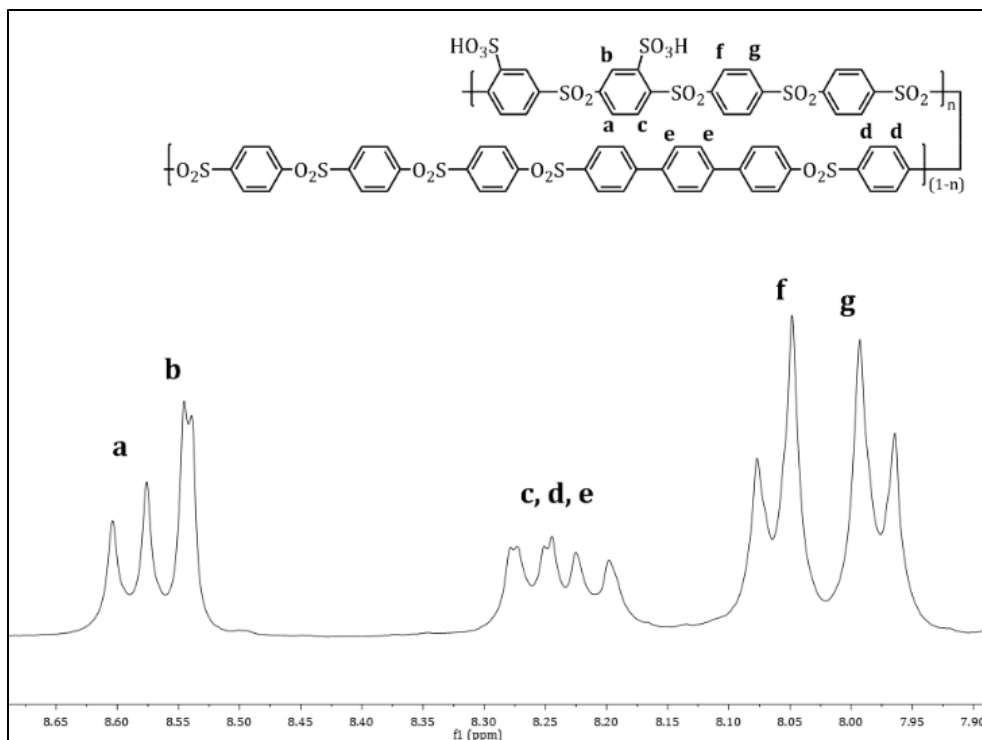


Figure 60. ^1H NMR spectrum of sPPS-410-*p*-TP-XXL in $\text{DMSO-}d_6$

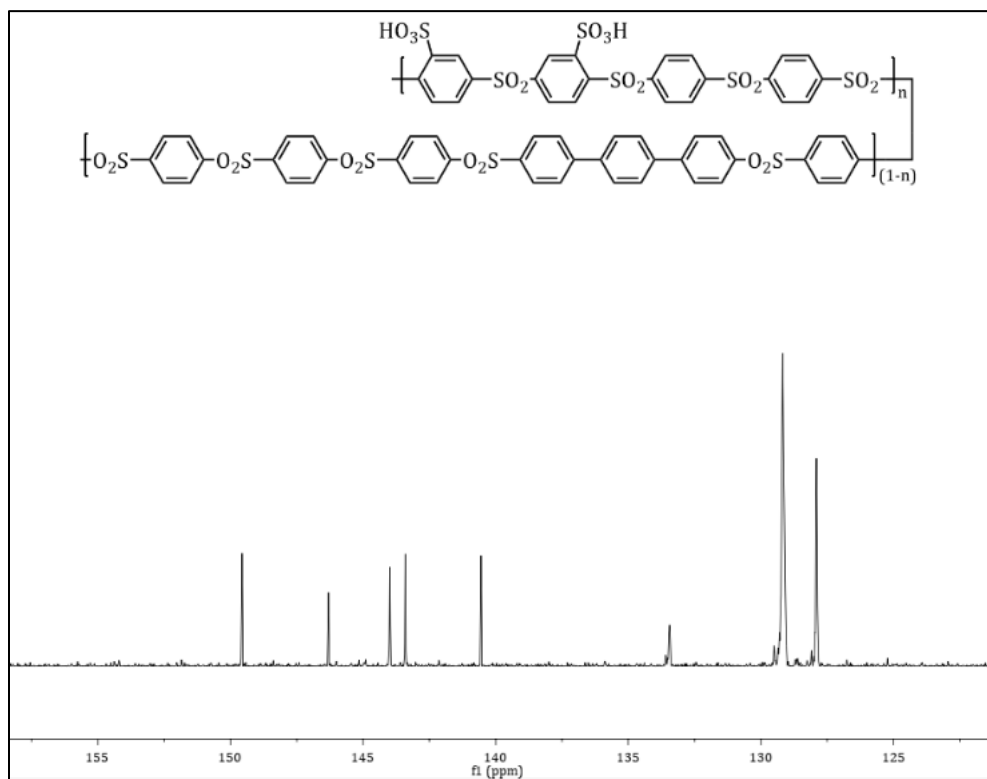


Figure 61. ^{13}C NMR spectrum of sPPS-410-*p*-TP-XXL in $\text{DMSO-}d_6$

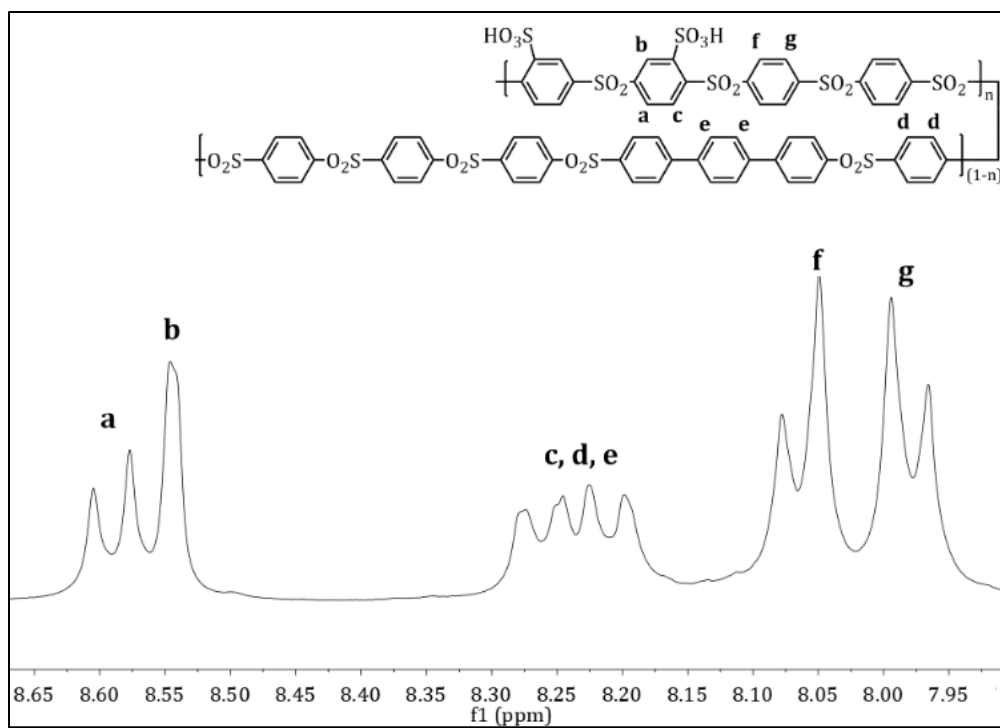


Figure 62. ¹H NMR spectrum of sPPS-430-*p*-TP-XXL in DMSO-*d*₆

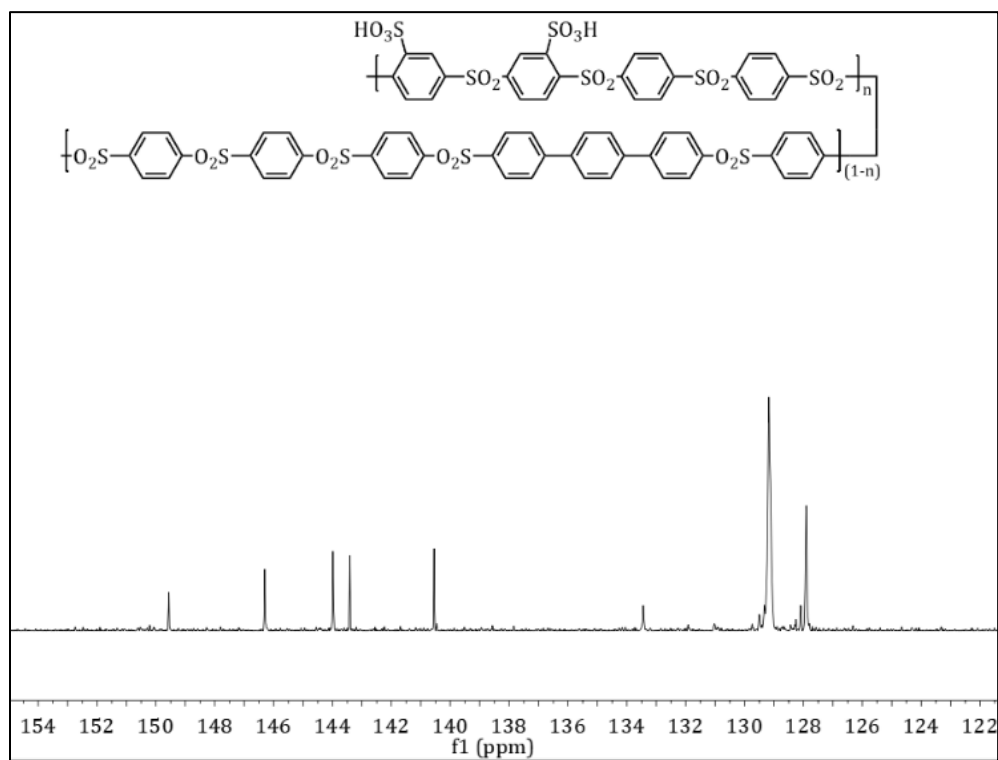


Figure 63. ¹³C NMR spectrum of sPPS-430-*p*-TP-XXL in DMSO-*d*₆

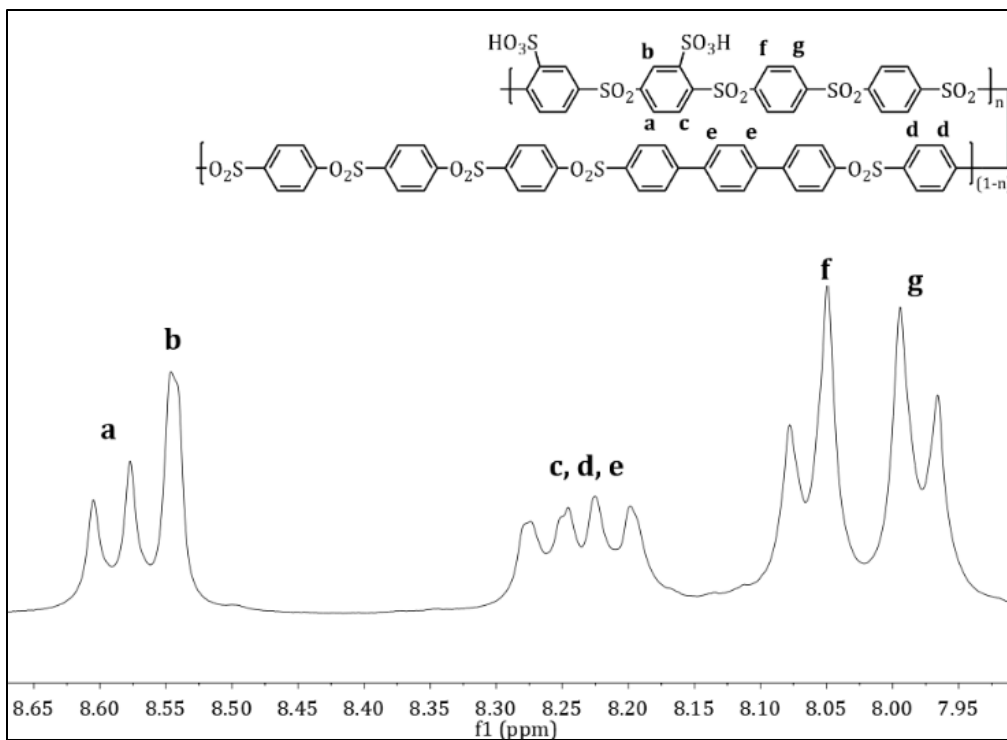


Figure 64. ^1H NMR spectrum of sPPS-450-*p*-TP-XXL in $\text{DMSO-}d_6$

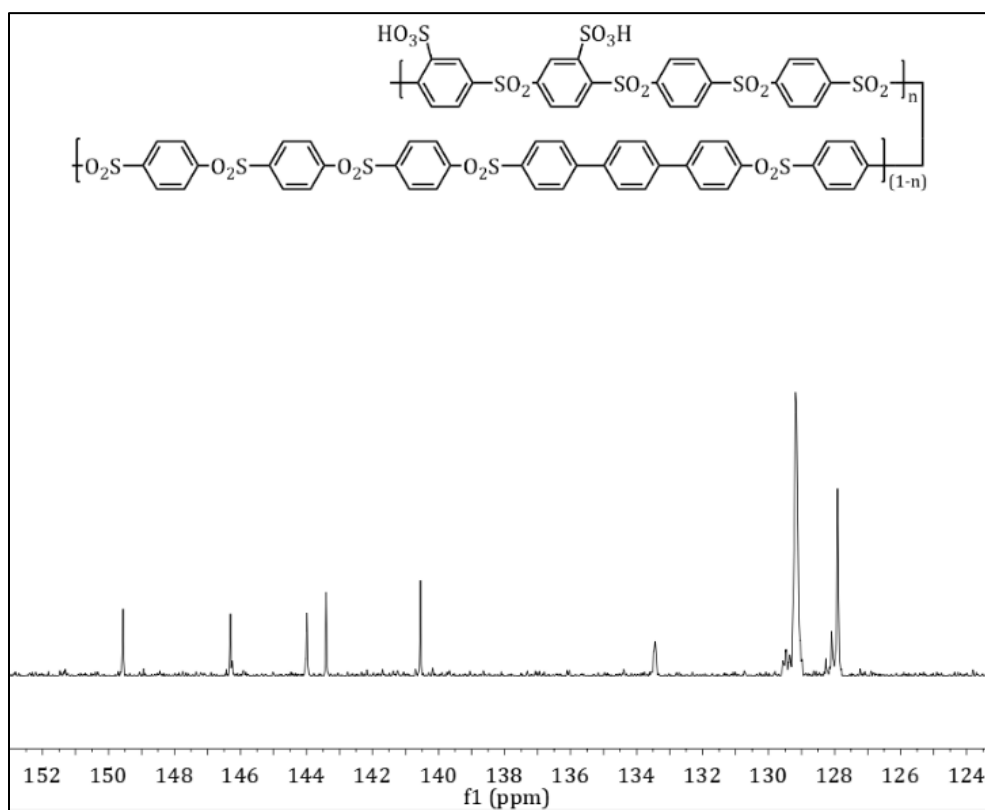


Figure 65. ^{13}C NMR spectrum of sPPS-450-*p*-TP-XXL in $\text{DMSO-}d_6$

The intrinsic viscosities of the synthesized polymers were determined and are summarized in the table below:

Table 8. Intrinsic viscosities of microblock copolymers containing phenylene fragments

Sample (H-form)	Intrinsic Viscosity [η], dL/g
sPPS-400-BP-XXL	1.75
sPPS-410- <i>p</i> -TP-XXL	2.10
sPPS-430- <i>p</i> -TP-XXL	2.26
sPPS-450- <i>p</i> -TP-XXL	3.04

In order to determine the film-forming ability of polymers, their solutions in DMSO were prepared, after which they were filtered with a syringe filter and poured onto a petri dish. The results are summarized in the table below:

Table 9. Film forming abilities of microblock copolymers containing phenylene fragments

Sample (H-form)	Film formation ability
sPPS-400-BP-XXL	+
sPPS-410- <i>p</i> -TP-XXL	+
sPPS-430- <i>p</i> -TP-XXL	+
sPPS-450- <i>p</i> -TP-XXL	+

Solubility of polyelectrolytes in different solvents was studied. The table below summarizes the solubility results of microblock copolymers containing biphenyl and terphenyl segments:

Table 10. Solubilities of microblock copolymers containing phenylene fragments in different solvents

Sample (H-form)	H ₂ O	DMAc	DMSO	DMF	NMP	NEP
sPPS-400-BP-XXL	-	-	+	-	+	+

sPPS-410- <i>p</i> -TP-XXL	-	-	+	-	+	+
sPPS-430- <i>p</i> -TP-XXL	-	-	+	-	+	+
sPPS-450- <i>p</i> -TP-XXL	-	-	+	-	+	+

The water uptake of polymers in liquid water at 80 °C was determined. The results are summarized in the table below:

Table 11. λ values of microblock copolymers containing phenylene fragments at 80 °C

Sample (H-form)	$\lambda_{80\text{ °C}} = [\text{H}_2\text{O}]/[-\text{SO}_3\text{H}]$
sPPS-400-BP-XXL	31-33
sPPS-410- <i>p</i> -TP-XXL	24-25
sPPS-430- <i>p</i> -TP-XXL	24-25
sPPS-450- <i>p</i> -TP-XXL	24-25

The comparison between copolymers containing phenylene fragments and those containing alkyl fragments reveals interesting insights into their water uptake behavior:

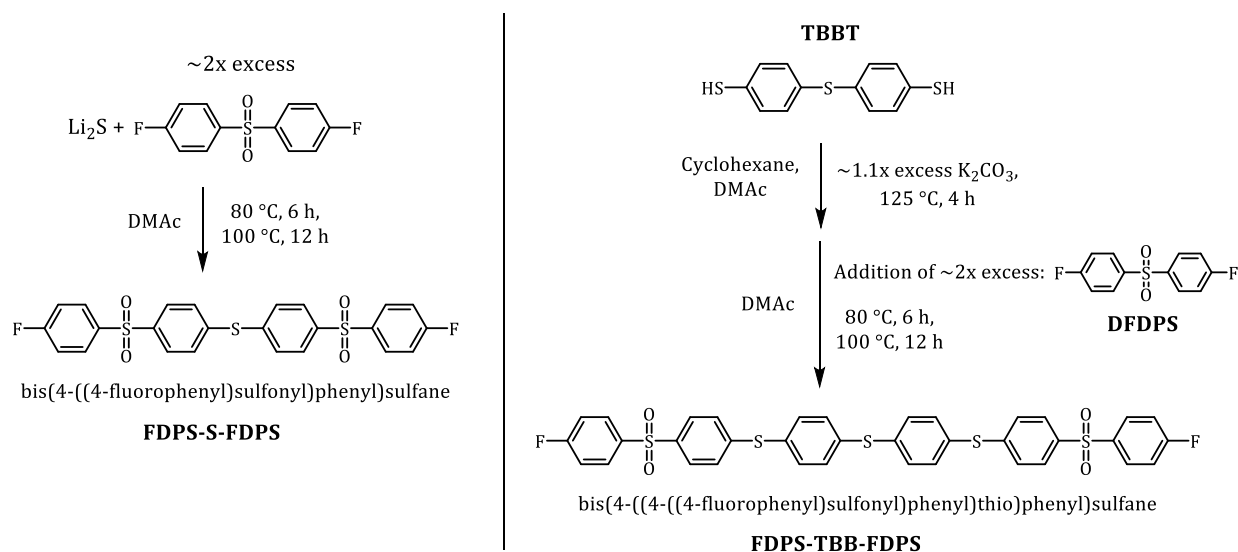
- Copolymers containing phenylene fragments exhibit water uptake levels comparable to those containing alkyl fragments. This suggests that the introduction of phenylene microblock segments into the polymer chain does not result in a significant additional decrease in water uptake. The low effect of phenylene fragments can be explained by their relatively low fraction (around 10-18 mol %).
- Furthermore, polymers containing biphenyl fragments have a higher λ value (indicating a higher hydration number) compared to those containing *p*-terphenyl fragments. This difference can be attributed to the more hydrophobic nature of *p*-terphenyl fragments and underscores the importance of the specific structural arrangement in influencing water uptake behavior.

3.4.3. Synthesis of microblock copolymers containing merely sulfone units

In this part is discussed the synthesis of microblock monomers containing merely sulfide and sulfone units, and then – their corresponding poly(phenylene sulfone)s that consist solely of sulfone units and phenyl rings in the main backbone.

3.4.3.1. Synthesis of microblock monomers containing merely sulfur and sulfone units

Microblock monomers containing merely sulfur and sulfone units were synthesized according to the scheme below:



Scheme 64. Synthesis scheme of FDPS-S-FDPS and FDPS-TBB-FDPS

The chemical structures of FDPS-S-FDPS and FDPS-TBB-FDPS was confirmed by ^1H , ^{13}C and ^{19}F NMR analysis. The purification of FDPS-S-FDPS involved column chromatography and resulted in a relatively low yield of 32 %. In contrast, for FDPS-TBBT-FDPS, recrystallization followed by washing with water and *i*-PrOH was sufficient, yielding 68 %.

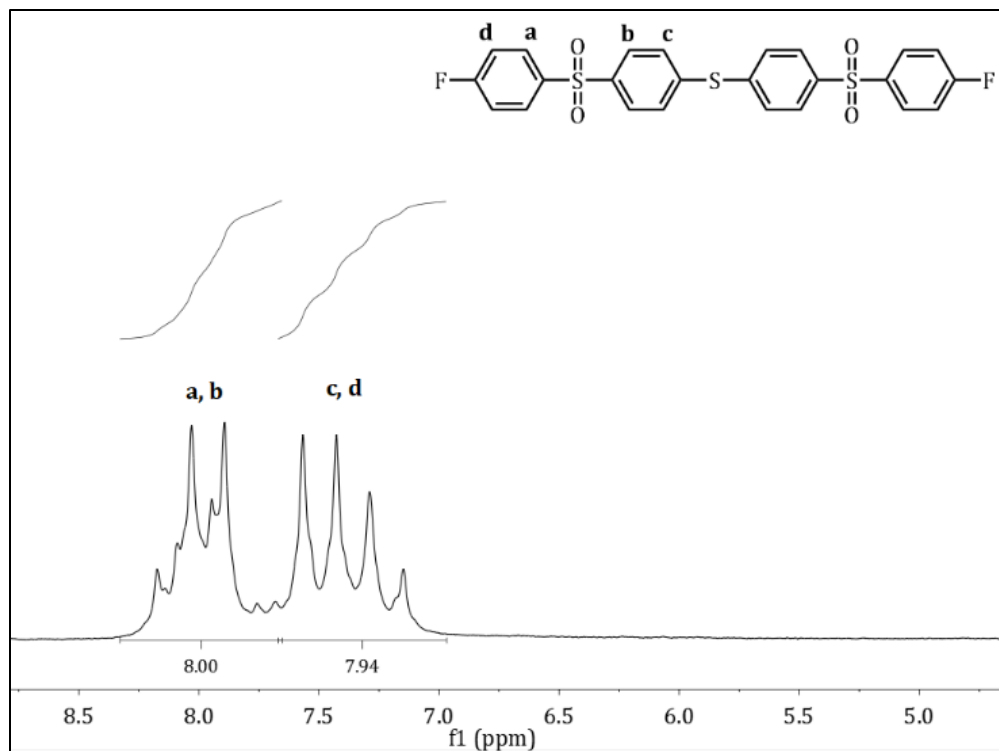


Figure 66. ^1H NMR spectrum of FDPS-S-FDPS in CDCl_3

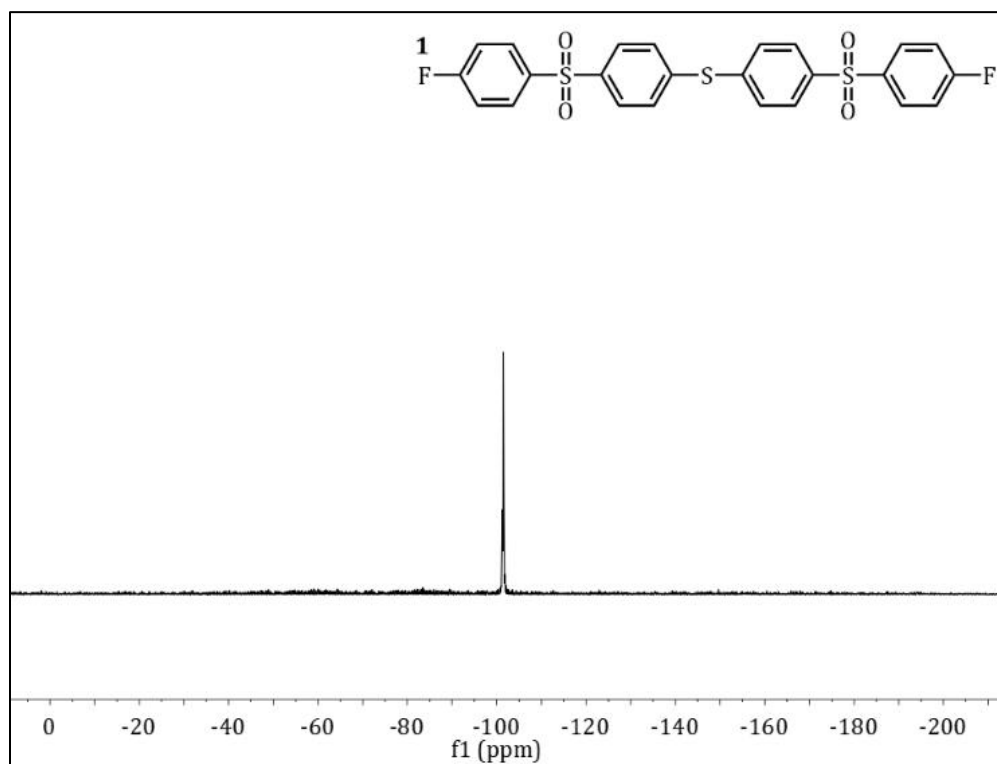


Figure 67. ^{19}F NMR spectrum of FDPS-S-FDPS in CDCl_3

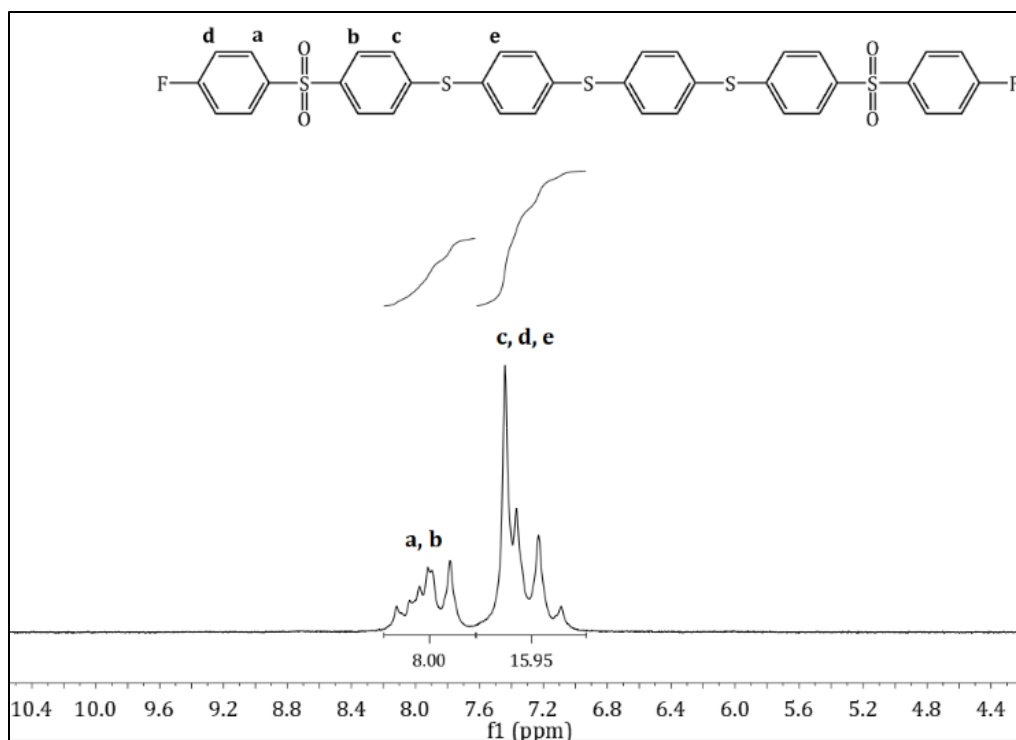


Figure 68. ¹H NMR spectrum of FDPS-TBB-FDPS in CDCl₃

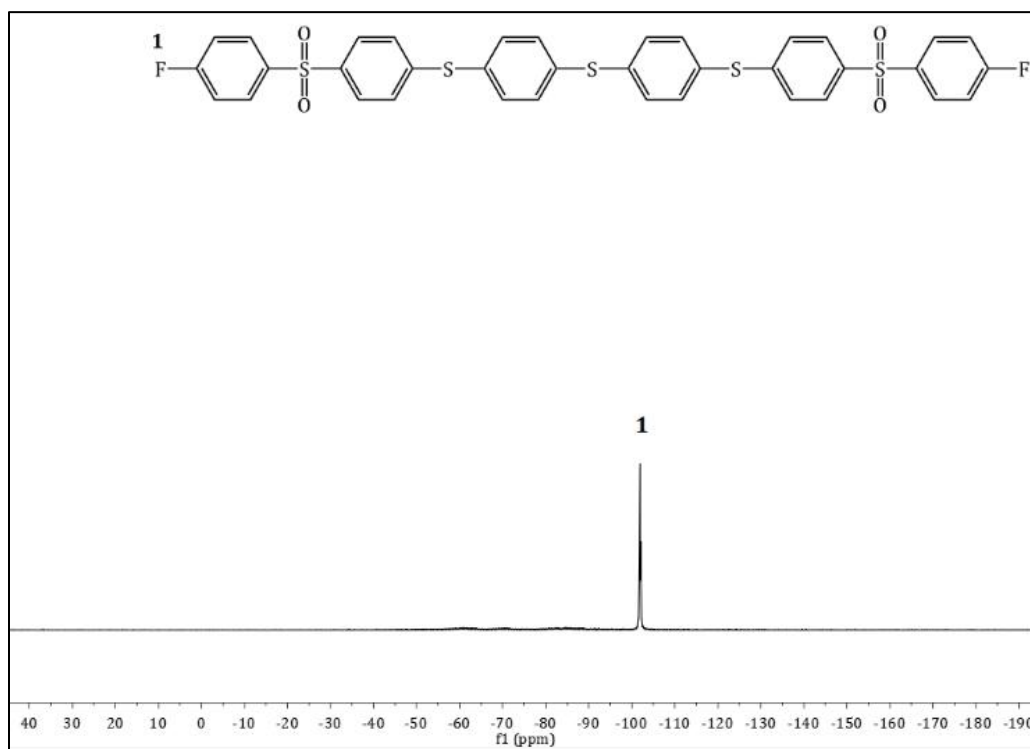
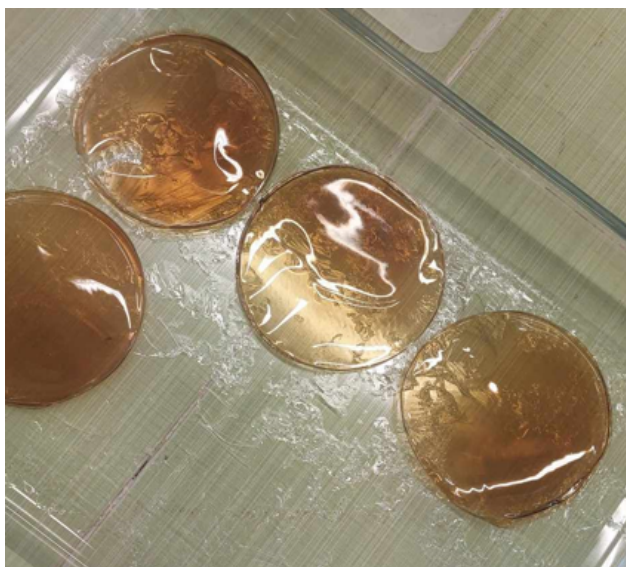


Figure 69. ¹⁹F NMR spectrum of FDPS-TBB-FDPS in CDCl₃



Picture 2. Precipitate of the unoxidized precursor of sPPS-390-XXL in *i*-PrOH



Picture 3. Films of the unoxidized precursor of sPPS-390-XXL

The chemical structure of synthesized polymers was confirmed by NMR analysis.

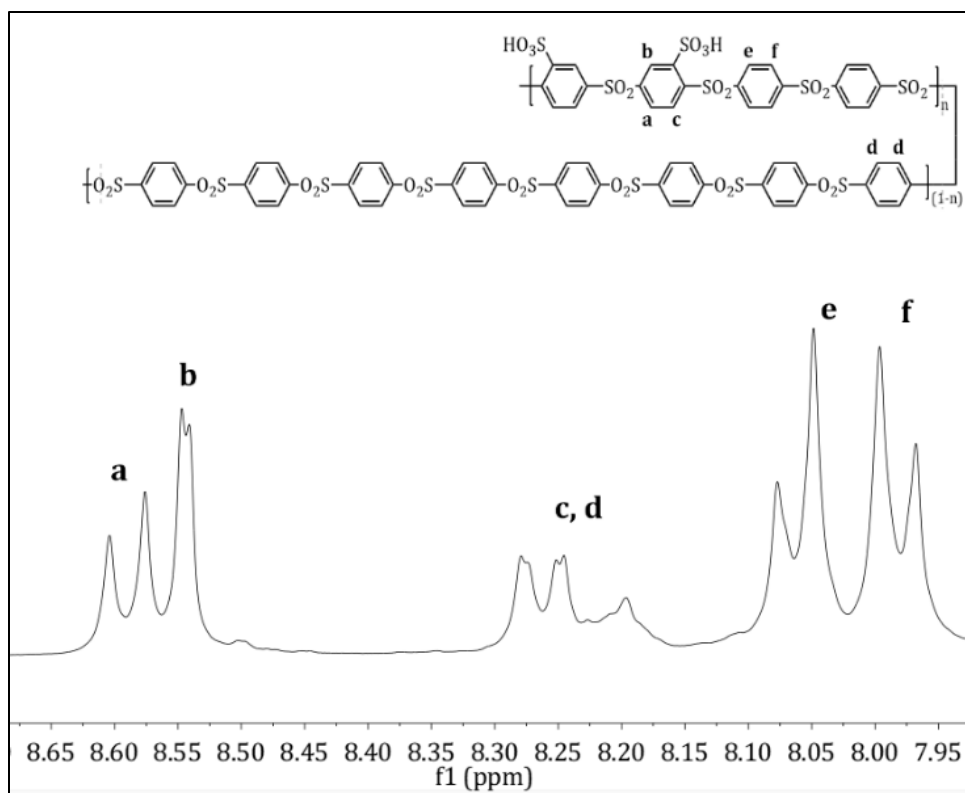


Figure 70. ^1H NMR spectrum of sPPS-390-XXL in $\text{DMSO-}d_6$

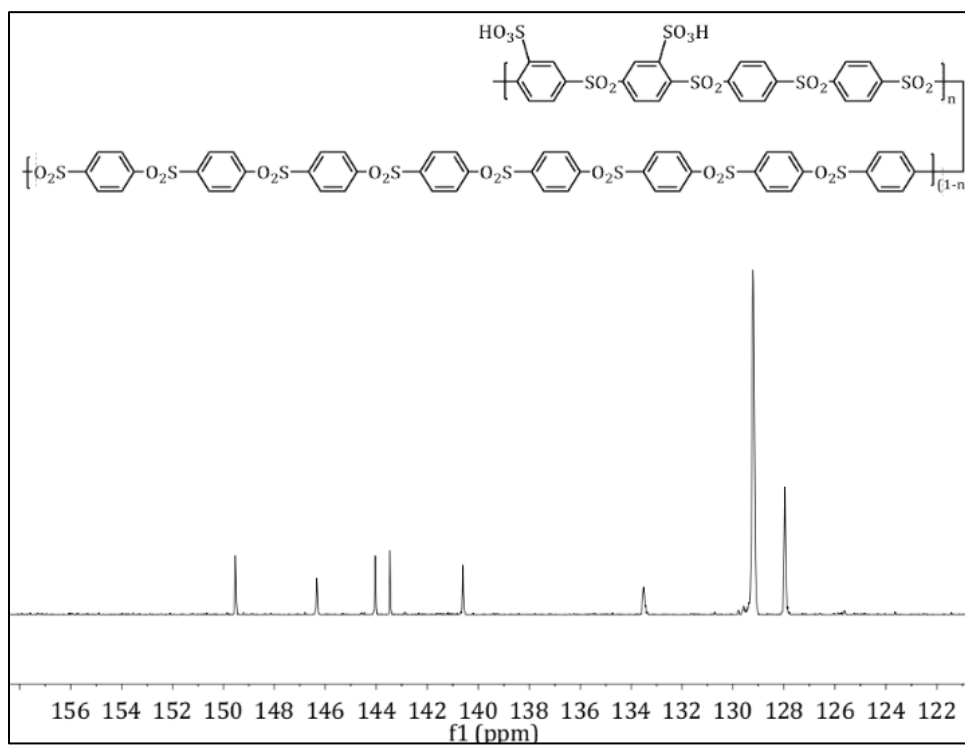


Figure 71. ^{13}C NMR spectrum of sPPS-390-XXL in $\text{DMSO-}d_6$

The intrinsic viscosities of the synthesized polymers were determined and are summarized in the Table 12:

Table 12. Intrinsic viscosities of microblock copolymers containing merely sulfone units

Sample (H-form)	Intrinsic Viscosity [η], dL/g
sPPS-400-L	1.56
sPPS-390-XXL	1.67

In order to determine the film-forming ability of polymers, their solutions in DMSO were prepared, after which they were filtered with a syringe filter and poured onto a petri dish. The results are summarized in the table below:

Table 13. Film forming abilities of microblock copolymers containing merely sulfone units

Sample (H-form)	Film formation ability
sPPS-400-L	+
sPPS-390-XXL	+



Picture 4. Film of sPPS-390-XXL

Solubility of polyelectrolytes in different solvents was studied. The table below summarizes the solubility results of microblock copolymers containing merely sulfone units:

Table 14. Solubilities of microblock copolymers containing merely sulfone units in different solvents

Sample (H-form)	H ₂ O	DMAc	DMSO	DMF	NMP	NEP
sPPS-400-L	-	-	+	-	+	+
sPPS-390-XXL	-	-	+	-	+	+

The water uptake of polymers in liquid water at 80 °C was determined. The results are summarized in the table below:

Table 15. λ values of microblock copolymers containing merely sulfone units at 80 °C

Sample (H-form)	$\lambda_{80\text{ }^\circ\text{C}} = [\text{H}_2\text{O}]/[-\text{SO}_3\text{H}]$
sPPS-400-L	32-33
sPPS-390-XXL	24-25

The observed decrease in water uptake with the growth of the non-sulfonated microblock segment can be attributed to several factors:

- **Increased Hydrophobicity:** As the non-sulfonated microblock segment lengthens, its relatively hydrophobic nature becomes increasingly dominant. Hydrophobic segments tend to repel water molecules, reducing the overall water uptake of the polymer. This effect is due to the unfavorable interactions between water molecules and hydrophobic groups, leading to decreased solvation and swelling of the polymer matrix;
- **Increased Polymer Packing and Crystallinity:** An increase in the length of the non-sulfonated poly(phenylene sulfone) microblock enhances intermolecular interactions, leading to higher crystallinity and, consequently, lower water uptake. It has to be noted, that pristine poly(*p*-phenylene sulfone) according to the X-ray powder diffraction analysis is highly crystalline (ca. 90 %) polymer [207], which is completely insoluble in any organic solvent and correspondingly is poorly characterized. Even the low molecular analogue consisting of 5 phenyl rings merely connected with 4 sulfone units is extremely insoluble [208]. Diaryl sulfone units,

which exhibit nearly perfect open-book conformations, crystallize with the aromatic rings of adjacent chains aligned essentially parallel. The crystal packing is primarily governed by $S=O^{\delta-} \cdots \delta^+H-C$ interactions, which are interpreted as weak but cooperative hydrogen bonding interactions.

For testing in a water electrolyzer, porous polyethylene (PE) was used to improve mechanical properties and reinforced sPPS-390-XXL was manufactured. The results of proton conductivity measurements are shown in the graph below:

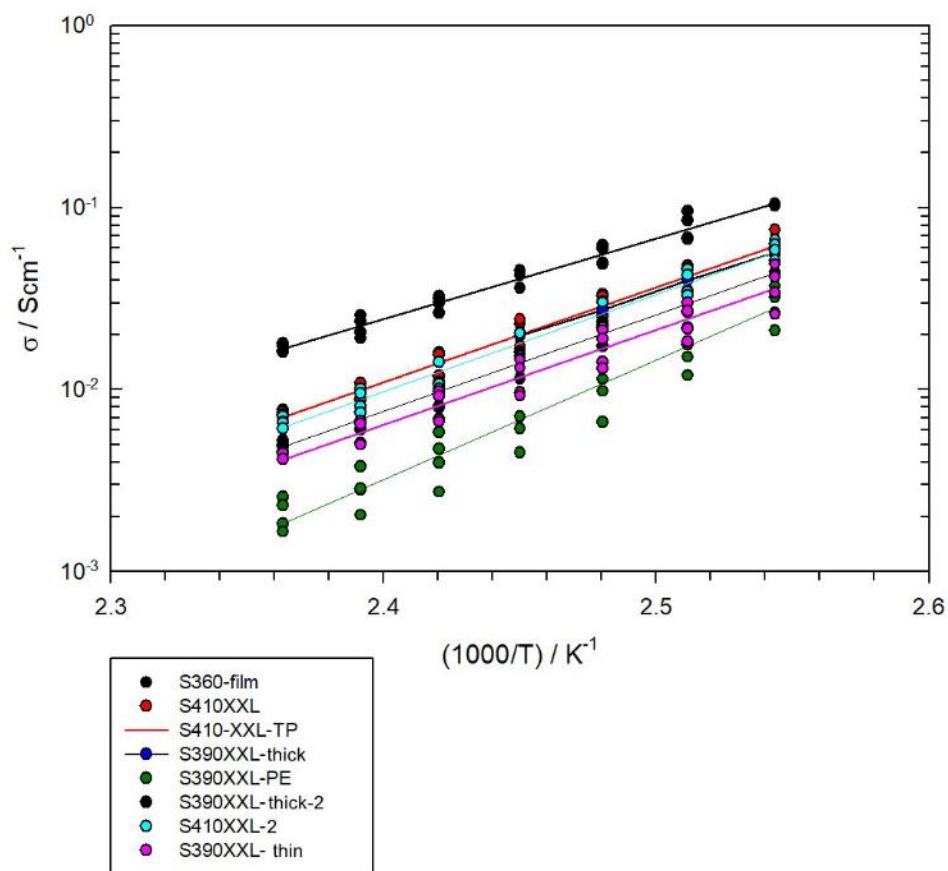


Figure 72. Graph of proton conductivities of sPPS-390-XXL, sPPS-390-XXL-PE and sPPS-410-p-TP-XXL

3.4.3.2.1. Electrochemical performance of sPPS-390-XXL

To examine the electrochemical performance of sPPS-390-XXL, we cast the membranes into porous PE (> 70 % porosity). The PE reinforcement effectively prevents XY dimensional swelling, whereas the non-reinforced membrane exhibits approximately 5 %

XY swelling. This reinforcement is critical for PEMs, enhancing both their mechanical properties and ease of handling. The thickness of the PE reinforcement is 5 μm , while the membrane total thickness is 10 μm . CCMs were fabricated by ultrasonic spray-coating using Nafion as binding ionomer with an IrO_2 anode ($1 \text{ mg}_{\text{Ir}}/\text{cm}^2$) and a Pt/C cathode ($0.5 \text{ mg}_{\text{Pt}}/\text{cm}^2$).

As shown in Figure 73, the sPPS-390-XXL membrane outperforms the reference N212-CCM and demonstrates similar performance to N211. It should be noted that the electrodes are not yet optimized, leaving room for further improvement.

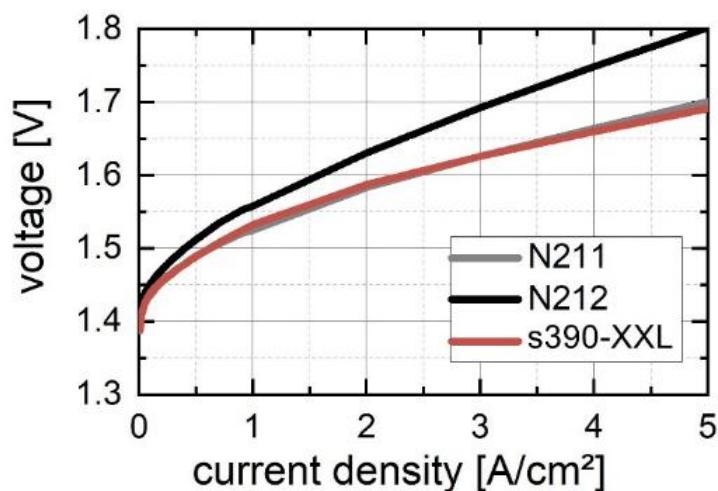


Figure 73. Graph of dependence of voltage and current density

To evaluate long-term stability, a constant current hold at $1 \text{ A}/\text{cm}^2$ was performed for 600 hours at $80 \text{ }^\circ\text{C}$, showing stable performance with a degradation rate of $< 20 \text{ } \mu\text{V}/\text{h}$ (Figure 74). This is one of the longest durations reported for hydrocarbon membranes in PEM water electrolysis. The extremely low degradation rate is attributed to the reduced water uptake, which is directly linked to the unique molecular structure of the microblock copolymers, and to the PE reinforcement, which limits dimensional swelling.

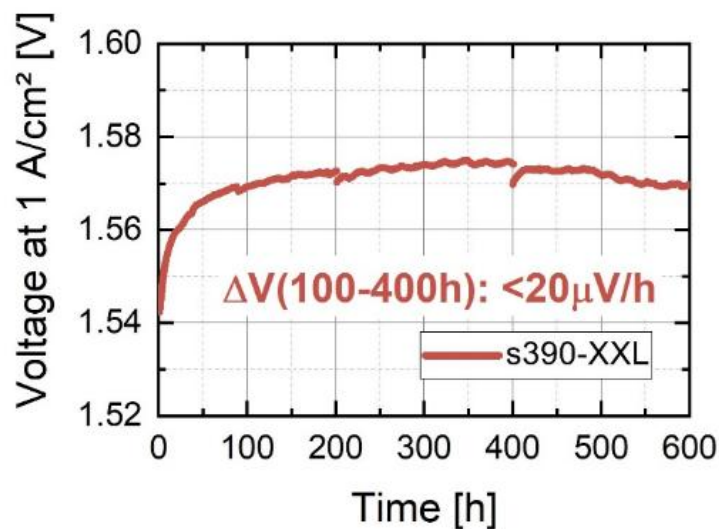


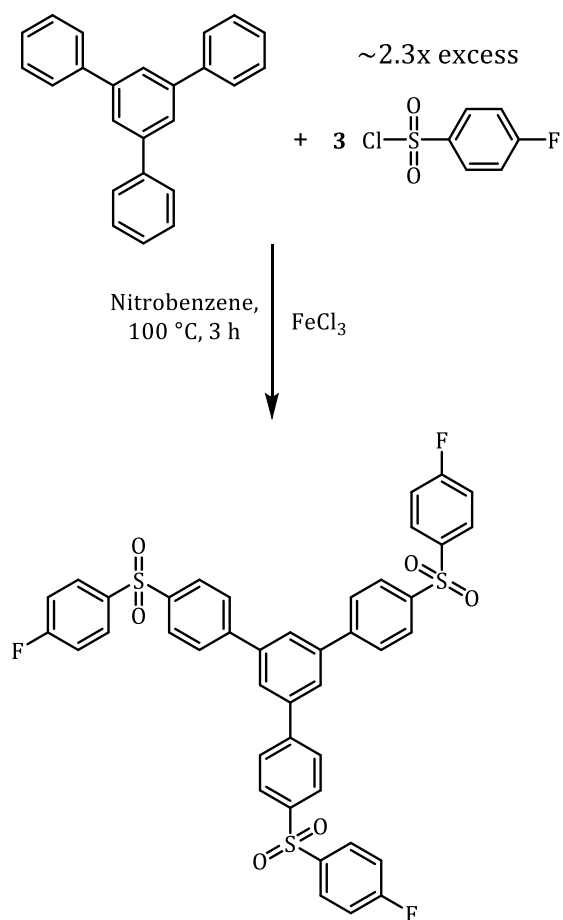
Figure 74. Graph of dependence of voltage (1 A/cm²) and time

3.4.4. Synthesis of microblock copolymers with different branching degree

In this part is discussed the synthesis of the branching monomer and then the synthesis of the microblock copolymers with different branching degree. Polymer branching results in less dense packing and lower crystallinity, leading to increased solubility and improved flexibility, which is expected to enhance water uptake. Our goal was to synthesize branched polymers that improve mechanical properties while maintaining the same water uptake as linear μ -block sPPSs.

3.4.4.1. Synthesis of the branching agent

The branching agent was synthesized using a Friedel-Crafts reaction, which proceeded with a yield of 58 %, and the product was purified using column chromatography. The detailed scheme for the synthesis is provided below:



4,4''-bis((4-fluorophenyl)sulfonyl)-5'-((4-fluorophenyl)sulfonyl)-1,1':3,1''-terphenyl

1,3,5-FPS-PB

Scheme 67. Synthesis scheme of the branching monomer (1,3,5-FPS-PB)

The chemical structure of 1,3,5-FPS-PB was confirmed by ^1H and ^{19}F NMR analysis.

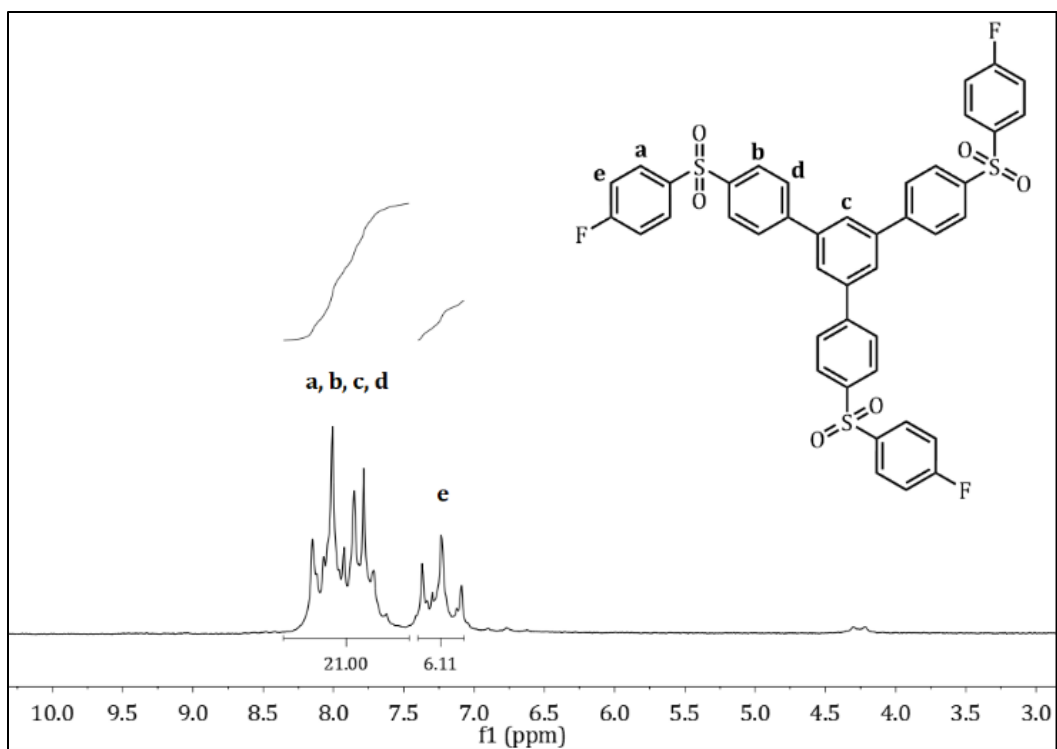


Figure 75. ^1H NMR spectrum of 1,3,5-FPS-PB in CDCl_3

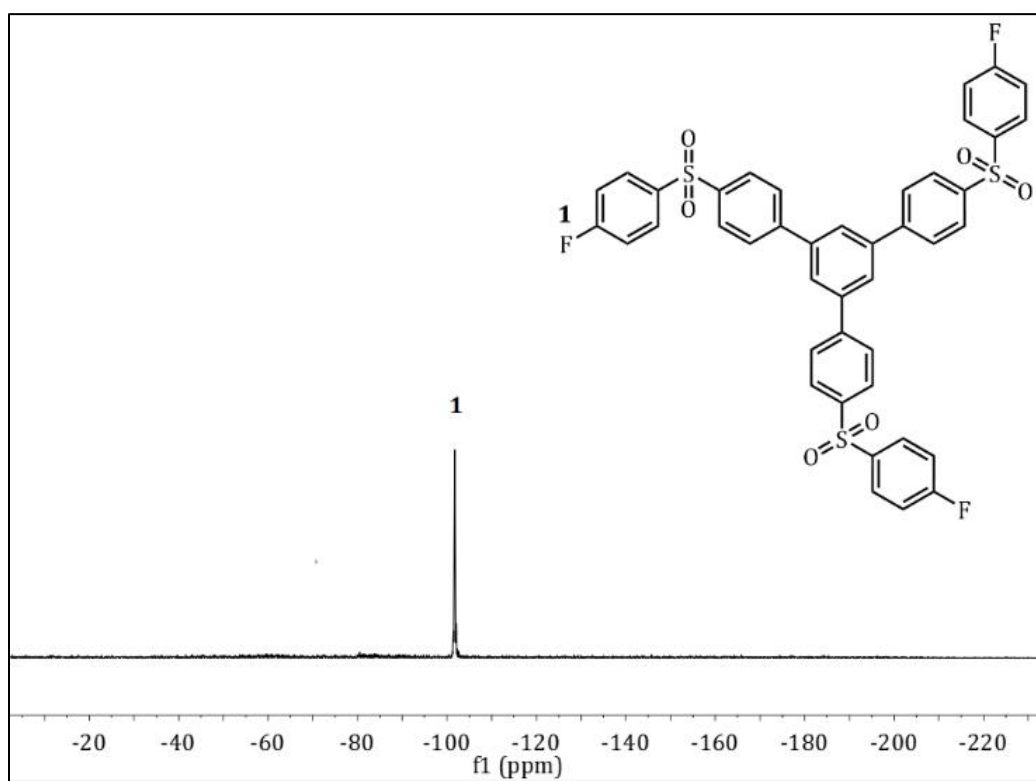
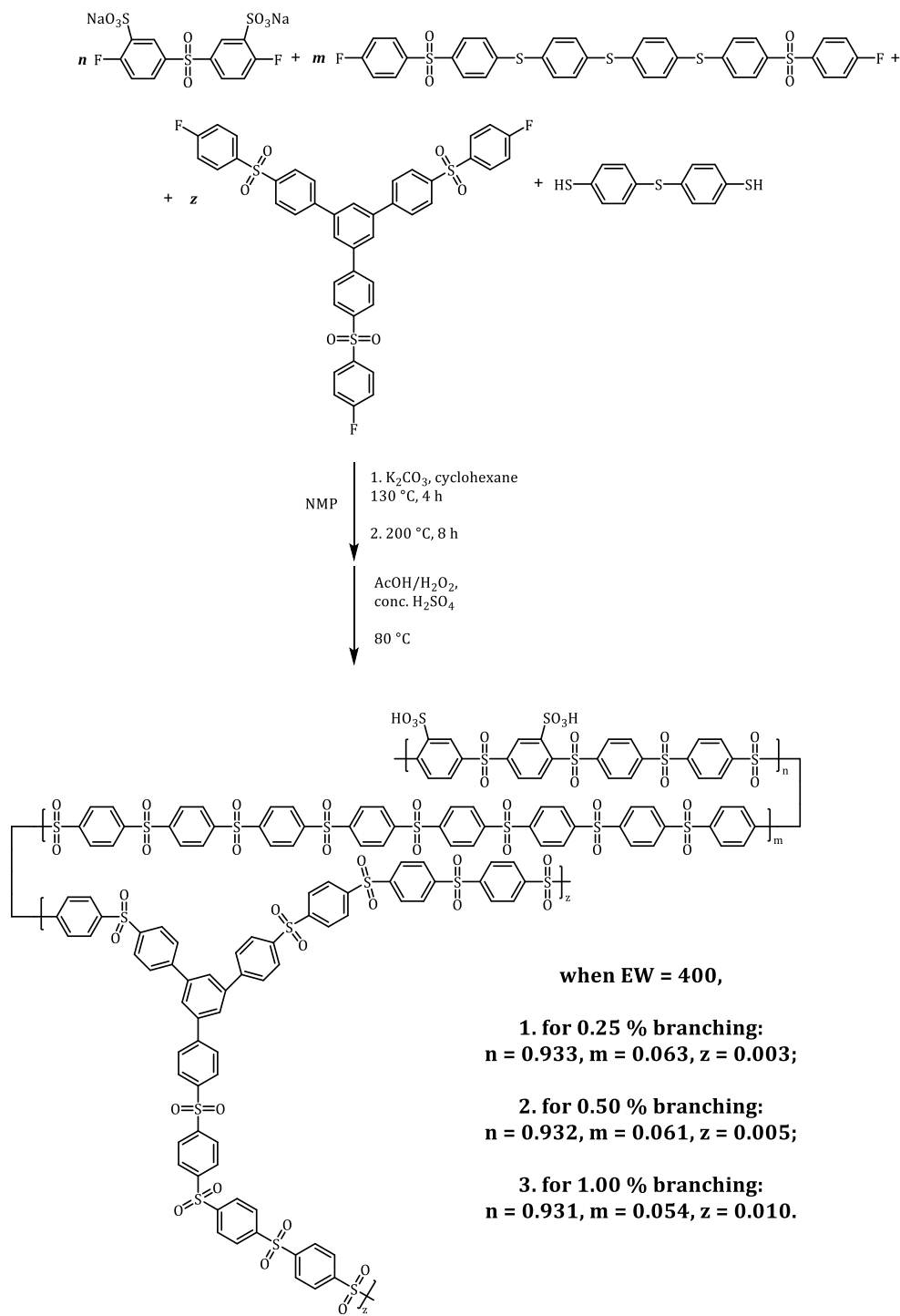


Figure 76. ^{19}F NMR spectrum of 1,3,5-FPS-PB in CDCl_3

3.4.4.2. Synthesis of branched poly(phenylene sulfone)s with microblock segments

By co-polymerization of the branching agent with TBBT, SDFDPS and FDPS-TBB-FDPS, oxidation and ion-exchange, polymers with EW = 400 and different branching degree (0.25 %, 0.50 %, 1.00 %) were obtained. Different degrees of branching were achieved by varying the molar ratio of the co-monomers.



branched sPPS-XXL

Scheme 68. General synthesis scheme of branched microblock copolymers containing merely sulfone units

The intrinsic viscosities of the synthesized branched polymers were determined and are summarized in the table below:

Table 16. Intrinsic viscosities of branched microblock copolymers containing merely sulfone units

Sample (H-form)	Intrinsic Viscosity [η], dL/g
branched (0.25 %) sPPS-400-XXL	3.33
branched (0.50 %) sPPS-400-XXL	2.87
branched (1.00 %) sPPS-400-XXL	2.26

As shown in Table 16, branching led to high molecular weight sPPSs, which are crucial for both film-forming properties and mechanical strength. In order to determine the film-forming ability of branched polymers, their solutions in DMSO were prepared, after which they were filtered with a syringe filter and poured onto a petri dish. The results are summarized in the table below:

Table 17. Film forming abilities of branched microblock copolymers containing merely sulfone units

Sample (H-form)	Film formation ability
branched (0.25 %) sPPS-400-XXL	+
branched (0.50 %) sPPS-400-XXL	+
branched (1.00 %) sPPS-400-XXL	+

Solubility of branched polyelectrolytes in different solvents was studied. The table below summarizes the solubility results of branched microblock copolymers containing merely sulfone units:

Table 18. Solubilities of branched microblock copolymers containing merely sulfone units in different solvents

Sample (H-form)	H ₂ O	DMAc	DMSO	DMF	NMP	NEP
-----------------	------------------	------	------	-----	-----	-----

branched (0.25 %) sPPS-400-XXL	-	-	+	-	+	+
branched (0.50 %) sPPS-400-XXL	-	-	+	-	+	+
branched (1.00 %) sPPS-400-XXL	-	-	+	-	+	+

The water uptake of polymers in liquid water at 80 °C was determined. The results are summarized in the table below:

Table 19. λ values of microblock copolymers containing merely sulfone units at 80 °C

Sample (H-form)	$\lambda_{80\text{ °C}} = [\text{H}_2\text{O}]/[-\text{SO}_3\text{H}]$
branched (0.25 %) sPPS-400-XXL	28-32
branched (0.50 %) sPPS-400-XXL	28-32
branched (1.00 %) sPPS-400-XXL	28-32

Table 19 shows that water uptake values are similar to those of linear polymers, with only a slight increase, while molecular weights have improved significantly. This suggests that the properties of branched μ -block sPPSs are primarily influenced by microblocks, with branching mainly contributing to the increase in molecular weight.

4. Conclusions

The presented thesis is focused on the development of membrane materials for PEM fuel cell and PEM electrolyzer applications. It includes development of as new monomers, as well new polymer electrolytes.

1. New method for preparation of sulfonated dihalo monomers was developed. Sulfonation of dihalomonomers is carried out using fuming sulfuric acid, followed by quantitative removal of excess sulfuric acid by neutralization with BaCO_3 . This leads to precipitation of excess H_2SO_4 as insoluble BaSO_4 which is easily separated from the sulfonated monomers in their soluble Ba-forms by filtration. Compared to conventional methods, the new approach leads to higher yields drastically reduces the number of purification steps and can easily be expanded to the preparation of other sulfonated monomers. Developed method was successfully used for preparation of 6 different monomers: SDFDPS, SBFPPPO, **DS-1,4-DFB**, **DS-1,3-DFB**, DS-1,4-DCB, DS-1,3-DCB and DS-1,4-DBB, among them 2 are reported for the first time (highlighted with bold). All monomers were characterized by ^1H , ^{13}C , ^{19}F NMR and IR spectroscopy.

2. It was found that sPPS with sulfonyl ($-\text{SO}_2$) linking groups exhibit superior stability due to their lower susceptibility to oxidative attack compared to those containing carbonyl ($-\text{C}=\text{O}$) or oxygen ($-\text{O}-$) linking groups. Oxidative stability of poly(phenylene sulfone) were investigated using the Fenton's test. By copolymerizing SDFDPS, DFDPS and DFDPK with TBBT, sPPS with carbonyl bridges was obtained; similarly, copolymerization of SDFDPS and DFDPS with OBBT produced sPPS with oxygen bridges. The stability of these copolymers was compared to that of pure sPPS, highlighting the significant influence of linking group composition on the polymer's resistance to oxidative degradation.

3. High molecular weight sulfonated poly(phenylene sulfone)s with high ion exchange capacities were synthesized by polymerizing SDFDPS, DFDPS, and Li_2S . The dependence of molecular weight on the particle size of Li_2S powder was investigated. For the first time, we demonstrated a significant influence of Li_2S powder particle size (5 μm , 50-75 μm , and 500 μm) on sPPS molecular weights. High molecular weight sPPS

with IECs of 3.5–4.1 meq/g were used to prepare sPPS/PBI-O acid-base blends, which are promising membrane materials. We showed that increasing the molecular weight prevents polymer electrolyte leaching from the blend at elevated temperatures.

4. sPPSs with alkyl groups in the main chain with varying IECs were synthesized using microblocks of 1,6-bis((4-fluorophenyl)sulfonyl)hexane and 1,10-bis((4-fluorophenyl)sulfonyl)decane, which were prepared for the first time via a two-step process and characterized by ^1H , ^{13}C and ^{19}F NMR spectroscopy. All sPPSs containing alkyl fragments exhibited good film-forming properties and moderate water uptake ($\lambda_{80\text{ }^\circ\text{C}} = 26\text{-}30$). To further reduce water uptake, the μ -block sPPSs were irradiated with an electron beam, resulting in partial crosslinking and a slight reduction in water uptake to $\lambda_{80\text{ }^\circ\text{C}} = 24\text{-}25$.

5. Sulfonated poly(phenylene sulfone)s containing phenylene fragments of varying lengths and ion-exchange capacities were synthesized using microblocks of 4,4'-bis((4-fluorophenyl)sulfonyl)-1,1'-biphenyl and 4,4''-bis((4-fluorophenyl)sulfonyl)-1,1':4',1''-terphenyl, which were prepared via Friedel-Crafts reactions. Both microblocks led to sPPS copolymers with excellent film-forming properties. The water uptake of the biphenyl-fragment-containing sPPS was $\lambda_{80\text{ }^\circ\text{C}} = 31\text{-}33$, while that of the terphenyl-fragment-containing sPPS was $\lambda_{80\text{ }^\circ\text{C}} = 24\text{-}25$, indicating that the length of the unsulfonated fragments significantly influences water uptake. The phenylene fragments provide a suitable basis for further sulfonation and thermal crosslinking.

6. μ -Block sPPS polymers with backbones containing only electron-accepting sulfone units ($-\text{SO}_2-$) connecting the phenyl rings were prepared using the μ -blocks bis(4-((4-fluorophenyl)sulfonyl)phenyl)thio)phenyl)sulfane (FDPS-TBB-FDPS) and bis(4-((4-fluorophenyl)sulfonyl)phenyl)sulfane (FDPS-S-FDPS). Both μ -blocks were synthesized for the first time: FDPS-TBB-FDPS was obtained by condensation reaction of DFDPS with TBBT with a high yield, while FDPS-S-FDPS was synthesized via condensation of DFDPS with Li_2S , yielding a lower yield. All synthesized polymers were characterized by ^1H and ^{13}C NMR spectroscopy, and viscosity measurements.

The sPPS with longer unsulfonated fragments (sPPS-XXL) exhibited lower water uptake $\lambda_{80\text{ }^\circ\text{C}} = 24\text{-}25$ compared to sPPS with shorter unsulfonated fragments (sPPS-L) $\lambda_{80\text{ }^\circ\text{C}} = 32\text{-}33$. This directly shows that the increase of the length of the non-sulfonated poly(phenylene sulfone) microblock enhances intermolecular interactions, leading to greater crystallinity and, consequently, reduced water uptake. In addition, the PE-reinforced sPPS-390-XXL membrane outperformed the reference N212-CCM and demonstrated similar performance to N211. This is attributed to its reduced water uptake (0 % XY swelling) and enhanced mechanical strength.

7. Microblock copolymers with varying degrees of branching were synthesized. The branching agent, 1,3,5-FPS-PB, was prepared via a Friedel-Crafts reaction, and its chemical structure was confirmed by ^1H , ^{13}C and ^{19}F NMR analysis. sPPS copolymers were then synthesized by polymerizing SDFDPS, FDPS-TBB-FDPS, and 1,3,5-FPS-PB with TBBT, followed by oxidation. It was observed that branching did not significantly affect the mechanical properties or water uptake, as these properties are primarily governed by the sPPS fragments. In some cases, branching resulted in extremely high molecular weights, making it a promising approach for achieving high molecular weights while retaining the properties of the linear sPPSs.

References

- 1 S. Chu, A. Majumdar, *Nature* **2012**, *488*, 294.
- 2 V. Sharma, A. Cortes, U. Cali, *IEEE Access* **2021**, *9*, 114690.
- 3 M. A. Hickner, H. Ghassemi, Y. S. Kim, B. R. Einsla, J. E. McGrath, *Chem. Rev.* **2004**, *104*, 4587.
- 4 Z. P. Cano, D. Banham, S. Ye, A. Hintennach, J. Lu, M. Fowler, Z. Chen, *Nat. Energy* **2018**, *3*, 279.
- 5 [https://en.wikipedia.org/wiki/File:Proton Exchange Fuel Cell Diagram.svg](https://en.wikipedia.org/wiki/File:Proton_Exchange_Fuel_Cell_Diagram.svg) (last checked on 15.01.2025).
- 6 <https://commons.wikimedia.org/wiki/File:PEMelectrolysis.jpg> (last checked on 17.01.2025).
- 7 L. Carrette, K. A. Friedrich, U. Stimming, *Fuel Cells* **2011**, *1*, 5.
- 8 K. D. Kreuer, *Solid State Ion.* **2013**, *252*, 93.
- 9 H. Ito, T. Maeda, A. Nakano, H. Takenaka, *Int. J. Hydrog. Energy* **2011**, *36*, 10527.
- 10 K. D. Kreuer, *J. Membr. Sci.* **2001**, *185*, 29.
- 11 J. Peron, Z. Shi, S. Holdcroft, *Energy Environ. Sci.* **2011**, *4*, 1575.
- 12 M. Feng, R. Qu, Z. Wei, L. Wang, P. Sun, Z. Wang, *Sci. Rep.* **2015**, *5*, 9859.
- 13 S. H. Shin, A. Kodir, D. Shin, S. H. Park, B. Bae, *Electrochim. Acta* **2019**, *298*, 901.
- 14 M. Schuster, K. D. Kreuer, H. T. Andersen, J. Maier, *Macromolecules* **2007**, *40*, 598.
- 15 M. Schuster, C. C. de Araujo, V. Atanasov, H. T. Andersen, K. D. Kreuer, J. Maier, *Macromolecules* **2009**, *42*, 3129.
- 16 Z. Katcharava, T. Saatkamp, A. Muenchinger, N. Dumbadze, K. D. Kreuer, M. Schuster, G. Titvinidze, *Polym. Adv. Technol.* **2022**, *33*, 2336.
- 17 V. Atanasov, M. Buerger, A. Wohlfarth, M. Schuster, K. D. Kreuer, J. Maier, *Polym. Bull.* **2012**, *68*, 317.
- 18 G. Titvinidze, K. D. Kreuer, M. Schuster, C. C. de Araujo, J. P. Melchior, W. H. Meyer, *Adv. Funct. Mater.* **2012**, *22*, 4456.
- 19 T. Saatkamp, *Ph.D. Thesis*, University of Stuttgart, **2021**.
- 20 N. Dumbadze, *Master's Thesis*, Free University of Tbilisi and Agricultural University of Georgia, **2021**.
- 21 C. Heitner-Wirguin, *J. Membr. Sci.* **1996**, *120*, 1.
- 22 A. Steck, H. L. Yeager, *Anal. Chem.* **1979**, *51*, 862.
- 23 C. Zaluski, G. Xu, *Macromolecules* **1994**, *27*, 6750.

24. T. A. Zawodzinski, C. Derouin, S. Radzinski, R. J. Sherman, T. Springer, S. Gottesfeld, *J. Electrochem. Soc.* **1993**, *140*, 1041.
- 25 M. Rikukawa, K. Sanui, *Prog. Polym. Sci.* **2000**, *25*, 1463.
- 26 V. Arcella, C. Trogila, A. Ghielmi, *Ind. Eng. Chem. Res.* **2005**, *44*, 7646.
- 27 M. Gebert, A. Ghielmi, L. Merio, M. Corasantini, V. Arcella, *ECS Trans.* **2010**, *26*, 279.
- 28 X. Ren, T. E. Springer, S. Gottesfeld, *J. Electrochem. Soc.* **2000**, *147*, 92.
- 29 J. Cruickshank, K. Scott, *J. Power Sources* **1998**, *70*, 40.
- 30 M. Gil, X. Ji, X. Li, H. Na, J. E. Hampsey, Y. Lu, *J. Membr. Sci.* **2004**, *234*, 75.
- 31 A. Kusoglu, A. Z. Weber, *Chem. Rev.* **2017**, *117*, 987.
- 32 K. D. Kreuer, S. J. Paddison, E. Spohr, M. Schuster, *Chem. Rev.* **2004**, *104*, 4637.
- 33 J. B. Rose, *Polymer* **1974**, *15*, 456.
- 34 W. F. Hale, A. G. Farnham, R. N. Johnson, *ACS POLY* **1966**, *7*, 503.
- 35 W. F. Hale, A. G. Farnham, R. N. Johnson, *J. Polym. Sci., Polym. Chem. Ed.* **1967**, *5*, 2399.
- 36 R. N. Johnson, A. G. Farnham, R. A. Clendinning, W. F. Hale, C. N. Merriam, *J. Polym. Sci., Polym. Chem. Ed.* **1967**, *5*, 2375.
- 37 V. L. Rao, *J. Macromol. Sci., Rev. Macromol. Chem. Phys.* **1999**, *C39*, 655.
- 38 Z. Wu, Y. Zheng, H. Yan, T. Nakamura, T. Nozawa, R. Yosomiya, *Angew. Makromol. Chem.* **1989**, *173*, 163.
- 39 J. J. Dumais, A. L. Cholli, L. W. Jelinski, J. L. Hedrick, J. E. McGrath, *Macromolecules* **1986**, *19*, 1884.
- 40 L. M. Robeson, A. G. Farnham, J. E. McGrath, *Appl. Polym. Symp.* **1975**, *26*, 373.
- 41 R. N. Johnson, A. G. Farnham, *J. Polym. Sci., Polym. Chem. Ed.* **1967**, *5*, 2515.
- 42 T. E. Attwood, T. King, V. J. Leslie, J. B. Rose, *Polymer* **1977**, *18*, 369.
- 43 K. Ghosal, R. T. Chern, B. D. Freeman, *J. Polym. Sci. B: Polym. Phys.* **1993**, *31*, 891.
- 44 J. S. McHattie, W. J. Koros, D. R. Paul, *Polymer* **1991**, *32*, 2618.
- 45 J. M. Mohr, D. R. Paul, G. L. Tullos, P. E. Cassidy, *Polymer* **1991**, *32*, 2387.
- 46 J. S. McHattie, W. J. Koros, D. R. Paul, *Polymer* **1991**, *32*, 840.
- 47 G. A. Olah, S. Kobayashi, J. Nishimura, *J. Am. Chem. Soc.* **1973**, *95*, 564.
- 48 B. E. Jennings, M. E. Jones, J. B. Rose, *J. Polym. Sci., Polym. Symp.* **1967**, *16*, 715.
- 49 M. E. A. Cudby, R. G. Feasey, S. Gaskin, M. E. B. Jones, J. B. Rose, *J. Polym. Sci., Polym. Symp.* **1967**, *22*, 747.
- 50 M. E. A. Cudby, R. G. Feasey, S. Gaskin, V. Kendall, J. B. Rose, *Polymer* **1968**, *9*, 265.

- 51 J. Meisenheimer, *Justus Liebigs Ann. Chem.* **1902**, 323, 205.
- 52 R. Alexander, E. C. F. Ko, A. J. Parker, T. J. Broxton, *J. Am. Chem. Soc.* **1968**, 90, 5049.
- 53 R. Fuchs, L. L. Cole, *J. Am. Chem. Soc.* **1973**, 95, 3194.
- 54 J. F. Bunnett, R. E. Zahler, *Chem. Rev.* **1951**, 49, 273.
- 55 A. Ben-Haida, P. Hodge, M. Nisar, M. Helliwell, *Polym. Adv. Technol.* **2006**, 17, 682.
- 56 H. M. Colquhoun, D. F. Lewis, A. Ben-Haida, P. Hodge, *Macromolecules* **2003**, 36, 3775.
- 57 D. Xie, Q. Ji, H. W. Gibson, *Macromolecules* **1997**, 30, 4814.
- 58 P. Genova-Dimitrova, B. Baradie, D. Foscallo, C. Poinsignon, J. Y. Sanchez, *J. Membr. Sci.* **2001**, 185, 59.
- 59 C. Bailly, D. J. Williams, F. E. Karasz, W. J. MacKnight, *Polymer* **1987**, 28, 1009.
- 60 B. C. Johnson, L. Yilgor, C. Tran, M. Iqbal, J. P. Wightman, D. R. Lloyd, J. E. McGrath, *J. Polym. Sci., Polym. Chem. Ed.* **1984**, 22, 721.
- 61 A. Noshay, L. M. Robeson, *J. Appl. Polym. Sci.* **1976**, 20, 1885.
- 62 M. I. Litter, C. S. Marvel, *J. Polym. Sci., Polym. Chem. Ed.* **1985**, 23, 2205.
- 63 S. H. Tian, D. Shu, S. J. Wang, M. Xiao, Y. Z. Meng, *Fuel Cells* **2007**, 7, 232.
- 64 B. Liu, G. P. Robertson, D-S. Kim, M. D. Guiver, W. Hu, Z. Jiang, *Macromolecules* **2007**, 40, 1934.
- 65 C. Le Ninivin, A. Balland-Longeau, D. Demattei, P. Palmas, J. Saillard, C. Coutanceau, C. Lamy, J. M. Leger, *J. Appl. Polym. Sci.* **2006**, 101, 944.
- 66 M. T. Bishop, F. E. Karasz, P. S. Russo, K. H. Langley, *Macromolecules* **1985**, 18, 86.
- 67 J. Kerres, W. Cui, S. Reichle, *J. Polym. Sci., Part A: Polym. Chem.* **1996**, 34, 2421.
- 68 M. Ueda, H. Toyota, T. Ouchi, J. Sugiyama, K. Yonetake, T. Masuko, T. Teramoto, *J. Polym. Sci., Part A: Polym. Chem.* **1993**, 31, 853.
- 69 F. Wang, Y. Kim, M. Hickner, T. A. Zawodzinski, J. E. McGrath, *Polym. Mater. Sci. Eng.* **2001**, 85, 517.
- 70 Y. S. Kim, L. Dong, M. A. Hickner, T. E. Glass, V. Webb, J. E. McGrath, *Macromolecules* **2003**, 36, 6281.
- 71 Y. S. Kim, F. Wang, M. Hickner, S. McCartney, Y. T. Hong, W. Harrison, T. A. Zawodzinski, J. E. McGrath, *J. Polym. Sci., Part B: Polym. Phys.* **2003**, 41, 2816.
- 72 Y. S. Kim, M. A. Hickner, L. Dong, B. S. Pivovar, J. E. McGrath, *J. Membr. Sci.* **2004**, 243, 317.
- 73 W. L. Harrison, M. A. Hickner, Y. S. Kim, J. E. McGrath, *Fuel Cells* **2005**, 5, 201.
- 74 G. M. Bower, L. W. Frost, *J. Polym. Sci.* **1963**, 1, 3135.
- 75 J. A. Kreuz, A. L. Endrey, F. P. Gay, C. E. Sroog, *J. Polym. Sci., Polym. Chem. Ed.* **1966**, 4, 2607.

- 76 C. Genies, R. Mercier, B. Sillion, R. Petriaud, N. Cornet, G. Gebel, M. Pineri, *Polymer* **2001**, *42*, 5097.
- 77 S. Besse, P. Capron, O. Diat, G. Gebel, F. Jousse, D. Marsacq, M. Pineri, C. Marsetin, R. Mercier, *J. New Mater. Electrochem. Syst.* **2002**, *5*, 109.
- 78 C. Genies, R. Mercier, B. Sillion, N. Cornet, G. Gebel, M. Pineri, *Polymer* **2000**, *42*, 359.
- 79 N. Asano, K. Miyatake, M. Watanabe, *J. Polym. Sci., Part A: Polym. Chem.* **2006**, *44*, 2744.
- 80 N. Asano, K. Miyatake, M. Watanabe, *Chem. Mater.* **2004**, *16*, 2841.
- 81 N. Asano, M. Aoki, S. Suzuki, K. Miyatake, H. Uchida, M. Watanabe, *J. Am. Chem. Soc.* **2006**, *128*, 1762.
- 82 B. R. Einsla, Y. T. Hong, Y. S. Kim, F. Wang, N. Gunduz, J. E. McGrath, *J. Polym. Sci., Part A: Polym. Chem.* **2004**, *42*, 862.
- 83 T. D. Gierke, W. Y. Hsu, *ACS Symp. Ser.* **1982**, *180*, 283.
- 84 T. D. Gierke, G. E. Munn, F. C. Wilson, *ACS Symp. Ser.* **1982**, *180*, 195.
- 85 L. Rubatat, G. Gebel, O. Diat, *Macromolecules* **2004**, *37*, 7772.
- 86 P. C. Van der Heijden, L. Rubatat, O. Diat, *Macromolecules* **2004**, *37*, 5327.
- 87 K. A. Mauritz, R. B. Moore, *Chem. Rev.* **2004**, *104*, 4535.
- 88 T. P. Lodge, *Macromol. Chem. Phys.* **2003**, *204*, 265.
- 89 G. Krausch, R. Magerle, *Adv. Mater.* **2002**, *14*, 1579.
- 90 C. Park, J. Yoon, E. L. Thomas, *Polymer* **2003**, *44*, 6725.
- 91 H. Ghassemi, G. Ndip, J. E. McGrath, *Polymer* **2004**, *45*, 5855.
- 92 H. Wang, A. S. Badami, A. Roy, J. E. McGrath, *J. Polym. Sci., Part A: Polym. Chem.* **2006**, *45*, 284.
- 93 H. Ghassemi, J. E. McGrath, T. A. Zawodzinski, *Polymer* **2006**, *47*, 4132.
- 94 Y. Li, A. Roy, A. S. Badami, M. Hill, J. Yang, S. Dunn, J. E. McGath, *J. Power Sources* **2007**, *172*, 30.
- 95 Y. Xiang, A. Roy, J. E. McGrath, *Prepr. Symp. –Am. Chem. Soc., Div. Fuel Chem.* **2005**, *50*, 577.
- 96 A. Roy, X. Yu, S. Dunn, J. E. McGrath, *J. Membr. Sci.* **2009**, *327*, 118.
- 97 Z. Shi, S. Holdcroft, *Macromolecules* **2004**, *37*, 2084.
- 98 Y. Yang, Z. Shi, S. Holdcroft, *Eur. Polym. J.* **2004**, *40*, 531.
- 99 Y. Yang, Z. Shi, S. Holdcroft, *Macromolecules* **2004**, *37*, 1678.
- 100 J. Ding, Q. Tang, S. Holdcroft, *Aust. J. Chem.* **2002**, *55*, 461.
- 101 Q. F. Li, J. O. Jensen, R. F. Savinell, N. J. Bjerrum, *Prog. Polym. Sci.* **2009**, *34*, 449.

- 102 S. Yu, B. C. Benicewicz, *Macromolecules* **2009**, *42*, 8640.
- 103 J. A. Mader, *Macromolecules* **2010**, *43*, 6706.
- 104 D. J. Jones, J. Roziere, *J. Membr. Sci.* **2001**, *185*, 41.
- 105 M. Kawahara, M. Rikukawa, K. Sanui, N. Ogata, *Solid State Ionics* **2000**, *136*, 1193.
- 106 R. Guo, J. E. McGrath, *Polymer Science: A Comprehensive Reference* **2012**, Amsterdam, 377.
- 107 J. R. Rowlett, Y. Chen, A. T. Shaver, G. B. Fahs, B. J. Sundell, Q. Li, Y. S. Kim, P. Zelenay, R. B. Moore, S. Mecham, J. E. McGrath, *J. Electrochem. Soc.* **2014**, *161*, F535.
- 108 C. H. Lee, S. Y. Lee, Y. M. Lee, S. Y. Lee, J. W. Rhim, O. Lane, J. E. McGrath, *ACS Appl. Mater. Interfaces* **2009**, *1*, 1113.
- 109 H. Yu, T. W. Xu, *J. Appl. Polym. Sci.* **2006**, *100*, 2238.
- 110 M. Cai, M. Chen, Y. Yu, C. Song, *Polym. Adv. Technol.* **2013**, *24*, 466.
- 111 J. F. Ding, C. Chuy, S. Holdcroft, *Chem. Mater.* **2001**, *13*, 2231.
- 112 Y. Sakaguchi, K. Kimura, M. Omori, Y. Yamashita, *Polym. J.* **2002**, *34*, 219.
- 113 Y. Sakaguchi, M. Tokai, Y. Kato, *Polymer* **1993**, *34*, 1512.
- 114 K. J. Smith, I. D. H. Towle, M. G. Moloney, *RCS Adv.* **2016**, *6*, 13809.
- 115 Y. Wang, P. P. Wang, Q. Xu, T. Yan, M. Z. Cai, *J. Polym. Res.* **2014**, *21*, 533.
- 116 X. Shang, S. Tian, L. Kong, Y. Meng, *J. Membr. Sci.* **2005**, *266*, 94.
- 117 Y. Gao, G. P. Robertson, M. D. Guiver, S. D. Mikhailenko, X. Li, S. Kaliaguine, *Macromolecules* **2004**, *37*, 6748.
- 118 H. S. Lee, A. Roy, O. Lane, M. Lee, J. E. McGrath, *J. Polym. Sci., Part A: Polym. Chem.* **2010**, *48*, 214.
- 119 Y. Chen, C. H. Lee, J. R. Rowlett, J. E. McGrath, *Polymer* **2012**, *53*, 3143.
- 120 J. Miyake, K. Miyatake, *Polym. J.* **2017**, *49*, 487.
- 121 T. J. Peckham, S. Holdcroft, *Adv. Mater.* **2010**, *22*, 4667.
- 122 H. Hou, M. L. Di Vona, P. Knauth, *ChemSusChem*, **2011**, *4*, 1526.
- 123 S. Takamuku, P. Jannasch, *Macromolecules* **2012**, *45*, 6538.
- 124 E. A. Weiber, S. Takamuku, P. Jannasch, *Macromolecules* **2013**, *46*, 3476.
- 125 S. Granados-focil, M. Litt, *Prepr.Pap.-Am. Chem. Soc. Div. Fuel Chem.* **2004**, *49*, 528.
- 126 C. Fujimoto, M. Hickner, C. Cornelius, D. Loy, *Macromolecules* **2005**, *38*, 5010.
- 127 T. J. G. Skalski, B. Britton, T. J. Peckham, S. Holdcroft, *J. Am. Chem. Soc.* **2015**, *137*, 12223.

- 128 J. Miyake, R. Taki, T. Mochizuki, R. Shimizu, R. Akiyama, M. Uchida, K. Miyatake, *Sci. Adv.* **2017**, *3*, eaao0476.
- 129 G. Goldfinger, *J. Polym. Sci., Part A: Gen. Pap.* **1949**, *4*, 93.
- 130 G. A. Edwards, G. Goldfinger, *J. Polym. Sci., Part A: Gen. Pap.* **1955**, *16*, 589.
- 131 W. Ried, K. H. Bonnighausen, *Chem. Ber.* **1960**, *93*, 1769.
- 132 W. Ried, D. Freitag, *Naturwissenschaften* **1966**, *53*, 306.
- 133 J. K. Stille, *J. Polym. Sci., Part A: Gen. Pap.* **1964**, *2*, 1487.
- 134 G. Noren, J. K. Stille, *J. Polym. Sci. Macromol. Rev.* **1971**, *5*, 385.
- 135 H. F. VanKerckhoven, Y. K. Gilliams, J. K. Stille, *Macromolecules* **1972**, *5*, 541.
- 136 Ionomr Innovations Inc. Pemion® <https://ionomr.com/solutions/pemion/>.
- 137 A. J. Berresheim, M. Müller, K. Müllen, *Chem. Rev.* **1999**, *99*, 1747.
- 138 J. K. Stille, *Makromol. Chem.* **1972**, *154*, 49.
- 139 M. Remmers, B. Müller, K. Martin, H.-J. Räder, W. Köhler, *Macromolecules* **1999**, *32*, 1073.
- 140 A. Abdulkarim, F. Hinkel, D. Jänsch, J. Freudenberg, F. E. Golling, K. Müllen *J. Am. Chem. Soc.* **2016**, *138*, 16208.
- [141] J. K. Kallitsis, M. Rehahn, G. Wegner, *Makromol. Chem.* **1992**, *193*, 1021.
- 142 J. K. Kallitsis, H. Naarmann, *Synth. Met* **1991**, *44*, 247.
- 143 X. Zhang, T. Higashihara, M. Ueda, L.-J. Wang, *Polym. Chem.* **2014**, *5*, 6121.
- 144 K. Umezawa, T. Oshima, M. Yoshizawa-Fujita, Y. Takeoka, M. Rikukawa, *ACS Macro Lett.* **2012**, *1*, 969.
- 145 S. Granados-focil, M. Litt, *Prepr.Pap.-Am. Chem. Soc. Div. Fuel Chem.* **2004**, *49*, 528.
- 146 M. Litt, S. Granados-Focil, J. Kang, K. Si, R. Wycisk, *ECS Trans.* **2010**, *33*, 695.
- 147 K. Si, R. Wycisk, D. Dong, K. Cooper, M. Rodgers, P. Brooker, D. Slattery, M. Litt, *Macromolecules* **2013**, *46*, 422.
- 148 M. Litt, S. Granados-Focil, J. Kang, *ACS Symp. Ser.* **2010**, *1040*, 49.
- 149 K. Si, M. H. Litt, *ECS Trans.* **2011**, *41*, 1645.
- 150 K. Si, R. Wycisk, D. Dong, K. Cooper, M. Rodgers, P. Brooker, D. Slattery, M. Litt, *Macromolecules* **2013**, *46*, 422.
- 151 M. Litt, R. Wycisk, *Polym. Rev.* **2015**, *55*, 307.
- 152 Y. Takeoka, K. Umezawa, T. Oshima, M. Yoshida, M. Yoshizama-Fujita, M. Rikukawa, *Polym. Chem.* **2014**, *5*, 4132.

- 153 R. Shimizu, K. Otsuji, A. Masuda, N. Sato, M. Kusakabe, A. Iiyama, K. Miyatake, M. Uchida, *J. Electrochem. Soc.* **2019**, *166*, F3105.
- 154 K. Shiino, J. Miyake, K. Miyatake *Chem. Commun.* **2019**, *55*, 7073.
- 155 T. Kobayashi, M. Rikukawa, K. Sanui, N. Ogata, *Solid State Ionics* **1998**, *106*, 219.
- 156 H. Ghassemi, J. E. McGrath, *Polymer* **2004**, *45*, 5847.
- 157 C. Le Ninivin, A. Balland-Longeau, D. Demattei, C. Coutanceau, C. Lamy, J. M. Lèger, *J. Appl. Electrochem.* **2004**, *34*, 1159.
- 158 S. Wu, Z. Qiu, S. Zhang, X. Yang, F. Yang, Z. Li, *Polymer* **2006**, *101*, 944.
- 159 C. Le Ninivin, A. Balland-Longeau, D. Demattei, P. Palmas, J. Saillard, C. Coutanceau, C. Lamy, J. M. Lèger, *J. Appl. Polym. Sci.* **2006**, *101*, 944.
- 160 F. Ahmed, S. C. Sutradhar, T. Ryu, H. Jang, K. Choi, H. Yang, S. Yoon, M. M. Rahman, W. Kim *Int. J. Hydrogen Energy* **2018**, *43*, 5374.
- 161 S. C. Sutradhar, M. Rahman, F. Ahmed, T. Ryu, J. Lei, S. Yoon, S. Lee, Y. Jin, W. Kim *J. Power Sources* **2019**, *442*, 227233.
- 162 S. C. Sutradhar, M. M. Rahman, F. Ahmed, T. Ryu, S. Yoon, S. Lee, J. Kim, Y. Lee, Y. Jin, W. Kim *J. Ind. Eng. Chem.* **2019**, *76*, 233.
- 163 S. C. Sutradhar, M. Rahman, F. Ahmed, T. Ryu, S. Yoon, S. Lee, J. Kim, Y. Lee, Y. Jin, W. Kim *Int. J. Hydrogen Energy* **2019**, *44*, 11311.
- 164 C. Fujimoto, M. Hickner, C. Cornelius, D. Loy, *Macromolecules* **2005**, *38*, 5010.
- 165 S. M. Budy, D. A. Loy, *J. Polym. Sci. Part A: Polym. Chem.* **2014**, *52*, 1381.
- 166 M. Hickner, C. Fujimoto, C. Cornelius, *Polymer* **2006**, *47*, 4238.
- 167 E. G. Sorte, B. A. Paren, C. G. Rodriguez, C. Fujimoto, C. Poirier, L. J. Abbott, N. A. Lynd, K. L. Winey, A. L. Frischknecht, T. M. Alam, *Macromolecules* **2019**, *52*, 857.
- 168 L. He, L. Smith, J. Majewski, C. H. Fujimoto, C. J. Cornelius, D. Perahia, *Macromolecules* **2009**, *42*, 5745.
- 169 M. Adamski, T. Skalski, B. Britton, T. Peckham, L. Metzler, S. Holdcroft *Angew. Chem., Int. Ed.* **2017**, *56*, 9058.
- 170 C. C. de Araujo, K. D. Kreuer, M. Schuster, G. Portale, H. Mendil-Jakani, G. Gebel, J. Maier, *Phys. Chem. Chem. Phys.* **2009**, *11*, 3305.
- 171 N. Dumbadze, M. Viviani, K. D. Kreuer, G. Titvinidze, *RSC Advances* **2024**, *14*, 37272.
- 172 Y. Tan, K. Zhang, H. Liao, G. Xiao, Y. Yao, G. Sun, D. Yan, *J. Membr. Sci.* **2016**, *508*, 32.
- 173 L. Gubler, S. M. Dockheer, W. H. Koppenol, *J. Electrochem. Soc.* **2011**, *158*, B755.
- 174 L. Greenspan, *J. Res. Nat. Bur. Stand. A* **1977**, *81*, 89.

- 175 A. Kusoglu, A. Kwong, K. T. Clark, H. Gunterman, A. Z. Weber, *J. Electrochem. Soc.* **2012**, *159*, F530.
- 176 C. Y. Jung, S. C. Yi, *Electrochem. Commun.* **2013**, *35*, 34.
- 177 O. F. Solomon, B. S. Gottesman, *Macromol. Chem.* **1969**, *127*, 153.
- 178 D. E. Knox, *U.S. Patent No. 5.081.306*, **1992**.
- 179 S. Matsumura, A. R. Hlil, C. Lepiller, J. Gaudet, D. Guay, Z. Shi, S. Holdcroft, A. S. Hay, *Macromolecules* **2008**, *41*, 281.
- 180 Y. Li, R. A. VanHouten, A. E. Brink, J. E. McGrath, *Polymer (Guildf)*, **2008**, *49*, 3014.
- 181 Y. Zhang, J. Kim, K. Miyatake, *J. Appl. Polym. Sci.* **2016**, *133*, 44218.
- 182 B. Bae, K. Miyatake, M. Watanabe, *Macromolecules*, **2009**, *42*, 1873.
- 183 A. Haragirimana, P. B. Ingabire, Y. Zhu, Y. Lu, N. Li, Z. Hu, S. Chen, *J. Membr. Sci.* **2019**, *583*, 209.
- 184 S. Liu, Y. Wang, N. Li, Z. Hu, S. Chen, *J. Membr. Sci.* **2024**, *694*, 122431.
- 185 T. N. Ofei, B. Lund, A. Saasen, *J. Pet. Sci. Eng.* **2021**, *206*, 108908.
- 186 H. Cerfontain, *Mechanistic Aspects of Aromatic Sulfonation and Desulfonation*; Wiley: New York, 1968.
- 187 H. Liao, K. Zhang, G. Tang, G. Xiao, D. Yan, *Polym. Chem.* **2014**, *5*, 412.
- 188 H. Liao, G. Xiao, D. Yan, *Chem. Comm.* **2013**, *49*, 3979.
- 189 S. Takamuku, A. Wohlfarth, A. Manhart, P. Räder, P. Jannasch, *Polym. Chem.* **2015**, *6*, 1267.
- 190 G. Titvinidze, A. Kaltbeitzel, A. Manhart, W. H. Meyer, *Fuel Cells* **2010**, *10*, 390.
- 191 D. Yazili, E. Marini, T. Saatkamp, A. Münchinger, T. de Wild, L. Gubler, G. Titvinidze, M. Schuster, C. Schare, L. Jörissen, K. D. Kreuer, *J. Power Sources* **2023**, *563*, 232791.
- 192 J. P. Owejan, J. J. Gagliardo, S. R. Falta, T. A. Trabold, *J. Electrochem. Soc.* **2009**, *156*, B1475.
- 193 Q. Guo, H. Guo, F. Ye, C. F. Ma, *Energy Convers. Manag.* **2022**, *254*, 115288.
- 194 M. R. Berber, T. Fujigaya, K. Sasaki, N. Nakashima, *Sci. Rep.* **2013**, *3*, 1764.
- 195 N. Dumbadze, *Master's Thesis*, Free University of Tbilisi and Agricultural University of Georgia, **2021**.
- 196 N. Arakishvili, *Master's Thesis*, Free University of Tbilisi and Agricultural University of Georgia, **2023**.
- 197 M. Navrozashvili, *Bachelor's Thesis*, Agricultural University of Georgia, **2024**.
- 198 T. A. Zawodzinski, T. E. Springer, J. Davey, R. Jestel, C. Lopez, J. Valerio, S. Gottesfeld, *J. Electrochem. Soc.* **1993**, *140*, 1981.

- 199 P.V. Schroeder, *Z. Phys. Chem.* **1903**, 45, 75.
- 200 P. Choi, R. Datta, *J. Electrochem. Soc.* **2003**, 150, E601.
- 201 V. Freger, *J. Phys. Chem. B* **2009**, 113, 24.
- 202 C. Vallieres, D. Winkelmann, D. Roizard, E. Favre, P. Scharfer, M. Kind, *J. Membr. Sci.* **2006**, 278, 357.
- 203 G. Alberti, R. Narducci, M. Sganappa, *J. Power Sources* **2008**, 178, 575.
- 204 M. L. Di Vona, E. Sgreccia, S. Licoccia, G. Alberti, L. Tortet, P. Knauth, *J. Phys. Chem. B* **2009**, 113, 7505.
- 205 H. M. Colquhoun, P. L. Aldred, F. H. Kohnke, P. L. Herbertson, I. Baxter, D. J. Williams, *Macromolecules* **2002**, 35, 1685.
- 206 H. Hou, M. L. Di Vona, P. Knauth, *J. Membr. Sci.* **2012**, 423-424, 113.
- 207 D. R. Robello, A. Ulman, E. J. Urankar, *Macromolecules* **1993**, 26, 6718.
- 208 H. M. Colquhoun, P. L. Aldred, F. H. Kohnke, P. L. Herbertson, I. Baxter, D. J. Williams, **2002**, 35, 1685.